LIQUID-FILM DIFFUSION CONTROLLED ION-EXCHANGE MODELING — STUDY OF WEAK ELECTROLYTE MASS TRANSPORT AND FILM MASS-TRANSFER KINETICS

By

VIKRAM N. CHOWDIAH

Bachelor of Engineering
Bangalore University
Bangalore, India
1988

Master of Science
Oklahoma State University
Stillwater, Oklahoma
1990

Submitted to the Faculty of the
Graduate College of the
Oklahoma State University
in partial fulfillment of
the requirements for
the Degree of
DOCTOR OF PHILOSOPHY
May, 1996

LIQUID-FILM DIFFUSION CONTROLLED ION-EXCHANGE MODELING — STUDY OF WEAK ELECTROLYTE MASS TRANSPORT AND FILM MASS-TRANSFER KINETICS

Thesis Approved:

Gary L Foutch
Thesis Advisor

Arland H. Johannes

James R Whiteley

Warren T Ford

Martin S. High

Thomas C. Collins
Dean of the Graduate School

PREFACE

This study addresses two specific modeling issues in liquid-film diffusion controlled mixed bed ion-exchange (MBIE). First, mass transport of weak electrolytes in MBIE is modeled. Both ionic and nonionic components of the weak electrolyte are included to model the mass flux expression. The flux of the ionic part is modeled using Nernst-Planck equation while Fick's law is used for the nonionic component. Electrostatic influence of the ionic form of the weak electrolyte on the mass flux of other electrolytes in the system is considered. A column material balance equation is solved with the flux expression to obtain the effluent concentration profile. The weak electrolyte model is applied to exchange of amines in a mixed bed. Specifically, MBIE operation with three different amines — ammonia, ethanolamine, and morpholine — were studied.

The second issue dealt in this study was improving mass-transfer coefficient (MTC) predictions in MBIE. Existing mass-transfer correlations in literature, for predicting MTCs in MBIE, have been compared. Theoretical analysis of diffusion in the system — sodium-chloride-water — is presented; using this analysis, differences in MTC of sodium chloride exchange in a mixed bed are examined.

I would like to express my deepest appreciation to my advisor Dr. Gary L. Foutch, for his assistance, encouragement, and helpfulness throughout this study. His guidance and insight into many aspects of ion-exchange has been very valuable for completing my study. Grateful acknowledgement and deep appreciation is also extended to Dr. A. H. Johannes for his guidance, support and friendly advice. I am thankful to my committee members Dr. W. T. Ford, Dr. M. High, and Dr. R. J. Whiteley for serving on the advisory committee and for their technical assistance.

I would like to thank all the faculty members in the chemical engineering department for making my stay at OSU a good experience. I would like to thank Charles Baker for helpful assistance throught this study. Help of staff members — Pat, Vickie, Sherri, and Laura — in the department is also acknowledged.

Immeasurable contributions to my life have been made by my parents Kusuma and Murthy, my brother Vinayak, and friend Dr. Venu. Their encouragement, support, and understanding throughout the course of this study has been vital. I would like to thank them especially and express my deepest gratitude to them.

Special thanks to Avinash for his friendly assistance, helpful discussions, and contributions for completing this work. Thanks to Dr. Bates, Mr. D. Barber, Mr. D. Morgan, and Mr. R. Martin for discussions on varied aspects of ion exchange.

Thanks to my roommates Srikanth and Alagappan, and friends Desai, Lou, Manoj, Rashmi, and Ameya. Thanks to all the co-workers — Bulusu, Dennis, Vinay, Ashwin, Kalyan, and Liu — for having made this a good experience. Assistance of all individuals, not mentioned by name, is also gratefully acknowledged.

TABLE OF CONTENTS

Chapter Page

I. INTRODUCTION 1

- Ion Exchange 4
- Mixed-Bed Ion-Exchange (MBIE) Technology 6
- Mixed-Bed Ion-Exchange Modeling 10
- Objectives 12

II. WEAK ELECTROLYTE MASS TRANSPORT MODEL FOR MBIE 15

- Introduction 15
- Modeling MBIE 16
- MBIE Modeling Literature 20
- Diffusion of Strong Electrolytes 24
- Diffusion of Weak Electrolytes 25
- Assumptions for Modeling MBIE 27
- Mathematical Model Development 29
- Conclusions 38

III. MASS TRANSPORT OF AMINES IN MIXED-BED ION EXCHANGE 39

- Introduction 39
- Aqueous Amine Solution Equilibrium 43
- Amine-Exchange Model Development 48
- Model Validation 49
- Simulations of Industrial Operation 69
- Conclusions 93

IV. LIQUID PHASE MASS-TRANSFER COEFFICIENT IN MIXED-BED ION EXCHANGE 94

- Introduction 94
- Literature 96
- Comparison of Literature Mass-Transfer Correlations 101
- Mass Transfer Experiments with Ion-Exchange Resins 107
- Comparison of Experimental Ion-Exchange Mass-Transfer Coefficients with Correlations 113
- Conclusions 119

Chapter Page

V. EFFECT OF MASS-TRANSFER COEFFICIENT ON BINARY EXCHANGE OF SODIUM CHLORIDE IN MIXED-BED ION EXCHANGE 123

Introduction 123
Diffusion of Sodium Chloride in Water at Low Concentrations 126
Computation of Ion-Exchange Rate in a Packed Bed 131
Liquid-Phase Mass-Transfer Coefficient in a Mixed-Bed Exchanging Sodium Chloride 133
Effluent Concentration History of Sodium and Chloride from a Mixed Bed 148
Conclusions 169

VI. CONCLUSIONS AND RECOMMENDATIONS 171

BIBLIOGRAPHY 175

APPENDIXES 185

APPENDIX A — NUMERICAL SOLUTION OF THE MBIE COLUMN MODEL 186

APPENDIX B — CALCULATED MASS-TRANSFER COEFFICIENT COMPARISONS 193

APPENDIX C — CONCENTRATION EFFECTS ON MULTI-COMPONENT DIFFUSION OF NaCl IN WATER 195

APPENDIX D — COMPUTER CODE LISTING 199

LIST OF TABLES

Table Page

Chapter III

I. Amines Used in pH Control of Boiler Feed Water 43

II. Amine Properties used in MBIE Modeling 50

III. Selectivity and Diffusivity of Sodium and Chloride Ions 50

IV. Operating Conditions at Oldbury 51

V. Experimental Conditions of Miller and Asay (1991) 62

VI. Resin Selectivity Data 73

VII. 10% Breakthrough Times for Different Amines using Macro Cation-Exchange Resins (EPRI TR-104299) 83

Chapter IV

I. Literature Mass-Transfer Correlations for Calculating Sherwood Number 102

Chapter V

I. Diffusion Coefficients from Conductance Data (aqueous infinite value; Horvath, 1985), at 25°C 128

II. Estimated Diffusion Coefficients of NaCl in Water 129

III. Estimated Main-Term Diffusion Coefficients Presented as a Ratio of Single-Ion Diffusivity 130

IV. Predicted Mass-Transfer Coefficient Comparisons with Mixed Bed Sodium Data (inlet: 2.8×10^{-5}; Lee, 1994) 134

V. Predicted Mass-Transfer Coefficient Comparisons with Mixed Bed Sodium Data (inlet: 6.9×10^{-5}; Lee, 1994) 135

Table Page

VI. Predicted Mass-Transfer Coefficient Comparisons with Mixed Bed Chloride Data (inlet: 2.8×10^{-5}; Lee, 1994) 136

VII. Predicted Mass-Transfer Coefficient Comparisons with Mixed Bed Chloride Data (inlet: 6.9×10^{-5}; Lee, 1994) 137

VIII. Predicted Mass-Transfer Coefficient Comparisons with Mixed Bed Chloride Data (Harries, 1984) 138

IX. Predicted Mass-Transfer Coefficient Comparisons with Mono Bed Sodium Data (inlet: 2.8×10^{-5}; Lee, 1994) 139

X. Predicted Mass-Transfer Coefficient Comparisons with Mono Bed Sodium Data (inlet: 6.9×10^{-5}; Lee, 1994) 140

XI. Predicted Mass-Transfer Coefficient Comparisons with Mono Bed Chloride Data (inlet: 2.8×10^{-5}; Lee, 1994) 141

XII. Predicted Mass-Transfer Coefficient Comparisons with Mono Bed Chloride Data (inlet: 6.9×10^{-5}; Lee, 1994) 142

XIII. Input Data for Simulations 149

XIV. Mass-Transfer Coefficients Predicted from Correlations 166

Appendix B

I. Experimental Properties 193

II. Mass-Transfer Coefficient Comparison 194

LIST OF FIGURES

Figure Page

Chapter I

1. Schematic representation of a mixed-bed ion-exchange column 6

2. Skeletal diagram of the boiler-water cycle 9

Chapter II

1. Schematic of fixed bed with different exchange zones 17

2. Schematic of the film model 30

Chapter III

1. Effect of amine concentration and base strength (Table I) on ionization....... 45

2. Effect of hydroxide concentration on dissociation of morpholine 46

3. Comparison of model predictions with Oldbury plant data 53

4. Morpholine profile in the bed as exchange progresses 54

5. Effect of solid phase resistance on morhopline breakthrough 56

6. Comparison of predicted sodium throw with Nuclear Electric (UK) data...... 58

7. Predicted sodium effluent profile compared with Nuclear Electric (UK) data 59

8. Comparison of predicted sodium effluent profile with Nuclear Electric (UK) data 60

9. Flow rate variation to the mixed beds (data from Nuclear Electric, UK) 61

10. Predicted breakthrough profile compared with experimental data................ 63

11. Comparison of predicted profile with experiment data for gel-type cation-exchange resin 64

12. Predicted ETA breakthrough compared with experimental data 66

Figure Page

13. Comparison of predicted sodium profile with experimental data 67

14. Predicted sodium throw compared with experimental data 68

15. Predicted sodium profile with different flow rates at day 6.6 of operation ... 70

16. Sodium effluent transition at different times for step change from half to full flow (800 gpm) 72

17. Effluent sodium concentration at different regeneration efficiencies for Ambersep 252 74

18. Effluent sodium concentration at different regeneration efficiencies for Amberlite IR120 76

19. Effect of cation-to-anion resin volume ratio on predicted sodium and chloride effluent concentration 77

20. Bed profile of morpholine loading on the resin... 79

21. Predicted pH profile in the bed with different cation-to-anion resin volume ratios.. 80

22. Predicted amine breakthrough curves at operating pH of 9.65...................... 82

23. Predicted sodium effluent profile using different amines.............................. 84

24. Predicted chloride effluent profile using different amines............................. 85

25. Effluent sodium concentration for Ambersep 252 with a condenser leak...... 87

26. Predicted sodium profiles for a 10 ppb condenser leak on day 10 89

27. Predicted sodium profile for a leak scenario with different amines............... 90

28. Predicted chloride profile for a simulated leak scenario using different amines.. 91

Chapter IV

1. Comparison of literature mass-transfer correlations for predicting the Sherwood number.. 105

2. Mass transfer data for univalent ions 112

Figure Page

3. Mass transfer data for divalent ions 114

4. Mass transfer data comparison of univalent and divalent ions 115

5. Comparison of experimental data of Harries (1984) with literature mass-transfer correlations 116

6. Comparison of Lee's (1994) chloride mass transfer data with literature mass-transfer correlations 117

7. Comparison of experimental data with mass-transfer correlation of Dwivedi and Upadhyay (1977) correlation 118

8. Predicted J-factor compared with experimental mass transfer data 120

9. Comparison of J-factor predictions with experimental mass transfer data 121

Chapter V

1. Comparison of sodium effluent profile with different mass-transfer coefficients 150

2. Effect of mass-transfer coefficient on chloride effluent profile 151

3. Comparison of sodium effluent profile with different mass-transfer coefficients 153

4. Liquid phase sodium concentration profiles with different mass-transfer coefficients 155

5. Liquid phase chloride profile with different mass-transfer coefficients 156

6. Resin-phase loading profile of sodium with different mass-transfer coefficients 157

7. Resin-phase loading profile of chloride with different mass-transfer coefficients 158

8. Effect of mass-transfer coefficient on sodium effluent profile 159

9. Effect of mass-transfer coefficient on chloride effluent profile 160

10. Effluent concentration profile using Carberry (1960) correlation 162

Figure Page

11. Chloride effluent profile using Carberry (1960) correlation for calculating the mass-transfer coefficient 163

12. Predicted effluent profile using different mass-transfer correlations 164

13. Chloride effluent profile using different mass-transfer coefficient correlations 165

14. Effect of exponent used in the mass transfer correction on predicted effluent profile 167

15. Comparison of predicted effluent profile with different exponents in the mass-transfer correction 168

Appendix A

1. Grid structure for the numerical calculation 191

NOMENCLATURE

a_s	specific surface area	(cm^2/cm^3)
C	fluid-phase concentration	(meq/ml)
C_T	total concentration of weak electrolyte	(meq/ml)
d_p	particle diameter	(cm)
D	diffusion coefficient	(cm^2/s)
F	Faraday's constant	(C/mol)
j	ionic flux	(meq/(cm^2)(s))
K_B^A	selectivity coefficient	
K_b	base dissociation constant	
K_f	film mass-transfer coefficient	(cm/s)
K_w	water ionization constant	
L	bed depth	(cm)
q	resin-phase concentration	(meq/ml)
Q	resin capacity	(meq/ml)
R	Universal gas constant	
R_i	Correction factor	
T	temperature	
t	time	
u	superficial velocity	(cm/s)
V_M	molar volume at normal boiling point	cm^3/mole

X	liquid-phase fractional concentration	
Y	resin-phase fractional concentration	
z	bed depth	(cm)
Z_i	valence of ion 'i'	

Dimensionless numbers

J	J-factor for mass transfer	
Sh	Sherwood Number	$\frac{K_f d_p}{D}$
Re	Reynolds Number	$\frac{d_p u \rho}{\mu \varepsilon}$
Sc	Schmidt Number	$\frac{\mu}{\rho D}$
Pe	Peclet Number	(Re)(Sc)

Greek Symbols

δ	film thickness	(cm)
ε	bed void fraction	
ϕ	electric potential	
Φ	resin volume fraction	
λ	equivalent conductance	$cm^2/(mol)(mho))$
μ	viscosity	g/(cm(s))
ρ	fluid density	(g/cm^3)
τ	dimensionless time-distance variable	
ξ	dimensionless distance variable	

Subscripts

c	cation
a	anion
H	hydrogen
O	hydroxide
Na	sodium
Cl	chloride
p	pseudo coion
Mol	molecular form of ion 'i'

Superscripts

i	ion 'i'
*	interfacial concentration
o	bulk-phase concentration

CHAPTER I

INTRODUCTION

Earlier civilizations recognized the need for pure and clean water. The earliest recorded need for pure water is from the inscriptions found in India and Egypt (Baker, 1948). Indian medical lore described the purification of water by boiling, filtration, and addition of substances. Egyptian tombs have recorded water purification ceremonies on the walls of tombs. The Greek and Roman civilizations also advocated treated water for consumption. Hippocrates, the father of medicine, discussed the relationship of health and quality of water. Biblical lore also records an instance of water purification using a tree (Baker, 1948; Zecchini, 1990).

In the early part of the seventeenth century, in Europe, water was purified by filtration and boiling. Charcoal for filtration and odor removal became prevalent in the later half of the eighteenth century. The nineteenth century saw the advent of slow sand filtration for municipal drinking water treatment, and later electrolysis was discovered as a water purification method.

In the early twentieth century, chlorine was used as a disinfectant for water in conjunction with slow sand filtration for potable water. Albeit water softening was discovered in the eighteenth century, application as a water treatment process started only in the early part of the twentieth century. Slow sand filtration, chlorination, and water softening are still in vogue as water treatment methods.

According to Baker (1948), the earliest known industrial water purification plant was built in France. Industrial growth in the twentieth century, in different sectors — process, power, pharmaceutical, food, and microelectronics industries — has spurred the need for a tremendous volume of process water.

The effect of water quality on a process was very well understood as industrialization progressed; for example, in the early twentieth century, commercial ice manufacturers in the United States recognized the effect of water constituents on the quality of manufactured ice (Handbook of Ice, 1927). In the last quarter of the twentieth century, industrial water quality standards have become very stringent; the impurity level guidelines for process water is industry specific. The power and microelectronics industry are noteworthy for their requirement of large volumes of ultrapure water.

Water with dissolved impurity levels of less than one part-per-billion (ppb) is usually termed ultrapure water. Impurities in water may be of natural origin or, in some cases, anthropogenic. Production of ultrapure water involves the removal of particulate, inorganic, organic, dissolved, colloidal, and microbial impurities. Process operations like ion exchange, electrodialysis, and membrane techniques are used to produce ultrapure water from pre-treated water. Water sterilization, to divest process water of microbial impurity, also forms a treatment step in the production of ultrapure water.

The power industry is concerned about erosion-corrosion problems within the steam/water circuit of boilers. Ionic impurities in water corrode materials of construction of key components in the steam/water circuit. Corrosion and corrosion by-products affect the performance of power generating stations. Power outage and destruction of components results in economic losses. Nuclear power stations are concerned about ionic and particulate nuclide — radioactive precipitates of materials of construction — buildup. This increases the amount of radioactive wastes and their associated disposal costs. Hence ultrapure water is used in power generation.

In the final decade of the twentieth century, the semiconductor industry has risen to be one of the most technologically advanced. The semiconductor industry uses large quantitites of ultrapure water to rinse silicon wafers used in microchip manufacture. The increased degree of semiconductor device integration has led to very stringent water quality requirements. The rinse water needs to be of high purity, since contaminant deposition on wafer surfaces (being cleaned) will lead to component failure.

New water treatment methods, and fundamental scientific analysis of the previously used water treatment methods, have improved human capability to treat water. Novel methods using membrane technology, activated carbon, ion-exchange, electrodeionization, oxidation, ozonation, and new coagulants have tremendously increased the capability to remove impurities from water. Advanced impurity detection methods, analytical capability improvements, and bio-hazard evaluation of contaminants will force the search for new water treatment methods or water treatment protocols.

Current industrial practice for manufacturing ultrapure water is to use ion-exchange and/or reverse osmosis. Hence theoretical studies are required to better understand and improve these systems.

Ion Exchange

Ion-exchange units are used for manufacturing ultrapure water in large volumes. Ion exchange is a stoichiometric reaction; ions in the bulk liquid are replaced by an equivalent amount of ions from the ion-exchange resin. Ion-exchange units are usually operated as fixed beds. Ion-exchange beds consisting of cation and anion exchange resins are called mixed beds. Ion-exchange beds that contain either cation or anion exchange resins only are called mono beds.

The ion-exchange resin bead, the solid phase in packed-bed operation, is spherical in shape and contains ionogenic groups in a polymer network. The polymeric matrix contains polystyrene crosslinked with divinyl benzene. Crosslinking enhances the rigidity of the ion-exchange resin. An ion-exchange resin is classified as either a cation or anion exchanger depending on the charge of the exchanged species. A cation-exchange resin exchanges positively charged species, while an anion-exchange resin exchanges negatively charged species.

Ion-exchange behavior is controlled by resin chemical composition and the functional groups. Ion-exchange resins are classified as either strong or weak depending on the functional groups. Strong resins exhibit strong electrolyte characteristics, the groups are dissociated at all pH levels. But exchange characteristic of the weak group resins is pH dependent; this is consistent with weak electrolyte behavior.

Strong acid cation exchangers have sulfonic acid groups, while carboxylic acid groups are the functionality of weak acid exchangers. Strong base anion exchangers are usually based on quaternary ammonium groups, and weak base anion exchangers possess either primary, secondary, or tertiary amine groups, or a mixture of groups. Strong base anion exchangers are of two classes: 1) Type I, having a $N^+(CH_3)_3$ group as the active site, and 2) Type II with a $N^+(CH_3)_2(CH_2CH_2OH)$ group as the active site. Type II anionic resins have lower basicity and are easy to regenerate, but they are less chemically stable than Type I anionic resins. Resins with other functional groups are also manufactured for specific applications (example: chelating resins).

Major use of ion-exchange is to produce ultrapure water, however, there are other interesting applications of this technology. Some other applications using ion-exchange processes are:

1. Separations in analytical chemistry; for example, chromatography
2. Recovery of heavy metals from wastewater, sewage, and process waste streams (example: electroplating rinse water, Bolto and Pawlowski (1987))
3. Recovery of fission products from waste streams generated by reprocessing of nuclear fuels (Bibler, 1990)
4. Applications in hydrometallurgy (Streat, 1988)
5. Removal of nitrate from drinking water (Croll, 1993)
6. Food industry (decolorizing cane sugar solution, protein recovery and purification) (Streat, 1988; Miers, 1995)
7. Ion exchangers as catalysts (Helfferich, 1988)
8. Recovery of constituents from process streams; for example, recovery of ammonia from condensate in nitrogen fertilizer industry (Bolto and Pawlowski, 1987)
9. Treating process water for the manufacture of alcohol (Miers, 1995)
10. Artificial plant nutrient media (Soldatov, 1988)

Mixed-Bed Ion-Exchange (MBIE) Technology

Mixed-bed ion-exchange technology was conceived by Kunin and McGarvey (1951). Mixed-bed deionization is an economical and convenient method of producing ultrapure water. A mixed-bed ion-exchange column combines cation and anion exchange resins. Figure 1 presents a schematic diagram of a mixed-bed ion-exchange column. In particular, water with the lowest impurity level can be produced using the hydrogen-hydroxide (HOH) mode of operation. In this mode, the cation-exchange resin has hydrogen as the exchangeable ion, and the anion-exchange resin has hydroxide ions.

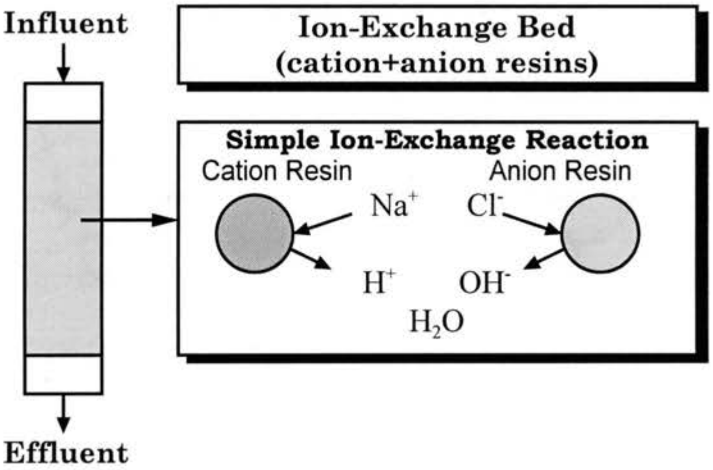
Influent
Ion-Exchange Bed (cation+anion resins)
Simple Ion-Exchange Reaction
Cation Resin
Anion Resin
Na^+
Cl^-
H^+
OH^-
H_2O
Effluent

Figure 1. Schematic representation of a mixed-bed ion-exchange column

The cation resin exchanges hydrogen ions for other positive ions in water, and the anion resin exchanges hydroxide ions for negative ions. The liberated hydrogen and hydroxide ions combine to form water. The reactions can be represented by:

$$R\text{-}H^+ + A^+ \Leftrightarrow R\text{-}A^+ + H^+ \quad \text{(cation exchange)}$$
$$R\text{-}OH^- + B^- \Leftrightarrow R\text{-}B^- + OH^- \quad \text{(anion exchange)}$$

$$H^+ + OH^- \Leftrightarrow H_2O \qquad \text{(water neutralization)}$$

where A^+ and B^- are the exchangeable ions in the bulk phase. Water neutralization decreases the amount of hydrogen and hydroxide ions in the bulk phase and minimizes reverse exchange. Thus reaction equilibria for exchange of other cations and anions in the column is favored. This mode of operating a mixed bed is called the service cycle.

The mixed bed is 'exhausted' when the concentration of a specific ion in the effluent exceeds a pre-determined threshold. The mixed bed is removed from service and 'rejuvenated.' This constitutes the regeneration cycle of a mixed bed. The cation and anion exchange resins are separated by backwashing, and are transferred to different process vessels. The ion-exchange resins are then regenerated using concentrated regenerant solutions specified by the ion-exchange resin manufacturer. After regeneration, the ion-exchange resins are transferred back to the service vessel and mixed using air; now the mixed bed is ready for service cycle operation.

Use of Mixed-Bed Ion-Exchange (MBIE) in Condenstate Polishing

The main goal of treating process water in the power industry is to reduce contaminants that corrode or assist in corrosion. Corrosion phenomenon is intimately associated with the ionic constituents and dissolved gas composition of water (Water Quality and Treatment, 1971). Corrosion is an electrochemical phenomenon requiring a cathode, anode and a connecting circuit (Snoeyink and Jenkins, 1980). In this case, an electrochemical cell will be formed by the metallic surfaces and water. The cathode and anode are areas on the metallic surface. Ions dissolved in water conduct electricity, thereby completing the circuit.

Absence of one of the components of the electrochemical corrosion cell — either the cathode, anode, or the circuit — will result in no corrosion. The corrosion cell component that can be controlled, in a power generating station, is the circuit. Removing ionic contaminants will decrease the current carrying capacity of the process water and minimize corrosion.

Also, localized accumulation of ions near metal surfaces leads to an acidic environment, aggravating any existing corrosive situation. Furthermore, presence of dissolved oxygen (in water) enhances oxidative reactions of the metal and results in precipitation of insoluble metal hydroxides (rust in the case of iron).

Hence the use of ion-exchange units in abating corrosion is two-fold: removal of ionic impurity and decreasing the current carrying capacity of water. Pure water, free from ionic contamination, has very low conductivity. Theoretically, pure water has a conductivity of 0.055 μS/cm (at 25 °C) — due to water dissociation.

Figure 2 presents a skeletal diagram of the boiler-water cycle; the main aim of the sketch is to descibe the relative place of the condensate polisher in the cycle. Mixed-bed ion-exchange units are used in treating make-up water, and in polishing the condensate returned from the turbines; they are also used to guard against condenser tube leaks. Condenser tube leaks can lead to ingress of impurities from the cooling water to the process water. Hence mixed-bed units are used to remove ionic impurity from process water and 'polish' the condensate. Mixed-bed units also act as filters when particulates (crud) and colloids (example: SiO_2) are present. In nuclear power plants MBIE units are also used for removing radionuclides in the ionic and particulate form (Lin, 1975).

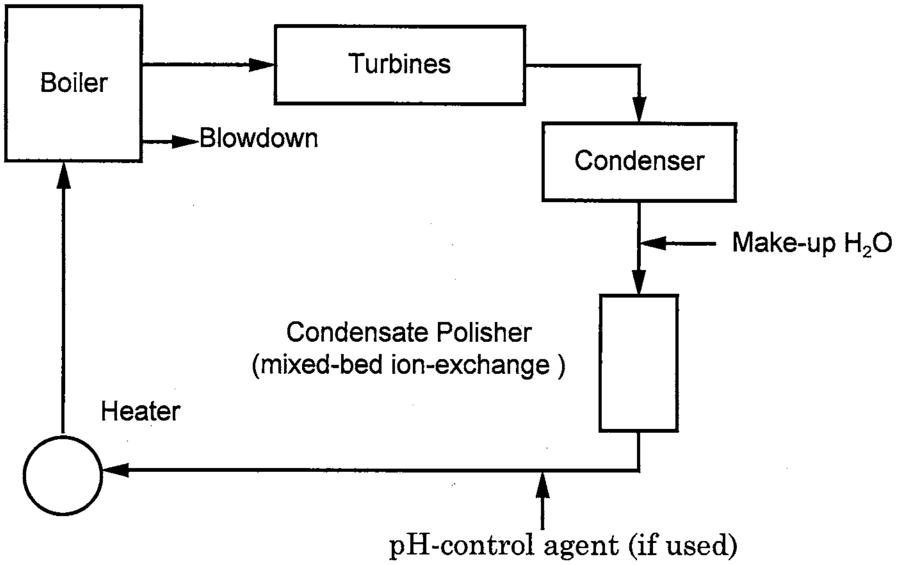
Boiler
Turbines
Blowdown
Condenser
Make-up H_2O
Condensate Polisher (mixed-bed ion-exchange)
Heater
pH-control agent (if used)

Figure 2. Skeletal diagram of the boiler-water cycle

Guidelines for ionic contaminant levels in boiler-feed water are set by the Electrical Power Research Institute (EPRI). To combat corrosion of materials of construction, EPRI recommends increasing the pH of boiler-feed water. To raise the pH of water, the power industry uses amines. The addition of amine to boiler-feed water leads to the amine cycle operation of MBIE units. Amine cycle operation of MBIE units can take one of two forms: cation-exchange resin in hydrogen form with amine in the bulk liquid, or cation-exchange resin in the amine form; industrially both forms of operation are prevalent. In the absence of amines, the MBIE units are operated in the hydrogen-hydroxide (HOH) form.

Mixed-Bed Ion-Exchange Modeling

Equilibrium principles or kinetics (rate models) govern the separation processes. The governing principles in conjunction with material and energy balances are used to model the separation process. Many industrial packed-bed operations are controlled by kinetics of the system, such a system is mass-transfer limited (Fogler, 1992). There are two regions of limitations: mass-transfer (diffusion), and reaction limited regimes. The system response to change in temperature and flow conditions will yield clues regarding the regimes of limitation.

Mixed-bed ion-exchange operations are controlled by system kinetics. The influent impurity concentration and resin characteristic determine the mass-transfer limitation. The time taken by the ions to travel from the bulk fluid to the resin exchange site becomes important. In MBIE, mass-transfer limitation can be further classified as being either diffusion or reaction controlled. Generally, mixed-bed units operating with strong (acidic or basic) resins and low influent impurity are diffusion limited. If weak (acidic or basic) resins are used, then reaction-limited processes need to be considere. Use of chelating resins may lead to the reaction limited regime.

In the diffusion limited regime, either film or particle diffusion is the rate-controlling step. Film-diffusion control applies when the ionic mobility through an assumed stagnant liquid film around the ion-exchange resin bead becomes the limiting factor. If the slowest step is the ionic movement within the resin bead, then particle diffusion is the rate controlling factor. A combination of the two factors may also determine the rate.

In this work, MBIE units operating with strong (acidic or basic) resins and low influent impurity concentrations (less than 0.0001 N) are assumed. In such cases, film diffusion is the rate limiting step; this has been experimentally verified by Frisch and Kunin (1960) and Helfferich (1962).

After establishing the rate-limiting condition, physical reality needs to be translated into a mathematical form. The first step is to describe ionic flux in the bulk liquid, and later the transport of ions into the ion-exchange resin for stoichiometric exchange. These equations need to be coupled with the model describing ion movement in the column due to fluid flow, to obtain a complete description of the process.

The presence of charged species — ions in this case — indicates that electrostatic forces, including other forces, are influencing mass transport. The Nernst-Planck equation is one method that can be used for computing ionic flux. The Nernst-Planck equation accounts for the chemical and electrical forces acting on an ion. The electrical force includes two parts: 1) applied external electrical field, and 2) electric-potential generated due to differing ionic mobilities. In MBIE, no external electric fields are applied, the electrical force represents only the electrostatic interaction of the ions.

The ionic flux equations (developed using the Nernst-Planck equation) are coupled with a fluid flow model. The aim is to connect the diffusion coefficients and hydrodynamics of the system. Since the system being studied here is heterogeneous, a lumped-parameter model — like the mass-transfer coefficient — is used to link diffusivity and hydrodynamics; film theory is applied for modeling this system.

According to film theory, there exists a stagnant fluid layer near the solid-fluid interface (Cussler, 1984). The fluid inside the film is stagnant and the outside fluid constitutes a well-mixed core. Mass transfer by diffusion, into the solid, is assumed to occur across the hypothetical film. The film model shows, in simple terms, the resistance encountered for mass transfer across the solid-fluid interface.

The total flux across the stagnant film is calculated by solving the Nernst-Planck equation for the ions. At ultra-low influent impurity concentrations, water dissociation reaction becomes important. Haub and Foutch (1986 a, b) incorporated the dissociation of water in computing a flux solution using the Nernst-Planck equation. The solution yields an effective-diffusion coefficient. The effective diffusion coefficient is used in a mass-transfer correlation (connects the hydrodynamics) to obtain the total ionic flux. This expression is combined with a differential column material balance equation to completely describe MBIE column operation.

Objectives

Traditionally, a full-scale separation process is designed based on information gained from experimental and pilot-plant work. This design approach is system specific, and evaluating the effect of system responses to changes in variables is very expensive. An easier approach, compared to experimental and pilot plant testing, is to build mathematical models of the separation process. Validated models can then be used to study the effect of different process parameters on system responses. Sensitivity of the system to perturbations on the different variables can also be tested. This is a cost-effective approach to system design.

System process models are developed from first principles, or by regressing experimental data to build correlations. First principle models are more rigorous and suitable for developing general models. Empirical correlations are system specific, and model extension beyond the range of data studied is uncertain. To obtain a working process model the modeling approaches are often combined. The objectives of this dissertation are:

1) To develop a mass transport model for weak electrolyte exchange.

The first objective of this dissertation is to model weak-electrolyte mass transport in MBIE. The goal is to develop a predictive tool for MBIE operations with a weak electrolyte in the influent. Weak electrolytes in aqueous solution contain an equilibrium mixture of dissociated and undissociated forms of the weak electrolyte. A model considering mass transport of both dissociated (ionic) and undissociated form (nonionic) of the weak electrolyte is presented. Also, the model considers exchange of sodium and chloride in the mixed bed. Only univalent ion-exchange is considered in this work. Chapter II presents the weak electrolye exchange model.

The weak electrolyte mass transport model is used to predict the effluent concentration history of amines from a MBIE column. The model parameters are all measured variables. The mathematical model is constructed to work with any amine, provided the physiochemical properties of the amine are known. The model predictions are compared with real-plant and experimental data. Chapter III presents the results of this comparison.

Chapter III also presents model use as a tool for testing hypothetical scenarios. This is one of the incentives for working on a process model. The process model — a simulation tool — can be used to test the responses of a mixed-bed ion-exchange column to change in system variables. Analysis of process parametric sensistivity and potential operating condition changes are presented. Perturbations on the influent concentration (condenser leak situations) are simulated to study impurity removal efficiency of the mixed beds.

2) To study film mass-transfer kinetics for improving effluent profile predictions.

To model mass transfer across the resin-fluid interface, a lumped parameter approach is used. Complexities of the system hydrodynamics and diffusive character are lumped into a MTC. MTCs are calculated using empirical correlations. Suitability of literature correlations for MBIE, at low solute concentrations, has not been studied. Hence the second objective of this dissertation is to study liquid-phase mass-transfer coefficients (MTC) for improving predictions of MBIE kinetics. In this work, available literature mass-transfer correlations are compared with existing ion-exchange mass transfer data of sodium chloride exchange in a mixed bed. This comparison is presented in Chapter IV.

Most packed bed mass-transfer correlations are obtained by regressing experimental data that excludes ion-exchange. The unsuitability of ion-exchange mass transfer data, for building empirical correlations, is due to complex analysis of the diffusion process in an ion-exchange system. Theoretical analysis of diffusion in the system — sodium-chloride-water — is presented; using this analysis, differences in the MTC of sodium chloride exchange in a mixed bed are examined. Chapter V presents this analysis.

CHAPTER II

WEAK ELECTROLYTE MASS TRANSPORT MODEL FOR MBIE

Introduction

Mathematical models of separation processes can be constructed either from first principles or functional relationships obtained empirically. Modeling a separation process by applying first principles is usually work intensive. The starting point for first-principles modeling is to recognize the governing equations of the system, and later solving these equations to obtain meaningful solutions. The latter approach — empirical method — is used when models serve the limited purpose of describing a specific separation scenario. Generalizing and extending these models to other situations should be done by applying engineering acumen. In most cases, additional experimental data are required to obtain a better model. Often, the two modeling approaches are used to describe different aspects of the system and combined to obtain a working model.

Mathematical modeling is undertaken to facilitate the design of separation processes. A tested system model can be used for evaluating different operating conditions, and for simulating a variety of hypothetical scenarios. First principle models make use of system properties that are easily measured. These properties are usually independent of the collective characteristics of the system. Hence building a mathematical model from first principles is attractive. These models are used for a priori prediction of certain system characteristics or responses to change in system properties.

The design of a MBIE unit involves the characterization of the effluent concentration history. The governing principles defining the MBIE system involves resin equilibrium and rate-controlling factors. The effluent concentration history, or the breakthrough curve, is the result of a specific combination of the fixed-bed and ion-exchange resin properties. The effluent concentration history depends on the physical and chemical properties of the ion-exchange resin and fluid, rate-controlling mechanisms, and hydrodynamics of the system. The inter-connective relationship between these factors is complex, and the relative effects are particular to an application.

The objective of this work is to develop a model capable of predicting effluent concentration history for MBIE operations using amines. Amines are weak electrolytes in aqueous solution. They form an equilibrium mixture of dissociated amine (ions), undissociated amine (molecular form), and hydroxyl ions. Development of a MBIE column model for weak electrolyte exchange is presented here.

Modeling MBIE

A fixed-bed column is the most commonly used configuration for operating MBIE units. The solid phase, ion-exchange resin in MBIE, is contacted by the moving fluid phase in the packed column. The fluid phase is usually water. Design of a MBIE unit usually involves characterizing the breakthrough curve of the different components in the influent. This determines impurity removal capability of the unit and process efficiency of a particular MBIE configuration.

The dynamic condition of the column can be visualized in terms of zones that move through the bed. The ion concentration changes as the zones move through the bed, this generates the breakthrough curve. Three zones can be distinguished for studying the dynamics of an ion-exchange column (Figure 1).

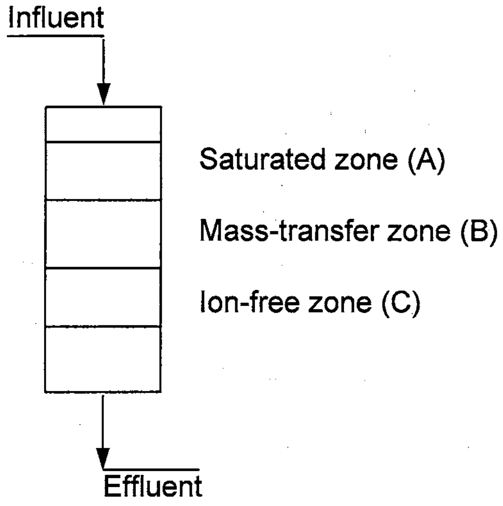

Figure 1. Schematic of fixed bed with different exchange zones

The zone near the feed inlet, zone A, is the saturated zone. The feed solution is in equilibrium with the loaded resin. The resin cannot achieve further ion loading in this zone if the feed conditions remain constant. Changes in the feed condition will result in either increasing or decreasing the resin loading of ions depending on the attainment of new equilibrium.

Zone B is the active exchange zone. The resin is not in equilibrium with the feed solution. Ions from the feed are being exchanged for ions from the resin in this zone. In the bottom section, zone C, ions in the feed have been reduced to very low levels; ionic concentration depends on the resin condition — new or regenerated. Again, in this section, the feed solution is in equilibrium with the resin. Higher resin-phase concentrations will result in ions leaching out of the resin into the bulk phase. Under these conditions, ion concentrations leaving the column are referred to as equilibrium leakage.

The first phase of developing a MBIE model involves description of mass transport. Ionic mass transport can be described in terms of an equilibrium approach or by a rate mechanism (kinetics). A simplistic view of the equilibrium phenomena is that the ions rearrange between the two phases given sufficient time. The rate mechanism is complex and involves the time taken by the ions to reach the resin exchange sites. Rate mechanisms are the most appropriate modeling methodologies when there is less contact time between the phases.

To model a column using a rate mechanism, the first step is to determine the rate-controlling factor. The possibilities being: 1) Film (liquid-film) diffusion control, 2) Particle-diffusion control, 3) Reaction-rate control, and 4) Combination of some of the previous steps. The slowest step limits mass transfer.

Film-diffusion control is when ionic mobility through an assumed stagnant film adhering to the resin bead controls mass transfer. Film-diffusion control theory gives simple physical insight into the mass-transfer resistance that might exist at a solid-fluid interface. This simple model suggests that a liquid-film adheres to the surface of the solid, and there is no convection in the film (Cussler, 1984). If the movement within the resin bead is slow, then particle diffusion is the rate-controlling mechanism. Helfferich's (1962) criteria can be used to determine whether a process is controlled by film diffusion or particle-diffusion. The criteria are based on resin properties and bulk-phase ion concentration. Helfferich (1990) discussed the application of different rate models in ion-exchange kinetics.

The rate-controlling step represents the resistance to mass transfer and models the physical process, but still a description is required for the ionic movement. This movement is described by diffusion which is a random process at the micro level (Bird et al., 1960; Cussler, 1984), ultimately the flux of the species describes mass transport at the macro level.

The first step for modeling a mass-transfer process is to describe chemical species flux. The chemical species flux depends on the driving forces — concentration, electric potential, pressure, and thermal gradients — that determine species movement. The flux expressions are applied to the physical process to obtain the total solute flux and concentration profiles. Modeling strong and weak electrolyte flux, as they are encountered in MBIE operations, is of interest in this work.

Modeling the system requires description of mass transfer of the chemical species, material balances, and hydrodynamics of the system. These equations form the set of governing equations. In MBIE, mass transfer to a single resin bead is solved first using a solute flux expression with the physical process model. This solution is then used with a description of the hydrodynamics of the fixed bed and a solute continuity equation for the mobile phase (fluid). This completes mathematical description of the MBIE column model. Mathematical models can then be used to design and study process parameter sensitivity of MBIE columns.

MBIE Modeling Literature

Extensive literature review of mixed-bed ion-exchange modeling has been carried out by Haub (1984), Yoon (1990), and Zecchini (1990). Bulusu (1994) has presented multicomponent mixed-bed ion-exchange modeling literature. These literature studies have focused on strong electrolyte exchange, weak electrolyte exchange has received relatively little attention. In this work, weak electrolyte ion exchange literature has been reviewed.

A weak electrolyte solution contains an equilibrium mixture of dissociated (ionic) and undissociated (molecular) forms of the electrolyte, and protons or hydroxyl ions liberated by equilibrium reaction with the solvent. Weak acid or base form of ion-exchangers have been used for separation of bases and acids from mixtures (Samuelson, 1963); weak electrolyte exchange has been studied in this context.

The sorption of weak electrolytes, specifically the undissociated part, has been treated as non-electrolyte or nonionic adsorption (Helfferich, 1962; Samuelson, 1963). The adsorption has been ascribed to van der Waals' interaction between the resin matrix and the undissociated part of the weak electrolyte. Dissociation of a weak electrolyte is pH dependent and so is the uptake of weak electrolyte by ion-exchange resins. Weak electrolytes were sorbed by ion-exchange resins in excess of their ion-exchange capacities (Helfferich, 1962).

Ion-exchange resin ability to adsorb nonionic or non-electrolyte species is used for separation processes. Ion-exclusion principle is applied for separation of a mixture of ionic and nonionic solutes using ion-exchange resins (Helfferich, 1962;

Vassiliou and Dranoff, 1962; Martinola, 1980). Ion exclusion is based on the Donnan effect; the strong electrolyte is excluded from the resin, whereas the nonionic solute is not excluded. Hence in ion exclusion, the nonionic or non-electrolyte is preferentially sorbed. The non-electrolyte is strongly sorbed and retained by the ion-exchange resin, the solute can later be recovered by elution.

Wagner and Dranoff (1967) were the first to model mass transfer of a weak electrolyte into a strong acid resin. Liquid-film diffusion controlled transport of ammonia was studied. They considered transport of both dissociated and undissociated form of the base. In their model they assumed that the resin-surface concentration of undissociated ammonia and ammonium ion was negligible, resulting in an analytical solution for the concentration profile. The model was validated with limited experimental data.

Helfferich and Bennett (1984) studied the effect of association-dissociation reactions on pH effects in ion-exchange columns. Sodium acetate-acetic acid and sodium carbonate-bicarbonate systems were studied. Co-ions and nonionic species were excluded from the resin interior in their equilibrium model. This assumption had no significant impact on the predicted results.

Ion-exchange chromatography has been used for component separation from a mixture based on: charges carried by the species, ionic size, differences in acid and base strength, and sorption of non-electrolytes. One of the applications in ion-exchange chromatography where non-electrolyte sorption needs to be considered is in amino acid separations (Helfferich, 1990). In equilibrium solution, amino acid dissociation is influenced by pH. The effective charge on the dissociated form varies in sign and magnitude with pH of the solution. Neutral species in the equilibrium mixture are adsorbed by the ion-exchange resin.

Hubner and Kadlec (1978), Helfferich and Hwang (1985), and Bhandari et al. (1992) have studied mass transfer using weak base resins. Bhandari et al. (1992) conducted batch experiments with formic acid and monochloroacetic acid. They concluded that transport of both dissociated and undissociated form of weak electrolytes is important. They modeled the system based on double layer theory and pore equilibrium. Pore diffusivity was obtained by regressing their experimental data. Film mass-transfer resistance was found to be negligible.

Dobbs et al. (1975) and Bolden et al. (1989) studied amine removal from solution using a copper loaded cation-exchange resin. Bolden et al. (1989) used a shrinking-core model to fit their experimental data for removal of amines. Different forms of amine transport were not considered. Predicted breakthrough curves were matched with experimental data.

Amine removal from wastewater using strong cation-exchange resin has also been studied by Yoshida et al. (1987, 1990). Yoshida and Kataoka (1987) found that amines with more than six carbon atoms adsorbed onto a strong cation-exchange resin by a multilayer mechanism. Adsorption of ammonia and amines on a strong cation-exchange resin in the hydrogen form, and elution with aqueous caustic solution were modeled. According to their model, the undissociated amine was immobilized by the resin by a neutralization reaction. The amount of amine (with less than six carbon atoms) adsorbed was found to be close to the exchange capacity of the resin. Hence they concluded that reaction with hydrogen ions in the exchanger was responsible for uptake of the undissociated amine, and that physical adsorption was absent. The breakthrough curve was modeled assuming that a combination of external and internal resistances were important. The predicted breakthrough curve was matched with their experimental data.

Lou (1993) modeled ion-exchange of boric acid, a weak electrolyte, on an anion-exchange resin bed. Transport of both ionic and nonionic forms of the weak electrolyte were considered in the model. The model predictions compared favorably with experimental data.

Weak electrolyte sorption is of interest in the study of soils too. Sorption affects the transport of organic and inorganic species in soil. Interaction between soil and organic species is complex; a number of transport mechanisms and reactions will be involved — ion-exchange reactions and adsorption are included. A comprehensive review of this subject is neither intended nor possible in this work; Stumm (1992), Schwarzenbach (1993), Petruzzeli and Helfferich (1993) have detailed reviews and references to the subject of soil and chemical species interaction. However, weak electrolyte multisite-multimechanism sorption is important in the study of transport in soils.

Weak electrolyte sorption by ion-exchangers is treated as an adsorption mechanism in most cases. Electrostatic influence of the dissociated weak electrolyte (the ionic form) on the mass transfer of other electrolytes is neglected. However, in MBIE at ultralow concentration of ionic impurities, the dissociated weak electrolyte influences mass transfer of the strong electrolytes. The model presented in this work considers the influence of the weak electrolyte on transport of other ionic components.

Diffusion of Strong Electrolytes

Strong electrolytes completely dissociate in a solvent yielding anion and cations; this solution conducts electricity. If complete dissociation occurs, a well mixed solution is assumed to have uniform distribution of anions and cations. Also, the solution can be pictured to have anions and cations moving independent of each other. But the situation is different; even in dilute solutions, the distribution of ions is not random (Newman, 1973) and the ions (anions and cations) are not free to move independent of each other (Cussler, 1984). This is a result of the electrostatic forces binding the anions and cations together. The net ionic flux is the same for both anions and cations, since they are 'tethered' to each other by the electrostatic force. The faster moving ion is retarded by the slower moving ion, hence their motion appears to be as that of a single entity.

Solute flux occurs due to the presence of gradients, concentration gradient being the most common. Such systems are modeled using Fick's law. But Fick's law is inadequate to model the flux expression when strong electrolytes are involved, since electrostatic forces are not included in Fick's model.

To model strong electrolyte flux, Nernst-Planck equation is used (Helfferich, 1962; Newman, 1973; Cussler, 1984). Graham and Dranoff (1982), Kraaijeveld and Wesselingh (1993) used the Maxwell-Stefan equations for modeling the diffusion flux of strong electrolytes; according to the authors, the Nernst-Planck equation is a special case of the Maxwell-Stefan equation.

The Nernst-Planck equation includes an electric potential gradient term in addition to the concentration gradient. The electric potential includes external electrical forces applied to the system, and electrostatic force induced by differing ion mobilities. In MBIE, no external electric field is applied to the system. The electric potential is a result of the different diffusion rates of the cations and anions. The Nernst-Planck equation is:

$$j_i = D_i\left(\frac{\partial C_i}{\partial r} + \frac{Z_i C_i F}{RT}\frac{\partial \phi}{\partial r}\right) \tag{II-1}$$

In Equation II-1, the second term in paranthesis is the electric potential gradient term. This term is a result of the influence of the electrostatic interactions of the ions present in the system. The charge of the ion, included in the second term of Equation II-1, also plays a role in influencing ion flux. Higher charge numbers will increase the value of the second term, and negative charges will reverse the direction of the electrical effect.

Diffusion of Weak Electrolytes

Solutes that incompletely dissociate in solution are called weak electrolytes. In an aqueous solution of weak electrolyte, different forms of the electrolyte will be in equilibrium. The equilibrium forms usually associated with a weak 1-1 electrolyte are: the dissociated electrolyte (ionic form), undissociated electrolyte (molecular form), and protons or hydroxyl ions. The degree of dissociation determines the concentration of the different species in the equilibrium mixture. Ostwald's dilution law defines the degree of dissociation, one in extremely dilute solutions and zero in concentrated solutions.

Vitagliano and Lyons (1956), Muller and Stokes (1957), and Dunn and Stokes (1965) have studied the effect of ionization on diffusion of weak electrolytes.

Wendt (1965) studied the diffusion coefficients of strong and weak electrolytes. The agreement between the estimated and observed values of diffusion coefficient for the weak electrolyte system H_2O-Na_2SO_4-H_2SO_4 was poor since dissociation-association reactions were ignored.

Leaist and Lyons (1981) have also studied multicomponent diffusion of electrolytes that are incompletely dissociated. They accounted for the association reaction in the multicomponent diffusion equation. Satisfactory agreement between experimental data and their predictions, for the experimental system — acetic acid-sodium acetate-water — was obtained by the authors.

Stokes (1965) and Cussler (1984) treat a weak 1-1 electrolyte equilibrium solution as a dimerization reaction. The ionic form or dissociated electrolyte is the monomer, and the undissociated electrolyte is treated roughly as the dimer of the same species. In the equilibrium solution, the monomeric form diffuses at a different rate compared to the dimeric form. As the total electrolyte concentration changes, the amount of monomer and dimer changes resulting in concentration dependent diffusivity. The total flux of a dimerizing solute is (Cussler, 1984):

$$j_T = -\left(\frac{D_1 + D_2\left[\sqrt{1+8kC_T} - 1\right]}{\sqrt{1+8kC_T}} \right) \frac{\partial C_T}{\partial r} \qquad \text{(II-2)}$$

Equation II-2 can be treated as a modified form of the Fickian diffusion equation. The total solute flux, j_T, is in equivalents. The term in the parantheses is an effective-diffusion coefficient representing the weak electrolyte system. The effective-diffusion coefficient approaches a diffusivity value of the monomer (D_1) as the total solute concentration decreases, and diffusivity value of the dimer (D_2) as the total solute concentration increases.

Assumptions for Modeling MBIE

Mechanism of Weak Electrolyte Removal

Polystyrene resins adsorb organics from solution. This property of ion-exchange resins has been used for removing organics and pesticides from water (Abrams, 1969; van Vliet et al., 1980; Cornel et al., 1986; Brattebo et al., 1987; Fu and Symons, 1990), and for analytical determination of organics in aqueous solution (Tateda and Fritz, 1978; Ammann and Ruttimann, 1995).

Experimental work shows ion-exchange resins remove organics from water by a combined mechanism of surface adsorption and ion exchange (Abrams, 1969; Afrashtehfar and Cantwell, 1982; Fu and Symons, 1990). Hence in this work, the ionic form of a weak electrolyte is assumed to exchange as a counterion with the ion-exchange resin, and the nonionic form is adsorbed by the resin.

The nonionic form is assumed to be adsorbed by an ion-exchange-resin site-sorbate interaction. Since a monolayer adsorption mechanism is assumed, the ion-exchange resin capacity determines the amount of nonionic form of the weak electrolyte adsorbed. Another reason for the assumed adsorption mechanism is the specificity of the ion-exchange resin to adsorb a particular nonionic species. Helfferich (1962) found that cation-exchange resins in the amine form (ion-exchange resin contains amino groups as the exchangeable species) adsorbed the nonionic form of the amine.

Other Assumptions

The following assumptions have been made to model the transport of weak electrolytes in mixed-bed ion exchange:

1. Since the solution is dilute there is no interference between electrolyte and non-electrolyte sorption. However, the dissociated weak electrolyte — ionic form — influences the transport of other electrolytes by electrostatic interaction.
2. Donnan principle — exclusion of ions, having the same charge as the fixed ion in the matrix, from the interior of the resin — does not affect nonionic sorption. This exclusion applies only to ionic form of the species.
3. Nernst-Planck equation models all the interactions between the ionic species.
4. Fick's law is used to model mass transport of the nonionic (or molecular) form.
5. Activity coefficients are assumed to be unity, since the solution is dilute.
6. Only univalent exchange is considered.
7. Film diffusion is assumed to be the rate determining step; this assumption is valid since ultra-low concentration of influent feed impurity is considered. Experimental verification for liquid-film diffusion control in MBIE has been provided by Frisch and Kunin (1960), and Helfferich (1962).
8. The weak electrolyte dissociation is considered to occur outside the film in the bulk phase only. Depending on the concentration of hydrogen and hydroxide ions, there may be reactions within the film (Haub and Foutch, 1986a,b). However, there is inadequate information to model film reactions for the case of amine exchange (Zecchini, 1990). Hence neutralization is limited to the bulk phase.

9. In the liquid film surrounding the resin bead: a) pseudo steady state exchange is assumed, b) co-ion flux is absent, c) curvature of the film is neglected, since thickness of the film is much smaller than the resin bead diameter, and d) there is no net current flow.
10. The solid-film interface is at equilibrium. Binary selectivity determines the equilibrium concentration at the interface. The concentration of the undissociated amine is assumed zero at the surface of the resin bead.
11. The localized and resin-phase concentrations are assumed to be uniform.
12. Ion-exchange reactions are assumed to be instantaneous compared to the overall rate of exchange.
13. In the mixed-bed ion-exchange column, plug flow is assumed. Axial dispersion is neglected.
14. The column is assumed to operate under isothermal and isobaric conditions.

Mathematical Model Development

The bulk phase consists of a mixture of ionized electrolytes, weak electrolytes, and an ionized solvent. The ionized solvent is water in typical MBIE operations. The concentration of strong electrolytes is small; in the parts-per-billion (ppb) range. Weak electrolyte concentration is in the range of parts-per-million (ppm). Hydrogen and hydroxyl ion concentrations, from water dissociation, are of comparable magnitude to the other strong electrolytes. This influences ionic flux, and hence the need to treat the bulk phase as an ionized solvent.

The flux of the strong electrolyte is expressed by the Nernst-Planck equation:

$$j_i = D_i\left(\frac{\partial C_i}{\partial r} + \frac{Z_i C_i F}{RT}\frac{\partial \phi}{\partial r}\right) \qquad \text{(II-1)}$$

The two terms on the right side of Equation II-1 represent: diffusion due to a concentration gradient, and motion due to an electric potential. The use of a psuedo steady-state assumption results in consideration of only space derivatives, time derivatives are ignored.

Convective terms are absent in Equation II-1. The film model for mass-transfer resistance is used to integrate Equation II-1. A schematic of the film model is given in Figure 2. Boundary conditions and additional equations are required to solve Equation II-1.

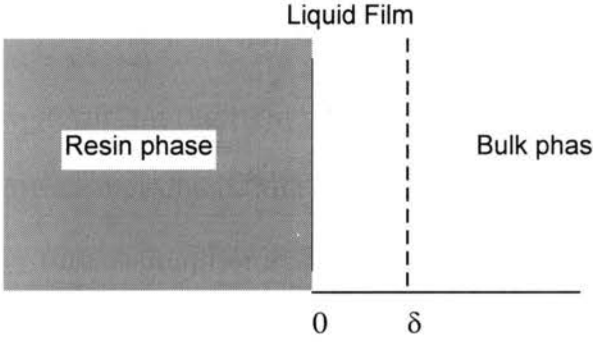

Figure 2. Schematic of the film model

Electrolytic solutions are assumed to be electrically neutral. This is one of the conditions that is assumed to be satisfied within the film. Electroneutrality is expressed as:

$$\sum Z_i C_i = 0 \qquad \text{(II- 3)}$$

Electroneutrality is violated very close to the interface of the solid-fluid film. A charge layer is setup near the interface due to preferential adsorption of certain ions. This leads to an electric field and violation of electroneutrality. Double layer theory is used to model this phenomena. However, in the case of the liquid-film model, the film thickness is very much greater than the electrical double layer (Wesselingh and Taylor, 1990; Newman, 1973). Hence the electroneutrality principle is applied to the film model.

Another conservation principle applicable to the film is conservation of electric charge. Charge density and current are related by the species continuity equation. In an electroneutral solution, the charge density is zero (Equation II-3). This results in no current flow, and is expressed as:

$$\sum Z_i j_i = 0 \tag{II - 4}$$

To solve Equation II-1, an expression is required for the electric potential gradient. Using Equations II-3, II-4, and no co-ion flux in the film, an expression relating the electric potential and concentration gradient of the ions is obtained. This relation is further used to determine the flux of the ionic species, and concentration profile in the film (Haub and Foutch, 1986a, b; Zecchini, 1990).

Haub and Foutch (1986a, b) first introduced the effect of water dissociation on the flux of ions in MBIE. An ionic flux expression for the binary exchange of univalent ions was derived, the equations were:

1) Concentration relationship between the ions in the liquid film is:

$$\frac{d}{dr}\left[\left(D_1 C_1 + D_2 C_2\right)\left(C_1 + C_2\right)\right] = 0 \tag{II-5}$$

At the edge of the film (thickness = δ), the concentration of the ions corresponds to the bulk-phase concentration ($C_1 = C_1^o$; $C_2 = C_2^o$). The resin surface concentrations of the ions ($C_1 = C_1^*$; $C_2 = C_2^*$) are in equilibrium with the resin-phase concentrations, and are related by the binary selectivity equation:

$$K_1^2 = \frac{C_1^* q_2}{C_2^* q_1} \tag{II-6}$$

2) The ionic flux is given by:

$$j_2 = -\left[\frac{2D_1D_2}{\delta(D_1 - D_2)}\right]\left(C_1^o + C_2^o - C_1^* - C_2^*\right) \tag{II-7}$$

(for cation exchange: Ion 1 is H^+, and Ion 2 is Na^+; for anion exchange: Ion 1 is OH^-, and Ion 2 is Cl^-)

Zecchini (1990) further expanded the expressions derived by Haub and Foutch (1986a,b) to include ternary exchange of univalent ions. Zecchini (1990) assumed that the co-ions present can be represented by a single pseudo co-ion. The pseudo co-ion concentration (C_p) is the sum of the concentration of all co-ions. The following expressions were derived:

1) Concentration relationship between the ions in the film is:

$$\frac{d}{dr}\left[\left(\frac{D_1}{D_2}C_1 + C_2 + \frac{D_3}{D_2}C_3\right)\left(C_1 + C_2 + C_3\right)\right] = 0 \tag{II-8}$$

Equation (II-8) is solved with the boundary conditions:

$C_1 = C_1^o$ $\quad C_2 = C_2^o$ $\quad C_3 = C_3^o$ $\quad$ (at the edge of the liquid film δ)

$C_1 = C_1^*$ $\quad C_2 = C_2^*$ $\quad C_3 = C_3^*$ $\quad$ (on the resin surface)

Binary selectivity is used as the equilibrium relation (assumption of solid-liquid interface equilibrium). The binary selectivity relations are:

$$K_1^2 = \frac{C_1^* q_2}{C_2^* q_1} \qquad K_1^3 = \frac{C_1^* q_3}{C_3^* q_1} \tag{II-9}$$

2) The flux for any ion (cation or anion) is given by:

$$j_i = \frac{2D_i\left(C_p^o - C_p^*\right)}{\delta}\left[\frac{C_i^o C_p^o - C_i^* C_p^*}{\left(C_p^*\right)^2 - \left(C_p^o\right)^2}\right] \quad \text{(II-10)}$$

The pseudo co-ion concentration (C_p) is the sum of either the cations or anions depending on cation or anion exchange; sum of the anions should be equal to sum of the cations due to electroneutrality.

Equation II-8 can be extended for four univalent ions, resulting in:

$$\frac{d}{dr}\left[\left(\frac{D_1}{D_2}C_1 + C_2 + \frac{D_3}{D_2}C_3 + \frac{D_4}{D_2}C_4\right)\left(C_1 + C_2 + C_3 + C_4\right)\right] = 0 \quad \text{(II-11)}$$

with the additional conditions:

$C_4 = C_4^o \qquad C_4 = C_4^*$

$$K_1^4 = \frac{C_1^* q_4}{C_4^* q_1} \quad \text{(II-12)}$$

Equation II-10 can still be used to obtain the ionic flux.

The flux of the weak electrolyte contains two parts: transport of the dissociated or ionic form and transport of the undissociated or molecular form. According to the assumptions for modeling weak electrolyte mass transfer, the transport of the two different forms are independent of each other. The ionic form only influences the mass transfer of strong electrolytes. The nonionic or molecular form transport follows Fickian diffusion, and the flux equation is:

$$j_{Mol} = -D_{Mol}\frac{dC_{Mol}}{dr} \quad \text{(II-13)}$$

Equation II-13 can be integrated across the assumed liquid film to obtain the total flux. The boundary conditions are: the concentration, at the edge of the film (δ), corresponds to the equilibrium value (due to dissociation-association reaction);

and is zero at the surface of the solid-fluid interface.

Equation II-1 involves a diffusion coefficient (D_i) of the ion, while in Equation II-13 a molecular diffusion coefficient (D_{Mol}) is required. Hence both values need to be quantified to apply the model.

Diffusivity measurements are necessary to obtain the transport coefficient. For strong electrolytes in dilute solutions, conductivity measurements are easier than measuring diffusion coefficients (Cussler, 1984) and diffusion can be related to conductance in solution (Horvath, 1985). In dilute solution, equivalent ionic conductance is related to ionic diffusion coefficient through mobility resulting in the Nernst relation. Nernst's expression for calculating the diffusion coefficient of a single ion is:

$$D_i = \left(\frac{RT}{Z_i F^2}\right)\lambda_i \qquad \text{(II-14)}$$

The diffusion coefficient obtained from Equation II-14 for an ionic species (or electrolyte) is termed single-ion diffusivity defined at infinite dilution. Tabulated values of the equivalent conductance (λ_i), at infinite dilution, for different ionic species is given by Robinson and Stokes (1955), Horvath (1985), and Lange (1985). The equivalent conductance varies with temperature and concentration.

Diffusivity of the molecular form of the weak electrolyte (in Equation II-13) can be calculated using the following correlation (Hayduk and Laudie, 1974):

$$D_{Mol} = \frac{13.26\left(10^{-5}\right)}{\mu_{water}^{1.4}\, V_{M,solute}^{0.589}} \qquad \text{(II-15)}$$

The correlation was developed by regressing experimental diffusivity data of 87 different species in dilute aqueous solutions. The molar volume (at normal boiling point) of the solute ($V_{M,solute}$) in Equation II-15 is estimated using the LeBas additive method, or by using the Tyn and Claus correlation with critical volumes (Reid, 1977).

MBIE Column Model

A column model is required to simulate the MBIE column and for generating breakthrough curves. MBIE columns can be designed with the prediction of breakthrough curves from equilibrium and kinetic property data. The starting point of a column model is the differential mass balance equation for an element of the ion-exchange column. The differential mass balance includes concentration of an exchangeable species in the fluid and resin phases. The column mass balance for a species is written as:

$$\frac{u}{\varepsilon}\frac{\partial C_i}{\partial z}+\frac{\partial C_i}{\partial t}+\Phi\left(\frac{1-\varepsilon}{\varepsilon}\right)\frac{\partial q_i}{\partial t}=0 \qquad \text{(II-16)}$$

The first two terms in Equation II-16 describe fluid-phase concentration distribution of a species. The third term in Equation II-16 is the mass balance for ion-exchange resin beads in the differential element of the column; in mixed-bed modeling, the factor Φ is the volume fraction of cation-exchange or anion-exchange resin in the column. If there are 'n' chemical species considered in the system, then 'n-1' column mass balance expressions are required.

The mass-transfer rate to the resin bead, assuming that the film model is applicable, can be written as:

$$\frac{\partial q_i}{\partial t}=K_{f,i}a_s\left(C_i^o-C_i^*\right) \qquad \text{(II-17)}$$

The mass-transfer rate in Equation II-17 has been defined by a simple linear driving force equation. K_f is an effective mass-transfer coefficient defined for each species, and is dependent on diffusive property of the species and prevailing hydrodynamic conditions. This is a lumped-parameter approach for modeling mass transfer into the ion-exchange resin. A lumped-parameter approach is used since mass transfer occurs across an interface. The hydrodynamic condition is built into the mass-transfer coefficient and need not be defined explicitly.

Empirical correlations are the usual route for obtaining mass-transfer coefficients. Specific correlations, matching hydrodynamics and diffusive characteristics of a particular column application can be used; else existing correlations can be extended to a particular application with caution.

Correlations developed by Carberry (1960) and Kataoka et al. (1973) are used for calculating mass-transfer coefficients in MBIE modeling. Carberry's (1960) correlation is used if the particle Reynolds number is greater than 20. For particle Reynolds number less than 20, Kataoka et al. (1972) correlation is used.

The mass-transfer coefficient calculated by Carberry (1960) or Kataoka et al. (1973) correlation represents a nonionic mass-transfer coefficient. Ionic mass-transfer coefficient is needed for defining mass transport of ionic species. Previously developed ionic flux expressions (Haub and Foutch, 1986a,b; Zecchini, 1990), defining the flux of ions in the liquid-film surrounding the resin bead, are used for calculating ionic mass-transfer coefficients. These ionic flux expressions do not connect the hydrodynamics and mass-transfer rate. But since the mass-transfer rate is equal to the total solute flux over the surface of the particle, the following equation can be written:

$$\frac{\partial q_i}{\partial t} = K_{f,i} a_s \left(C_i^o - C_i^* \right) = -j_i a_s \tag{II-18}$$

The ionic flux expression can be substituted in Equation II-18 and compared to define an effective diffusivity as:

$$D_{ei} = -\left[\frac{j_i \delta}{\left(C_i^o - C_i^* \right)} \right] \tag{II-19}$$

Van Brocklin and David (1972) have studied the effect of ionic migration on mass transfer. They defined a correction for mass transport as a ratio of the ionic-to-noionic mass-transfer coefficient. The correction, based on their definition, for MBIE is:

$$R_i = \left(\frac{D_{ei}}{D_i} \right)^{\frac{2}{3}} \tag{II-20}$$

The correction is applied to Equation II-17 and written as:

$$\frac{\partial q_i}{\partial t} = K_{f,i} R_i a_s \left(C_i^o - C_i^* \right) \tag{II-21}$$

Mass-transfer rate of strong electrolytes can be calculated using Equation II-21. But for weak electrolytes, the mass-transfer rate expression is:

$$\frac{\partial q_i}{\partial t} = K_{f,i} R_i a_s \left(C_i^o - C_i^* \right) + K_{f,Mol} a_s \left(C_{Mol,i}^o - C_{Mol,i}^* \right) \tag{II-22}$$

There is no R_i correction for the molecular form (second term in Equation II-22). The mass-transfer coefficient ($K_{f,M}$) is calculated using the molecular diffusivity (Equation II-15).

The concentration of the molecular form of weak electrolyte, in the differential column element, is calculated assuming that the bulk solution is in equilibrium. The dissociation reaction of the weak electrolyte, dissociation of water, and the charge balance are used to calculate the equilibrium composition of the bulk phase. The equations are:

$H_2O \Leftrightarrow H^+ + OH^-$ (water dissociation reaction)
$Amine + H_2O \Leftrightarrow Amine^+ + OH^-$ (weak electrolyte dissociation)
$\sum cations = \sum anions$ (charge balance)

Equation II-16 with II-21 (for strong electrolytes) or II-22 (for weak electrolytes) along with the solution equilibrium is solved with the appropriate initial and boundary conditions to predicit the dynamic behavior of the column. The initial and boundary conditions used in MBIE modeling, here, are:

$q_i = q_o$ (at t=0; $0 \le z \le L$)
$C_i = C_{Feed}$ (t > 0; at z=0, the top of the bed — near the feed entry point)
$C_i = C_{Effluent}$ (t > 0; at z=L, bottom of the bed)

The exchange isotherm in the case of ion exchange is more complex than isotherms seen in adsorption (for example: Langmuir or Freundlich isotherm). Analytical solution of this set of equations is not possible. Hence a numerical solution is developed (Appendix A).

Conclusions

A model for univalent weak electrolyte ion exchange in a mixed-bed column has been presented. The major simplifying assumptions have been kept to a minimum to develop a general model. This MBIE model is applicable only for low influent impurity concentration. A numerical solution is required to predict the dynamic behavior of the column.

CHAPTER III

MASS TRANSPORT OF AMINES IN MIXED-BED ION EXCHANGE

Introduction

Corrosion and corrosion products are detrimental to the operation of boilers. Corrosion products can form deposits on steam-generator tube surfaces, or block tube-support-plate broaches and increase feedwater flow resistance (Hepp et al., 1987; Thompson, 1991). Corrosion products will impede ion-exchange resin kinetics and hamper the impurity removal capability of resins. Corrosion will result in economic losses — chemical cleaning costs, power outage, and waste disposal. Iron corrosion products are common since the metal is very prevalent in the system. However, copper corrosion products are also relevant since copper is used. An increase in the local concentration of corrosion products acts as a corrosion initiator. Ion accumulations in the corrosion sludge will further result in a localized corrosive environment. Hence the need to reduce corrosion.

The chemistry of boiler water is controlled in power generating stations to combat corrosion-erosion problems. Water chemistry is controlled by the addition of desirable compounds and the removal of impurities. Weak electrolytes occur frequently in many of these operations. Weak electrolytes of significance to the power industry include borates, and amines and their breakdown products. Amines are used as pH-control agents to minimize corrosion.

To control corrosion, the feedwater pH guidelines recommended by EPRI are: 8.8-9.2 in the presence of copper and copper alloys; 9.3-9.6 in the absence of copper. The corrosion rate of carbon steel is a minimum at pH 10.0 (EPRI TR-102952, 1993). Plant-site economics determine the upper limit of achievable feedwater pH.

Selection of amines for pH control in boiler feedwater requires consideration of the following major factors: 1) base strength, 2) distribution coefficient (or volatility), 3) degradation characteristics, 4) toxicity, and 5) material compatibility. The base strength indicates the extent of amine ionization in water. Higher base strength, or basicity, is desired since smaller quantities of the weak base can be used for achieving certain pH. The distribution coefficient or the volatility determines how the amine partitions between the steam and water phase. Lower volatility is desired so that the water-phase concentration of amine is high, to prevent corrosion in wet steam areas, such as traps, drains and bypasses. The amine encounters a range of operating conditions in the boiler-water cycle; hence, a thermally stable amine is desired. The effect of degradation by-products must be considered if the amines are thermally unstable. Environmental effects and health hazards need to be considered too. Also, the amine needs to be compatible with the materials of construction. Finally, availability of the amine in bulk is an economical consideration.

Amine use in boiler feedwater results in reducing corrosion and iron transport in the system (Hepp et al., 1987; Fountain et al., 1990; Thompson, 1991; Harries et al., 1992). However, amines do not protect the system components from corrosion due to ionic impurities. The main impurities of concern are sodium, chloride, and sulfate. These ions, upon concentration, alter their local environment. The pH may become extremely acidic or basic, resulting in localized corrosion. Also, anions are involved in stress-corrosion cracking. Hence, even though amines are added, ionic impurity removal is a priority to avoid corrosion.

MBIE units are used to remove ionic impurities from process water. Use of MBIE units result in higher removal efficiency of ionic impurity compared to mono beds. The water neutralization reaction — hydrogen released from the cation-exchange resin combines with the hydroxide from the anion-exchange resin — will aid the exchange process.

There are two possible modes of operating MBIE units with amine dosed feedwater. The first mode is to convert the cation-exchange resin into the amine form and operate the mixed bed. The second mode is to use the HOH (hydrogen-hydroxide) cycle; the cation-exchange resin is in the hydrogen form, and amine is added to the feedwater. The cation-exchange resin removes the amine and other ionic impurities from the bulk phase. Removal of amine from the bulk phase results in a decrease of the effluent pH. Hence additional amine needs to be redosed to maintain the operating pH.

One of the disadvantages in water purification of amine dosed feedwater is sodium throw from the cation-exchange resin. Sodium on the cation-exchange resin is displaced by ionic form of the amine. Sodium ion from the cation-exchange resin is leached as the bed converts to the amine form. Sodium slip occurs due to differences in the concentration of the competing ions. The concentration of amine added is usually in the parts-per-million range, whereas other ionic impurity concentrations are in the parts-per-billion range. The type and concentration of amine determines the amount of sodium leak from the mixed bed.

The equilibrium concentration of sodium in the bulk phase is determined by the selectivity coefficient of the resin for sodium over the amine. The selectivity coefficient is represented by:

$$\text{R-Amine} + \text{Na}^{+} \Leftrightarrow \text{R-Na} + \text{Amine}^{+} \qquad \text{(III-1)}$$

$$K_{\text{Amine}}^{\text{Na}} = \frac{[\text{R} - \text{Na}][\text{Amine}^{+}]}{[\text{R} - \text{Amine}][\text{Na}^{+}]} \qquad \text{(selectivity coefficient)} \qquad \text{(III-2)}$$

When the selectivity coefficient is greater than one, the resin prefers the sodium ion over the ionic amine, a value less than one reverses the preference. The amount of sodium-ion leakage is determined by the selectivity coefficient, concentration of the ionic form of the amine, and sodium content of the resin. One of the assumptions made in writing this selectivity expression is that the ionic form of the amine is univalent — this is true for the amines used in this study.

Ammonia, a weak base, has been traditionally used as the pH-raising chemical in fossil fired power generating stations. The disadvantages of ammonia are: 1) high volatility — most ammonia is found in the steam phase, hence there is inadequate corrosion protection in the places where liquid water is present, and 2) cation-exchange resins have lower selectivity for sodium over ammonia; this results in higher sodium-ion leakages as the resin converts to the ammonium form. This decreases run length of the MBIE units with acceptable sodium-ion leakages. Therefore, alternative amines have been studied to replace ammonia (EPRI TR-102952, 1993). A summary of different amines used in pH control is presented in Table I.

TABLE I

Amines Used in pH Control of Boiler Feedwater

Amine	Mol. Weight	Base Strength (pK_b; 25°C)	Reference
Morpholine	87.0	5.51	Bates (1989)
Ammonia	17.0	4.75	Lange (1985)
2-Amino-2-methyl-1-propanol (AMP)	89.1	4.30	Bates (1989)
Dimethyl amino propanol (DAP)	104.1	4.50	Bates (1989)
Ethanolamine (ETA)	61.0	4.50	Lange (1985)
Quinuclidine	111.2	2.86	Bates (1989)
3-Hydroxyquinuclidine	127.2	4.20	Bates (1989)
Piperidine	85.0	2.89	Lange (1985)

The objective of this work is to predict the effluent concentration profile of amines using the weak electrolyte exchange model developed earlier (Chapter II) for MBIE. Along with the amine effluent profile, effluent concentrations of the other ions — sodium and chloride — are also predicted. All the ions considered here are univalent. The model is validated by comparing predicted effluent profiles with experimental and real-plant data. The use of the model to optimize plant performance by simulating potential operating scenarios is demonstrated.

Aqueous Amine Solution Equilibrium

Amines dissociate in an aqueous solution. The aqueous solution is an equilibrium mixture containing dissociated amine (ionic form), undissociated amine (molecular or nonionic form), and OH^- ions. This property is used for increasing solution pH. The reaction can be represented by:

$$\text{Amine} + H_2O \Leftrightarrow \text{Amine}^+ + OH^- \tag{III-3}$$

$$K_b = \frac{[\text{Amine}^+][OH^-]}{[\text{Amine}]} \tag{III-4}$$

The fraction of ionized amine depends on the base strength. Table I also presents the base strength of different amines. Figure 1 compares ionization of amines with different values of K_b. The hydroxide-ion concentration is proportional to the amount of dissociated amine. The fraction of ionized amine decreases as the concentration of amine increases. Hence higher pH cannot be achieved by increasing amine concentration since dissociation decreases.

Excess hydroxide in solution shifts the reaction (III-3) to the left. Conversely, lower amounts of OH^- will favor the reaction (III-3) to move towards the right. Figure 2 presents the effect of hydroxide on morpholine and morpholinium ion concentration. At higher hydroxide concentration, the amount of morpholinium ion is negligible, and morpholine — the unidissociated form — is dominant (the total amount of morpholine is 60 ppm).

The relative amounts of the different forms of amine and hydroxide-ion concentration are computed by a solution equilibrium calculation. The aqueous amine solution equilibrium is also affected by the presence of other ions. Other weak electrolytes in solution will influence the amount of OH^- produced. Water dissociation reaction plays a role in the equilibrium. Strong electrolytes influence the charge balance only. The following equations are used to determine the relative amounts of the dissociative species:

$$\text{Amine} + H_2O \Leftrightarrow \text{Amine}^+ + OH^- \tag{III-3}$$

$$H_2O \Leftrightarrow H^+ + OH^- \tag{III-5}$$

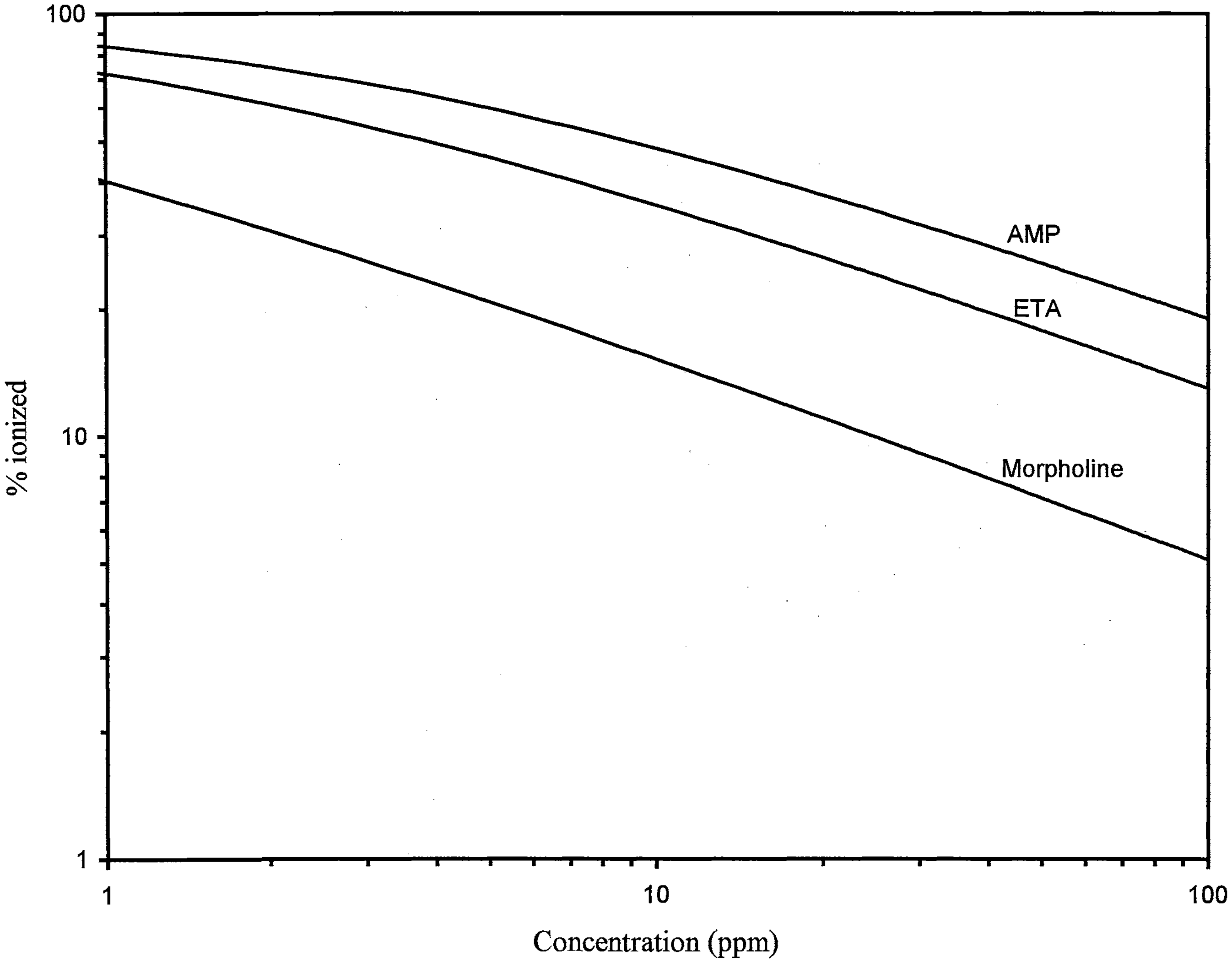

Figure 1. Effect of amine concentration and base strength (Table I) on ionization

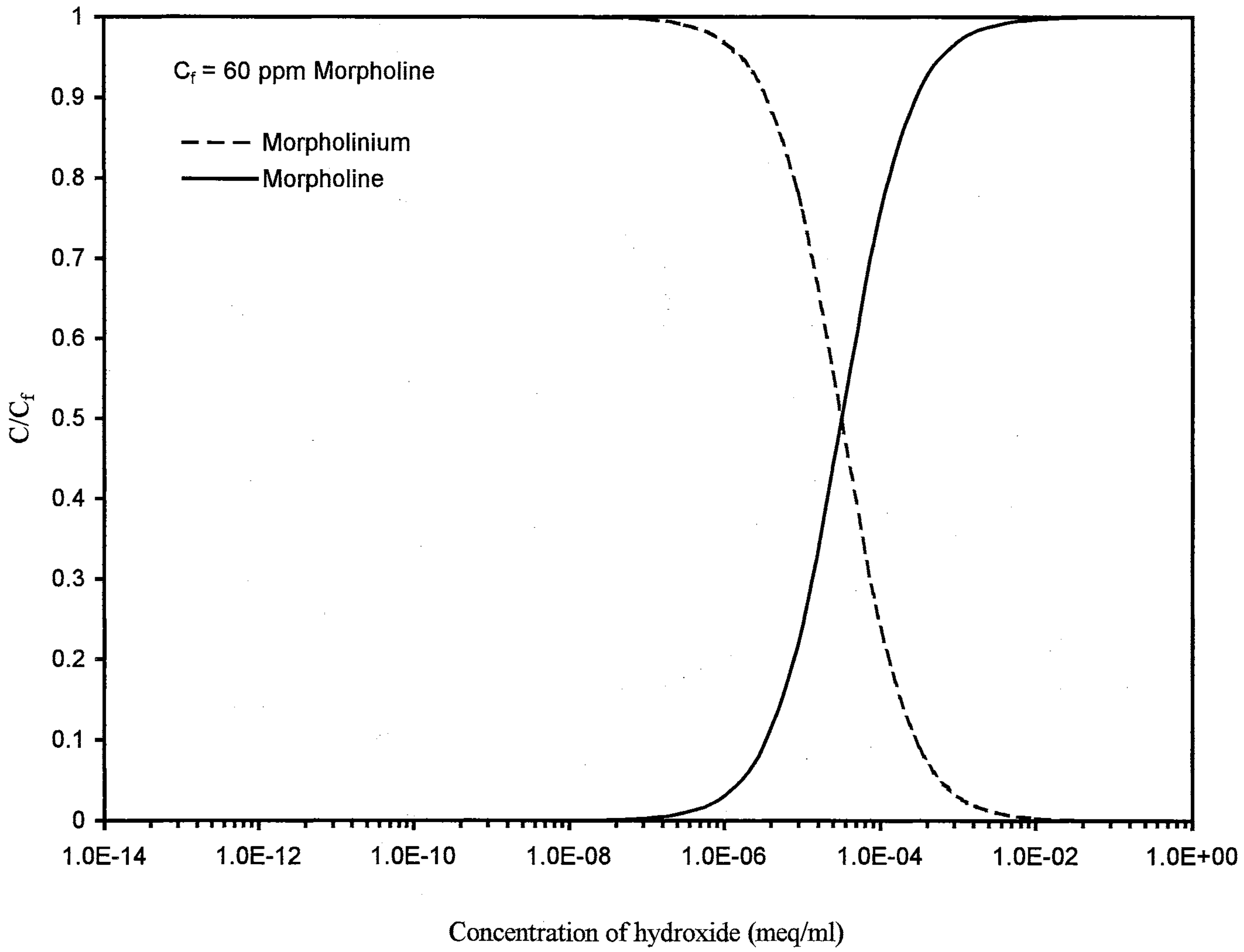

Figure 2. Effect of hydroxide concentration on dissociation of morpholine

$$K_b = \frac{C_{Amine^+} C_{OH^-}}{C_{Amine}} \qquad K_w = C_{H^+} C_{OH^-} \tag{III-6}$$

$$C_{Na^+} + C_{H^+} + C_{Amine^+} = C_{OH^-} + C_{Cl^-} \qquad \text{(charge balance)} \tag{III-7}$$

$$C_{Total,Amine} = C_{Amine^+} + C_{Amine} \qquad \text{(amine mass balance)} \tag{III-8}$$

The concentrations of sodium and chloride ions, and total amine concentration are known. The values of K_b and K_w are easily obtained, and are temperature dependent. In this work the temperature is assumed to be 25°C. Equations III-6 through III-8 are solved to determine the concentration of: ionic amine ($Amine^+$), noionic amine (Amine), hydrogen (H^+), and hydroxide (OH^-). To solve for the unknown concentrations, Equations III-6 to III-8 are written in terms of the hydroxide-ion concentration. The resulting polynomial is:

$$C_{OH}^3 + AC_{OH}^2 + BC_{OH} + D = 0 \tag{III-9}$$

where

$$A = K_b + C_{Cl^-} - C_{Na^+}$$

$$B = K_b\left(C_{Cl^-} - C_{Na^+} - C_{Total,Amine}\right) - K_w$$

$$D = (-1)K_b K_w$$

Equation III-9 is solved using a Newton-Raphson method to obtain the hydroxide-ion concentration. This determines pH of the solution. The hydroxide-ion concentration is later used to calculate the concentration of the other ions using Equations III-6 to III-8.

Amine-Exchange Model Development

The model developed earlier (Chapter II) for weak electrolyte mass transport is used to predict the effluent concentration history of amines. The ions considered in the ion-exchange process are: Na^+, $Amine^+$, H^+, Cl^-, and OH^-. Only univalent system of ions are considered. There are different kinds of amines studied as pH-control agents (Table I). Hence the model developed here is general, and applicable to any of the amines. However, the requirement that dissociated species are univalent still holds. The transport of the undissociated (molecular or noionic form) amine is considered in the model.

The model assumes that neutralization and equilibrium establishment reactions are instantaneous, compared with the ion-exchange rate. The model treats cation and anion exchange separately, rather than a combined approach — like a salt removal process. The material balance and ion-exchange rate for the resins are computed separately.

The cation-exchange resin is assumed to start in the hydrogen form and later convert to the amine form. Hence this is an HOH cycle with amine in the influent. A single type of amine is assumed to be present in the influent.

The ionic form of the amine is assumed to be stoichiometrically exchanged by the cation-exchange resin. The nonionic form is assumed to protonate with hydrogen ions on the cation-exchange resin. The mechanism is:

$\text{R-H} + \text{Amine}^+ \Leftrightarrow \text{R-Amine} + \text{H}^+$ (ion exchange)
$\text{R-H} + \text{Amine} \Leftrightarrow \text{R-H-Amine}$ (protonation)

The model requires transport property data of the amines. Cation-exchange resin selectivity coefficient of amine over sodium is also required (ion-exchange reaction equilibrium). Selectivity coefficients for organic ions are complicated by structure of the molecule and solution conditions (Semmens, 1975). For example, McNulty et al. (1992) show that the sodium/morpholinium selectivity of Ambersep 200 (cation-exchange resin) changes from 12 to 35 depending on solution morpholine concentration. Hence experimentally measured values for a particular system are best suited for use in the model. Table II summarizes properties of the amines. The amine selectivity over hydrogen can be calculated using the sodium-hydrogen selectivity coefficient.

The MBIE model also requires transport and equilibrium properties of inorganic ions — sodium and chloride ions in this work. The selectivity coefficient is dependent on the physio-chemical properties of the ion-exchange resin and the exchanging ions. The ionic diffusivity is calculated using Equation II-14. Selectivity coefficients and diffusivity are presented in Table III.

Apart from ionic selectivity and diffusivity, additional input data required by the model includes resin properties, inlet concentration of the ions, flow rate, temperature, initial resin loading, and the cation-to-anion resin ratio. These values are used in the model to simulate a particular operating scenario.

Model Validation

Model validation is an important phase of process model development. In this work the main goal was to develop a process model from first principles to predict column performance a priori. To validate process models, in certain system specific models, adjustable parameters are used; these parameters are obtained by regression with experimental data. This will lead to loss of model generality. In this work, parameter adjustment to fit experimental data has not been done; the model parameters are all measured values. However, parametric sensitivity has been studied with existing experimental data.

TABLE II

Amine Properties used in MBIE Modeling

Amine	V_M[1]	D_{Mol}[2]	D_{Ionic}[2]	Selectivity[3] for Na^+
Morpholine	94.1	1.06	1.57	2.1 [3]
Ammonia	25.4	2.23	1.92	0.77 [3]
2Amino-2methyl -1propanol (AMP)	117.8	0.93	1.74	4.50 [3]
Ethanolamine (ETA)	72.0	1.24	1.11	1.73 [4]

[1] Molar volume at normal boiling point (cm^3/mole)
[2] Diffusivity at 25°C (X 10^{-5} cm^2/s)
[3] K^{Na}_{Amine} ; 12%DVB crosslinked cation-exchange resin (Harries et al., 1989)
[4] 12% macro cation-exchange resin (EPRI TR-102952, 1993)

TABLE III

Selectivity and Diffusivity of Sodium and Chloride Ions

Ion	Diffusion Coefficient [1]	Selectivity
Sodium	1.38	$K^{Na}_{H}=1.5$
Chloride	2.04	$K^{Cl}_{OH}=17.0$

[1] 25°C (X 10^{-5} cm^2/s)

To validate the model, here, effluent concentration data from a real-plant and laboratory experimental setup have been used. Real-plant data is from Nuclear

Electric's Oldbury-on-Severn power station, United Kingdom. Miller and Asay's (1991) laboratory experimental data have also been used for purposes of comparison. Comparison of model prediction with data has been presented as two case studies.

Case 1: Condensate Polishing at Nuclear Electric's Oldbury Power Station

TABLE IV

Operating Conditions at Oldbury

Property	Value
Bed diameter (cms)	152.0
Resin depth (cms)	100.0
Cation-to-anion exchange resin (volumetric ratio)	1:1
Resin bead diameter (cm)	
Cation (Ambersep 252)	0.1
Anion (Ambersep 900)	0.066
Resin capacity (meq/ml)	
Cation	2.18
Anion	1.1
Temperature (°C)	25
Influent concentration (meq/ml)	1.74E-8
Initial loading on the resin (%)	
Cation (sodium)	0.2
Anion (chloride)	0.2

Table IV presents the operating conditions at Oldbury. Oldbury polishes 100% of the feedwater flow to the once-through boilers. This flow is distributed to five mixed beds, each 152 cms in diameter. Each service vessel is charged with equal volumes of Ambersep 252 (cation) and Ambersep 900 (anion) resins. The feedwater is dosed with 60 ppm morpholine, to give an operating pH of 9.65. Sodium chloride concentration in the feed is 1.74×10^{-8} milliequivalents-per-milliliter. Freshly regenerated beds are returned to service at half flow (400 gpm) to limit the morpholine removal rate by the hydrogen-form bed, and to dilute the sodium throw with throughput from the other beds in service. Beds are typically returned to full flow (800 gpm) after 6.6 days and remain in operation for a total of 30 days before regeneration.

The model predictions for morpholine breakthrough have been compared with Oldbury data. Figure 3 presents this comparison. There is variation in the four runs of presented plant data. The flow rate to the mixed bed is not constant; there is variation in the amount of flow to each bed. The corresponding fluctuation in the inlet feed concentration is neglected and a constant average feed rate is assumed. The model was used to predict morpholine breakthrough by changing the flow rates. The model predictions for morpholine breakthrough agree well with Oldbury data. Figure 3 also presents a predicted breakthrough curve neglecting molecular morpholine (nonionic) transport. The breakthrough is much earlier than expected and does not agree with plant data. The resin-phase concentration profile of morpholine in the mixed bed, as exchange progresses, is shown in Figure 4.

Since the concentration of molecular morpholine in the bulk phase is high, morpholine mass transport, assuming that solid-phase resistance is also important, has been tested. Linear addition of mass-transfer resistances is assumed (Ruthven, 1984). A linear driving force in the solid is used, and the ion-exchange rate for the molecular form (second term in equation II-22) is modified as:

$$\frac{\partial q_{\mathrm{Mol},i}}{\partial t} = \left(\frac{1}{K_{f,\mathrm{Mol}} a_s} + \frac{1}{K_{p,\mathrm{Mol}} a_p} \right)^{-1} \left(C^{o}_{\mathrm{Mol},i} - C^{*}_{\mathrm{Mol},i} \right) \qquad \text{(III-10)}$$

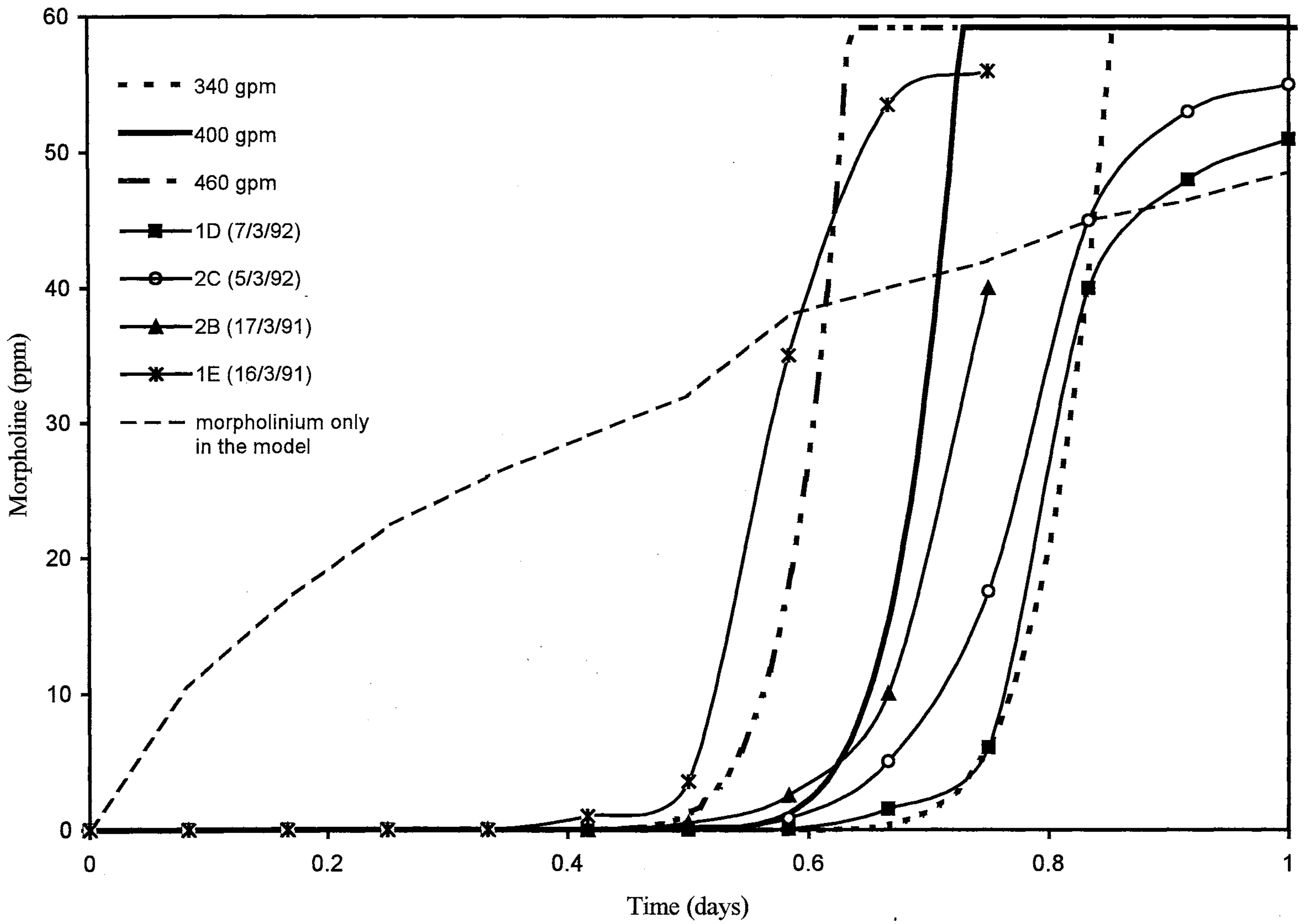

Figure 3. Comparison of model predictions with Oldbury plant data

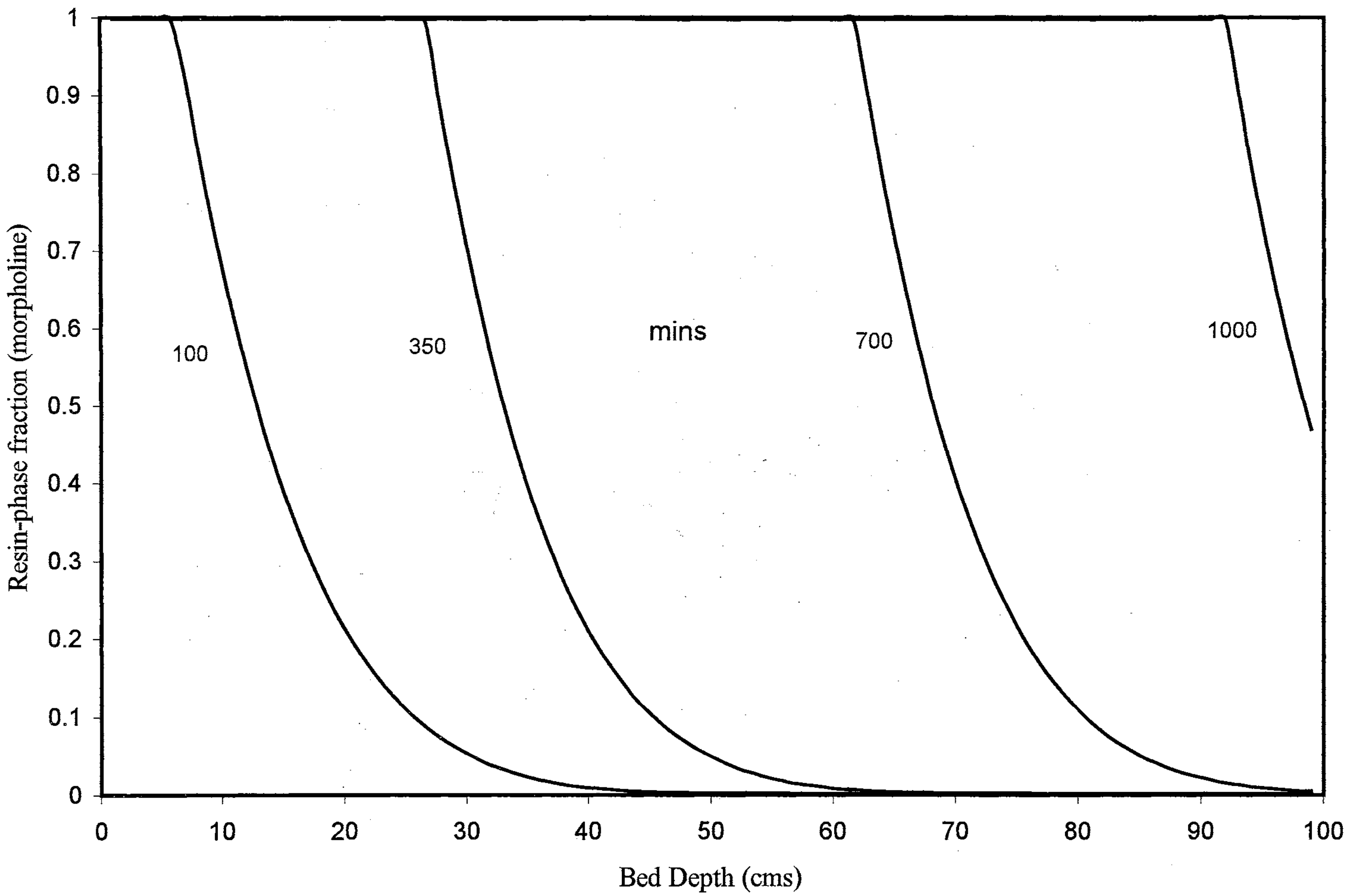

Figure 4. Morpholine profile in the bed as exchange progresses

where:

$$K_p a_p = 60 \frac{D_{eff}}{d_p^2} \tag{III-11}$$

The intraparticle diffusivity (D_{eff}) is not known; this parameter is system specific (depending on resin porosity, and molecular structure of the amine), and is to be estimated from experimental data. There are no reliable correlations for estimating this diffusivity from liquid-phase diffusivity.

Figure 5 shows the effect of including solid-phase resistance on morpholine breakthrough. The effective diffusivity used here is an approximate value. The S-shape pattern of the breakthrough curve is affected. Low resin-phase diffusivity results in earlier breakthrough of morpholine. Higher resin-phase diffusivity has no significant impact on the breakthrough profile since film diffusion dominates. Hence a model accounting for solid-phase resistance to mass transport is unnecessary.

The limiting factor in morpholine form operation is the increased impurity leakage, sodium — in this case — from the mixed beds. This is caused by the relatively high concentrations of morpholinium (ionic form of morpholine) and hydroxide ions present in the bed at pH 9.65. The sodium leakage is determined by the sodium/morpholinium selectivity coefficient (Equation III-2). The cation-exchange resin used at Oldbury, Ambersep 252, has a sodium/morpholinium selectivity coefficient of 2.1 (Sadler et al., 1988).

The maximum concentration for the sodium throw peak is controlled primarily by regeneration efficiency. For Oldbury conditions, a resin contamination of 0.2% sodium (percentage sites in sodium form) will result in a sodium throw

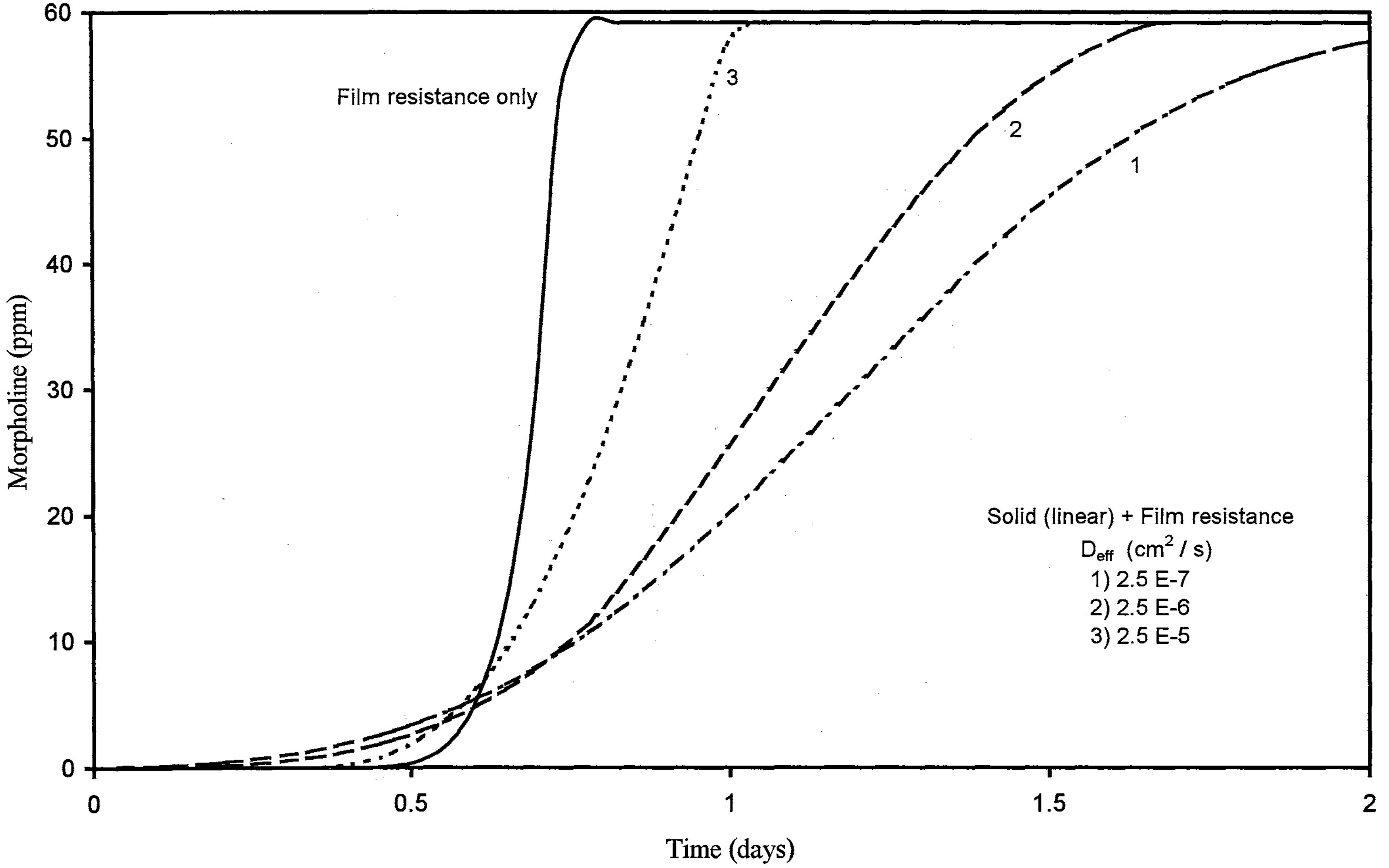

Figure 5. Effect of solid phase resistance on morpholine breakthrough

peak concentration of 0.8 ppb (Equation III-2). The average inlet sodium feed concentration is 0.4 ppb.

Predicted sodium effluent profile is compared with plant data in Figures 6, 7, and 8. Sodium effluent profiles were predicted by adjusting the initial resin loading and flow rate. Plant data indicated flow rate fluctuations to the mixed beds, hence an average flow rate has been assumed for predicting the sodium effluent profile. Plant records do not indicate the efficiency of regeneration or residual sodium on the cation-exchange resin. Hence the initial resin loading of sodium was obtained by trial-and-error to get the sodium-throw peak concentration. Also, the change in flow rate to the beds on day 6.6 of operation was inconsistent; time of the flow rate change as indicated by the plant record is used. Flow rate data is presented in Figure 9.

The plant sodium data presented in Figures 6 to 8 have an error of ±0.1 ppb (Bates, 1993). The predicted sodium effluent profile is within this error. The data obtained from full-scale equipment show variations. Operational and human (plant personnel) inconsistencies also influence the fluctuation of measured values. For example, in the flow rate data presented in Figure 9, the flow rate to bed 1C varies ±10% from the average flow rate after day 6 of operation. This flow rate variation affects the effluent sodium concentration. The model, here, assumes only average values for computation of the effluent profile. Taking into consideration these factors, the predicted profile compares favorably with plant data.

Chloride breakthrough profiles have not been presented here. The predicted chloride concentration is less than 0.20 ppb with operating conditions of Table IV,

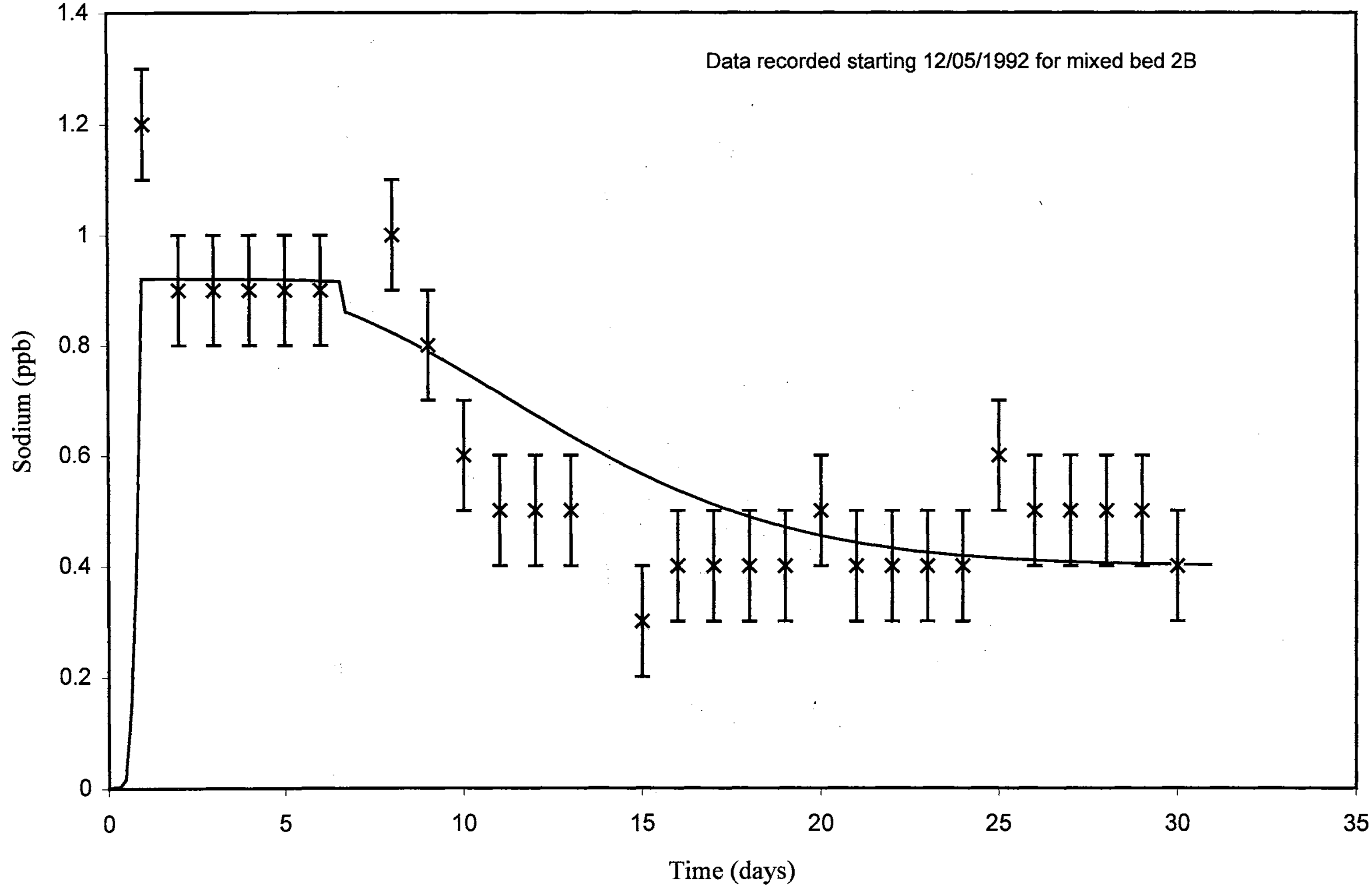

Figure 6. Comparison of predicted sodium throw with Nuclear Electric (UK) data

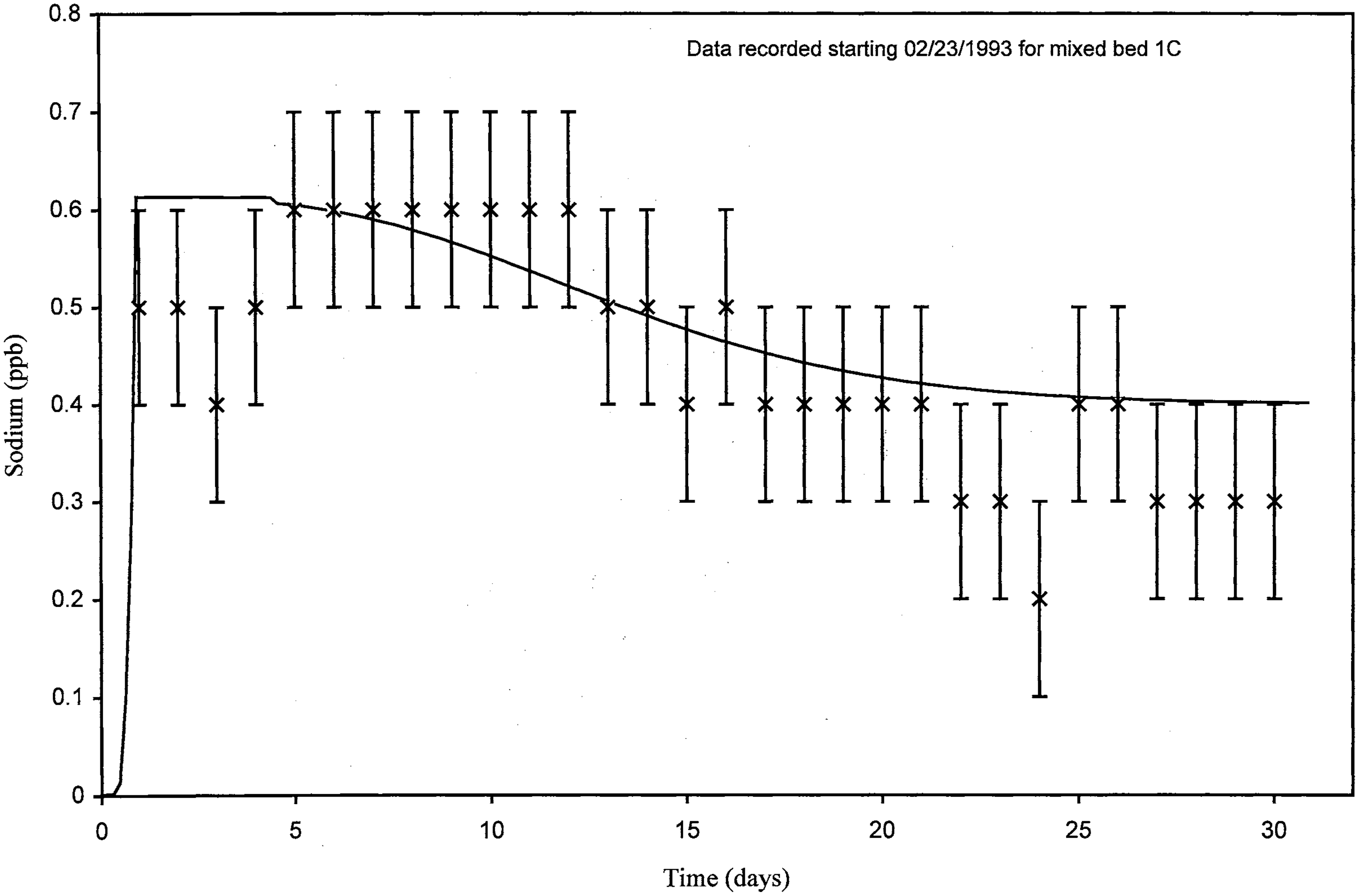

Figure 7. Predicted sodium effluent profile compared with Nuclear Electric (UK) data

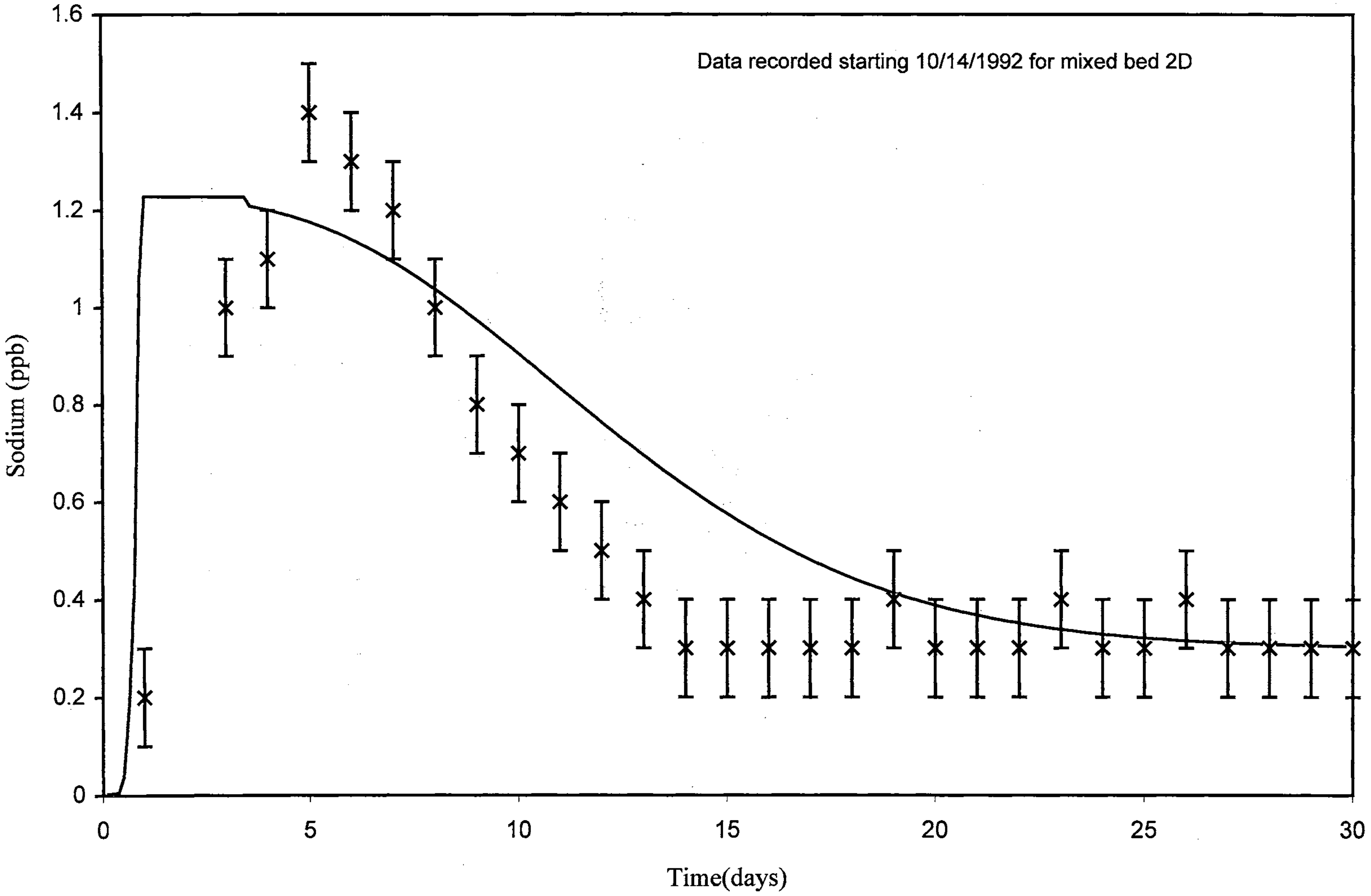

Figure 8. Comparison of predicted sodium effluent profile with Nuclear Electric (UK) data

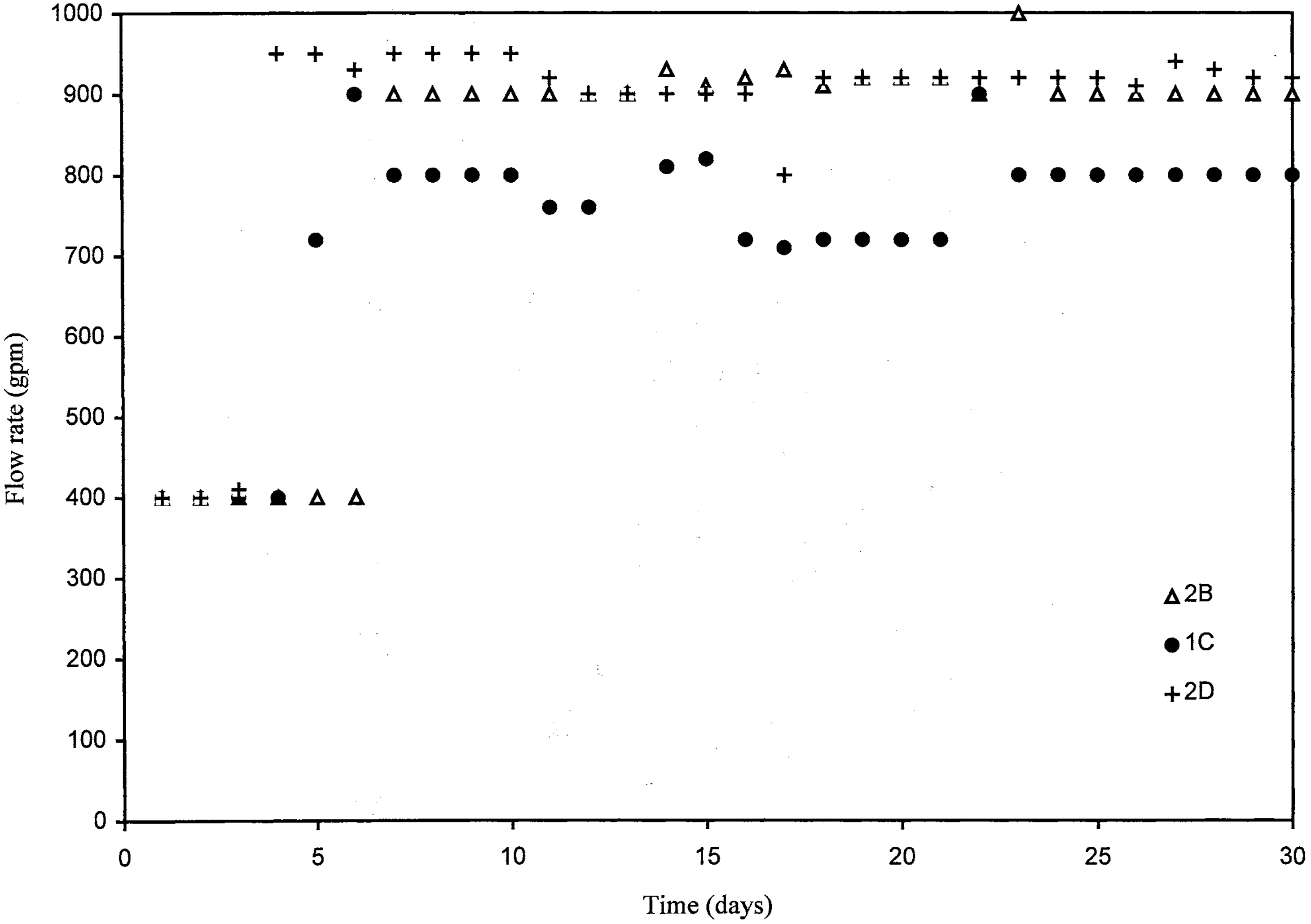

Figure 9. Flow rate variation to the mixed beds (data from Nuclear Electric, UK)

for the 30 day period of mixed bed operation. Low anion effluent concentrations, due to high hydroxide-ion concentration, is one of the advantages of using amines.

Case 2: Experimental data of Miller and Asay (1991)

Table V presents the operating conditions used by Miller and Asay (1991) in their experiments. They studied the effect of initial sodium loading on the resin and different amines on sodium throw. However, in this study, amine experimental data for morpholine, ETA, and AMP are used for comparisons since transport and equilibrium coefficients were readily available.

TABLE V

Experimental Conditions of Miller and Asay (1991)

Property	Value
Bed diameter (cms)	10.2
Resin depth (cms)	106.6
Cation-to-anion exchange resin (volumetric ratio)	2:1
Resin bead diameter (assumed; cms)	
Cation (Amberlite IR200)	0.08
Anion (Ambersep IR900C)	0.06
Resin capacity (meq/ml)	
Cation	2.18
Anion	1.1
Temperature (°C)	25
Flow rate (cm^3/s)	269.0

Figure 10 compares predicted effluent AMP profile with experimental data. The assumed average inlet concentration of AMP was 13 ppm. Figure 11 presents a

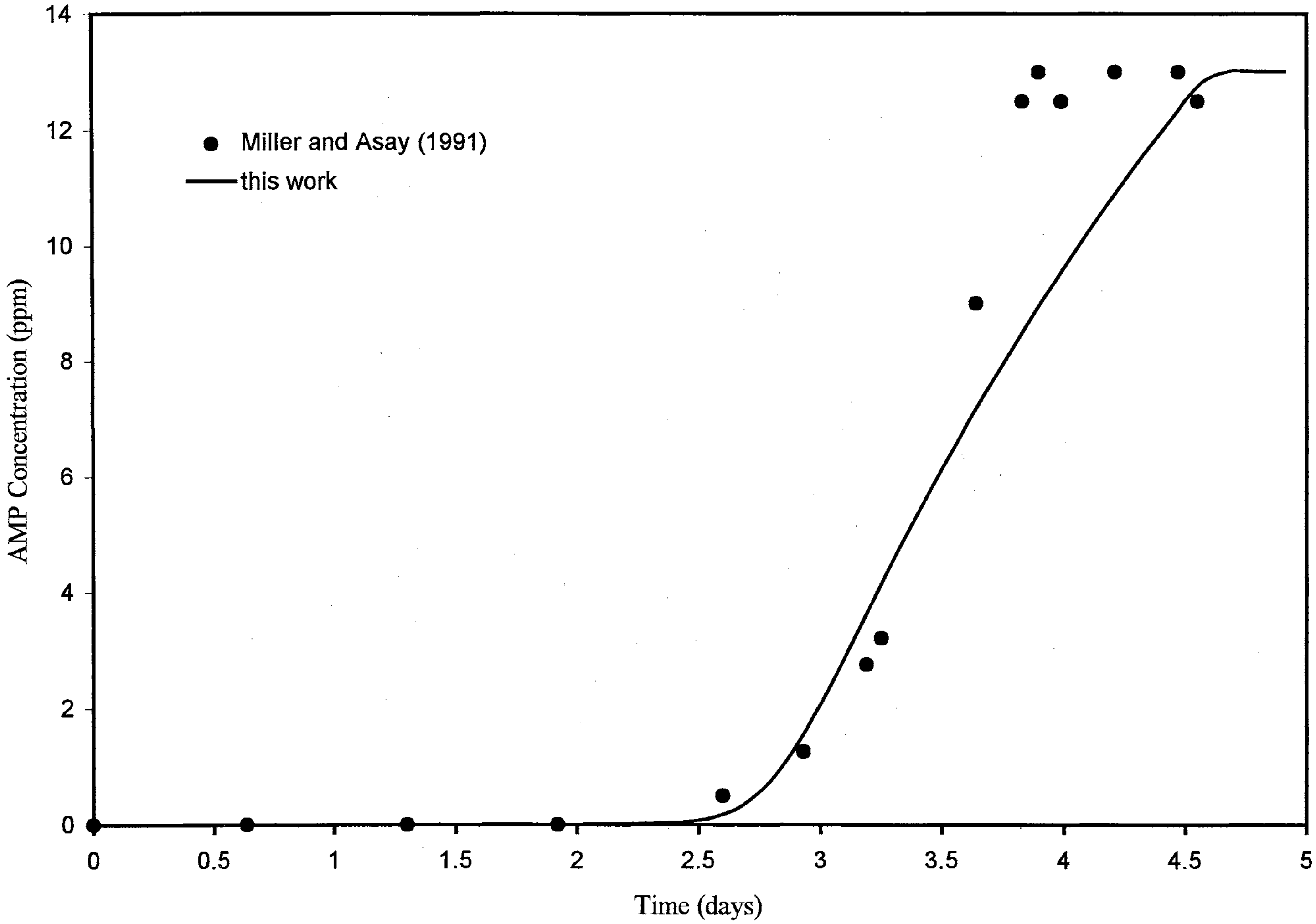

Figure 10. Predicted breakthrough profile compared with experimental data (macro cation-exchange resin)

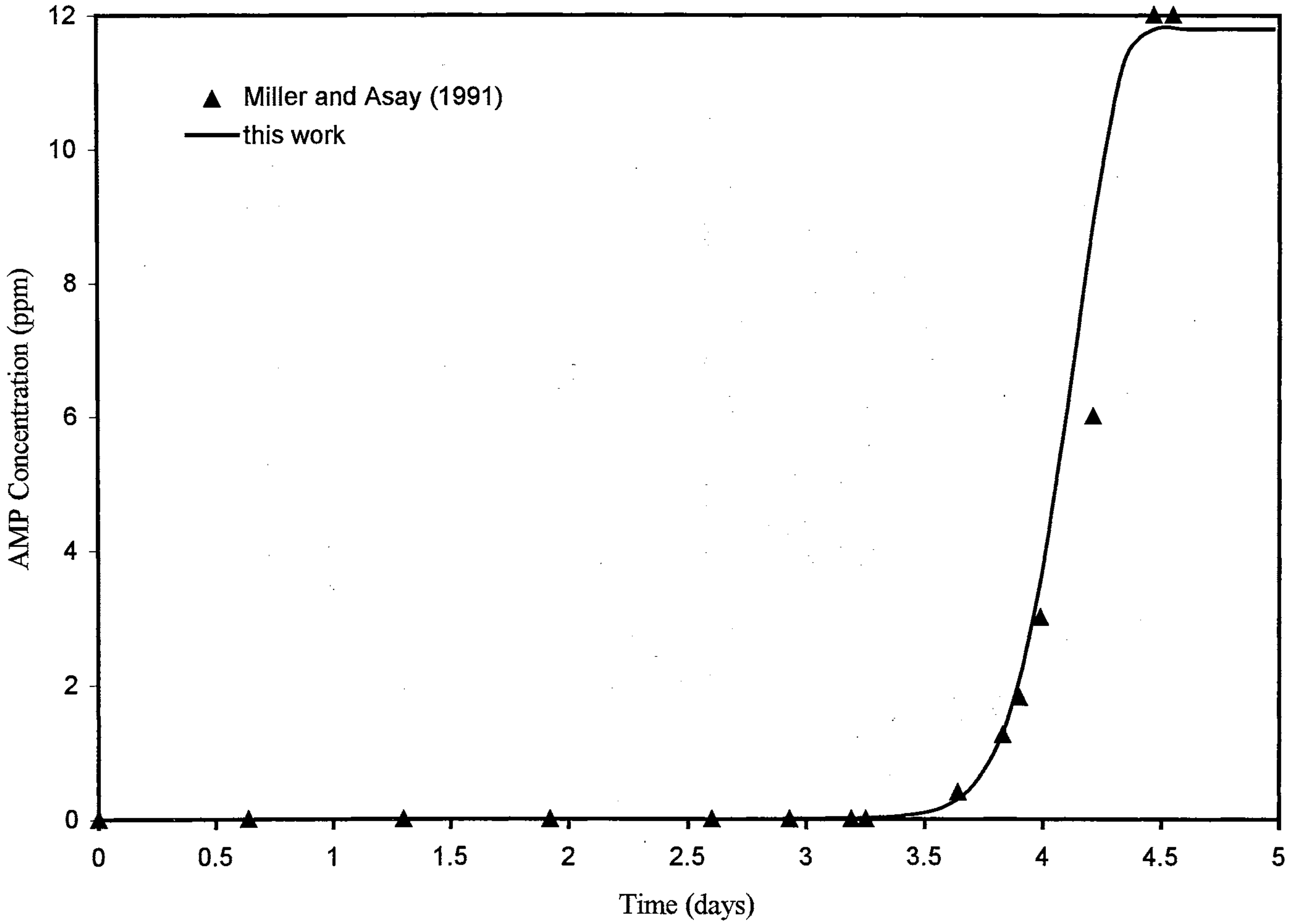

Figure 11. Comparison of predicted profile with experiment data for gel-type cation-exchange resin

comparison of experimental data with predicted AMP effluent profile. For this experiment, a different cation-exchange resin was used — gel-type resins were used (cation-exchange resin was HGR-W2, and anion-exchange resin was SBRP); assumed influent concentration of AMP was 12 ppm for model predictions.

The predicted ETA effluent profile is compared with experimental data in Figure 12. The data presented by Miller and Asay (1991) shows that the ETA influent concentration varied from 10 ppm to 13 ppm. Hence an average concentration of 11.5 ppm ETA was assumed for the model predictions.

Figures 13 and 14 compare predicted sodium effluent profile with experimental data. The inlet concentration of sodium was not constant, and hence an average value is assumed. The selectivity coefficient for the cation-exchange resin was calculated using the sodium-throw peak concentration reported by Miller and Asay (1991). The sodium/amine selectivity values used were: 14.0 for sodium/morpholine exchange (Figure 13), and 5.3 for sodium/ETA exchange in Figure 14.

The model predictions compared with Miller and Asay's (1991) experimental data are in good agreement for the amines. However, evaluation of the predicted sodium profile with their experimental data is difficult. There is considerable scatter in the presented experimental data; this may be due to operation of analytical equipment near the detection limit or loss of calibration. Other contributing factors may be fluctuations in the input values; for example, flow rate and influent concentration of ions. Miller and Asay (1991) have not reported any error analysis. Hence an estimate on the error values of the experimental data is not presented here.

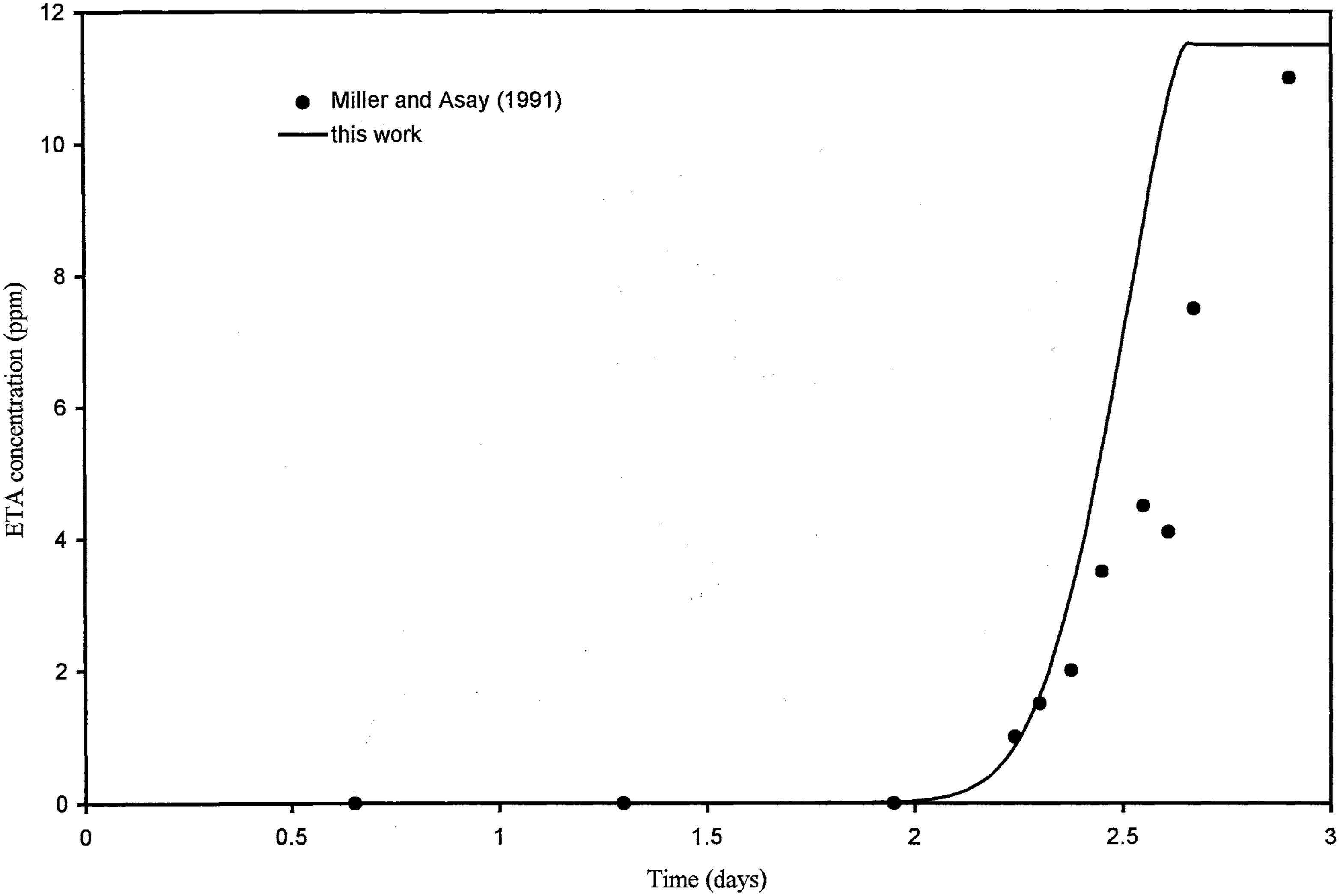

Figure 12. Predicted ETA breakthrough compared with experimental data

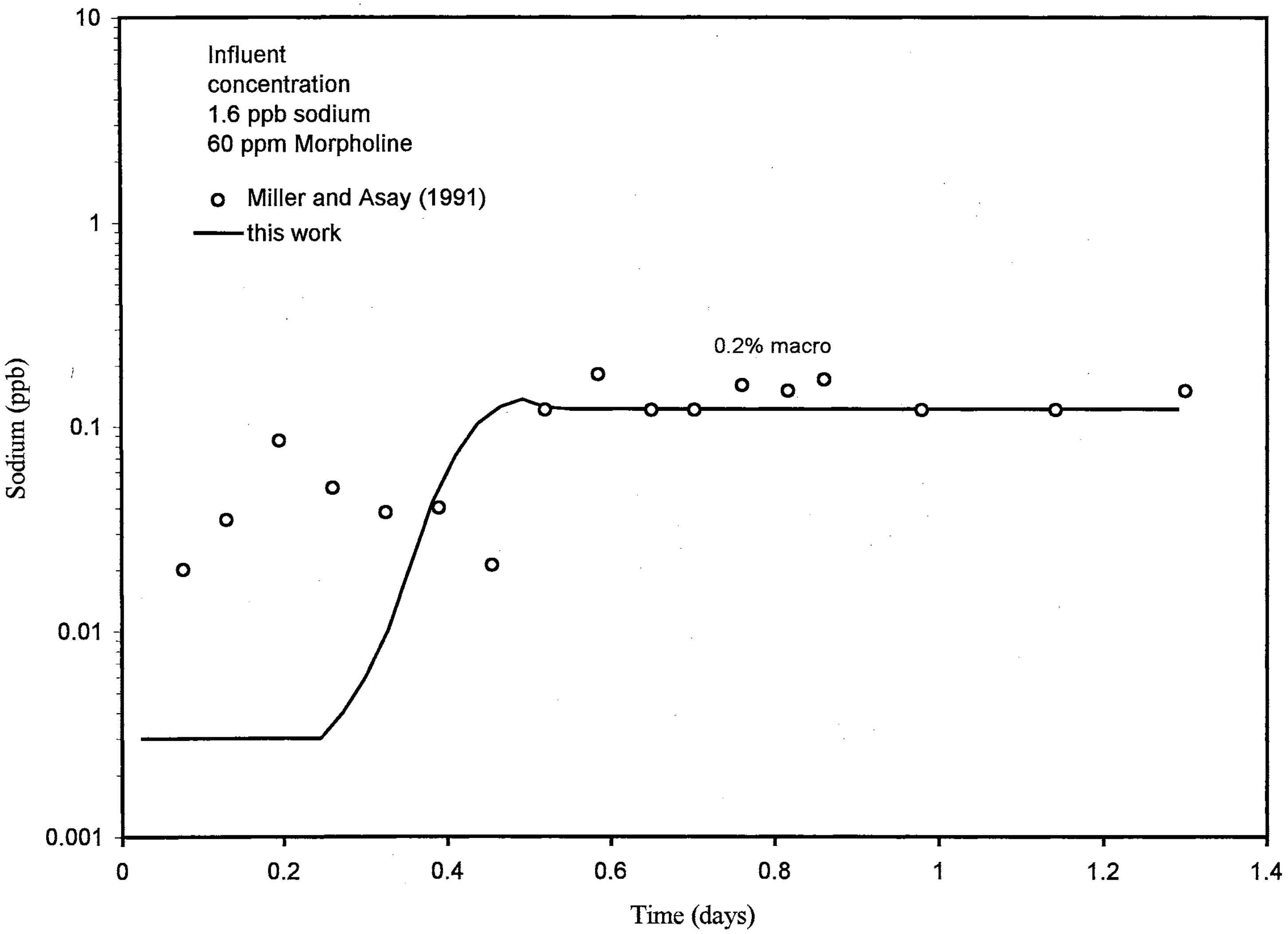

Figure 13. Comparison of predicted profile with experimental data

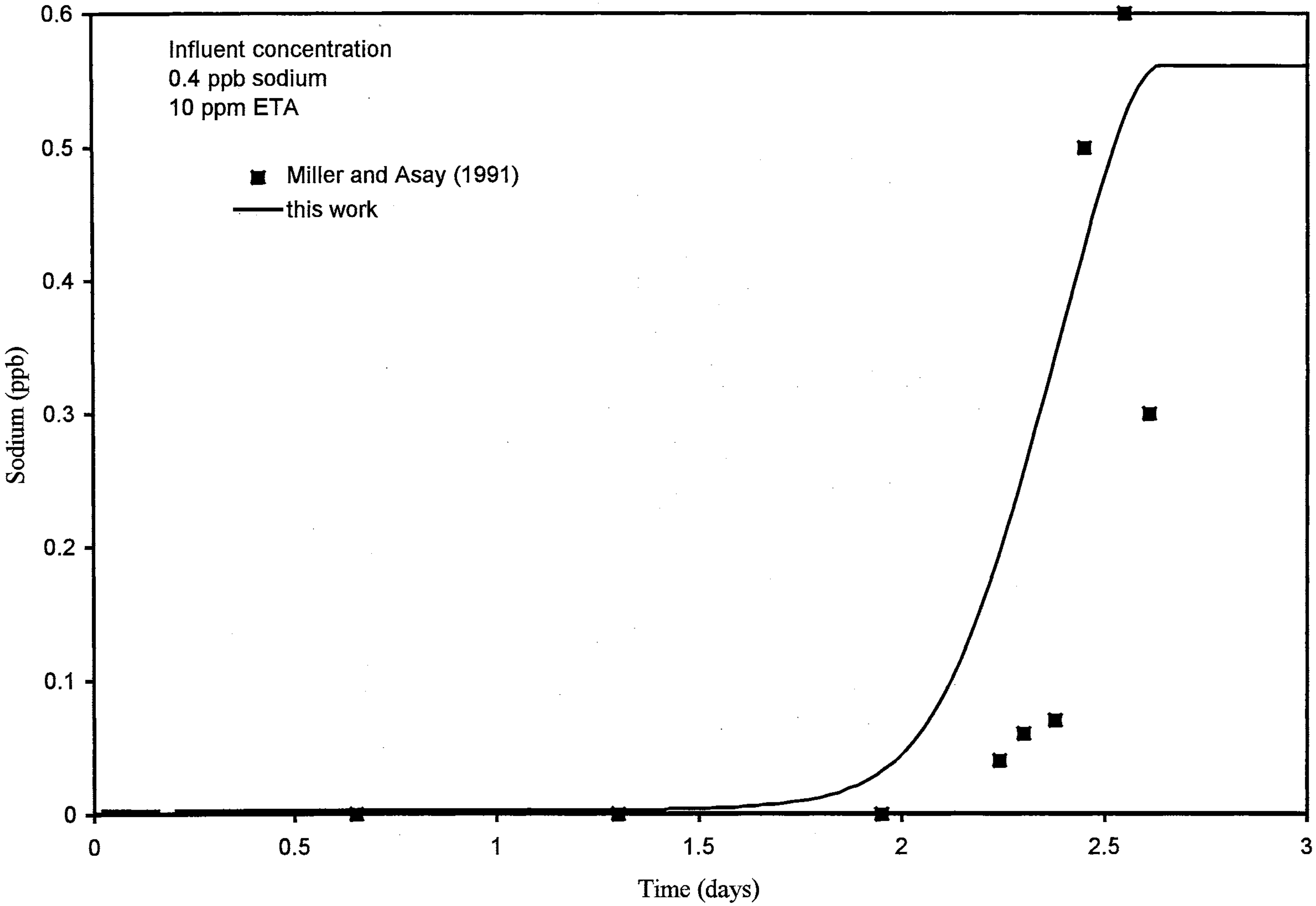

Figure 14. Predicted sodium throw compared with experimental data

Simulations of Industrial Operation

A model that can predict accurately the effluent concentrations for both the amine and primary ionic contaminants can be used to analyze potential operating conditions and the timing for resin regeneration. Instead of expensive trial-and-error experimentation, a relatively inexpensive way of testing hypothetical scenarios is by simulating them. The model can be used for simulating such scenarios. The model can also be used as a tool to evaluate long-term operating criteria.

The capability of the model as a simulation tool is demonstrated here. Operating conditions at Oldbury power station (Table IV) have been used as the model input parameters. A series of computer runs are presented and their potential impact on Oldbury operation are evaluated. The analysis presented here is case specific. Hence results of the simulations cannot be concluded as being generally applicable to other scenarios. Simulation and result analysis has to be undertaken on a case-by-case basis since system properties differ; these differences have the potential to impact some of the conclusions.

Effect of Flow Rate Change

Oldbury operates a newly regenerated bed initally at 400 gpm for 6.6 days in order to dilute the sodium concentration with the total flow from the other beds. After 6.6 days the flow rate to the bed is doubled to a value of 800 gpm. Figure 15 presents predicted sodium effluent curves as a function of the percentage of full flow

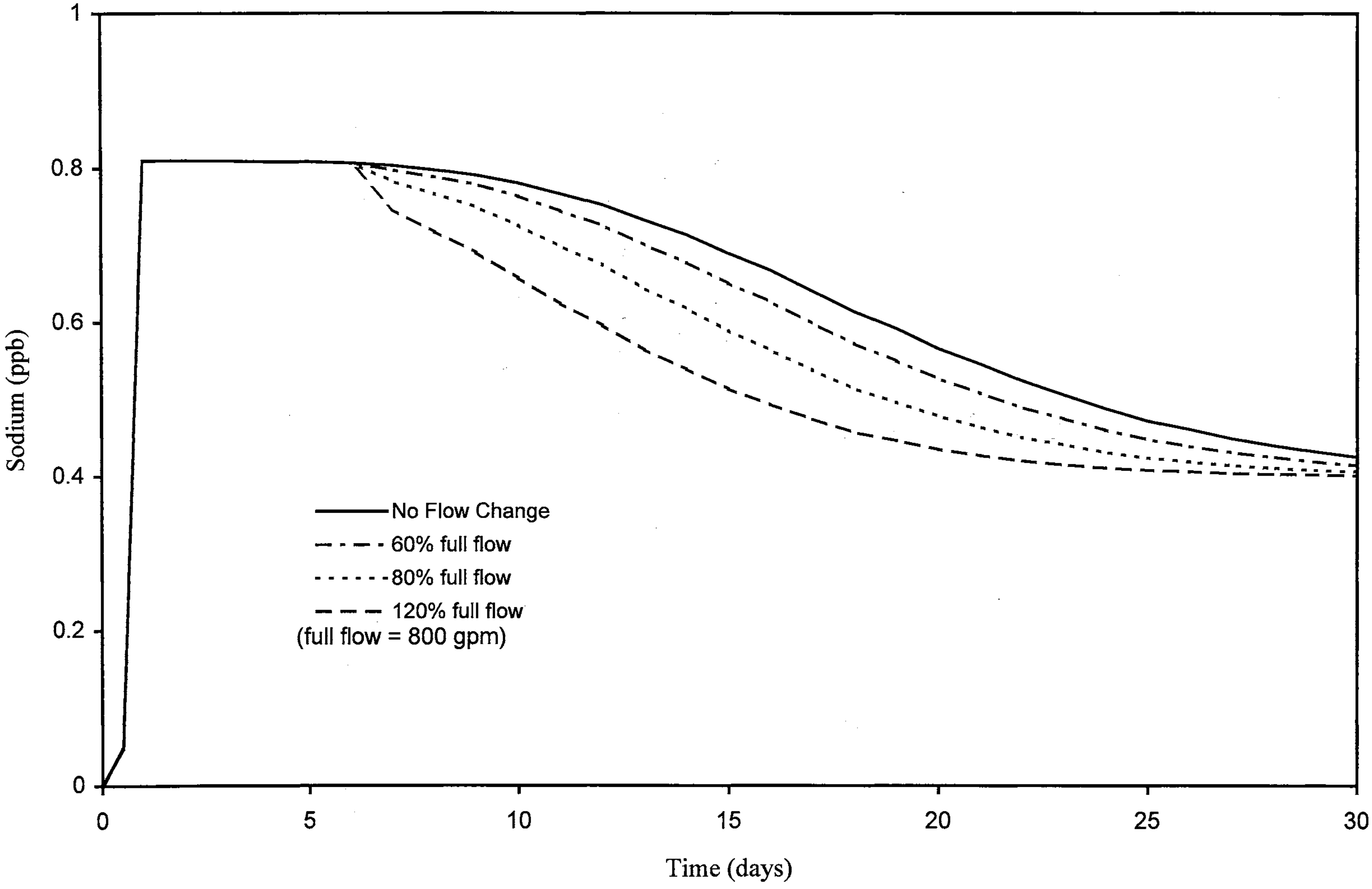

Figure 15. Predicted sodium profile with different flow rates starting at day 6.6 of operation

used after 6.6 days. In Figure 15, no flow change represents continued operation at 50% of full flow, or 400 gpm. The primary observation is that different operating lines exist at each flow rate. Changing the flow rate results in a shift to a new sodium throw curve. Increasing the flow rate dilutes the sodium released from a particular bed, since a finite amount of sodium fixed on the resin is released into an increased amount of processed water. All curves approach the 0.4 ppb feed concentration asymptotically.

Figure 16 presents simulations for different times at which full flow is initiated. Bed operation is most efficient at full flow (800 gpm). As a result, the initial reduced flow should be increased — to full flow — as early as possible. At the current operating condition, with flow increasing at 6.6 days, a concentration drop of 0.04 ppb is predicted. But changing to full flow at 4.6 days will give a lower effluent sodium concentration for a longer duration, and eventually gives the same sodium effluent concentration as the other operating lines.

The point at which the sodium throw curves intersect represents the earliest possible time at which full flow could be used without expecting an increase in sodium concentration from the bed. This point occurs at about three days. If sodium concentration from a bed operating at half flow is averaged with full flow from three additional beds each having a 0.4 ppb effluent concentration, the overall sodium concentration is expected to be 0.46 ppb. Doubling the flow at day three for this bed will result in a concentration of 0.5 ppb. Waiting until 6.6 days would give an expected total concentration of only 0.01 ppb less. This difference would not be detectable in operation.

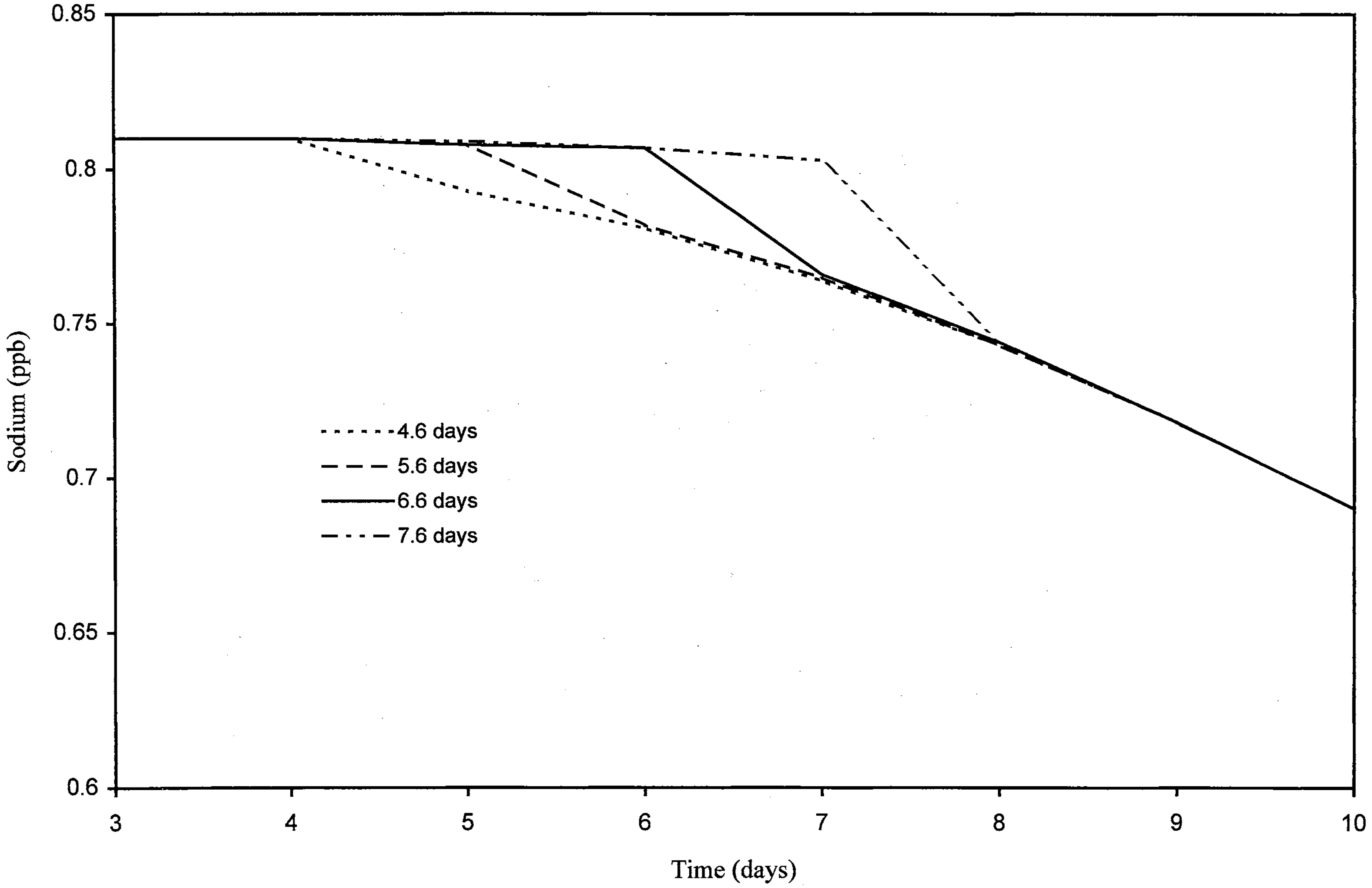

Figure 16. Sodium effluent transition at different times for the step change from half to full flow (800 gpm)

Effect of Initial Resin-Phase Sodium Concentration on Sodium Throw

The efficiency of resin regeneration is critical to the effluent concentration observed during sodium throw. In this study, regeneration efficiency is defined as the percentage of residual cation-exchange sites in the sodium form when the bed is returned to service. The sodium/amine selectivity of the cation-exchange resin also influences the sodium-throw peak concentration. For modeling purposes, the actual selectivity of the resin should be determined in order to get an accurate prediction of the bed performance. Table VI presents the selectivity coefficient of resins used in this study. The selectivities were measured for condensate polishing plant conditions at Oldbury (Sadler et al., 1988).

TABLE VI

Resin Selectivity Data

Resin	Type	Ion in the resin-phase	Exchanging bulk-phase ion	Selectivity Coefficient
Ambersep 900	Anion	Hydroxide	Chloride	17.0
Ambersep 252	Cation	Hydrogen	Sodium	2.0
		Morpholinium	Sodium	2.1
Ambersep 200	Cation	Hydrogen	Sodium	2.5
		Morpholinium	Sodium	46.0
Amberlite IR120	Cation	Hydrogen	Sodium	1.5
		Morpholinium	Sodium	0.96

Figure 17 presents predicted curves as a function of resin regeneration efficiency for Ambersep 252. A residual sodium concentration of 0.2% gives a sodium throw of 0.81 ppb; 0.6% gives 3.1 ppb; 1.0% gives 5.2 ppb; and 2.0% gives 10.3 ppb. The need to minimize the sodium loading after regeneration is obvious.

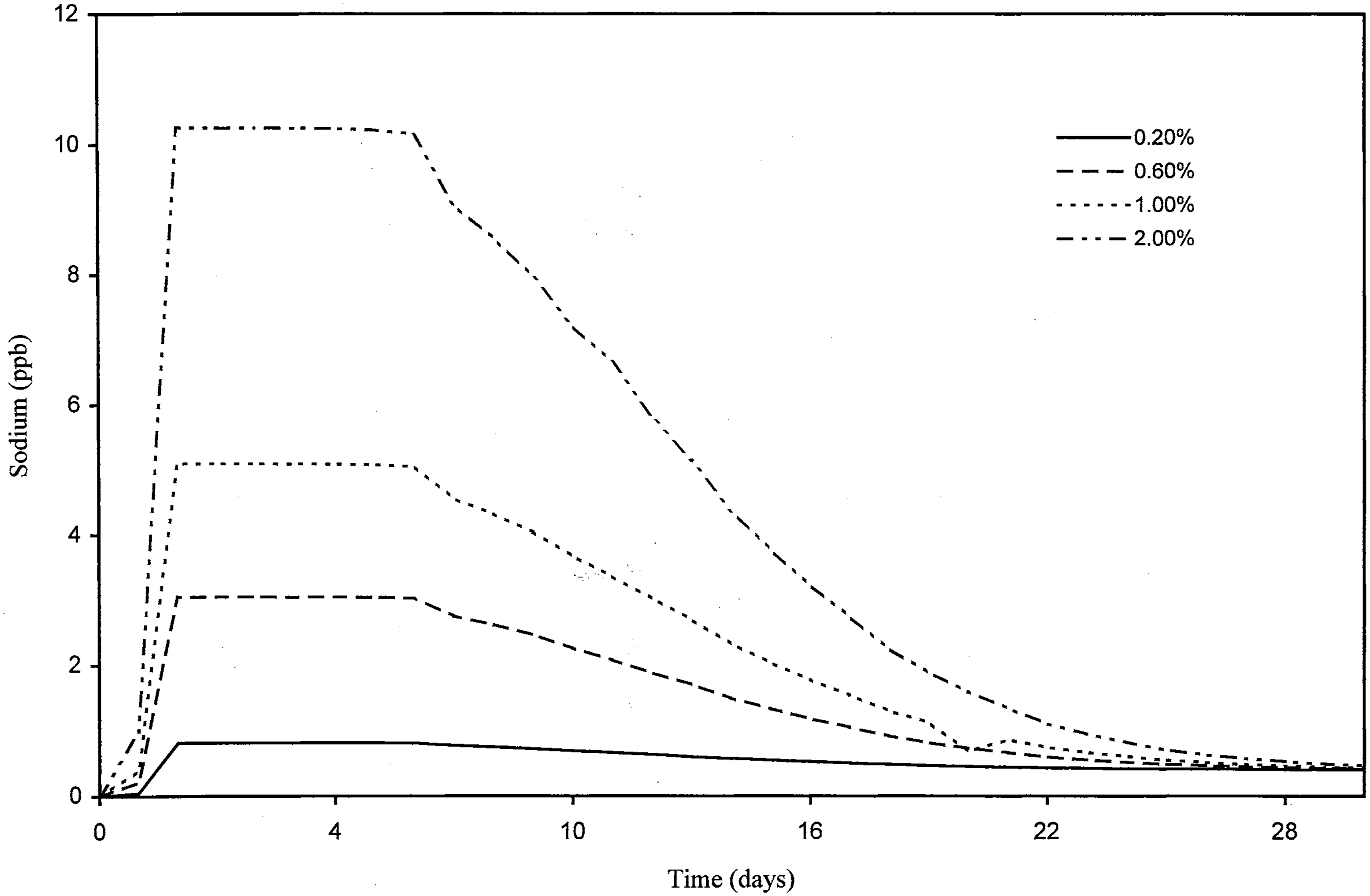

Figure 17. Effluent sodium concentration at different regeneration efficiencies for Ambersep 252

Figure 18 presents similar curves for Amberlite IR120. The expected sodium throw is much greater, but the rinse down time to the feed concentration is also much improved. The area under the curve above the feed concentration should be the same for both resins using the same initial sodium loading.

Effect of Changing Cation-to-Anion Resin Volume Ratio

Figure 19 presents the effect of changing the cation-to-anion resin volume ratio on the predicted sodium and chloride effluent concentrations. An inlet concentration of 0.4 ppb sodium and 0.62 ppb chloride is used. Inlet water is dosed with 60 ppm morpholine. The cation-exchange resin converts to the morpholine form in less than a day. A bed with 2:1 cation-to-anion resin volume ratio takes a slightly longer time to morpholiniate than a bed with 1:1 ratio, due to the higher cation-exchange capacity.

The sodium-throw peak concentration is 0.94 ppb. This value is independent of the cation-to-anion resin volume ratio, but depends on the initial sodium loading on the cation-exchange resin. Hence there is a minor difference in the initial sodium concentration exiting the bed and not the sodium-throw peak concentration. However, a longer time is taken by the bed with higher cation-exchange resin volume to achieve feed concentration due to higher sodium content.

Figure 19 also presents the chloride effluent profile. The effluent chloride concentration is low compared to sodium concentration. The high anion-exchange resin selectivity for chloride will result in higher chloride removal. The anion-exchange resin has nearly an order of magnitude higher selectivity for chloride

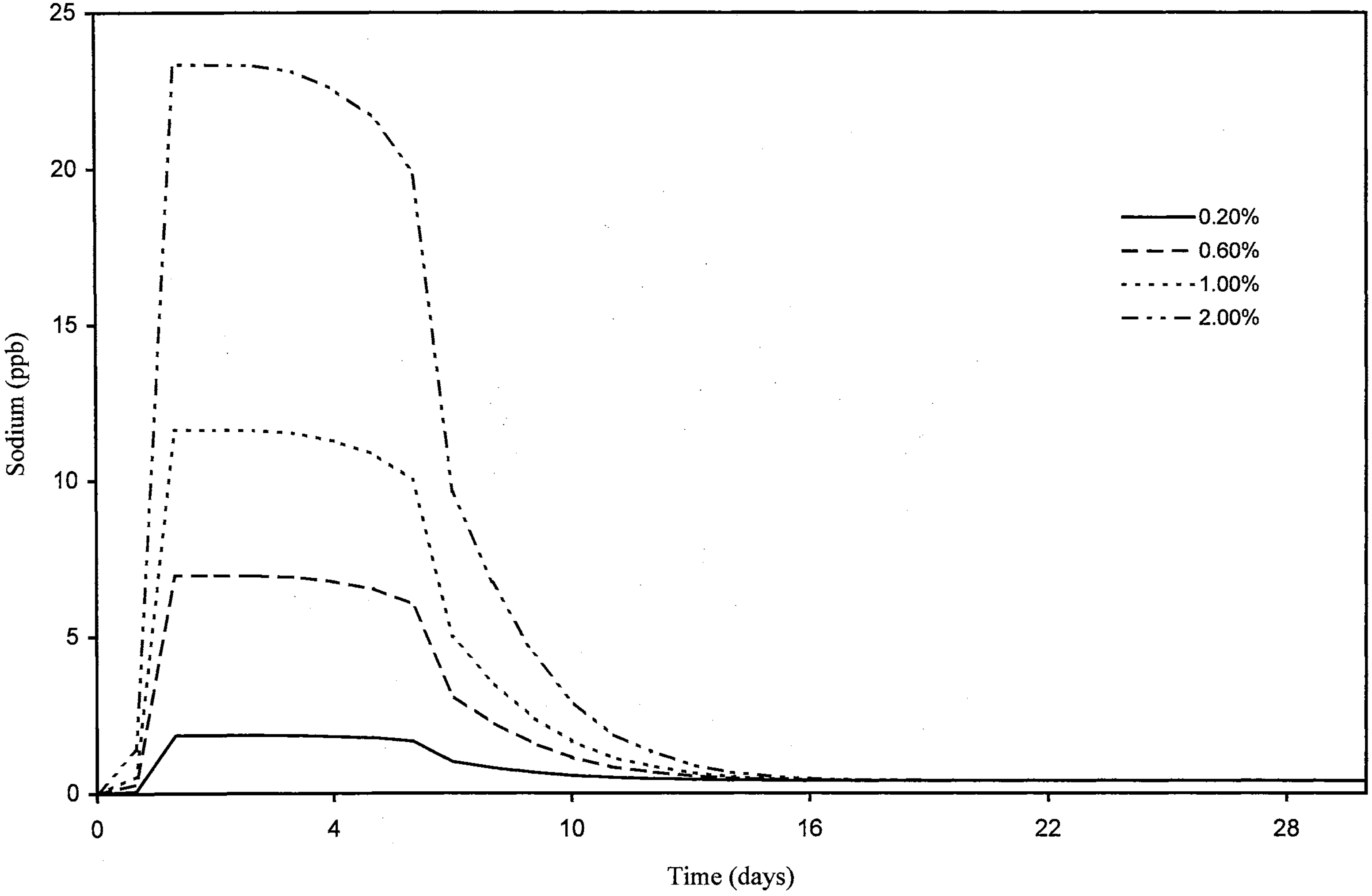

Figure 18. Effluent sodium concentration at different regeneration efficiencies for Amberlite IR 120

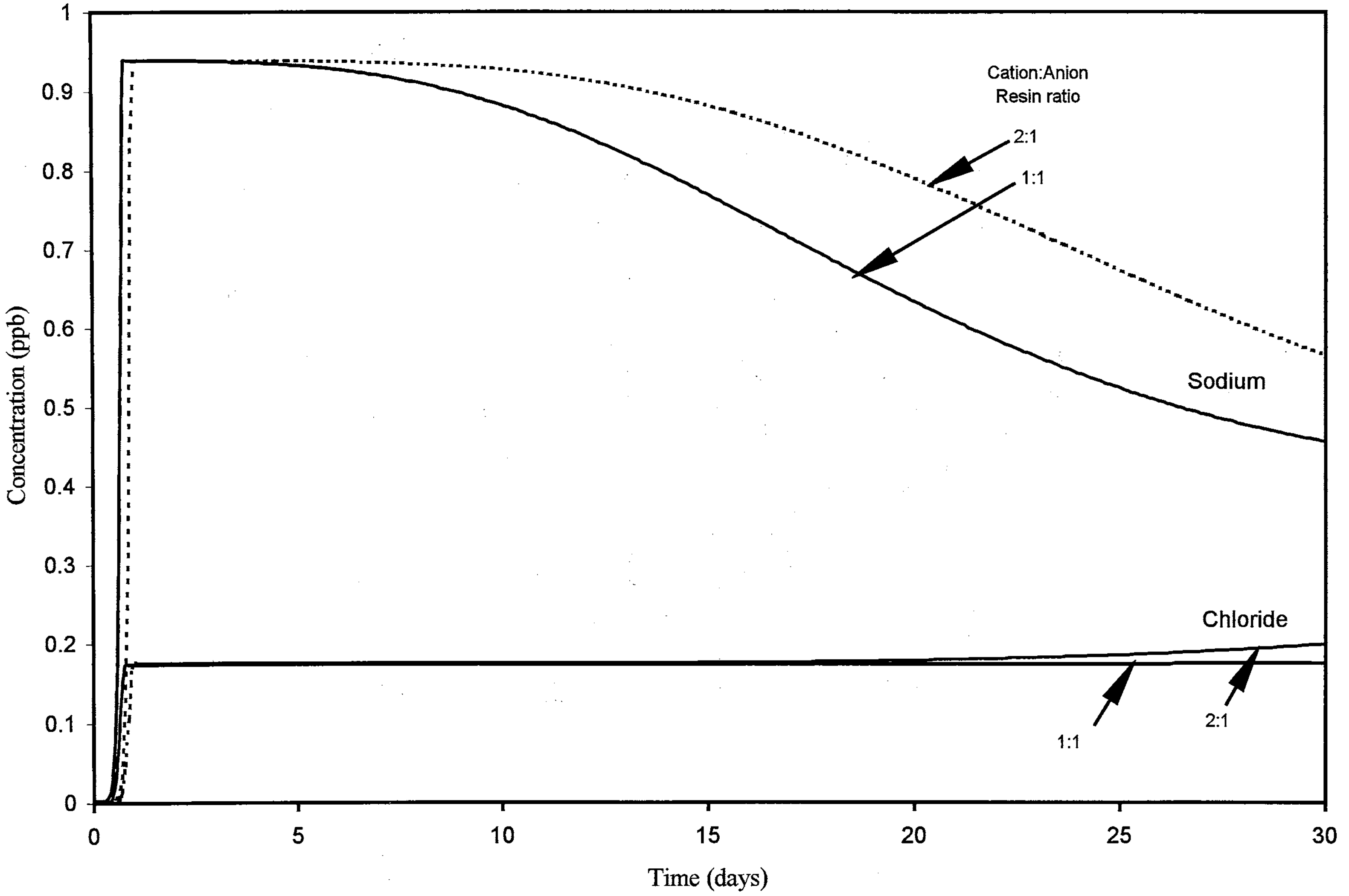

Figure 19. Effect of cation-to-anion resin volume ratio on predicted sodium and chloride effluent concentration

when compared to sodium selectivity of the cation-exchange resin. The higher hydroxide concentration in the bed, due to the amine, also favors chloride exchange.

Chloride concentration from the bed with higher cation-exchange resin increases earlier than the bed with a lower cation-exchange resin volume. This can be explained by the change in effective capacity. An increase in the cation-to-anion resin volume fraction from 1:1 to 2:1 represents a capacity gain of 34% for the cation-exchange resin and a capacity loss of 67% for the anion-exchange resin (resin capacities are given in Table IV). Hence higher chloride leak concentrations can be expected.

Figure 20 shows the bed profile of resin-phase morpholine concentration. Higher cation-exchange resin fraction in the bed results in higher concentration of morpholine being removed. This is one of the drawbacks of operating at higher cation-to-anion resin ratio. The reduced morpholine concentration at the outlet will decrease pH, and hence additional morpholine has to be dosed. This increases the cost of operation. Figure 21 presents the associated pH profile in the bed. The pH in a bed containing higher cation-exchange resin fraction is lower compared to a bed with lower cation-exchange resin fraction due to greater removal of morpholine. The pH rises to the operating value of 9.65 as the cation-exchange resin in the bed saturates with morpholine.

Effect of Using Different Amines

Several different amines have been tested as pH-control agents (EPRI TR-102952, 1993). The effect of amines on effluent sodium and chloride concentration

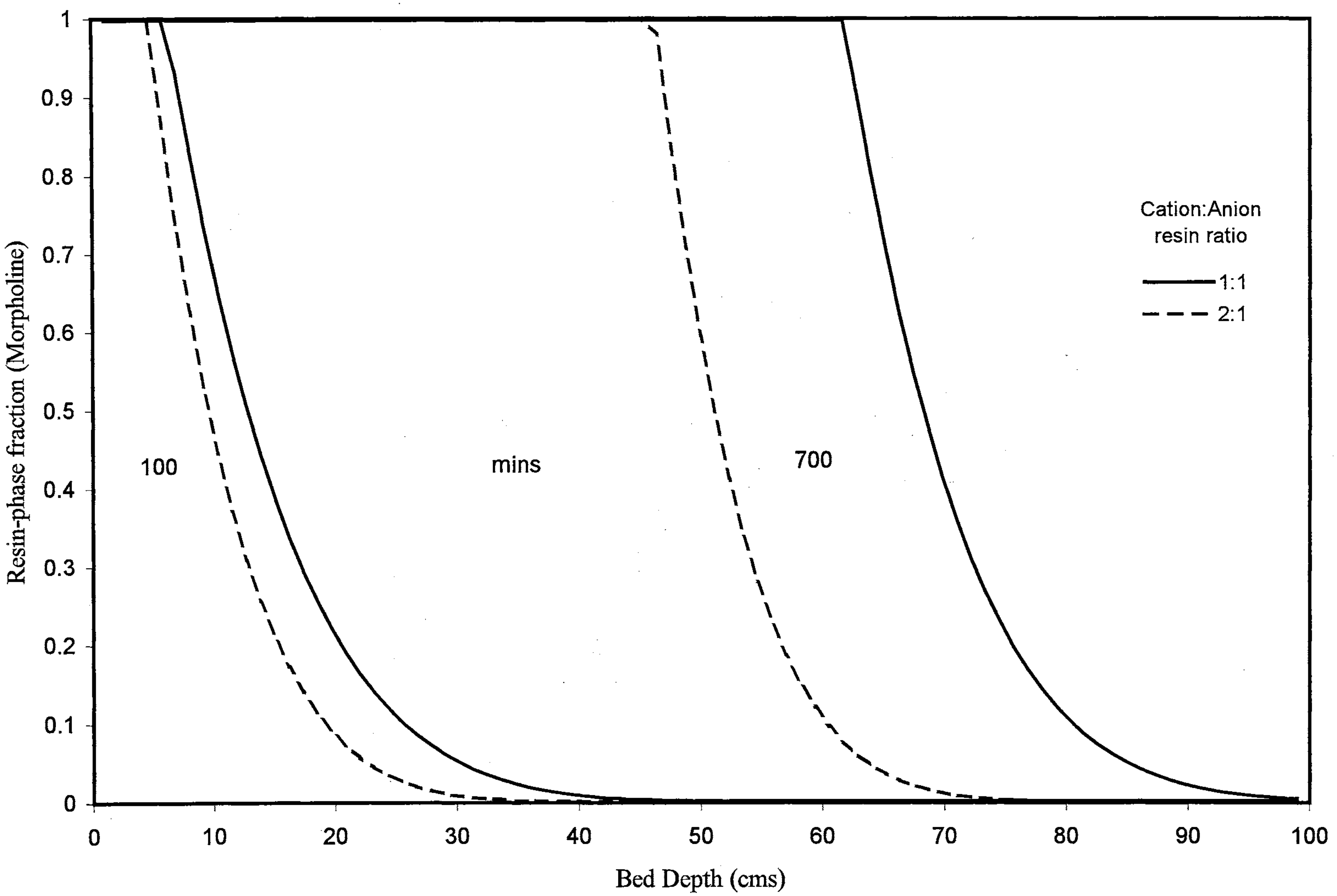

Figure 20. Bed profile of morpholine loading on the resin

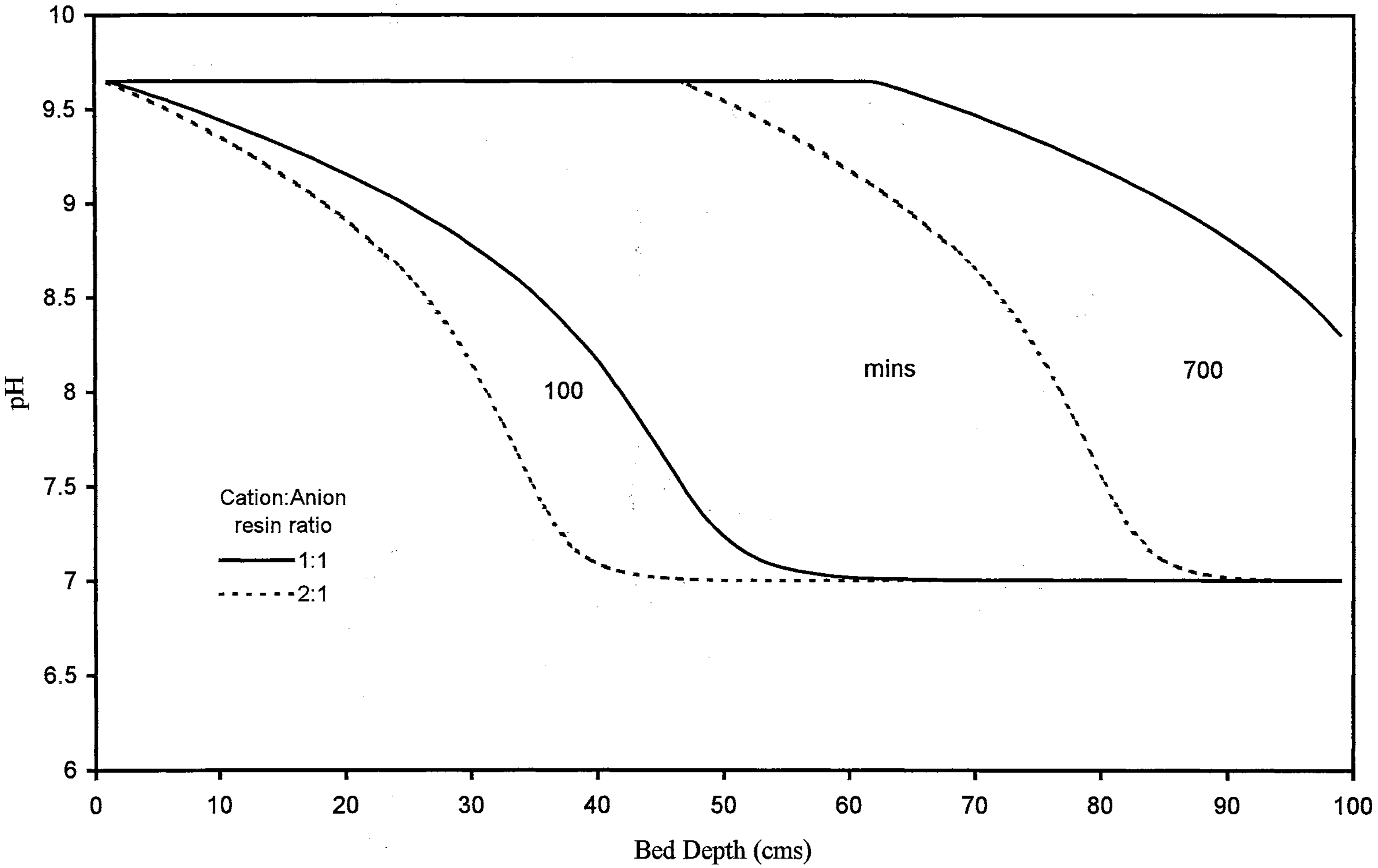

Figure 21. Predicted pH profile in the bed with different cation-to-anion resin volume ratios

is studied. For purposes of comparison, three amines were choosen — ammonia, ETA, and morpholine. All operating criteria were held constant. An operating pH of 9.65 is used. Different feed concentration of the amines — 2.6 ppm ammonia, or 6.5 ppm ETA, or 60 ppm morpholine — had to be used to obtain a pH of 9.65, due to differing base strength of the amines. Transport and equilibrium coefficients for the amines are presented in Table II.

Figure 22 presents a comparison of the breakthrough profile of different amines. The concentration of morpholine in the feed is extremely high, and hence saturates the cation-exchange resin very quickly. This results in an early breakthrough of morpholine. Ammonia and ETA breakthrough take a longer time, 3.8 and 5.4 days, respectively. An important observation is that ETA has a delayed breakthrough compared to ammonia even though the feed concentration is higher.

The differences in breakthrough times are due to dissociation of the amines. At any given concentration, percent ionization of ETA is higher than ionization of ammonia. For example, at 5 ppm concentration, 45% of ETA is ionized while only 22% of ammonia is ionized. The different concentration of undissociated and dissociated amine results in different transport rates, and hence the difference in breakthrough time. Lower concentration of ionized amine results in earlier breakthrough. Experimental data presented in Table VII validates this observation.

The experimental conditions for the data presented in Table VII were identical for all experiments, only inlet amine concentrations were different. The difference in breakthrough times for ETA and AMP are small compared to ammonia breakthrough time; although the concentration of ETA was five times greater, and the concentration of AMP was six times greater than ammonia concentration.

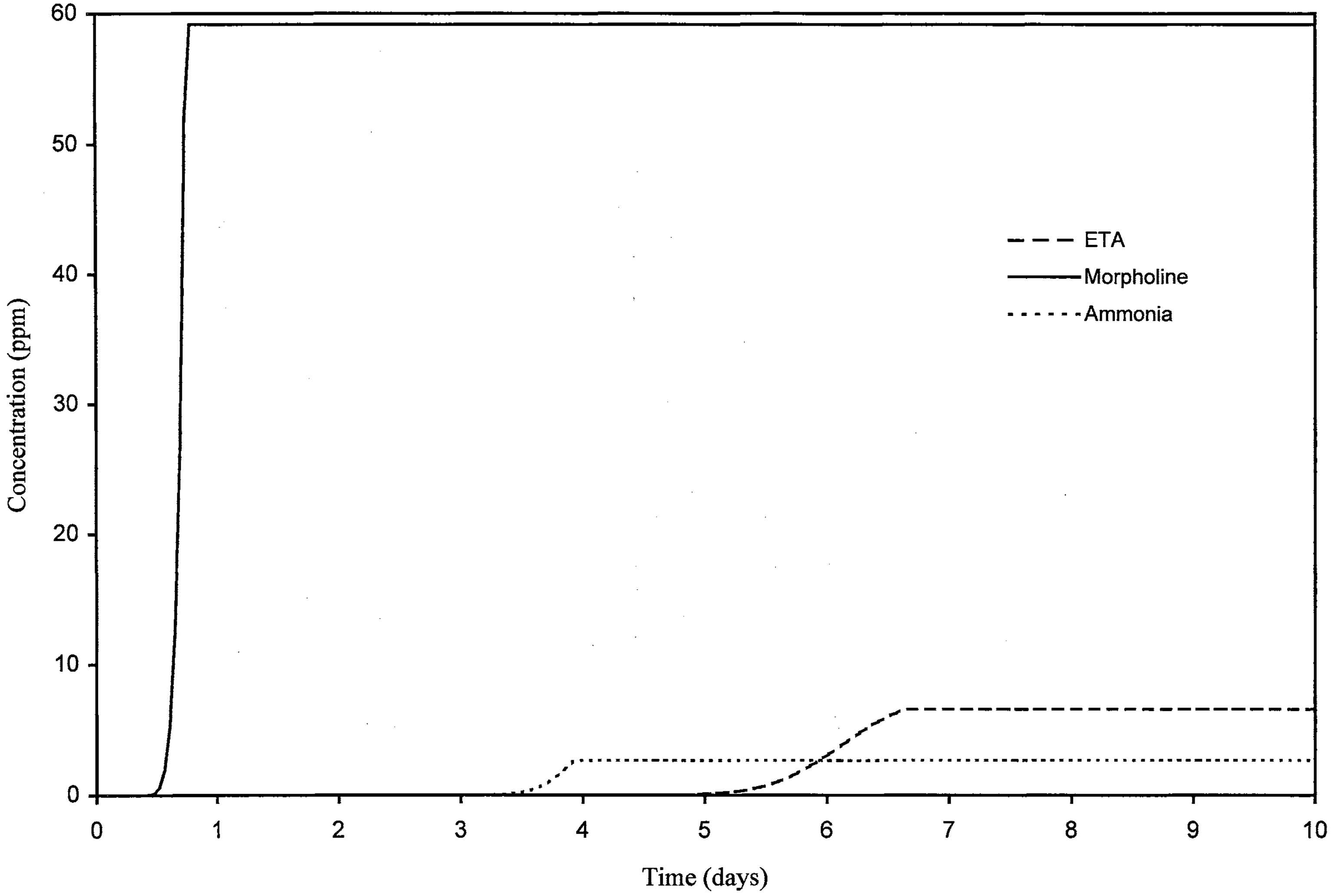

Figure 22. Predicted amine breakthrough curves at operating pH of 9.65

TABLE VII

10% Breakthrough Times for Different Amines using Macro Cation-Exchange Resins (EPRI TR-104299)

Amine	Feed concentration (ppm)	Breakthrough time (days)	pK_b
Ammonia	2.0	3.5	4.75
ETA	10.0	2.5	4.5
AMP	12.0	3.0	4.3

Early saturation of the cation-exchange resin is expected at higher concentrations of the amine. Hence very early breakthrough of ETA and AMP should have been expected compared to ammonia. But the difference in base strength results in very close breakthrough times of the amines to each other. Ammonia has low base strength compared to ETA and AMP.

Figures 23 and 24 present the effluent profile of sodium and chloride. Operation with ammonia gave a very high sodium-throw peak concentration (4.3ppb). The sodium throw concentration with morpholine was 0.8 ppb, and operation with ETA gave the lowest concentration of 0.45 ppb. The differences in selectivity of amine over sodium determines the sodium throw concentration. Selectivities of the amines over sodium is presented in Table III. Sodium throw concentration with ammonia operation levels to the feed sodium concentration very rapidly.

The effluent chloride concentrations, shown in Figure 24, are below 0.2 ppb for 10 days of operation. Operating with ETA gave the lowest initial chloride leak values, but was slightly higher than operation with other amines after the bed converts to the amine form.

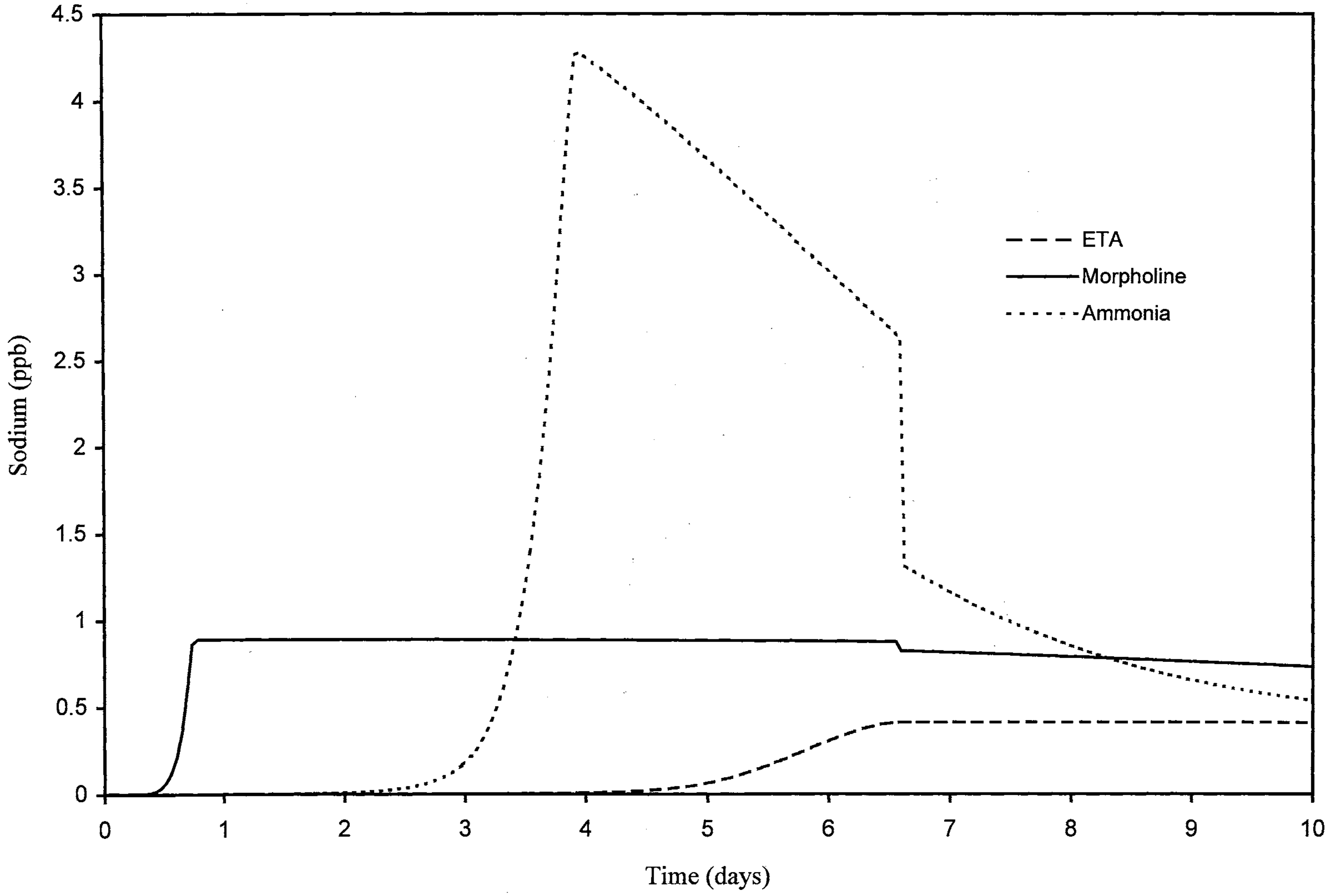

Figure 23. Predicted sodium effluent profile using different amines

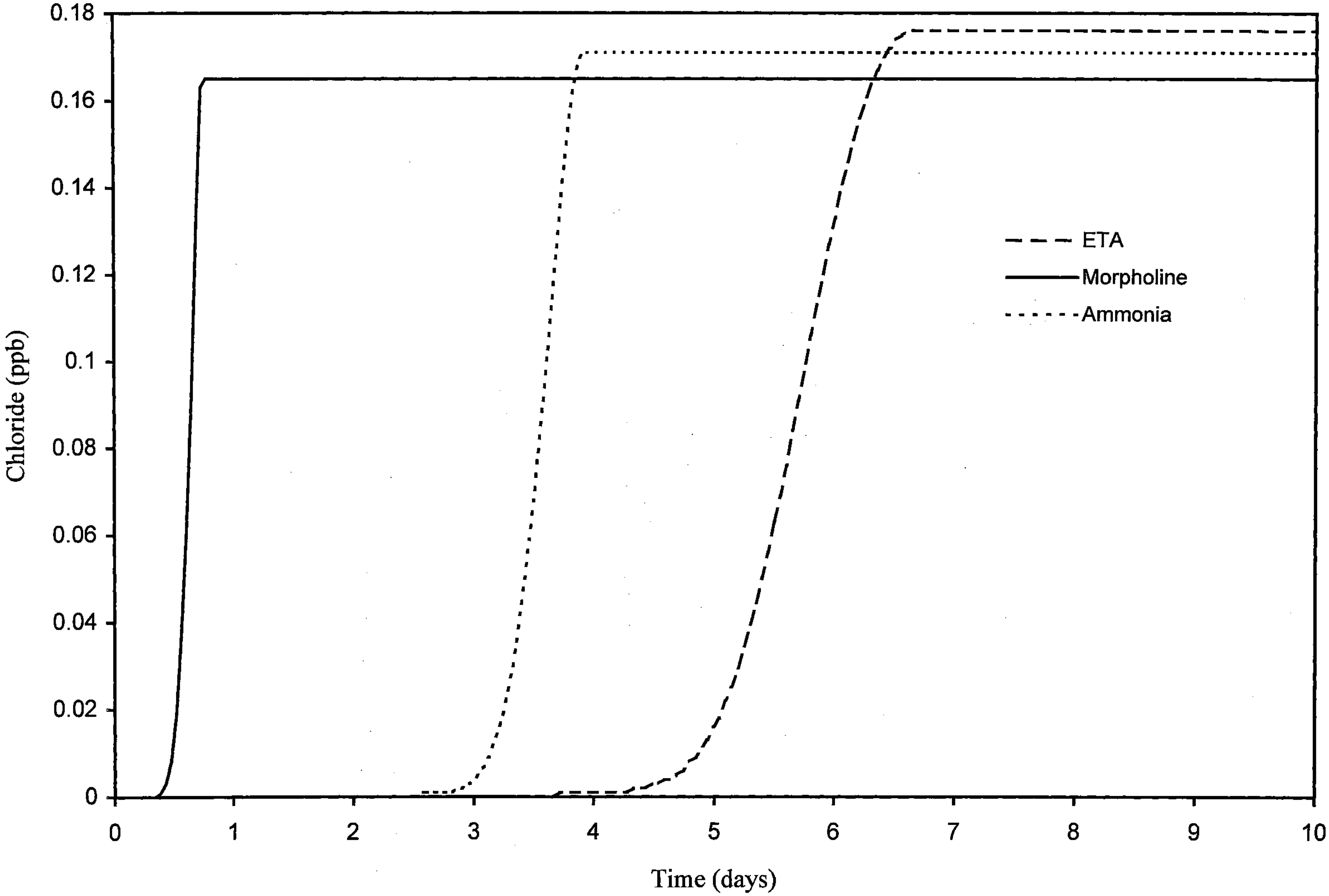

Figure 24. Predicted chloride effluent profile using different amines

Effect of Tube Leaks on Mixed Bed Performance

Effectiveness of mixed beds can also be measured by their capacity to contain condenser leaks. Cooling water ingress contributes to both suspended and dissolved solids in the condensate. Plants using brackish water or sea water will have additional concerns due to higher in-leakage concentrations. For example, a 0.5 gpm sea water leak (average dissolved solids concentration of 35,000 ppm) into a condensate flow rate of 1000 gpm can increase the dissolved solids concentration by 17.5 ppm. Hence the impurity removal efficiency of mixed beds at increased influent concentrations need to be known. Effectiveness of the mixed bed is determined by knowing how long an existing bed can operate under tube leak conditions before reaching mandatory shutdown conditions.

MBIE units provide protection against tube leaks to a certain extent. Sadler et al. (1988) found that a morpholine form bed had contained a short duration (5 hours) 120 ppb sodium leak successfully in a simulated condenser leak experiment. The mixed bed responded to the short duration leak by a slight increase in the effluent sodium concentration from 0.4 to 0.5 ppb. The sodium leak gradually increased to 2 ppb in 4 days. There was no detectable change in chloride concentrations. They found that the polished effluent maintained a sodium concentration of less than 1 ppb for more than two weeks after an actual plant leak incident. The cation-exchange resin was in the morpholine form and the tube leak was about 10 ppb.

Figure 25 presents the sodium profile expected for Ambersep 252 with an initial sodium loading of 0.2% for a 120 ppb sodium feed beginning on day 10 and

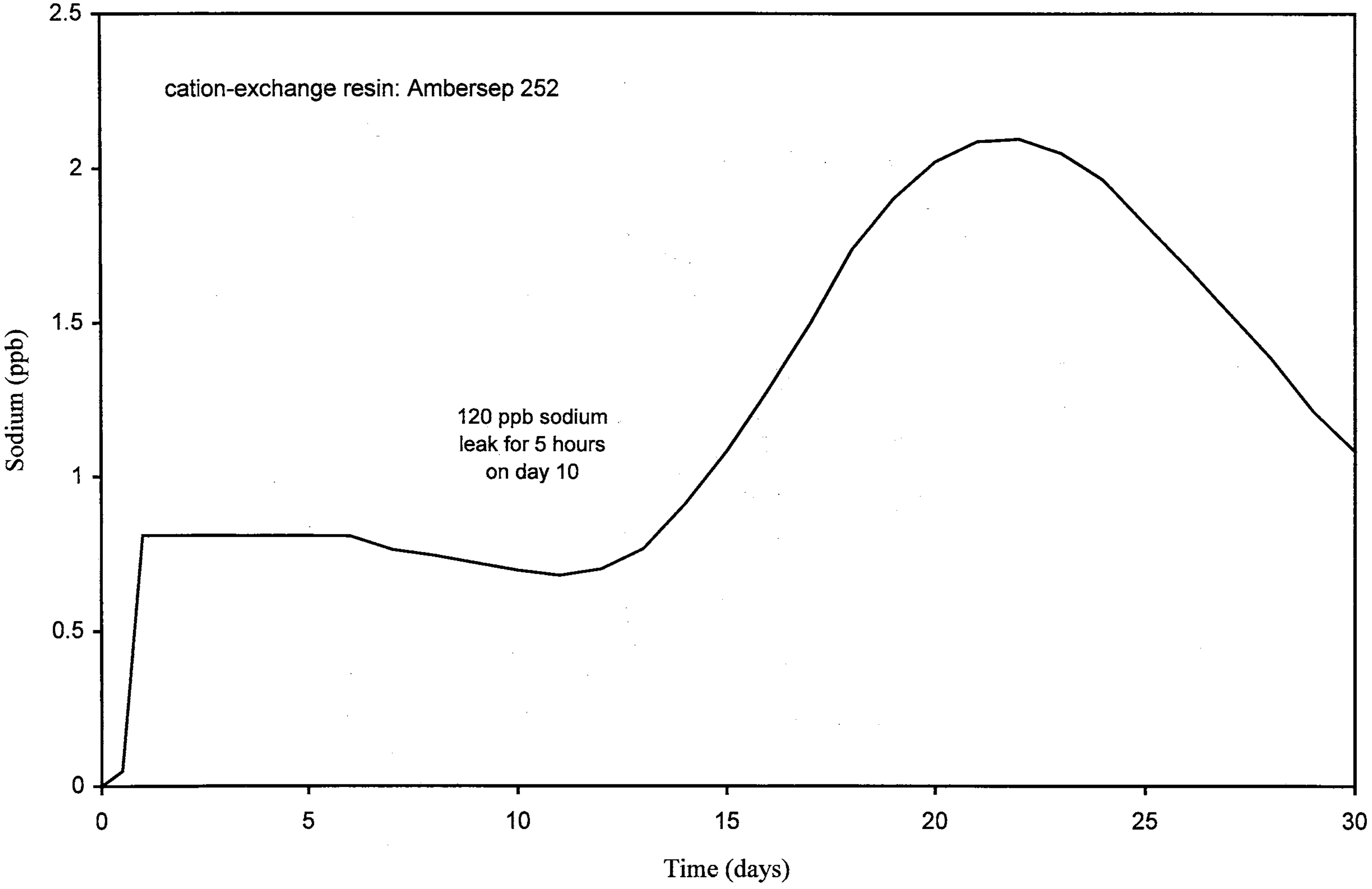

Figure 25. Effluent sodium concentration with a condenser leak

lasting for five hours. For a short duration leak of this type, the bed has significant exchange capacity and the 120 ppb feed concentration is not approached within 30 days of operation. A residual sodium throw curve is predicted due to kinetic leakage as a result of the significantly higher concentration of sodium fed to the bed during the leak.

Figure 26 presents a comparison of resin types for a step change from 0.4 to 10 ppb sodium at day 10. Compared to Figure 25, the same amount of additional sodium is added in 60 hours, but in this case the 10 ppb sodium concentration remains constant for the next 20 days. The result is that the effluent sodium concentration increases gradually to the feed concentration. This result is reasonable for amine cycle operation where the resin prefers morpholine to sodium, however, the same effect would not be expected in the hydrogen cycle where sodium is preferred over hydrogen. Figure 26 also shows the effect of sodium-morpholinium selectivity on the effluent sodium concentration in a condenser leak scenario. Ambersep 200 had the highest morpholine-sodium selectivity (Table VI), hence the lowest sodium effluent concentration compared to the other two resins.

Mixed bed behavior with different amines, in a simulated condenser leak scenario, is presented in Figures 27 and 28. The operating pH used was 9.65 — to obtain this pH, 2.6 ppm ammonia or 60 ppm morpholine is used. A short duration (5 hours) sodium chloride leak on day 10 was simulated. By day 10, the cation-exchange resin in the mixed bed has been converted completely into the amine form. High concentrations of sodium (4 ppm) and chloride (6.2 ppm) were used for the leak simulation.

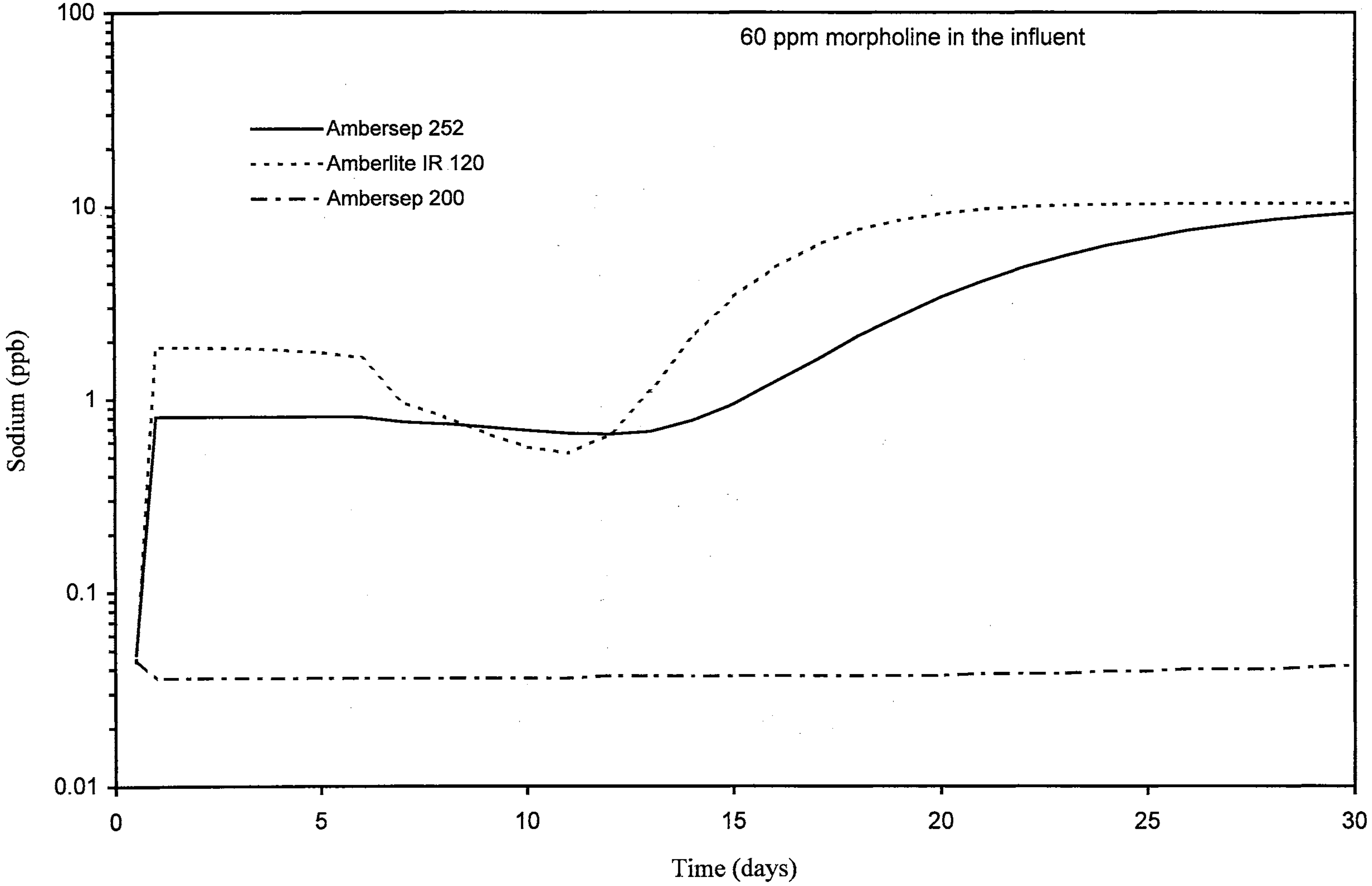

Figure 26. Predicted sodium profiles for a 10 ppb condenser leak on day 10

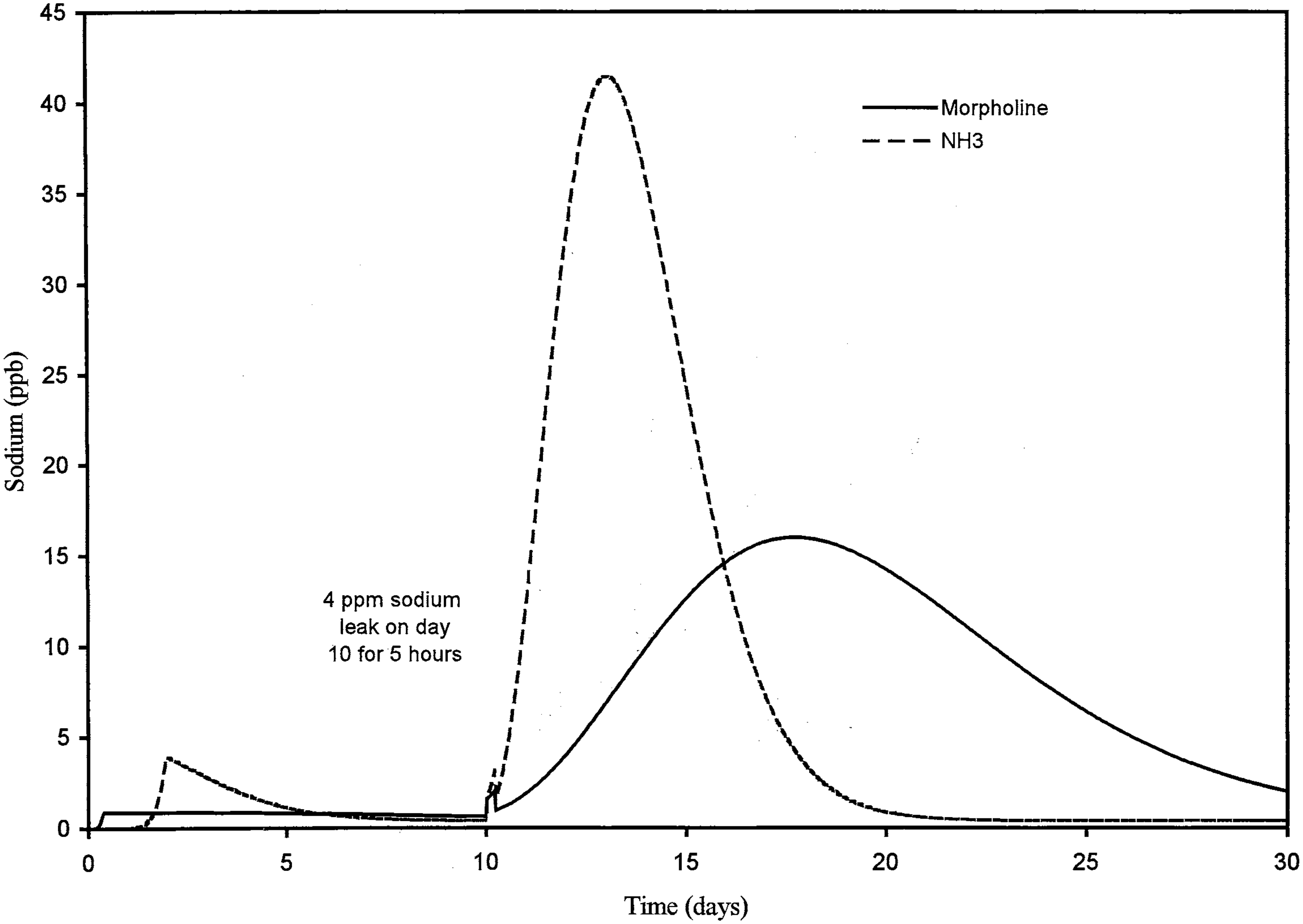

Figure 27. Predicted sodium profile for a condenser leak scenario with different amines

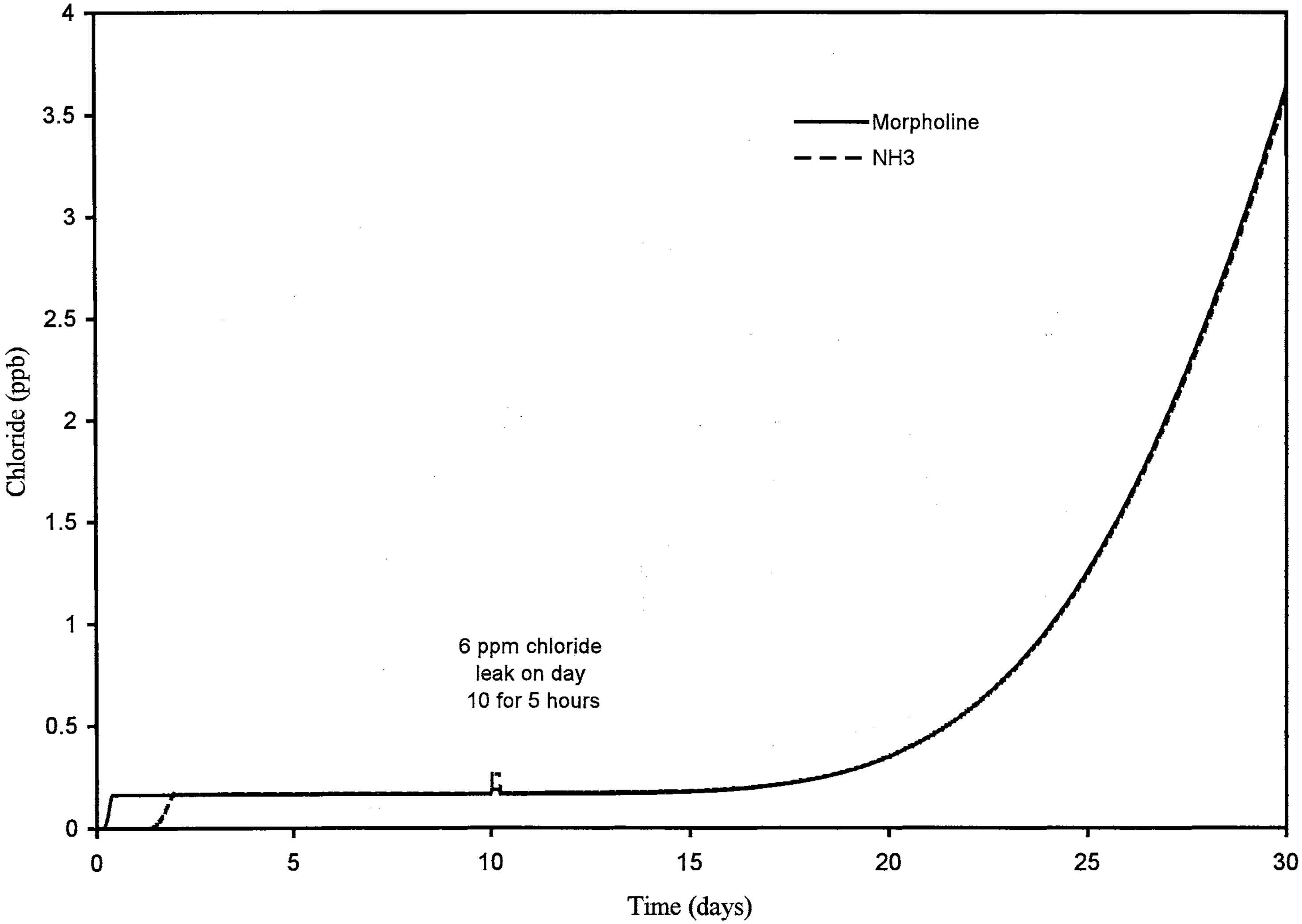

Figure 28. Predicted chloride profile for a simulated condenser leak scenario using different amines

Figure 27 shows the sodium effluent profile. Sodium slip from the bed operating with ammonia reaches a peak concentration of 42 ppb by day 12. The bed operating with morpholine shows a small sodium spike immediately following the leak; the peak sodium concentration reaches around 15.5 ppb on day 18. Cation-exchange resin selectivity of amine over sodium results in different sodium profiles; ammonium ion is preferred over the sodium ion. However, when operating with morpholine, the cation-exchange resin prefers the sodium ion over the morpholinium ion. The high concentration of sodium ions during the leak, comparable to ionic amine concentration, will favor and increase the ion-exchange rate. Hence sodium removal capability of the mixed bed is good. Due to the selectivity advantage in morpholine operation, lower sodium effluent concentrations are observed.

Figure 28 presents the predicted chloride profile with a condenser leak. Using the two different amines did not produce any difference in predicted effluent chloride profiles. The anion exchange rate is favored in amine cycle operation due to high hydroxide concentration in the bulk phase. The predicted chloride profile shows a small increase in outlet concentration initially following the leak, kinetic leakage may be the contributing factor. But chloride concentration in the effluent is 0.2 ppb till day 18. The chloride effluent concentration reaches a value of 3.6 ppb by day 30. The mixed bed performed very well in containing the 6.2 ppm chloride leak.

Conclusions

Weak electrolyte mass transport models available in literature ignore electrostatic influence of ionic form of the weak electrolyte on mass flux of other electrolytes in solution. In this work, electrostatic influence of the ionic form of the weak electrolyte on mass flux of other electrolytes in the system is accounted. Importance of mass transport of the different forms of weak electrolyte is presented.

The weak electrolyte model has been used to describe amine transport in mixed bed ion-exchange. Amine, sodium, and chloride effluent concentration profiles from an MBIE column have been predicted. The model predictions were compared with laboratory data and data from an operating power station; the predictions compared favorably. The predicted sodium effluent profile was in the range ±10% of the data. The predicted amine effluent concentrations matched the data very well.

Specifically, the amines studied were: ammonia, ETA, and morpholine. The model presented here is not specific to a particular type of amine. Availability of physiochemical properties data limited this study to the three amines. Use of the model as a tool to optimize performance and enhance mixed bed operation is demonstrated.

CHAPTER IV

LIQUID PHASE MASS-TRANSFER COEFFICIENT IN MIXED BED ION-EXCHANGE

Introduction

Mixed-bed ion-exchange (MBIE) units, usually operated as fixed beds, are used extensively in manufacturing high-purity water. Mixed beds consist of a mixture of cation and anion exchange resins; this accomplishes the removal of cation and anions simultaneously. Mixed bed ion-exchange is used to manufacture ultrapure water by the microelectronics and power industry. Steam condensate and make-up water is treated using MBIE in the power industry. The microelectronics industry uses high-purity water for cleaning wafer surfaces.

The shape of the effluent concentration profile (breakthrough curve) from an ideal mixed bed would be similar to the influent concentration profile. However, the effluent profile will have a time lag accounting for the residence time in the bed. But in a real system the effluent concentration profile is distorted. Mass-transfer resistances and dispersion influence the shape of the effluent concentration profile. Mass-transfer effects may be due to external or internal resistance, or a combination of both resistances. The kinetics of mixed bed ion-exchange, at low influent solute concentration, is controlled by external mass-transfer resistance.

This has been experimentally verified by Frisch and Kunin (1960) and Helfferich (1962).

The study of the kinetics of ion-exchange resins is an important tool for troubleshooting the operation of mixed beds. Deterioration of the mass-transfer kinetics, which manifests as a decrease in mass-transfer coefficient, results in poor quality effluent. Low mass-transfer coefficients result in the slippage of impurity from the column without exchange. Kinetic deterioration of anion-exchange resins in the power industry is a significant problem (Harries, 1984; Mc Nulty et al. 1986). Hence determining the kinetics of ion-exchange resins is critical. Harries (1984, 1987), McNulty et al. (1986), and Lee (1994) have done experimental work on ion-exchange kinetics.

Mass-transfer coefficient is one of the important parameters required for the design of a mixed bed ion-exchange column. The external mass-transfer coefficient, also called the film mass-transfer coefficient, is needed to predict the effluent concentration history. Mass-transfer coefficient is also used in predicting the dynamics of the system.

The mass-transfer coefficient is calculated using empirical or semi-empirical correlations, and is expressed as a Sherwood number or as the Chilton and Colburn factor (J-factor). Forced convection mass-transfer correlations make use of dimensionless groups: Sherwood, Schmidt, and Reynolds numbers (Cussler, 1984; Hines and Maddox, 1985). The hydrodynamic condition and diffusive transport are characterized by the Reynolds number and Schmidt number, respectively. Dimensionless groups such as particle diameter to bed height or particle-to-column diameter ratio are also used to improve correlations.

Some of the mass-transfer correlations under-predict the mass-transfer coefficient for the case of mixed bed ion-exchange. Most mass-transfer correlations exclude ion-exchange kinetic data. Ion-exchange experiments are not used due to complexity in analyzing the diffusion process. Hence the suitability of these correlations to predict mass-transfer coefficients in mixed bed ion-exchange needs to be studied.

Predicting ion-exchange mass-transfer coefficients is an important aspect of numerical modeling of the ion-exchange process, and hence the breakthrough curve. The objective of this work is to find a mass-transfer correlation to predict ion-exchange resin mass-transfer coefficient at low influent concentrations. Existing mass-transfer correlations are compared with mixed bed ion-exchange mass-transfer coefficient data (at low influent concentrations) .

Literature

Numerous experimental investigations and a wide range of empirical mass transfer correlations are available in the literature. McCune and Wilhelm (1949), Gaffney and Drew (1950), Evans and Gerald (1953), Gilliland and Baddour (1953), Selke et al. (1956), Bar-Ilan and Resnick (1957), Moison and O'Hern (1959), Carberry (1960), Frisch and Kunin (1960), Williamson et al. (1963), Pfeffer (1964), Rao and David (1964), Wilson and Geankoplis (1966), Kunii and Suzuki (1967), Turner and Snowdown (1968), Karabelas et al. (1971), Kataoka et al. (1972), Levins et al. (1972), Nelson and Galloway (1975), Miyauchi et al. (1975), Appel and Newman (1976), Novak (1976), Dwivedi and Upadhyay (1977), Koloini et al. (1977), Wakao and Funazkri (1978), Rahman and Streat (1981), Ohashi et al. (1981), Kikuchi et al. (1984), Zarraa (1992), and Livingstone and Nobel (1993) are some of the authors who have correlated mass-transfer data. The purpose of this section is not intended to present all mass-transfer correlations available in literature. Correlations that included ion-exchange experiment data and those that included dispersion analysis have been considered in this work.

Mass transfer data has been gathered by dissolution, sublimation, evaporation, surface controlled reactions, and by ion-exchange experiments. Most correlations contain data from dissolution experiments. Benzoic acid spheres dissolving in aqueous media has been frequently used; this system has been relatively simple to use for obtaining good mass transfer data (Cussler, 1984). Correlations that included mainly dissolution data have not been considered in this study.

Mass-transfer correlations include the flow dynamics and physiochemical features of the systems under study. Mass-transfer data have been accumulated over a range of Reynolds numbers for fixed and fluidized beds — flow characteristics of fixed and fluidized beds being very much different (Tournie et al., 1979; Yutani et al., 1987).

A physical characteristic of the fixed bed that affects mass-transfer coefficient is the surface roughness of the particles. The effect of surface roughness on mass-transfer coefficient has been studied by Dawson and Trass (1972), Tantirige and Trass (1984), and Van Vliet and Weber (1988). Van Vliet and Weber (1988) found that mass-transfer enhancement was dependent on the surface roughness of the particle rather than the shape of the particle. In their experiments with adsorbents, they found that rough particles showed a seven-fold increase in mass transfer when compared with smooth particles.

Mass-transfer data have also been gathered by performing single particle experiments. These mass-transfer coefficients are incorrect for a packed bed. The measured mass-transfer coefficient in a packed bed represents an average over the entire set of particles. Particles in a randomly packed bed are under the influence of a varying environment (Jolls and Hanratty, 1969; Nelson and Galloway, 1975); neighboring particles affect the mass-transfer rate in a packed bed. In a dumped bed, the active surface of the particle available for mass transfer varies, and every particle is under the influence of a slightly different concentration gradient and flow pattern around the particle.

Carberry (1960) analysed packed-bed mass transfer by the boundary-layer theory. The packed bed was viewed as a series of discrete surfaces separated by void cells. Carberry (1960) assumed that development and destruction of the boundary layer occurs over a distance equal to one particle diameter, approximately. Solute transfer occurs by diffusion to the fixed surface during development of the boundary layer. The boundary layer gets destroyed at the mixing points.

Frisch and Kunin (1960) studied mixed-bed deionization of sodium chloride solutions. Experiments were conducted at flow rates of 3 to 70 gal/(min).(sq ft), bed depths of 0.25 to 3.2 ft, and solution concentrations of 0.0002 to 0.01N were used. The experiments were also conducted at 15°C and 45°C. Liquid-film mass transfer was the rate controlling step at the low concentrations used in their experiments. They compared their correlation with that of Wilke and Hougen (1945). The coefficient in their correlation was higher than Wilke and Hougen's (1945). The increase in magnitude of the coefficient was attributed to: 1) the film mass-transfer coefficient being composition dependent, and 2) surface roughness of the beads leading to larger surface areas than accounted for by the particle size.

Kunii and Suzuki (1967) interpreted mass and heat transfer in packed beds in the low Peclet number region using a simple model accounting for channelling in the bed. At low Reynolds numbers, the boundary conditions describing heat or mass transfer in flowing media is quite different from those of an isolated particle system. Hence a channelling length factor was introduced in the equation. The channelling factor is assumed to be one at no-channelling flow conditions.

Kataoka et al. (1972) analyzed liquid-phase mass transfer using the hydraulic-radius model. They assumed that laminar flow mass transfer in a packed bed is analogous to mass transfer between a pipe surface and a stream of liquid having laminar velocity profile. The effective diffusivity of the system calculated using the hydraulic-radius model was compared with effective diffusivity calculated from the film model. The correlation included data from dissolution experiments. Kataoka et al. (1976) demonstrated the applicability of their correlation to liquid-phase-controlled ion-exchange accompanied by chemical reaction.

Miyauchi et al. (1975) used cationic exchange resin beads in dilute alkaline solution in their experiments. The limiting Sherwood number at low Peclet numbers was determined experimentally for liquid-phase mass transfer in packed beds. A pulse response method was used to increase measurement accuracy. The limiting Sherwood number at low Peclet number was found to be 16.7 ($\varepsilon=0.4$).

Dwivedi and Upadhyay (1977) correlated available fixed and fluidized bed data. Their aim was to deduce a general mass-transfer correlation. They correlated gas-phase and liquid-phase mass transfer data using iterative least squares with minimization of residual errors. They used 18 data sets for correlating the liquid-phase mass-transfer coefficient. The average deviation of liquid-phase experimental data from their correlation was 17.95%.

Wakao and Funazkri (1978) corrected mass-transfer coefficients for axial dispersion. They correlated data obtained from dissolution experiments and surface diffusion controlled reactions for liquid-phase mass-transfer coefficients. Mass-transfer data obtained at particle Reynolds numbers below three were not used due to concerns of natural convection effects. Liquid-phase mass-transfer coefficients were relatively unaffected by dispersion when the Reynolds number was greater than three.

Rahman and Streat (1981) conducted mass-transfer experiments with single ion-exchange beads falling at their terminal settling velocities, and also fluidized bed experiments. Experiments were conducted with strong cation-exchange resin and dilute sodium hydroxide solution. There is a neutralization reaction in this system. The equilibrium concentration of sodium on the solid-fluid interface was assumed to be zero.

Ohashi et al. (1981) analyzed mass-transfer data using the rate of energy dissipation for a single particle. A specific power group was introduced into the correlation instead of a Reynolds number. Shallow-bed ion-exchange experiments were conducted. Using the specific power group, their mass-transfer correlation is applicable to stirred tanks, suspended bubble columns, and two-phase tube-flow.

Comparison of Literature Mass-Transfer Correlations

The definitions of the dimensionless numbers used in mass-transfer correlations are not uniform in literature. In particular, the definition of Sherwood and Reynolds numbers varies. The definitions include a characteristic length term. Generally, for mass-transfer correlations, the characteristic length term in a packed bed is the diameter of the particle. Some authors have used the hydraulic diameter for the characteristic length, or a shape factor in conjuction with particle diameter for non-spherical particles. Three different definitions of the Reynolds number have been used in the literature for correlating mass-transfer coefficients (Dwivedi and Upadhyay, 1977; Barber, 1994). In this study, the characteristic length used is the particle diameter, and the definition of Reynolds number is:

$$\mathrm{Re} = \frac{d_p u \rho}{\mu \varepsilon} \qquad \text{(IV-1)}$$

Literature mass-transfer correlations are presented in Table I. Some of these are re-grouped equations. Re-grouping of the terms was necessary due to non-uniformity in the definitions of the dimensionless numbers. The correlations in Table I have a different format than those presented by the original authors.

The mass-transfer coefficient has been presented as a Sherwood number. Equation IV-1 defines the Reynolds number in all the correlations in Table I. Most correlations in Table I show a dependence on Schmidt number with a one-third exponent, and a Reynolds number exponent one-half or slightly higher. Kunii and Suzuki (1967) correlation stands-out, the exponent on Schmidt and Reynolds number is one.

TABLE I

Literature Mass-Transfer Correlations for Calculating Sherwood Number

Reference	Correlation	Limits	Remarks
Frisch and Kunin (1960)	$\mathrm{Sh} = 16.6\left[\frac{\varepsilon}{6(1-\varepsilon)}\right]^{0.52} \mathrm{Re}^{0.52}\,\mathrm{Sc}^{0.32}$		Fixed bed correlation; Ion exchange experiments
Carberry (1960)	$\mathrm{Sh} = 1.15\,\mathrm{Sc}^{\frac{1}{3}}\,\mathrm{Re}^{\frac{1}{2}}$	Re < 1000	Fixed bed correlation; Correlation included ion exchange data
Kunii and Suzuki (1967)	$\mathrm{Sh} = \frac{\phi_s \varepsilon}{6(1-\varepsilon)\xi}\mathrm{Pe}$	$0 < \varepsilon\,(\mathrm{Re})(\mathrm{Sc}) < 10$	ϕ_s : shape factor ξ : channeling
Kataoka et al. (1972)	$\mathrm{Sh} = 1.85\left(\frac{\varepsilon}{1-\varepsilon}\right)^{-\frac{1}{3}} \mathrm{Sc}^{\frac{1}{3}}\,\mathrm{Re}^{\frac{1}{3}}$	$\left(\frac{\varepsilon}{1-\varepsilon}\right)\mathrm{Re} < 100$	Fixed bed correlation; Correlation included ion exchange data
Nelson and Galloway (1975)	$\mathrm{Sh} = \dfrac{2\zeta + \left\{\dfrac{2\zeta^2(1-\varepsilon)^{\frac{1}{3}}}{\left[1-(1-\varepsilon)^{\frac{1}{3}}\right]^2} - 2\right\}\tanh\zeta}{\dfrac{\zeta}{\left[1-(1-\varepsilon)^{\frac{1}{3}}\right]} - \tanh\zeta}$	$0.08 < \mathrm{Re} < 100$	$\zeta = \left[\frac{1}{(1-\varepsilon)^{\frac{1}{3}}} - 1\right]\frac{\alpha}{2}\mathrm{Re}^{\frac{1}{2}}\,\mathrm{Sc}^{\frac{1}{3}}$ α is the Frossling number and is equal to 0.6

TABLE I (contd)

Dwivedi and Upadhyay (1977)	$Sh = Sc^{\frac{1}{3}} Re\left[\frac{0.765}{(\varepsilon Re)^{0.82}} + \frac{0.365}{(\varepsilon Re)^{0.386}}\right]$	$0.01 < \varepsilon Re < 15{,}000$	Data included fixed and fluidized beds.
Wakao and Funazkri (1978)	$Sh = 2 + 1.1 Sc^{\frac{1}{3}} \varepsilon^{0.6} Re^{0.6}$	$3 < Re < 10{,}000$	Included dispersion effects
Rahman and Streat (1981)	$Sh = 0.75 Re^{\frac{1}{2}} Sc^{\frac{1}{3}}$	$7 < Re < 95$	Re is calculated using the terminal settling velocity of the particle
Rahman and Streat (1981)	$Sh = \frac{0.86}{\varepsilon^{0.5}} Sc^{\frac{1}{3}} Re^{\frac{1}{2}}$	$2 < Re < 25$	Fluidized bed data adapted for fixed beds
Ohashi, et al. (1981)	$Sh = 2 + 0.51\left(\frac{E^{\frac{1}{3}} d^{\frac{4}{3}}}{\gamma}\right)^{0.60} Sc^{\frac{1}{3}}$	$0.2 < \left(\frac{E^{\frac{1}{3}} d^{\frac{4}{3}}}{\gamma}\right) < 4600$ $505 < Sc < 70600$	E is energy disspation rate per unit mass of liquid flowing around a particle
Zarraa (1992)	$Sh = 0.85 Re^{0.54} Sc^{0.33}\left(\frac{d_p}{d}\right)^{-0.75}\left(\frac{d_p}{L}\right)^{0.41}$	$0.23 < Re < 2.27$ $0.52 < \varepsilon < 0.87$ $0.0127 < d_p/d < 0.0417$ $0.0095 < d_p/L < 0.125$	Fluidized bed correlation; experiments with cationic resin and copper sulfate solution

The numerical coefficients differ between the correlations. Some correlations have extra terms accounting for corrections of void volume, or channelling, or particle shape.

The equations presented by Carberry (1960) show that the exponent of the Schmidt number lies between one-half and two-thirds. The exponent approaches one-half for Schmidt numbers below unity. For high Schmidt numbers the mass-transfer resistance lies in the hydrodynamic boundary layer, and at low Schmidt numbers the concentration boundary layer becomes larger than the hydrodynamic boundary layer.

Bar-Ilan and Resnick (1957) reported that the exponent of the Schmidt number changes from one in cases of pure laminar flow, as suggested by Von Karman (1939), to two-third in the turbulent regime.

Film theory predicts that the exponent of diffusivity is one in the mass-transfer coefficient. Penetration and Surface Renewal theory predict that the mass-transfer coefficient depends on the diffusion coefficient to one-half power (Cussler, 1984). However, from experimental data, the mass-transfer coefficient is proportional to two-thirds power of diffusivity (Hines and Maddox, 1985).

A graphical comparison of the different mass-transfer correlations is presented in Figure 1. Most correlations presented in Table I can be used to calculate mass transfer coefficients in the Reynolds number range ten to one-hundred. The Nelson and Galloway (1975) correlation predicts the lowest Sherwood number, while the Frisch and Kunin (1960) correlation predicts the highest Sherwood number, compared to the other correlations.

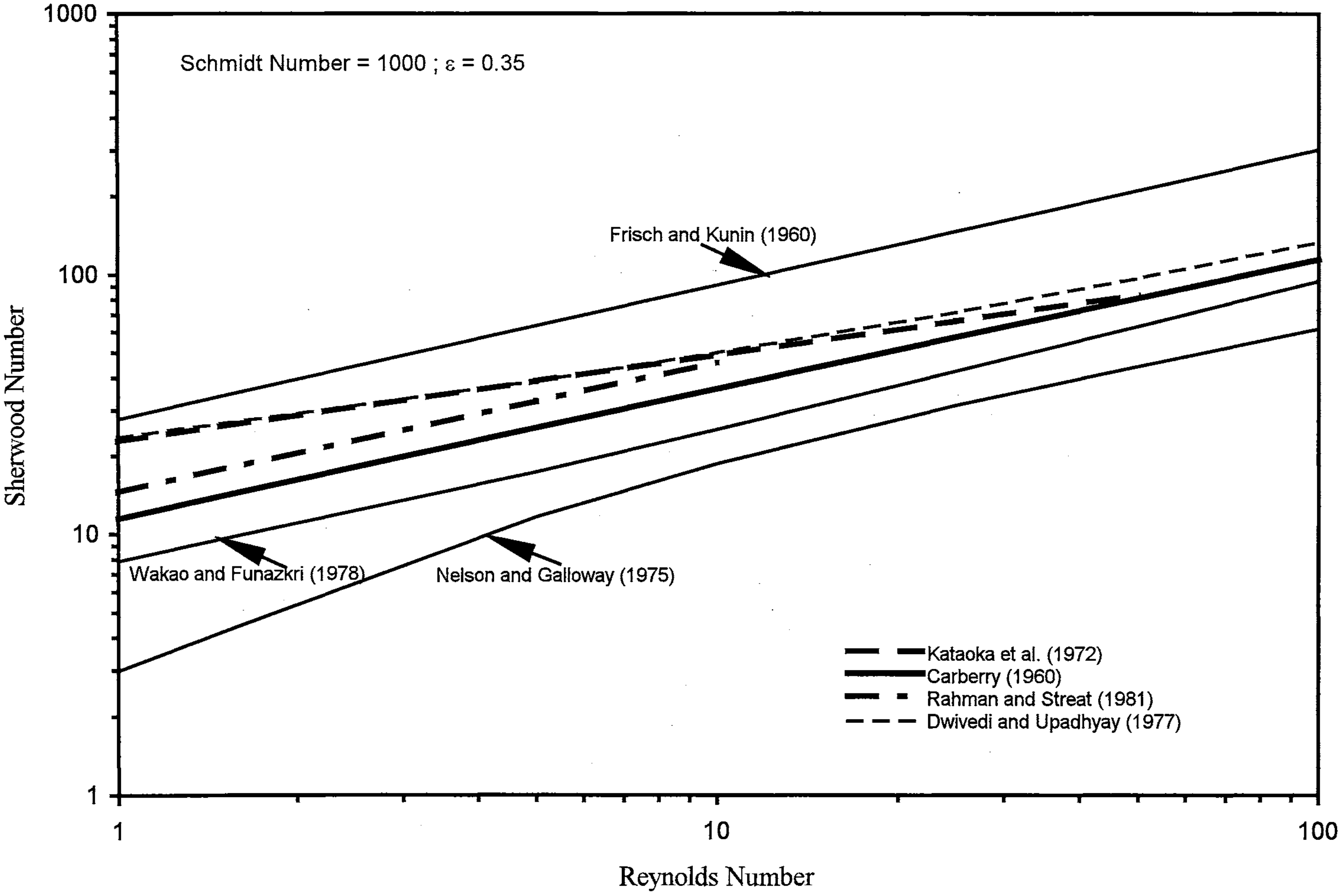

Figure 1. Comparison of literature mass-transfer correlations for predicting the Sherwood number

Experimental data suggest that the slope of the Sherwood number line changes as the Reynolds number decreases (Radcliffe et al., 1982). The slope of the Sherwood number line, predicted by Nelson and Galloway's (1975) correlation, changes in the Reynolds number region one to ten. No change of slope of the Sherwood number line in the Reynolds number region one to hundred is seen with other correlations. Sherwood number predicted by Kataoka et al. (1972) and Dwivedi and Upadhyay (1977) in the Reynolds number range one to ten is almost equal.

Limiting Value of Sherwood Number

For a single sphere, in an infinite stagnant fluid, the differential equation describing transport has a steady-state solution with a non-zero transfer rate. This leads to a limiting value of 2 for the Sherwood number at low Reynolds number. According to Wakao and Kagei (1982) a limiting value of 2 for Sherwood number (at low Reynolds number) is reached in packed beds too. But Aminzadeh et al. (1974), Nelson and Galloway (1975), and Novak (1976) have shown that in a packed bed the Sherwood number can have a value less than 2.

Nelson and Galloway (1975) questioned the validity of applying single sphere correlations ($Sh = 2$) to a dense system of particles. In a packed bed, all the particles are participating in the transfer process; hence the boundary conditions change for the assembly of particles compared to a single particle. The change in boundary condition leads to a value of zero for the Sherwood number at no-flow conditions. They proposed a new model for packed-bed mass transfer using a boundary condition where the gradient of concentration vanishes symmetrically between particles.

Mass Transfer Experiments with Ion-Exchange Resins

Gilliland and Baddour (1953), Selke et al. (1956), Moison and O'Hern (1959), Frisch and Kunin (1960), Rao and David (1964), Turner and Snowdown (1968), Kataoka et al. (1973), Miyauchi et al. (1975), Koloini et al. (1977), Rahman and Streat (1981), Ohashi et al. (1981), Kikuchi et al. (1984), Harries (1984), McNulty et al. (1986), Zarraa (1992), and Lee (1994) have conducted mass transfer experiments using ion-exchange resins. Fixed bed, fluidized bed, and single particle experiments have been conducted using ion-exchange resins. Single particle ion-exchange data have been studied by Van Brocklin (1968). Mixed bed ion-exchange mass transfer at low influent concentrations is the main concern of this study.

Short beds are used to obtain kinetic characteristics of adsorbents in column studies (Smith and Weber, 1989). Shallow-bed columns have been used for measuring the kinetic characteristics of ion-exchange resins. They simulate a differential part of a deep bed, and hence the hydrodynamics and the physiochemical characteristics of the system. Also, the results of shallow-bed column studies are more amenable to theoretical interpretation without making too many assumptions. In shallow-bed column experiments, the influence of resin saturation and intraparticle diffusion are eliminated since concentration data are collected in the first few minutes of breakthrough. The main concern in a shallow-bed experiment is the entrance and exit effect (Novak, 1976).

Harries (1984) devised a shallow-bed column methodology for testing the kinetic characteristics of ion-exchange resins in a mixed bed. The test results were interpreted in terms of a mass-transfer coefficient. Harries (1984) adapted the Frisch and Kunin (1960) mass-transfer equation for determining mass-transfer coefficients of cations or anions in a mixed bed. The mass-transfer equation uses the measured values: bed height, resin particle diameter, flowrate, diameter of the column, volume fraction of resin, and influent concentration. Harries (1984) method for obtaining kinetic data of ion-exchange resins has been used by McNulty et al. (1986) and Lee (1994).

Mathematical Model for Shallow-Bed Column Ion Exchange

The solute continuity equation in a fixed-bed ion-exchange column, ignoring axial dispersion (since the fluid phase is a liquid), is

$$\frac{u}{\varepsilon}\frac{\partial C}{\partial z}+\frac{\partial C}{\partial t}+\Phi\left(\frac{1-\varepsilon}{\varepsilon}\right)\frac{\partial q}{\partial t}=0 \tag{IV-2}$$

The first term of Equation IV-2 accounts for convective transport of the ions axially, and the second term represents accumulation in the fluid phase. The third term accounts for accumulation in the solid phase; Φ is the volumetric fraction of cation or anion exchange resin, depending on whether Equation IV-2 was written for cation or anion material balance. For a shallow-bed column, the second term in Equation IV-2 can be neglected, simplifying Equation IV-2 to

$$\frac{u}{\varepsilon}\frac{\partial C}{\partial z}+\Phi\left(\frac{1-\varepsilon}{\varepsilon}\right)\frac{\partial q}{\partial t}=0 \tag{IV-3}$$

The rate law (assuming that initial breakthrough is controlled by external-film resistance), using a Nernst film model, can be written as:

$$\frac{\partial q}{\partial t} = K_f a_s \left(C - C^*\right) \qquad \text{(IV-4)}$$

In the rate law, Equation IV-4, C^* is assumed to be zero (Frisch and Kunin, 1960; Koloini et al., 1977; Rahman and Streat, 1981). Cooney (1991) has discussed the validity of using a zero interfacial concentration. Equation IV-3 with IV-4 can be integrated using the boundary conditions

$$\begin{aligned} C &= C_{inf} && \text{at } z = 0 \\ C &= C_{eff} && \text{at } z = L \end{aligned} \qquad \text{(IV-5)}$$

to obtain

$$\ln\left(\frac{C_{eff}}{C_{inf}}\right) = -\left[\frac{(1-\varepsilon)\Phi K_f a_s L}{u}\right] \qquad \text{(IV-6)}$$

The specific surface area (a_s) for a spherical particle is defined by the product:

$$a_S\, d_p = 6$$

Equation IV-6 can be written as:

$$\ln\left(\frac{C_{eff}}{C_{inf}}\right) = -\left[\frac{6\Phi(1-\varepsilon)K_f L}{u d_p}\right] \qquad \text{(IV-7)}$$

Using Equation IV-7 the film mass transfer coefficient (K_f) can be calculated from experimental values of C_{inf} and C_{eff}.

Experimental Ion-Exchange Mass-Transfer Data

Mass-transfer experiments conducted at low influent concentrations, less than 0.01 N only, have been considered. At higher influent concentrations the solid phase contributes to mass-transfer resistance, hence such systems are not truly film mass-transfer limited. Mass-transfer experiments have been conducted in mono and mixed ion-exchange beds. Frisch and Kunin (1960), Harries (1984), McNulty et al. (1986), and Lee (1994) have studied mixed bed ion-exchange mass transfer using low influent concentrations of sodium chloride (around 2 x 10^{-4} N or less).

The data considered in this study is in the Reynolds number range 10 to 100. Mass transfer data below Reynolds number 10 have not been used, since the influence of natural convection needs to be considered at low Reynolds number ranges.

Most mass-transfer experimental data have been reported in terms of the Sherwood number or the K_f value. K_f, ε, Schmidt and Reynolds numbers are variant between the experimental data of different authors — this is obvious since different systems have been studied. The number of variables needs to be reduced for comparing experimental data with literature correlations. For comparison, on a two-dimensional plot, only three variables can be accomodated; but in this case, there are four variables — K_f, ε, Schmidt and Reynolds numbers. Hence a J-factor form for representing the mass-transfer data is used. By this method the number of variables for comparison has been reduced to two, and is on an uniform basis.

The original experimental mass-transfer data of the different authors have been expressed as a J-factor. The J-factor is calculated using the following equation:

$$J = \frac{K_f \varepsilon}{u} (Sc)^{\frac{2}{3}} \tag{IV-8}$$

The diffusion coefficient, used in the Schmidt number calculation, is obtained from conductance data measured at infinite dilution (Equation II-14). For an uniform basis of comparison, all mass-transfer data have been adjusted to a temperature of

25°C and a void volume value of 0.35. The Reynolds number from the individual authors has been recalculated according to Equation IV-1.

Figure 2 compares experimental mass-transfer data for univalent ions obtained by different authors. Selke et al. (1956) data, obtained using shallow beds for silver (argentum) ions, shows more scatter than the other data. Their experimental mass-transfer coefficients have a higher value compared with other data presented in Figure 2. Moison and O'Hern (1959) reported that the concentration range used by Selke et al. (1956) for the experimental system Ag-H was 0.003-0.06N ($AgNO_3$). Radcliffe et al. (1982) also observed that the data of Selke et al. (1956) was 70% higher than that calculated using solid dissolution correlations.

Moison and O'Hern (1959) used deep beds in their experiments. The average bed depth was 40 cms or more. They conducted experiments with sodium chloride in mono beds (cation or anion exchange resins only, in a packed-bed), and influent concentrations ranging from 0.01 to 0.1N. Mass transfer data taken at a concentration of 0.01N have been used in Figure 2. Since data of Selke et al. (1956) shows a lot of scatter and Moison and O'Hern (1959) conducted experiments in deep beds, their data are not used further in this analysis.

Harries (1984) conducted mixed bed ion-exchange experiments with chloride and sulfate. Lee (1994) used Harries (1984) method to obtain mass-transfer data of sodium and chloride in mono and mixed beds. Lee (1994) conducted experiments at different influent concentrations (3×10^{-6} to 1.4×10^{-4}N) and flow rates (60, 80, and 105 m/h). Lee's (1994) data, taken at an influent concentration of 2.8×10^{-5}N, have

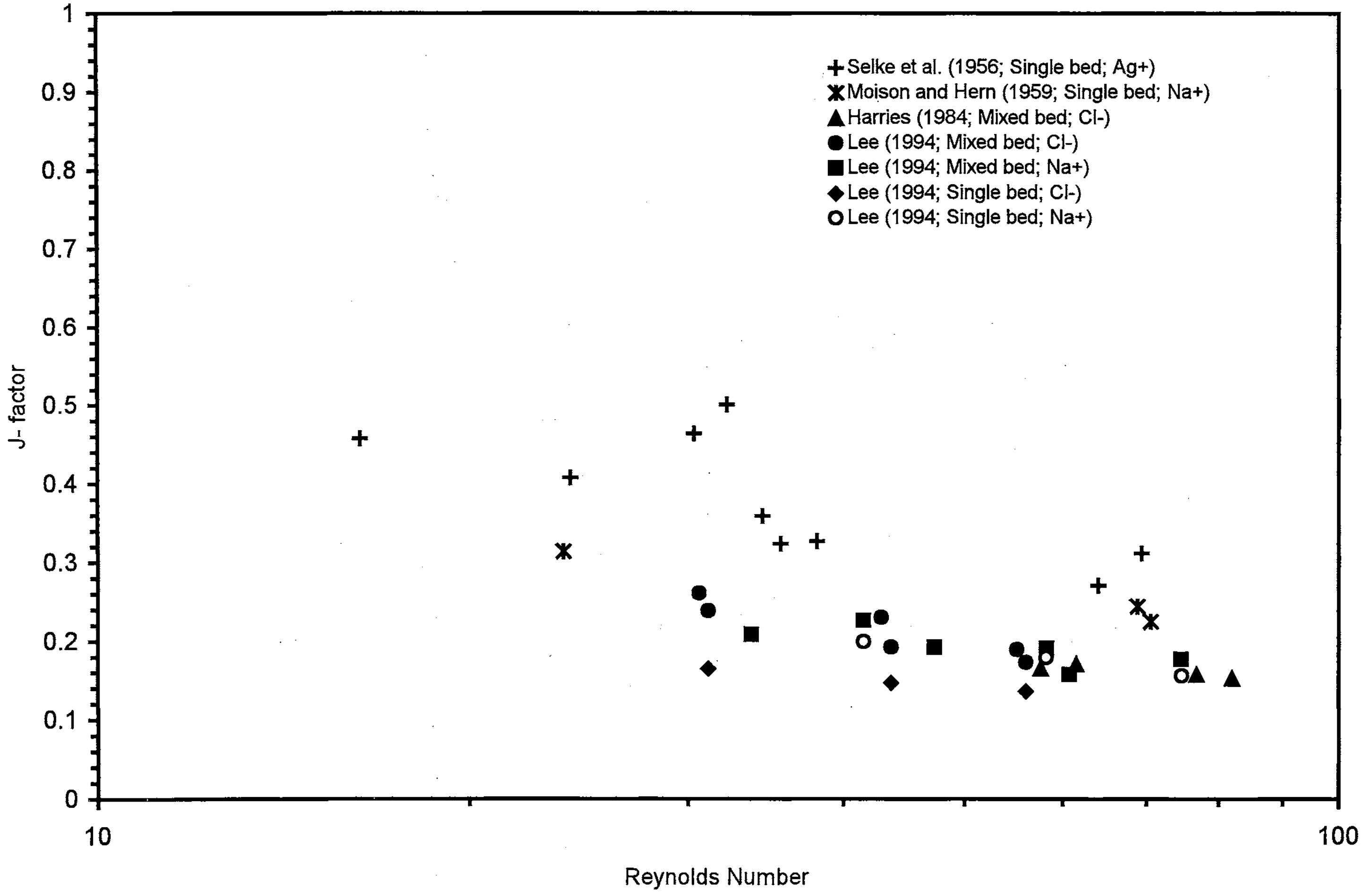

Figure 2. Mass tranfer data for univalent ions

been used in Figure 2. Experimental data collected with a bed composition of 2:1 — cation-to-anion resin volume ratio — have been used in this study.

Figure 3 compares mass-transfer data obtained for divalent ions. Rao and David (1964) conducted single particle experiments in a packed bed of inert particles. They studied the mass transfer of cupric ions to a cation-exchange resin in copper sulfate solution. Kataoka et al. (1973) studied the exchange of zinc nitrate, copper nitrate, and cesium nitrate with sodium form cation-exchange resin in a mono bed. Their data were taken at an influent concentration of 0.01N. Figure 4 presents mass-transfer coefficient comparison of both univalent and divalent ions in mono and mixed beds.

Comparison of Experimental Ion-Exchange Mass-Transfer Coefficients with Correlations

Carberry (1960), Kataoka et al. (1972), and Dwivedi and Upadhyay (1977) correlations have been used for comparing experimental mass-transfer data. Figures 5 and 6 give a Sherwood number comparison of experimental data with the literature mass-transfer correlations.

In Figure 5, experimental chloride mass-transfer coefficient of Harries (1984) is compared with the predicted mass-transfer coefficient. The experimental Sherwood number is under-predicted by Carberry (1960) and Kataoka's (1972) correlations, while Dwivedi and Upadhyay (1977) correlation gives a better estimate. The same trend is seen with Lee's (1994) chloride mass-transfer data, Figure 6. In Figure 7, ion-exchange mass-transfer data of Harries (1984) and Lee

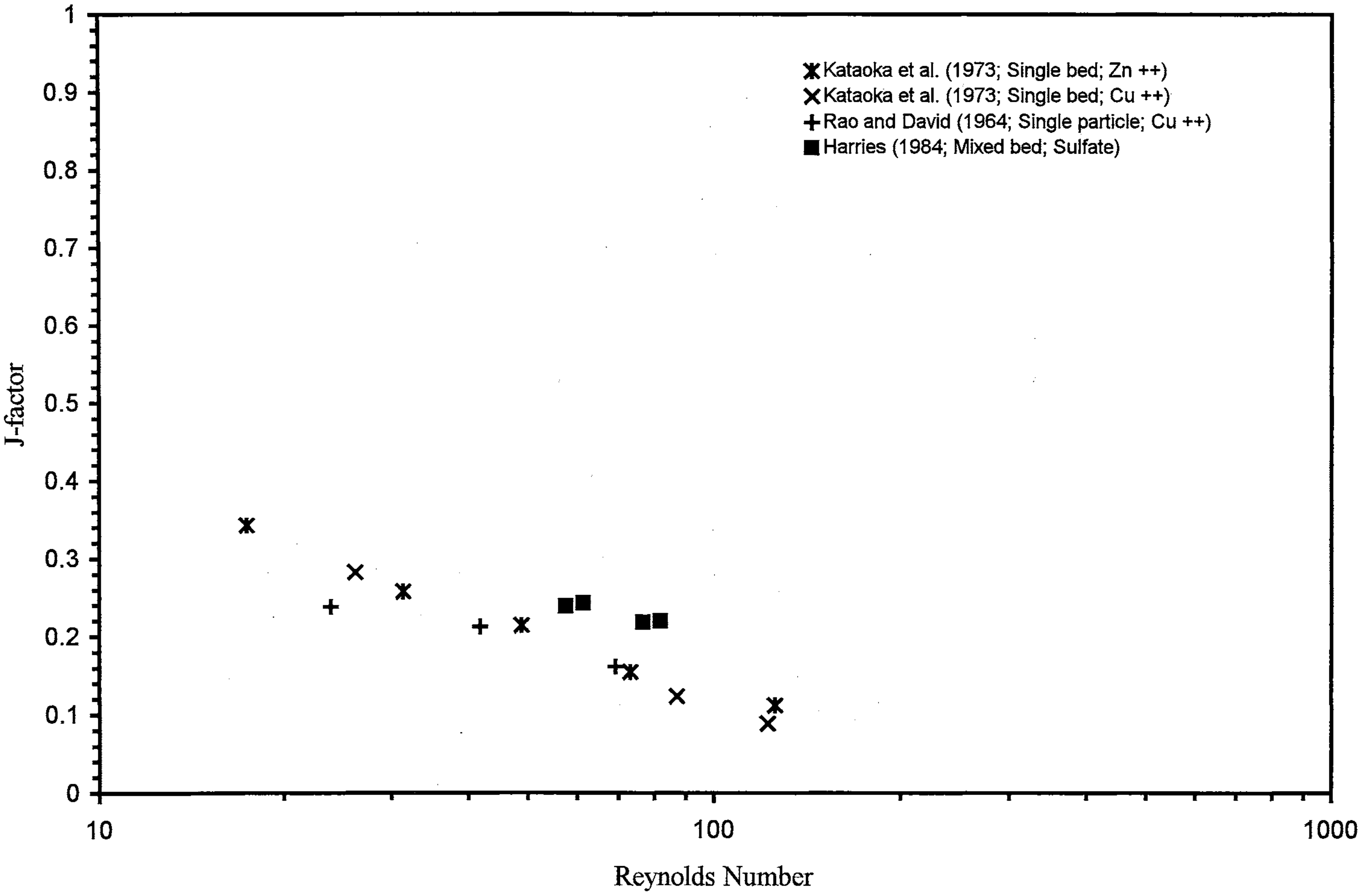

Figure 3. Mass transfer data for divalent ions

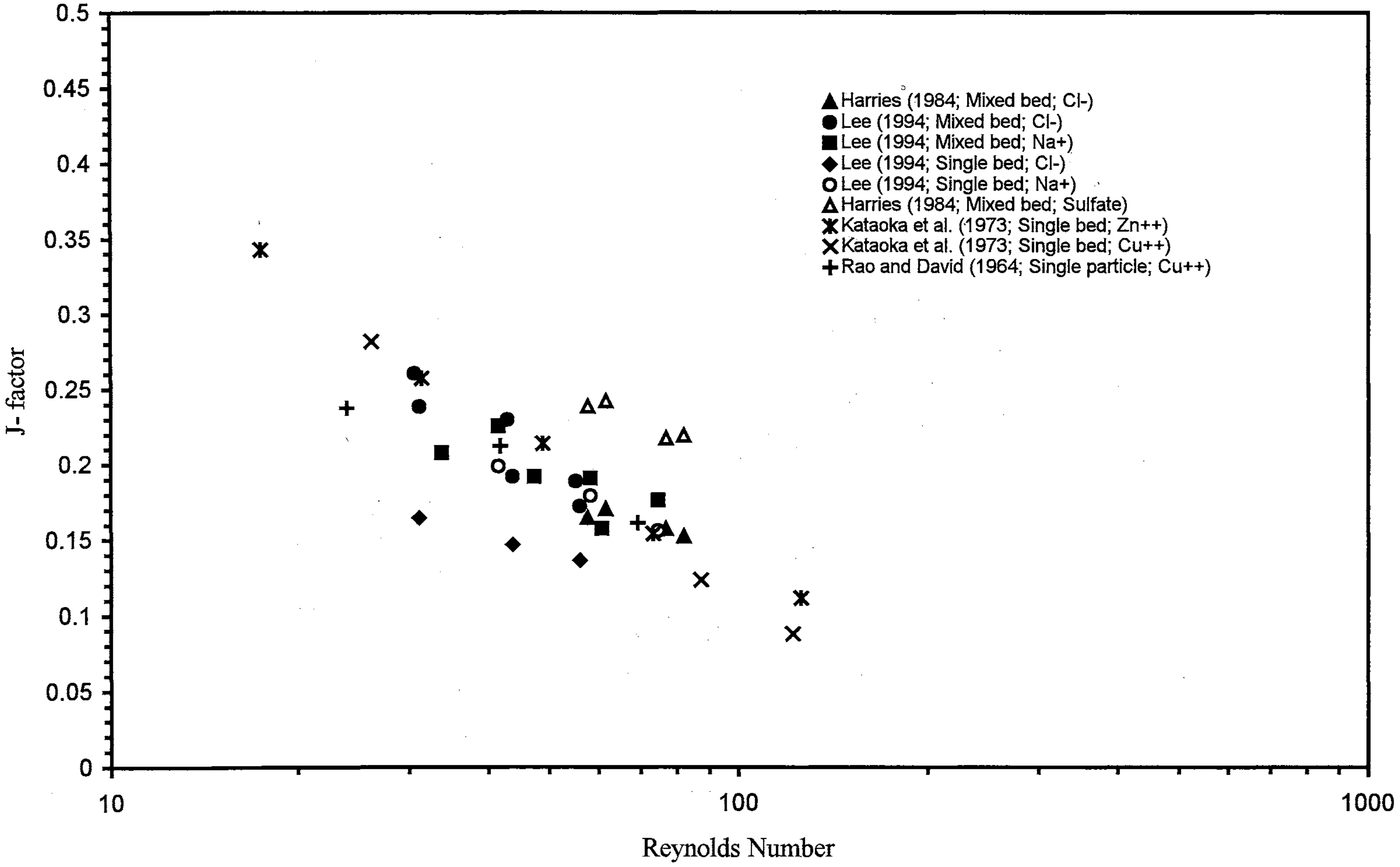

Figure 4. Mass transfer data comparison of univalent and divalent ions.

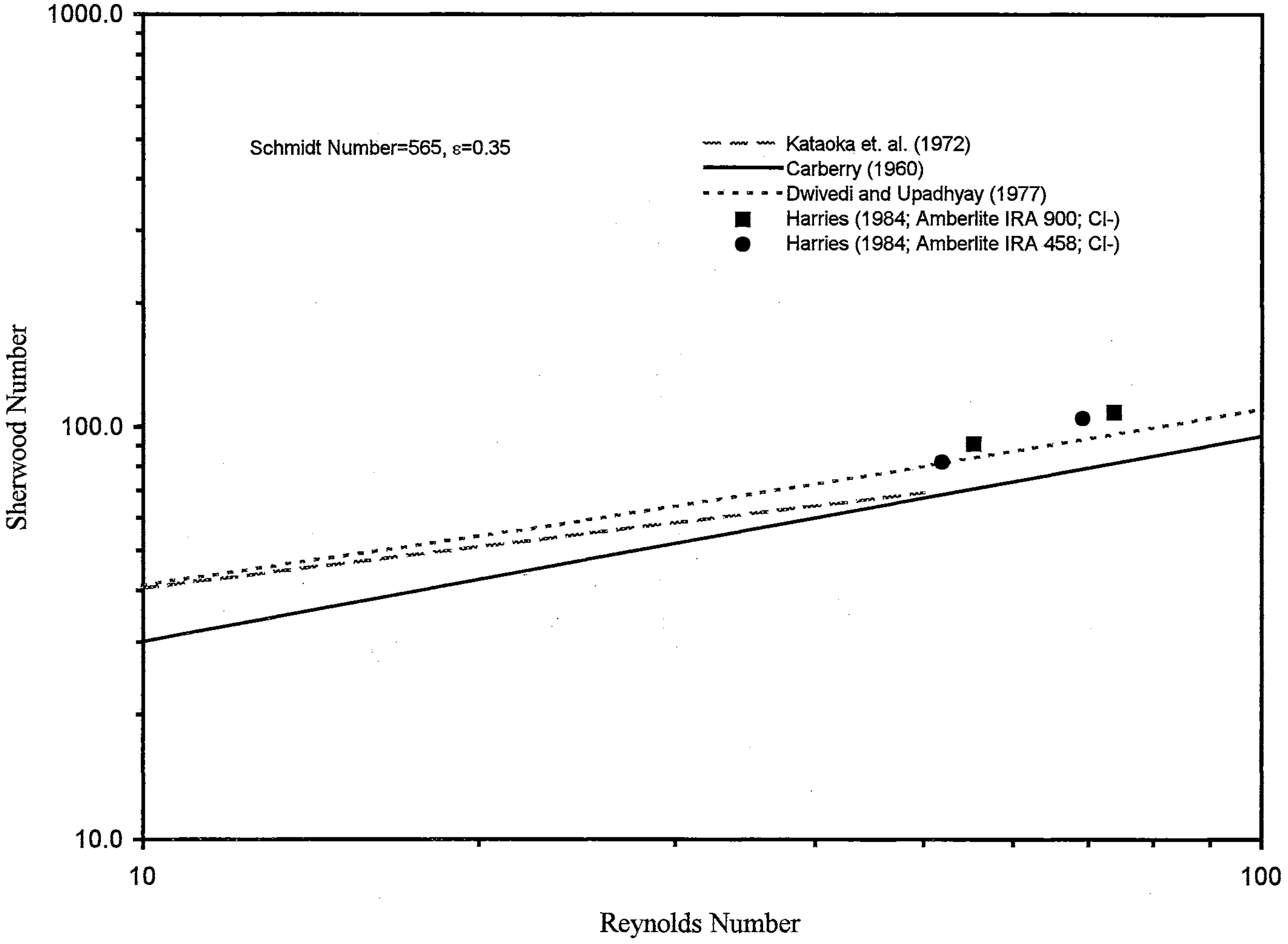

Figure 5. Comparison of Harries (1984) experimental data with literature mass-transfer correlations.

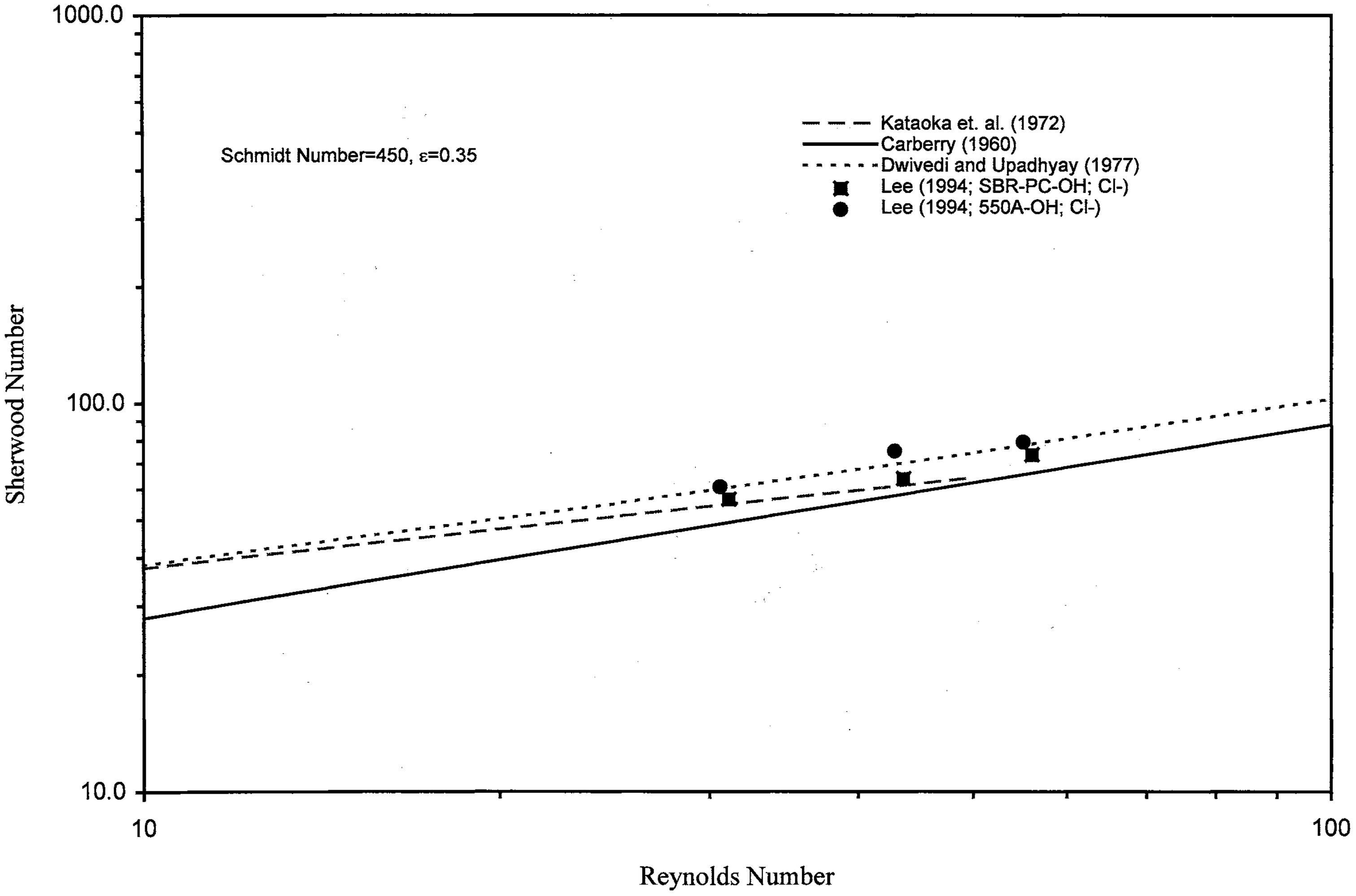

Figure 6. Comparison of Lee's (1994) chloride mass transfer data with literature mass-transfer correlations

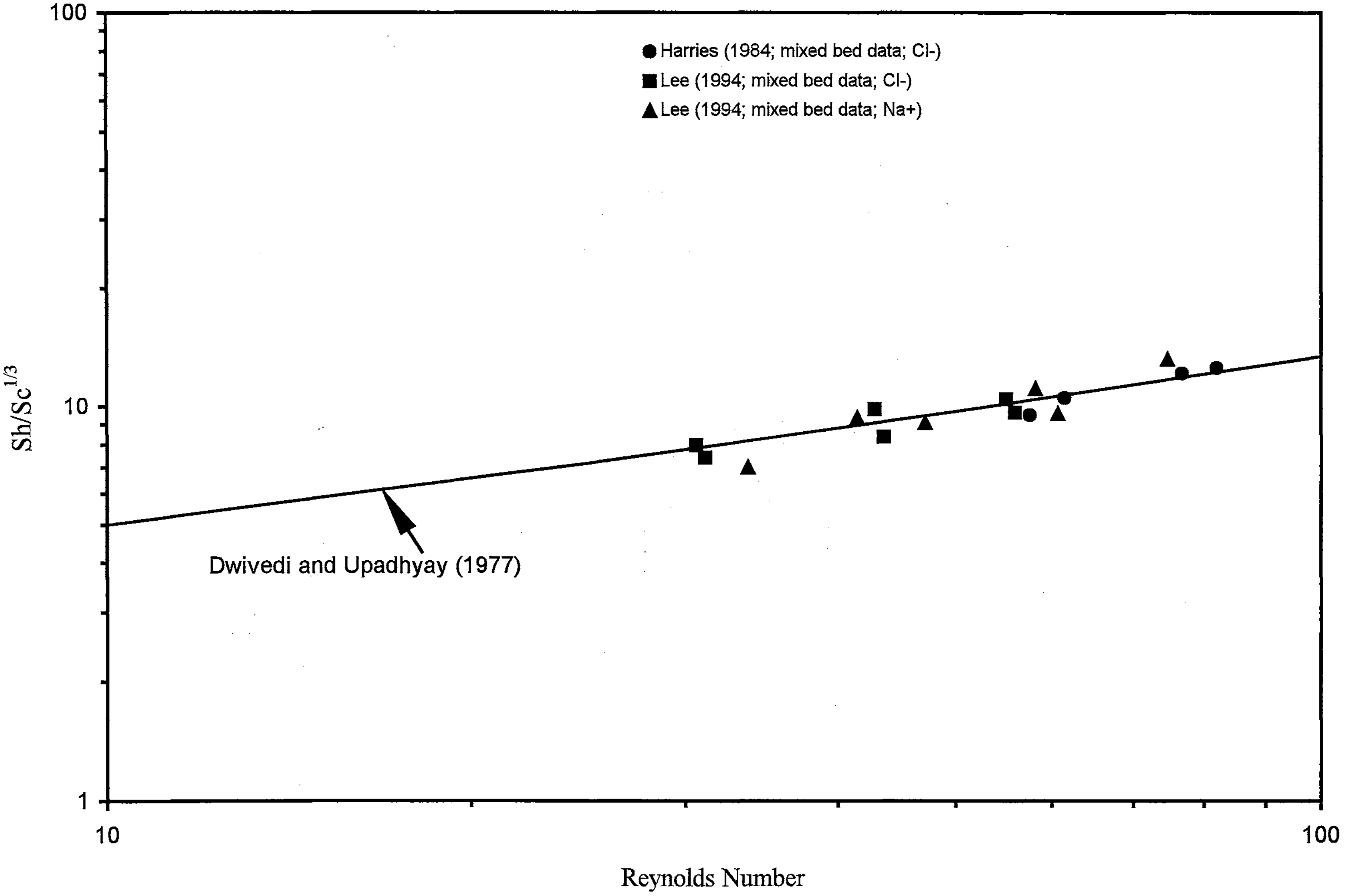

Figure 7. Comparison of Dwivedi and Upadhyay (1977) correlation with experimental mass transfer data

(1994) are compared with Dwivedi and Upadhyay (1977) correlation; the mass-transfer data correlate very well.

Figure 8 presents a comparison of J-factor calculated using Carberry (1960) correlation with experimental data. A ±20% variation of the Carberry (1960) J-factor is also shown in Figure 8, most of the experimental data lies within this range. Figure 9 compares predicted J-factor using Carberry (1960) and Dwivedi and Upadhyay (1977) correlations. The J-factor predicted from Dwivedi and Upadhyay (1977) correlation is higher than that predicted by Carberry (1960) correlation. Appendix B compares mass-transfer coefficient calculated using these correlations with experimental data.

From Table I, both Carberry (1960) and Dwivedi and Upadhyay (1977) correlation show a one-third power dependence on diffusivity (Schmidt number). The differences between the correlations are in the Reynolds number dependence and the numerical coefficients. The Reynolds number functionality in Dwivedi and Upadhyay (1977) correlation is more elaborate than that presented by Carberry (1960) correlation.

Conclusions

Literature mass-transfer correlations were presented with uniform definition of the dimensionless numbers. The Schmidt number, in all correlations, was calculated using the aqueous single-ion diffusion coefficient at infinite dilution. The ion-exchange mass-transfer coefficient obtained by shallow-bed column experiments has been analyzed as an average mass-transfer coefficient. The ion-exchange mass-

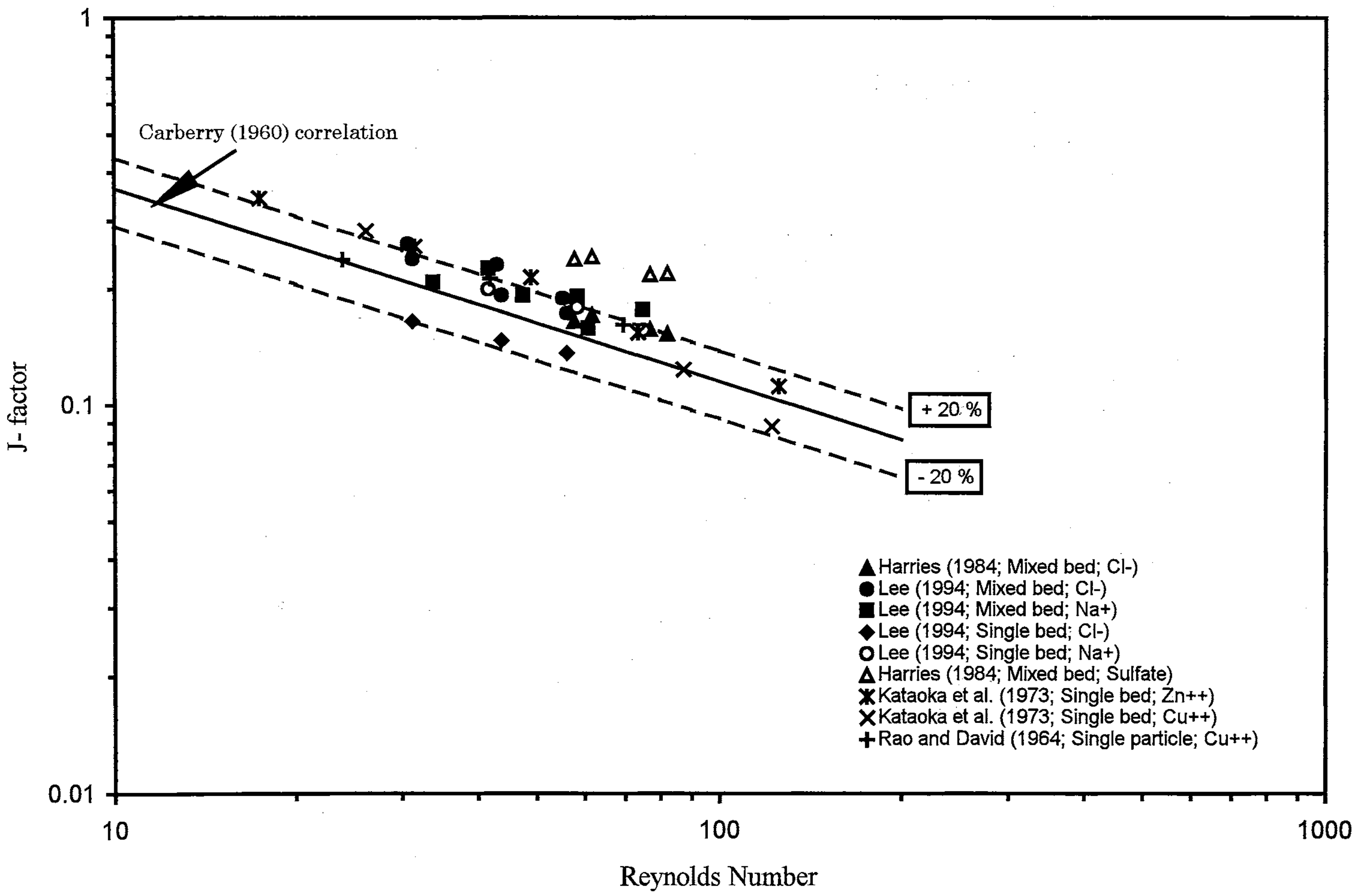

Figure 8. Predicted J-factor compared with experimental mass transfer data.

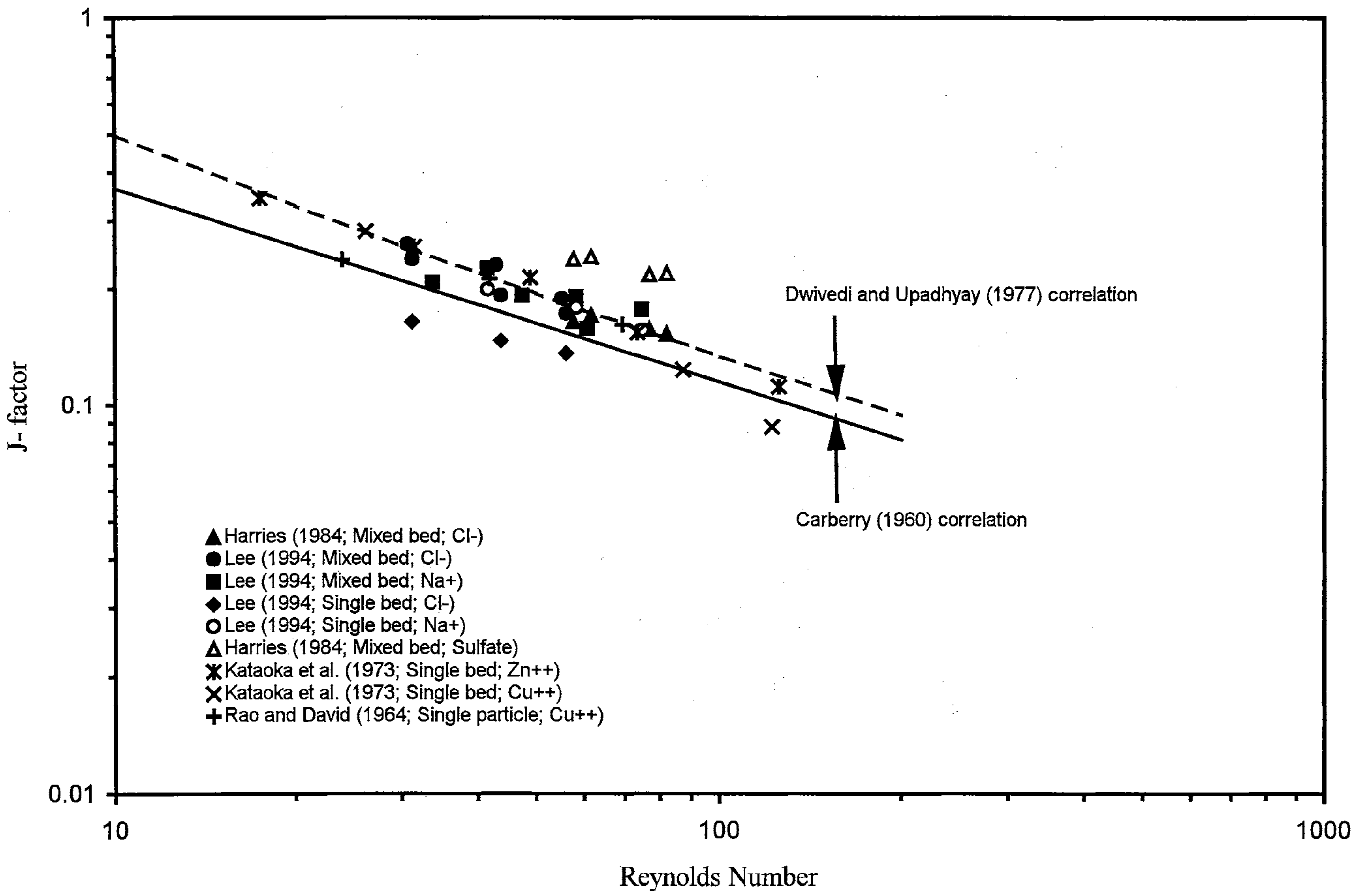

Figure 9. Comparison of J-factor predictions with experimental mass transfer data

transfer coefficient data were correlated well by Dwivedi and Upadhyay (1977) correlation. Dwivedi and Upadhyay (1977) correlation predicted the mass-transfer coefficient within ±10% of the experimental data. Carberry's (1960) correlation under-predicted the mass-transfer coefficient by 20%.

CHAPTER V

EFFECT OF MASS-TRANSFER COEFFICIENT ON BINARY EXCHANGE OF SODIUM CHLORIDE IN MIXED-BED ION EXCHANGE

Introduction

A lumped-parameter, the mass-transfer coefficient, is generally used to model packed-bed operations. Packed-bed systems can be easily described using a mass-transfer coefficient model. External mass-transfer coefficients for a system can be calculated using empirical correlations (Cussler, 1984). The previous chapter described various mass-transfer correlations available for calculating mass-transfer coefficients for mixed-bed ion exchange. The mass-transfer coefficient involves the diffusion coefficient and hydrodynamics of the system.

Most diffusion processes in dilute solution can be modeled using Fick's law. Fick's law is usually combined with a mass balance equation to calculate mass flux and mass-transfer coefficient across any given interface. Fick's model describes the transport of molecular species considering only the concentration gradient. The model does not account for other external forcings like: thermal gradient, electric-potential gradient, and pressure gradient.

In an electrolytic solution, like sodium chloride in water, solute-solute interactions are important; diffusing solute molecules interact with other solute molecules and the solvent. This gives rise to a diffusion coefficient that has a different value than the individual species diffusion coefficient.

Electrostatic interactions are primarily responsible for most of the diffusion effects seen in a solution containing ions. Ionic mass transport is usually modeled using the Nernst-Planck equation. The Nernst-Planck equation accounts for the chemical and electrical forces that affect ionic flux. The electrical force includes applied potential on the system and potential generated due to difference in diffusivities of the ions.

Non-electrolyte mass-transfer coefficients are used to calculate the ionic flux. Ion migration effects are unaccounted for in non-electrolyte mass-transfer coefficients. But in an ion-exchange system, ionic migration effects are important due to differences in the diffusivities of the ionic species. Van Brocklin and David (1972) have defined a correction that can be applied to ion-exchange systems using non-electrolyte mass-transfer correlations.

Haub and Foutch (1986) used an effective-diffusion coefficient for correcting the mass-transfer coefficient calculated using non-electrolyte mass-transfer correlations. The effective-diffusion coefficient accounts for the interaction of the different ionic species (Kataoka et al., 1973; Wildhagen et al., 1985; Haub and Foutch, 1986; Zecchini, 1990). The effective-diffusion coefficient depends on the concentration of the ions in the bulk liquid, and the equilibrium concentration at the solid-fluid interface. Hence the effective-diffusion coefficient varies though the ion-exchange process.

Haub and Foutch (1986) used the Nernst-Planck equation to model film-mass-transfer limited ion-exchange of sodium chloride in a mixed bed. The Nernst-

Planck equation was used in conjunction with Nernst film or stagnant-film theory to model mixed bed ion-exchange. Diffusion of an ionic species from the bulk fluid to the surface of the resin is assumed to occur across a stagnant fluid layer (Nernst film); albeit, convective flow is present in the bulk fluid. Convective flow reduces to zero as the resin surface is approached in the radial direction. The absence of convection gives rise to a stagnant fluid layer, which satisfies the condition of no-slip at the particle boundary.

Intuitively, a stagnant fluid layer around a single resin particle can be visualized, but is difficult to do in the case of a packed bed. In a packed bed, the resin particles are in contact with each other, hence, a well-defined boundary layer around each particle is abstract. However, for purposes of modeling the kinetics of film-diffusion controlled ion-exchange, in a packed bed, the notion of a stagnant layer around each particle makes the problem tractable. The applicability of this model states that the film kinetics is controlled by hydrodynamics.

The purpose of this chapter is to study the effect of mass-transfer coefficient on mixed-bed ion exchange. Diffusion of sodium chloride in water at low concentration has been theoretically analyzed. The contribution of ionized water towards transport of the ions involved in this system forms the basis for defining some of the observed multi-component effects. Existing experimental ion-exchange mass-transfer data have been analyzed in this work. Effect of mass-transfer coefficient on numerical predictions of the breakthrough curve has also been studied.

Diffusion of Sodium Chloride in Water at Low Concentrations

Sodium chloride — a strong electrolyte — completely ionizes in water (at low concentrations). At low concentration of NaCl, in an aqueous environment, water ionization contributes ions (hydrogen and hydroxide) to form a multicomponent system. Presence of substantial amount of hydroxyl ions influences mass transport of sodium chloride (water contains 1.7 ppb hydroxyl ions at 25°C and pH 7).

The ionic flux of Na^+, Cl^-, H^+, and OH^-, in the bulk liquid, can be modeled using the Nernst-Planck equation with constraints of electroneutrality and no electric current.

$$j_i = -D_i\left[\frac{\partial C_i}{\partial r} + \frac{Z_i C_i F}{RT}\frac{\partial \phi}{\partial r}\right] \tag{V-1}$$

$$\sum_{i=1}^{i=n} Z_i C_i = 0 \tag{V-2}$$

$$\sum_{i=1}^{i=n} Z_i j_i = 0 \tag{V-3}$$

where i = Na^+, Cl^-, H^+, and OH^-

The water dissociation equilibrium can be written as:

$$\frac{\partial}{\partial r}\left(C_H C_O\right) = 0 \tag{V-4}$$

Equations V-1 to V-4 can be solved for the flux expressions of the ions in the bulk liquid. The electric-potential gradient (second term in eq V-1) can be solved in terms of concentration gradient of the ions. Furthermore, since all the ions are univalent the valence terms in the equations have been dropped. The result of solving Equations V-1 through V-4, for Na^+ and Cl^- is (Appendix C)

$$j_{Na} = D_{11}\frac{\partial C_{Na}}{\partial r} + D_{12}\frac{\partial C_{Cl}}{\partial r} \tag{V-5}$$

$$j_{Cl} = D_{21}\frac{\partial C_{Na}}{\partial r} + D_{22}\frac{\partial C_{Cl}}{\partial r} \qquad \text{(V-6)}$$

where

$$\zeta = \frac{D_H C_H^2 + D_O K_w}{C_H^2 + K_w} \qquad \text{(V-7)}$$

$$D_{11} = \frac{1}{\sum_{i=1}^{n} D_i C_i}\left[-D_{Na}\sum_{i=1}^{n} D_i C_i + D_{Na}^2 C_{Na} + D_{Na} C_{Na}\zeta\right] \qquad \text{(V-8)}$$

$$D_{12} = \frac{(-1)}{\sum_{i=1}^{n} D_i C_i}\left[D_{Na} D_{Cl} C_{Na} + D_{Na} C_{Na}\zeta\right] \qquad \text{(V-9)}$$

$$D_{21} = \frac{(-1)}{\sum_{i=1}^{n} D_i C_i}\left[D_{Na} D_{Cl} C_{Cl} + D_{Cl} C_{Cl}\zeta\right] \qquad \text{(V-10)}$$

$$D_{22} = \frac{1}{\sum_{i=1}^{n} D_i C_i}\left[-D_{Cl}\sum_{i=1}^{n} D_i C_i + D_{Cl}^2 C_{Cl} + D_{Cl} C_{Cl}\zeta\right] \qquad \text{(V-11)}$$

The summation (Σ) is done over all the ions; i = Na^+, H^+, Cl^-, and OH^-

Equations V-5 to V- 11 describe a multi-component diffusion problem. The equations describe the specific interactions of the ionic species arising due to electrostatic coupling. Equations V-7 to V-11 present the role played by water dissociation on liquid-phase transport of sodium chloride (at low concentrations). D_{11} and D_{22} are the main-term diffusion coefficients; D_{12} and D_{21} are the cross-term diffusion coefficients (Cussler, 1976).

Table I lists the value of diffusion coefficients for different ionic and molecular species. The single ion diffusion coefficients have been calculated from conductance data using the Nernst-Hartley equation (Horvath, 1985).

Table II lists the calculated diffusion coefficients of sodium chloride in water using Equations V-7 to V-11. The concentrations of sodium and chloride have been adjusted for electroneutrality at the given pH value. At pH 7 and sodium chloride concentration greater than 1.0×10^{-5} milliequivalents-per-milliliter, the main-term diffusion coefficient (D_{11}) of sodium takes on a value equivalent to the sodium hydroxide diffusion coefficient (Table I). The diffusion coefficient (D_{22}) of chloride has a value near that of the hydrochloric acid molecule. The main-term diffusion coefficients decrease as the concentration of sodium chloride decreases. The main-term diffusion coefficients become negative as the concentration approaches that of the hydrogen and hydroxyl ions. This indicates that diffusion may well be against the concentration gradient.

TABLE I

Diffusion Coefficient from Conductance Data
(at aqueous infinite dilution; Horvath, 1985), at 25°C

Species	Diffusion Coefficient x 10^5 (cm^2/s)
Sodium (Na^+)	1.38
Chloride (Cl^-)	2.04
Hydrogen (H^+)	9.35
Hydroxide (OH^-)	5.32
NaCl	1.61
NaOH	2.13
HCl	3.33
Sulfate	1.67
H_2SO_4	2.59
Na_2SO_4	1.23
Cu^{2+}	0.74
Zn^{2+}	0.72
Ag^+	1.65

TABLE II

Estimated Diffusion Coefficients of NaCl in Water

pH	Sodium Conc (meq/ml)	Chloride Conc (meq/ml)	D_{11} (cm^2/s)	D_{12} (cm^2/s)	D_{21} (cm^2/s)	D_{22} (cm^2/s)
6	1.00E-04	1.01E-04	2.79E-05	-4.42E-05	-6.24E-05	4.58E-05
	1.00E-05	1.10E-05	1.85E-05	-3.43E-05	-5.26E-05	3.54E-05
	1.00E-06	1.99E-06	-3.85E-06	-1.05E-05	-2.92E-05	1.07E-05
	1.00E-07	1.09E-06	-1.25E-05	-1.33E-06	-2.02E-05	1.05E-06
	1.00E-08	1.00E-06	-1.36E-05	-1.36E-07	-1.90E-05	-1.90E-07
	1.00E-09	9.91E-07	-1.37E-05	-1.37E-08	-1.89E-05	-3.18E-07
7	1.00E-01	1.00E-01	2.13E-05	-3.78E-05	-8.22E-06	3.56E-05
	1.00E-02	1.00E-02	2.13E-05	-3.78E-05	-8.22E-06	3.56E-05
	1.00E-03	1.00E-03	2.13E-05	-3.77E-05	-8.22E-06	3.56E-05
	1.00E-04	1.00E-04	2.12E-05	-3.76E-05	-8.18E-06	3.53E-05
	1.00E-05	1.00E-05	1.99E-05	-3.62E-05	-7.88E-06	3.33E-05
	1.00E-06	1.00E-06	1.08E-05	-2.64E-05	-5.75E-06	1.88E-05
	1.00E-07	1.00E-07	-7.13E-06	-7.13E-06	-1.55E-06	-9.83E-06
	1.00E-08	1.00E-08	-1.30E-05	-8.59E-07	-1.88E-07	-1.91E-05
8	1.01E-04	1.00E-04	1.31E-05	-2.95E-05	-3.94E-05	2.29E-05
	1.10E-05	1.00E-05	1.11E-05	-2.73E-05	-3.36E-05	1.65E-05
	1.99E-06	1.00E-06	4.34E-06	-1.99E-05	-1.35E-05	-5.59E-06
	1.09E-06	1.00E-07	4.35E-07	-1.56E-05	-1.93E-06	-1.83E-05
	1.00E-06	1.00E-08	-1.50E-07	-1.50E-05	-2.02E-07	-2.02E-05
	9.91E-07	1.00E-09	-2.11E-07	-1.49E-05	-2.03E-08	-2.04E-05

The estimated diffusion coefficients in Table II are presented as a ratio of main-term diffusivity to single-ion diffusion coefficient (Table I) in Table III. The ratios are expressed as:

$$\alpha_{11} = \frac{D_{11}}{D_{Sodium}} \qquad \alpha_{22} = \frac{D_{22}}{D_{Chloride}}$$

TABLE III

Estimated Main-Term Diffusion Coefficients Presented as a Ratio of Single-Ion Diffusivity

pH	Sodium Conc (meq/ml)	Chloride Conc (meq/ml)	α_{11}	α_{22}
6	1.00E-04	1.01E-04	2.02	1.91
	1.00E-05	1.10E-05	1.34	1.48
	1.00E-06	1.99E-06	-0.28	0.44
	1.00E-07	1.09E-06	-0.91	0.04
	1.00E-08	1.00E-06	-0.99	-0.01
	1.00E-09	9.91E-07	-1.00	-0.01
7	1.00E-01	1.00E-01	1.55	1.74
	1.00E-02	1.00E-02	1.55	1.74
	1.00E-03	1.00E-03	1.54	1.74
	1.00E-04	1.00E-04	1.53	1.73
	1.00E-05	1.00E-05	1.44	1.63
	1.00E-06	1.00E-06	0.78	0.92
	1.00E-07	1.00E-07	-0.52	-0.48
	1.00E-08	1.00E-08	-0.94	-0.94
8	1.01E-04	1.00E-04	0.95	1.12
	1.10E-05	1.00E-05	0.81	0.81
	1.99E-06	1.00E-06	0.31	-0.27
	1.09E-06	1.00E-07	0.03	-0.90
	1.00E-06	1.00E-08	-0.01	-0.99
	9.91E-07	1.00E-09	-0.02	-1.00

At pH 8, the chloride-ion diffuses slower compared to its diffusion coefficient (D_{22}) at pH 6. The chloride ion, concentration $1.0x10^{-6}$ milliequivalents-per-milliliter, diffuses against the concentration gradient at pH 8 but still maintains a positive diffusion velocity at pH 6. However, the sodium-ion shows opposite behavior. The sodium-ion diffuses in the direction of the concentration gradient at pH 8 and against the concentration gradient at pH 6 (the sodium-ion concentration is $1.0x10^{-6}$ milliequivalents-per-milliliter).

Multi-component effects cannot be ignored when the concentration of H^+, OH^-, Na^+, and Cl^- are of comparable magnitude (in equivalents). The effect of hydrogen and hydroxyl ions on the bulk phase transport of sodium chloride is shown in Table II (or Table III). In mixed-bed ion exchange, the net diffusion coefficient of a particular ion is influenced by hydrogen and hydroxyl ions resulting in increased or decreased mass-transfer coefficient for the particular ion. Harries's (1991) observation of ion-exchange rate dependence on pH can be seen in Table II.

Equations V-5 through V-11 need to be solved for obtaining ionic flux. The flux expressions (Equations V-5 and V-6) are solved with the continuity equation of the species to get a concentration profile. Equations V-5 to V-11 forms a set of non-linear equations, since the main-term and cross-term diffusion coefficients are concentration dependent. The solution for ionic flux can be obtained by linearizing Equations V-5 and V-6 (Toor, 1964; Taylor, 1982), by defining concentration in the diffusion coefficients (Frey, 1986).

Computation of Ion-Exchange Rate in a Packed Bed

Ionic species diffusion, from the bulk liquid to the resin surface, can be viewed as molecular diffusion, or as effective diffusion accounting for the interaction due to the presence of other ions. This effect is evident from Equations V-5 and V-11. If molecular form of diffusion is appropriate, then the diffusion coefficient can take values of the salt or acid/base form. The ion-exchange rate can then be calculated using the diffusion coefficient in a mass flux expression.

The rate of ion-exchange, in a mixed bed, is computed as the product of the ionic flux and the resin-particle surface area. When film mass-transfer controls ion-exchange in a mixed bed, the rate is equal to the product of film mass-transfer coefficient and a concentration gradient defined across the boundary of a pre-defined region. The rate of ion-exchange is:

$$\frac{\partial q}{\partial t} = K_f a_s \left(C_i - C_i^*\right) = -j_i a_s \tag{V-12}$$

To compute the rate, Equations V-5 and V-6 need to be solved and used in Equation V-12. Solving Equations V-5 to V-11 is a very tedious procedure. However, Haub (1986) obtained an analytical rate expression for binary univalent exchange by making simplifying assumptions. An effective diffusion coefficient has been calculated by Haub (1986) for binary-univalent exchange in an ion-exchange system (hydrogen in the resin phase exchanging for sodium ions in the liquid) as:

$$j_i = D_{ei} \frac{\partial C_i}{\partial r} \tag{V-13}$$

where

$$D_{ei} = \frac{2D_N D_H}{\left(D_H - D_N\right)} \left[\frac{\left(C_N^o + C_H^o\right) - \left(C_N^* + C_H^*\right)}{\left(C_N^o + C_N^*\right)} \right] \tag{V-14}$$

Van Brocklin and David (1972) studied the effect of ionic migration on liquid-phase mass transfer and applied a correction to Equation V-12. A factor, R_i, was formulated to be applied in conjunction with existing non-electrolyte mass-transfer correlations. The R_i factor was defined as the ratio of diffusion coefficient of the ions exiting-to-entering the ion-exchanger. They modeled ionic mass transfer using film, penetration, and boundary-layer theories. Using boundary-layer theory, the R_i factor was proportional to two-third power of the ratio of diffusion coefficients. The exponent on the diffusion coefficient ratio was one from film theory, and one-half from penetration theory.

Haub (1986) used the effective-diffusion coefficient, Equation V-14, and applied the R_i correction. The R_i factor, defined by Haub (1986), was the ratio of the effective diffusion coefficient (Equation V-14) to single-ion diffusion coefficient of the ionic species with a two-thirds exponent.

$$R_i = \left(\frac{D_{ei}}{D_i}\right)^{2/3} \tag{V-15}$$

The non-electrolyte mass-transfer coefficient was calculated using either Carberry (1960) or Kataoka et al. (1972) correlation depending on the Reynolds number. The ion-exchange rate expression with correction is:

$$\frac{\partial q}{\partial t} = K_f a_s R_i \left(C_i - C_i^*\right) \tag{V-16}$$

Liquid-Phase Mass-Transfer Coefficient in a Mixed-Bed Exchanging Sodium Chloride

Usually the diffusion coefficient used in the Schmidt number, for mass-transfer coefficient calculations, is the single-ion diffusion coefficient at infinite dilution. In a mixed-bed ion-exchange system, the single ionic diffusion coefficient does not represent the true value of diffusivity. The mobility of the exchanging ion is strongly influenced by the presence of other ions around the exchanger. Since charge separation cannot occur, the species diffusion coefficient is different from the single-ion diffusion coefficient.

Tables IV through XII present a comparison of mass-transfer coefficients calculated using different diffusion coefficient values. Non-electrolyte mass transfer

TABLE IV

Predicted Mass-Transfer Coefficient Comparsions with Mixed Bed Sodium Data (inlet: 2.8 x 10^{-5} N; Lee, 1994)

Cationic Resin		HGR-W2-H (particle dia: 0.08 cm)			650C-H (particle dia: 0.065 cm)		
Reynolds number (superficial velocity, cm/s)		41 (1.65)	58 (2.3)	75 (3.0)	34 (1.65)	47 (2.3)	61 (3.0)
Diffusion coefficient used in Schmidt number calculation (cm^2/s)	Schmidt number	MTC [a], cm/s (% dev from experimental value: 0.014 cm/s)	MTC [a], cm/s (% dev from experimental value: 0.017 cm/s)	MTC [a], cm/s (% dev from experimental value: 0.020 cm/s)	MTC [a], cm/s (% dev from experimental value: 0.013 cm/s)	MTC [a], cm/s (% dev from experimental value: 0.017 cm/s)	MTC [a], cm/s (% dev from experimental value: 0.018 cm/s)
Ionic diffusion coefficient at infinite dilution (1.33x10^{-5})	678	0.011 (-22.5)	0.013 (-22.7)	0.015 (-26.0)	0.012 (-6.6)	0.014 (-14.7)	0.016 (-8.2)
Diffusion as NaCl (1.61x10^{-5})	560	0.012 (-11.9)	0.015 (-12.1)	0.017 (-16.0)	0.014 (6.1)	0.016 (-3.1)	0.018 (4.4)
Diffusion as NaOH (2.13x10^{-5})	424	0.015 (6.0)	0.018 (5.8)	0.021 (1.1)	0.016 (27.7)	0.019 (16.6)	0.022 (25.6)
Correction for the calculated value of effective diffusion coefficient [b]		0.019 (37.0)	0.023 (36.3)	0.026 (30.3)	0.021 (64.5)	0.025 (50.3)	0.028 (62.0)

MTC: Mass Transfer Coefficient [a] calculated from Carberry (1960) correlation [b] Van Brocklin and David (1978)

TABLE V

Predicted Mass Transfer Coefficient Comparsions with Mixed Bed Sodium Data (inlet: 6.9×10^{-5} N; Lee, 1994)

Cationic Resin		HGR-W2-H (particle dia: 0.08 cm)			650C-H (particle dia: 0.065 cm)		
Reynolds number (superficial velocity, cm/s)		41 (1.65)	58 (2.3)	75 (3.0)	34 (1.65)	47 (2.3)	61 (3.0)
Diffusion coefficient used in Schmidt number calculation (cm^2/s)	Schmidt number	MTC[a], cm/s (% dev from experimental value: 0.014 cm/s)	MTC[a], cm/s (% dev from experimental value: 0.016 cm/s)	MTC[a], cm/s (% dev from experimental value: 0.019 cm/s)	MTC[a], cm/s (% dev from experimental value: 0.013 cm/s)	MTC[a], cm/s (% dev from experimental value: 0.017 cm/s)	MTC[a], cm/s (% dev from experimental value: 0.017 cm/s)
Ionic diffusion coefficient at infinite dilution (1.33×10^{-5})	678	0.011 (-20.8)	0.013 (-21.7)	0.015 (-22.5)	0.012 (-4.4)	0.014 (-15.7)	0.016 (-2.6)
Diffusion as NaCl (1.61×10^{-5})	560	0.012 (-10.0)	0.015 (-11.0)	0.017 (-12.0)	0.014 (8.6)	0.016 (-4.3)	0.018 (10.6)
Diffusion as NaOH (2.13×10^{-5})	424	0.015 (8.4)	0.018 (7.1)	0.02 (6.0)	0.016 (30.6)	0.019 (15.2)	0.022 (33.2)
Correction for the calculated value of effective diffusion coefficient[b]		0.019 (39.6)	0.023 (38.0)	0.026 (36.6)	0.021 (68.5)	0.025 (48.5)	0.028 (71.7)

MTC: Mass Transfer Coefficient [a] calculated from Carberry (1960) correlation [b] Van Brocklin and David (1978)

TABLE VI

Predicted Mass-Transfer Coefficient Comparsions with Mixed Bed Chloride Data (inlet: 2.8×10^{-5} N; Lee, 1994)

Anionic Resin		SBR-PC-OH (particle dia: 0.06 cm)			550A-OH (particle dia: 0.059 cm)		
Reynolds number (superficial velocity, cm/s)		31 (1.65)	43 (2.3)	56 (3.0)	31 (1.65)	43 (2.3)	55 (3.0)
Diffusion coefficient used in Schmidt number calculation (cm^2/s)	Schmidt number	MTC [a], cm/s (% dev from experimental value: 0.019 cm/s)	MTC [a], cm/s (% dev from experimental value: 0.022 cm/s)	MTC [a], cm/s (% dev from experimental value: 0.025 cm/s)	MTC [a], cm/s (% dev from experimental value: 0.021 cm/s)	MTC [a], cm/s (% dev from experimental value: 0.026 cm/s)	MTC [a], cm/s (% dev from experimental value: 0.027 cm/s)
Ionic diffusion coefficient at infinite dilution (2.03×10^{-5})	445	0.017 (-13.5)	0.020 (-9.5)	0.022 (-10.8)	0.017 (-20.2)	0.02 (-23.7)	0.022 (-18.0)
Diffusion as NaCl (1.61×10^{-5})	560	0.014 (-26.0)	0.017 (-22.4)	0.019 (-23.5)	0.014 (-31.6)	0.017 (-34.6)	0.019 (-29.6)
Diffusion as HCl (3.33×10^{-5})	271	0.023 (20.4)	0.027 (26.0)	0.031 (24.1)	0.023 (11.0)	0.028 (6.0)	0.031 (14.2)
Correction for the calculated value of effective diffusion coefficient [b]		0.037 (90.7)	0.043 (99.5)	0.049 (96.7)	0.037 (76.0)	0.044 (68.0)	0.05 (81.0)

MTC:Mass Transfer Coefficient [a] calculated from Carberry (1960) correlation [b] Van Brocklin and David (1978)

TABLE VII

Predicted Mass-Transfer Coefficient Comparsions with Mixed Bed Chloride Data (inlet: 6.9×10^{-5} N; Lee, 1994)

Anionic Resin		SBR-PC-OH (particle dia: 0.06 cm)			550A-OH (particle dia: 0.059 cm)		
Reynolds number (superficial velocity, cm/s)		31 (1.65)	43 (2.3)	56 (3.0)	31 (1.65)	43 (2.3)	55 (3.0)
Diffusion coefficient used in Schmidt number calculation (cm^2/s)	Schmidt number	MTC [a], cm/s (% dev from experimental value: 0.019 cm/s)	MTC [a], cm/s (% dev from experimental value: 0.021 cm/s)	MTC [a], cm/s (% dev from experimental value: 0.024 cm/s)	MTC [a], cm/s (% dev from experimental value: 0.020 cm/s)	MTC [a], cm/s (% dev from experimental value: 0.025 cm/s)	MTC [a], cm/s (% dev from experimental value: 0.026 cm/s)
Ionic diffusion coefficient at infinite dilution (2.03×10^{-5})	445	0.017 (-11.0)	0.020 (-9.5)	0.022 (-8.6)	0.017 (-17.0)	0.02 (-20.4)	0.022 (-14.0)
Diffusion as NaCl (1.61×10^{-5})	560	0.014 (-23.0)	0.017 (-20.6)	0.019 (-21.5)	0.014 (-28.8)	0.017 (-31.6)	0.019 (-25.8)
Diffusion as HCl (3.33×10^{-5})	271	0.023 (25.0)	0.027 (28.9)	0.031 (27.1)	0.023 (15.5)	0.028 (10.7)	0.031 (20.3)
Correction for the calculated value of effective diffusion coefficient [b]		0.037 (98.0)	0.043 (104.3)	0.049 (101.5)	0.037 (83.0)	0.044 (75.0)	0.05 (91.0)

MTC:Mass Transfer Coefficient [a] calculated from Carberry (1960) correlation [b] Van Brocklin and David (1978)

TABLE VIII

Predicted Mass-Transfer Coefficient Comparsions with Mixed Bed Chloride Data (Harries, 1984)

Anionic Resin		Amberlite IRA 900 (particle diameter: 0.079 cm)			Amberlite IRA 458 (particle diameter: 0.074 cm)		
Reynolds number (superficial velocity, cm/s)			55 (2.5)	74 (3.3)		52 (2.5)	69 (3.3)
Diffusion coefficient used in Schmidt number calculation (cm^2/s)	Schmidt number	MTC [a], cm/s (% dev from experimental value: cm/s)	MTC [a], cm/s (% dev from experimental value: 0.021 cm/s)	MTC [a], cm/s (% dev from experimental value: 0.025 cm/s)	MTC [a], cm/s (% dev from experimental value: cm/s)	MTC [a], cm/s (% dev from experimental value: 0.020 cm/s)	MTC [a], cm/s (% dev from experimental value: 0.026 cm/s)
Ionic diffusion coefficient at infinite dilution ($1.81x10^{-5}$)	554		0.016 (-21.0)	0.019 (-23.5)		0.017 (-15.4)	0.020 (-23.4)
Diffusion as NaCl ($1.43x10^{-5}$)	699		0.014 (-32.3)	0.016 (-34.5)		0.014 (-27.6)	0.017 (-34.4)
Diffusion as HCl ($2.97x10^{-5}$)	337		0.023 (10.0)	0.026 (6.5)		0.024 (17.6)	0.027 (6.6)
Correction for the calculated value of effective diffusion coefficient [b]			0.036 (72.6)	0.041 (67.0)		0.037 (84.5)	0.043 (67.1)

MTC:Mass Transfer Coefficient [a] calculated from Carberry (1960) correlation [b] Van Brocklin and David (1978)

TABLE IX

Predicted Mass-Transfer Coefficient Comparsions with Mono Bed Sodium Data (inlet: 2.8 x 10^{-5} N; Lee, 1994)
(cationic resin: HGR-W2-H, particle diameter: 0.08 cm)

Reynolds Number (Superficial Velocity, cm/s)		41 (1.65)		58 (2.3)		75 (3.0)	
Diffusion Coefficient used in Schmidt number calculation (cm^2/s)	Schmidt Number	Mass transfer Coefficient [a] (cm/s)	% deviation from experimental value:0.014 cm/s	Mass transfer Coefficient [a] (cm/s)	% deviation from experimental value:0.014 cm/s	Mass transfer Coefficient [a] (cm/s)	% deviation from experimental value:0.014 cm/s
Ionic diffusion coefficient at infinte dilution (1.33x10^{-5})	679	0.011	-12.5	0.013	-17.7	0.015	-16.3
Diffusion as NaCl (1.61x10^{-5})	560	0.012	-0.5	0.015	-6.5	0.017	-4.8
Diffusion as NaOH (2.13x10^{-5})	424	0.015	19.7	0.018	12.5	0.02	14.5
Correction for the calculated value of effective diffusion coefficient [b]		0.019	54.3	0.023	45.0	0.026	47.6

[a] calculated from Carberry (1960) correlation [b] Van Brocklin and David (1978)

TABLE X

Predicted Mass-Transfer Coefficient Comparsions with Mono Bed Sodium Data (inlet: 6.9 x 10^{-5} N; Lee, 1994)
(cationic resin: HGR-W2-H, particle diameter: 0.08 cm)

Reynolds Number (Superficial Velocity, cm/s)		41 (1.65)		58 (2.3)		75 (3.0)	
Diffusion Coefficient used in Schmidt number calculation (cm^2/s)	Schmidt Number	Mass transfer Coefficient [a] (cm/s)	% deviation from experimental value:0.012 cm/s	Mass transfer Coefficient [a] (cm/s)	% deviation from experimental value:0.015 cm/s	Mass transfer Coefficient [a] (cm/s)	% deviation from experimental value:0.018 cm/s
Ionic diffusion coefficient at infinte dilution (1.33x10^{-5})	679	0.011	-11.0	0.013	-16.6	0.015	-16.7
Diffusion as NaCl (1.61x10^{-5})	560	0.012	1.1	0.015	-5.3	0.017	-5.3
Diffusion as NaOH (2.13x10^{-5})	424	0.015	21.6	0.018	14.0	0.02	13.8
Correction for the calculated value of effective diffusion coefficient [b]		0.019	56.8	0.023	46.4	0.026	46.7

[a] calculated from Carberry (1960) correlation [b] Van Brocklin and David (1978)

TABLE XI

Predicted Mass-Transfer Coefficient Comparsions with Mono Bed Chloride Data (inlet: 2.8×10^{-5} N; Lee, 1994) (anionic resin: SBR-PC-OH, particle diameter: 0.06cm)

Reynolds Number (Superficial Velocity, cm/s)		31 (1.65)		43 (2.3)		56 (3.0)	
Diffusion Coefficient used in Schmidt number calculation (cm^2/s)	Schmidt Number	Mass transfer Coefficient [a] (cm/s)	% deviation from experimental value: 0.013 cm/s	Mass transfer Coefficient [a] (cm/s)	% deviation from experimental value: 0.017 cm/s	Mass transfer Coefficient [a] (cm/s)	% deviation from experimental value: 0.020 cm/s
Ionic diffusion coefficient at infinte dilution (2.03×10^{-5})	445	0.017	25.0	0.020	18.4	0.022	12.6
Diffusion as NaCl (1.61×10^{-5})	560	0.014	7.1	0.017	1.5	0.019	-3.5
Diffusion as HCl (3.33×10^{-5})	271	0.023	73.7	0.027	64.6	0.031	56.7
Correction for the calculated value of effective diffusion coefficient [b]		0.037	175.3	0.043	161.0	0.049	148.3

[a] calculated from Carberry (1960) correlation [b] Van Brocklin and David (1978)

TABLE XII

Predicted Mass-Transfer Coefficient Comparsions with Mono Bed Chloride Data (inlet: 6.9 x 10^{-5} N; Lee, 1994) (anionic resin: SBR-PC-OH, particle diameter: 0.06cm)

Reynolds Number (Superficial Velocity, cm/s)		31 (1.65)		43 (2.3)		56 (3.0)	
Diffusion Coefficient used in Schmidt number calculation (cm^2/s)	Schmidt Number	Mass transfer Coefficient [a] (cm/s)	% deviation from experimental value: 0.014 cm/s	Mass transfer Coefficient [a] (cm/s)	% deviation from experimental value: 0.017 cm/s	Mass transfer Coefficient [a] (cm/s)	% deviation from experimental value: 0.019 cm/s
Ionic diffusion coefficient at infinte dilution (2.03×10^{-5})	445	0.017	16.1	0.020	12.9	0.022	16.7
Diffusion as NaCl (1.61×10^{-5})	560	0.014	-0.4	0.017	-3.2	0.019	0.1
Diffusion as HCl (3.33×10^{-5})	271	0.023	61.6	0.027	-57.0	0.031	62.4
Correction for the calculated value of effective diffusion coefficient [b]		0.037	156.1	0.043	149.0	0.049	157.0

[a] calculated from Carberry (1960) correlation [b] Van Brocklin and David (1978)

coefficient is calculated using the Carberry (1960) correlation. Mass-transfer coefficient applying the correction used by Haub (1986) has also been computed. Assuming that the interfacial concentrations are zero, Equation V-14 reduces to:

$$D_{ei} = \frac{2D_N D_H}{D_H - D_N}\left[1 + \frac{C_H^o}{C_N^o}\right] \qquad \text{(V-17)}$$

The term inside the parantheses will never have a value less than one. Hence the minimum value D_{ei} can have is equal to the term outside the parantheses. However, in Equation V-14, D_{ei} can be a negative value if the sum of the interfacial concentrations is greater than the sum of the bulk concentrations. Equation V-17 has been used for calculating an effective-diffusion coefficient with the concentration term being neglected.

Tables IV through XII present the value of deviation of the calculated mass-transfer coefficients from the experimental values. Tables IV and V compare the calculated sodium mass-transfer coefficient with Lee's (1994) experimental data. Sodium mass-transfer coefficient, for the cation-exchange resin HGR-W2-H, calculated using NaOH diffusivity gives better estimates than the other diffusion coefficients. While for the resin 650C-H, mass-transfer coefficient calculated using NaCl diffusivity deviates less from the experimental value.

The cation-exchange resin HGR-W2-H had a particle diameter of 0.08 cm, and the cation-exchange resin 650C-H had a diameter of 0.065 cm. All other experiment variables were identical. Since the resin HGR-W2-H had a bigger particle size, the exchange kinetics were unfavorable compared to the resin 650C-H. Due to the bigger particle size there is increased ionic leakage (Foutch, 1991). The effluent concentration using HGR-W2-H at 59 m/hr and an influent concentration of

2.8×10^{-5} N, as reported by Lee (1994), was 1.13×10^{-6} N. For similar experimental conditions, an effluent concentration value of 6.9×10^{-7} N was obtained using the cation-exchange resin 650C-H.

The deviation of calculated mass-transfer coefficient using different diffusivities in Tables IV and V can be explained by results from computation in Table II. From Table II, at pH 7, the main-term diffusion coefficient (for sodium, D_{11}) decreases from the value of NaOH diffusivity to a value near to the sodium single-ion diffusion coefficient as the concentration of sodium chloride decreases. Since a lower effluent concentration is obtained using the cation-exchange resin 650C-H, NaCl diffusivity with Carberry's (1960) correlation gives a better estimate of the sodium mass-transfer coefficient. While using NaOH diffusivity gives a better value of sodium mass-transfer coefficient for the cation-exchange resin HGR-W2-H.

In mixed bed experiments, Lee (1994) used the resin mixture: HGR-W2-H with SBR-PC-OH, and 650C-H with 550A-OH. SBR-PC-OH and 550A-OH are anion-exchange resins. Particle diameter of the two different anion-exchange resins is almost equal (0.06 cm). Tables VI to VIII compare the calculated mass-transfer coefficient of chloride with experimental data.

Chloride mass-transfer coefficient calculated with single-ion diffusivity was good for the anion-exchange resin SBR-PC-OH. Mass-transfer coefficient predicted with hyrochloric acid molecule diffusivity gave an average deviation of ± 15% from the experimental value for the anion-exchange resin 550A-OH.

Higher sodium leakage using the cation-exchange resin HGR-W2-H resulted in slowing down the chloride ion; whereas, the cation-exchange resin 650C-H gave lower sodium effluent concentration and hence faster anion exchange kinetics. This effect can be seen by comparing the experimental chloride mass-transfer coefficients. Chloride mass-transfer coefficient was higher using a combination of resins 550A-OH and 650C-H when compared to the resin mixture SBR-PC-OH and HGR-W2-H. This demonstrates the effect of cation-exchange resin on anion kinetics. Also, data presented by Harries (1988) show a reduction in chloride mass-transfer coefficient when the cation-exchange resin bead size increases in a mixed bed.

Table VIII presents Harries (1984) data for chloride mass-transfer coefficient. Experiments were conducted with the anion-exchange resins Amberlite IRA900 and Amberlite IRA458. The cation-exchange resin used by Harries (1984) was Amberlite 200C. Chloride mass-transfer coefficient predictions with hydrochloric acid molecule diffusivity in Carberry's (1960) correlation compared well with experimental data. The average deviation of predicted value from the experimental mass-transfer coefficient was ± 10%. This agrees with the predictions for Lee's (1994) chloride mass-transfer coefficient using the anion-exchange resin 550A-OH (Tables VI and VII).

Lee's (1994) experimental mass-transfer data from mono beds are compared with calculated mass-transfer coefficients in Tables IX to XII. Lee (1994) conducted mono bed experiments with the cation-exchange resin HGR-W2-H, and the anion-exchange resin SBR-PC-OH. Using NaCl diffusivity in Carberry's (1960) correlation gave a deviation of ± 5% from the experimental mass-transfer coefficients of sodium and chloride.

Applying the correction of Van Brocklin and David (1972), as used by Haub

(1986), overpredicts the mass-transfer coefficient. Haub's (1986) model, Equation V-14, was derived using the Nernst film theory, but the R_i correction applied had an exponent two-thirds derived from the boundary-layer theory. The Schmidt number exponent in Carberry's (1960) correlation matches the exponent on the R_i factor, and is two-thirds. Hence the product of mass-transfer coefficient (calculated using Carberry's (1960) correlation) and the R_i factor (as defined by Haub (1986)) results in canceling the single-ion diffusion coefficient term — found in the definition of Schmidt number and the factor R_i (Equation V-15). This is equivalent to re-calculating the mass-transfer coefficient with the effective-diffusion coefficient. The predicted mass-transfer coefficient deviates from the experimental data by more than 30%.

Also, neglecting interfacial concentration in Equation V-17 can lead to an erroneous result. The interfacial concentration of hydrogen can be large compared to that of the sodium ion, since hydrogen is the primary ion exiting the cation resin after ion-exchange. The effect of R_i correction on improving mass-transfer coefficient predictions (Tables IV to XII) is inconclusive since concentration terms have been ignored in D_{ei} (Equation V-17).

Discussion

The mobility of an ionic species is directly proportional to its diffusivity. This fact is used for calculating diffusion coefficients from mobility data using the Nernst-Einstein equation (Cussler, 1984). In the sodium-chloride-water system, the hydrogen ion has a higher diffusivity than the rest of the species. The hydrogen ion has a diffusivity nearly an order of magnitude higher than the sodium ion. But this difference in diffusivity does not result in large differences in the mass-transfer coefficient. The appropriate diffusivity for the system depends on all the participating species and their concentration. Hence caution has to be exercised when using individual species diffusivity for calculating mass-transfer coefficient in the mixed-bed ion-exchange system.

The cation (sodium) mass-transfer coefficient showed less improvement compared to the anion (chloride) mass-transfer coefficient when put into mixed beds. The local composition in the bed is acidic due to the excess cation-exchange resin. This results in a water neutralization reaction near the surface of the anion resin, and an increased hydroxide ion gradient. The change in local pH, tending towards pH 7, around the anion-exchange resin results in a net increase in the chloride-ion diffusion coefficient (D_{22}, Table II). Therefore the chloride-ion mass-transfer coefficient increases in a mixed bed. Hence the multi-component nature of this system cannot be ignored.

Reducing the cation-exchange resin content in the mixed bed will decrease the mass-transfer coefficient of the chloride ion. This is a result of decrease in hydrogen ion concentration available for neutralizing hydroxide ions. Mass-transfer data presented by Harries (1988) validates this observation; changing the mixed-bed composition from a cation-to-anion resin ratio of 2:1 to 1:1 resulted in a 15% decrease of the chloride mass-transfer coefficient. The resin particle diameter also influences composition changes in the bed — higher leakages are expected as the particle diameter increases.

Local composition affects the diffusion of a species and hence the local mass-transfer coefficient. The experimental film mass-transfer coefficient, from shallow-bed experiments, is actually an average mass-transfer coefficient. The internal liquid-phase concentration gradient has been neglected and only the effluent concentration was measured. Hence the local mass-transfer coefficient will be different from the average mass-transfer coefficient.

The solid-liquid interfacial concentration is assumed zero in the analysis of mass-transfer data. Neglecting interfacial concentration in Haub's (1986) effective-diffusion coefficient resulted in a poor approximation of the mass-transfer coefficient. The solid-liquid interface concentration is determined by selectivity. This defines the local concentration gradient under which mass transfer occurs. Hence the total ionic flux also relates to selectivity of the resin for a particular species.

Effluent Concentration History of Sodium and Chloride from a Mixed Bed

The effluent profiles of sodium and chloride have been numerically computed. The ion-exchange rate expression (Equation V-16) is solved with the column material balance Equation (IV-2; Appendix A) to obtain the effluent concentration profile (Haub, 1986). The input data for the simulations is summarized in Table XIII.

In this work on mixed bed ion-exchange mass transfer, importance has been given to diffusion processes and not the hydrodynamics of the system. System hydrodynamics influences mixed bed ion-exchange at two places: 1) axial dispersion in the system and, 2) mass transfer around the resin particles. Flow fields are undoubtedly important in determining the efficiency of mass transfer. Stanek (1994) has dealt with the subject of packed-bed hydrodynamics extensively. In the analysis presented here, the assumptions are: 1) axial dispersion is absent, and 2) mass-transfer correlations adequately represent the effect of hydrodynamics.

TABLE XIII

Input Data for Simulations

Property	Value
Bed diameter (cms)	150.0
Resin depth (cms)	100.0
C:A (volumetric ratio)	2:1
Resin bead diameter (cm)	
Cation	0.08
Anion	0.06
Resin capacity (meq/ml)	
Cation	2.18
Anion	1.1
Temperature (C)	25
Influent concentration (meq/ml)	4.82×10^{-5}
Initial loading on the resin (%)	
Cation (sodium)	0.01
Anion (chloride)	0.01

Figures 1 and 2 compare the predicted effluent profile of sodium and chloride with different mass-transfer coefficients. The non-electrolyte mass-transfer coefficient was calculated using Carberry's (1960) correlation. The R_i correction has been used in the numerical calculation procedure.

Figures 1 and 2 show that the mass-transfer coefficient has little influence on the time taken to achieve equilibrium; the differences are minor. However, the mass-transfer coefficient does affect effluent concentration before the equilibrium condition is reached. In Figure 2, a 25% increase in chloride-ion mass-transfer

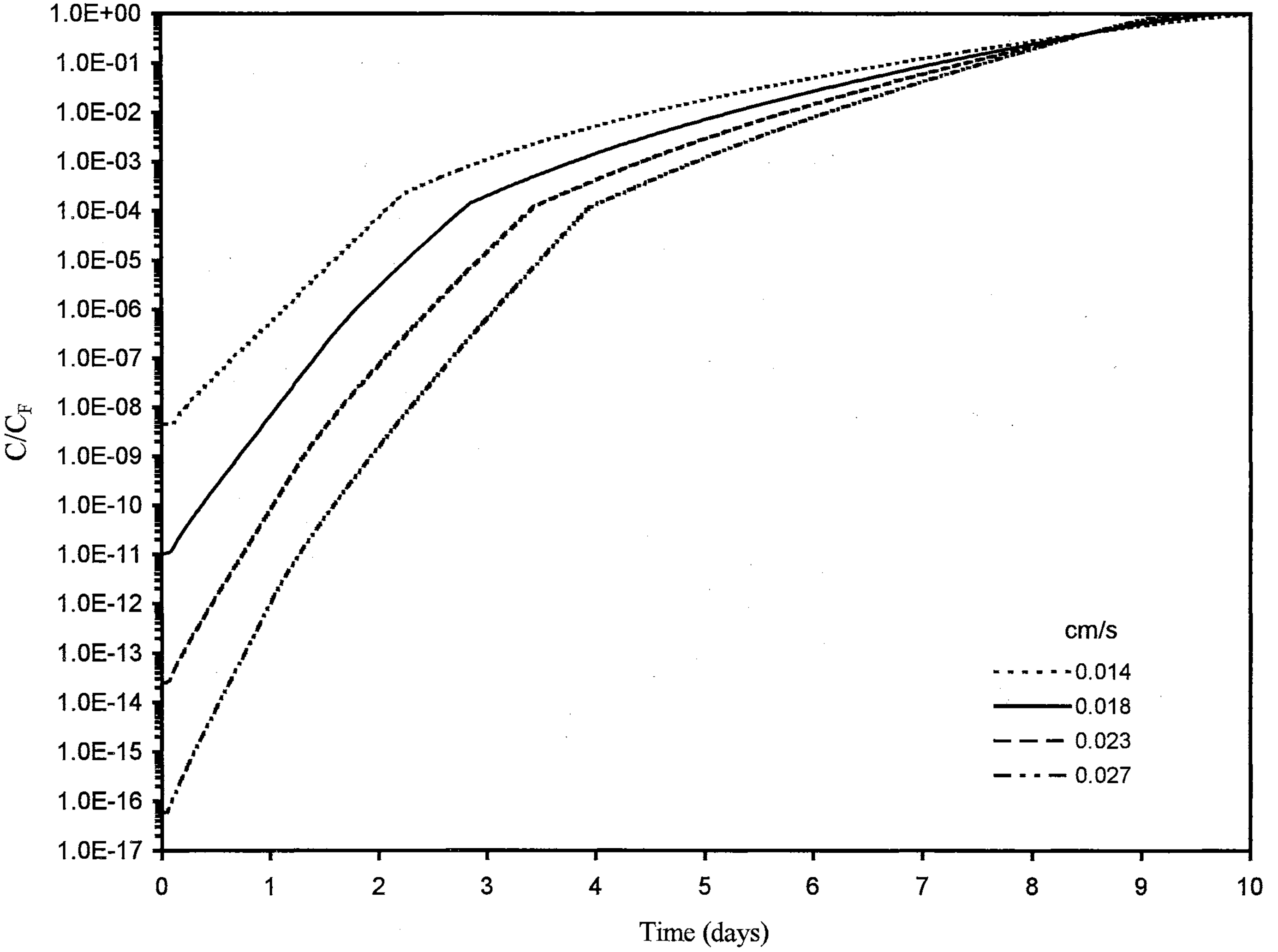

Figure 1. Comparison of sodium effluent profile with different mass-transfer coefficients.

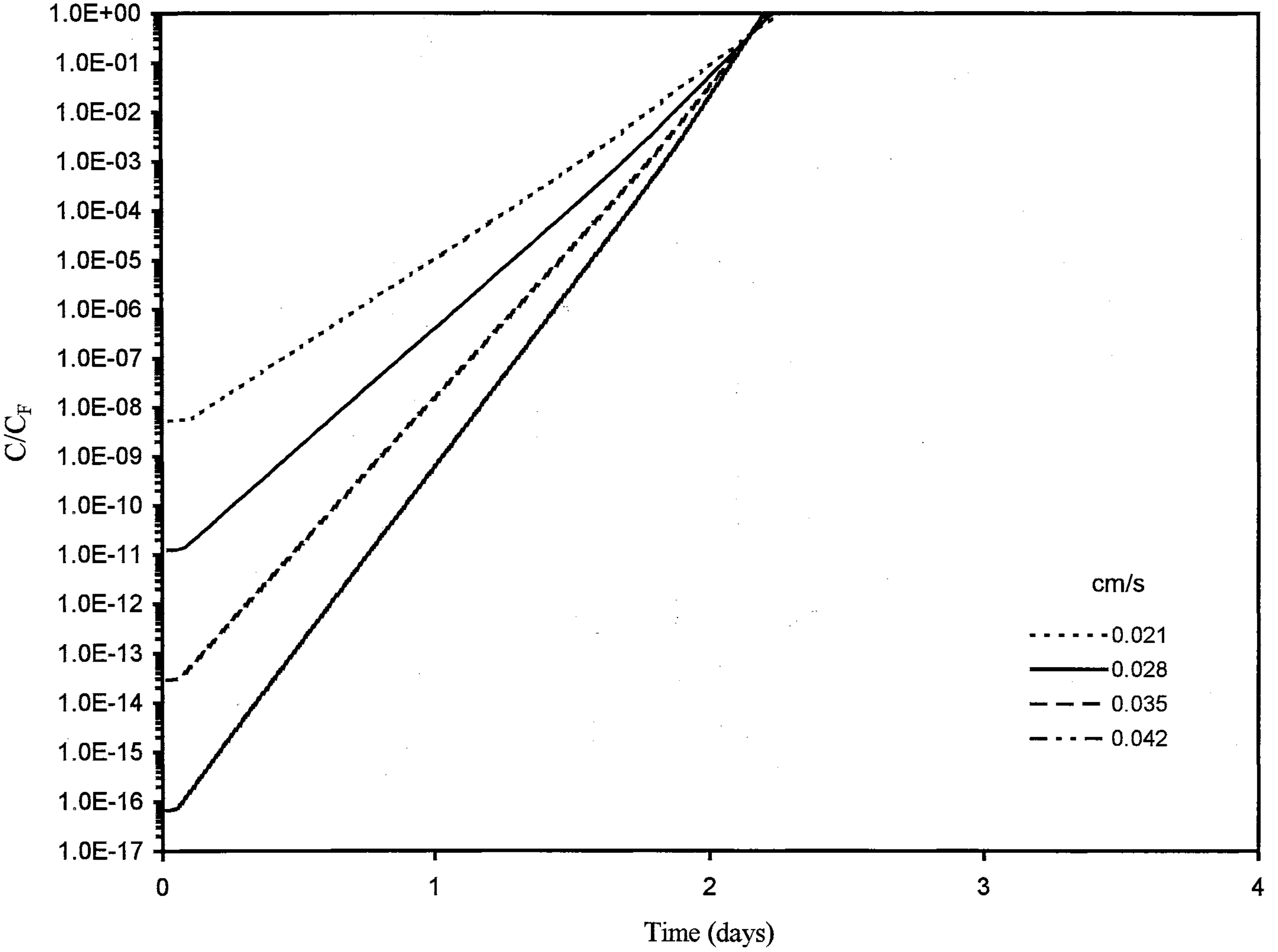

Figure 2. Effect of mass-transfer coefficient on chloride effluent profile.

coefficient, from 0.021 cm/s to 0.028 cm/s, resulted in three orders of magnitude decrease in the initial leakage. Similar effect of the mass-transfer coefficient on initial leakage is also seen in the predicted sodium effluent profile, Figure 1. The effect of mass-transfer coefficient is more pronounced during the earlier part of the breakthrough curve.

The cation-exchange resin capacity was more than the anion-exchange resin capacity since the mixed bed composition was 2:1 cation-to-anion resin ratio. Complete chloride ion breakthrough was achieved by 2.5 days. But the sodium ion exchanged even after chloride breakthrough. The rate of sodium exchange decreased after the chloride ion breakthrough. This is evident from the change in slope of the breakthrough profiles of sodium ion on the semi-linear plot (Figure 1). After complete anion exhaustion, the mixed bed exchanges only the cation — sodium in this case — and behaves like a mono bed. The effluent pH drops to the acidic range (pH 4.31 predicted for the operating conditions given in Table XIII) affecting sodium ion-exchange rate.

Figure 3 is a re-plot of Figure 1 using a linear scale. There is a cross-over point around day 8.5 in the predicted sodium effluent profiles. Around day 9, lower effluent concentration is obtained with low mass-transfer coefficient compared to effluent concentration at higher mass-transfer coefficient. The effluent profile cross-over occurs due to unused capacity in the bed at lower mass-transfer coefficient. The breatkthrough profile is sharp at higher mass-transfer coefficients, since most of the ion-exchange capacity has been used during the initial period of mixed-bed operation. The cation-exchange resin capacity was completely utilised by day 10.

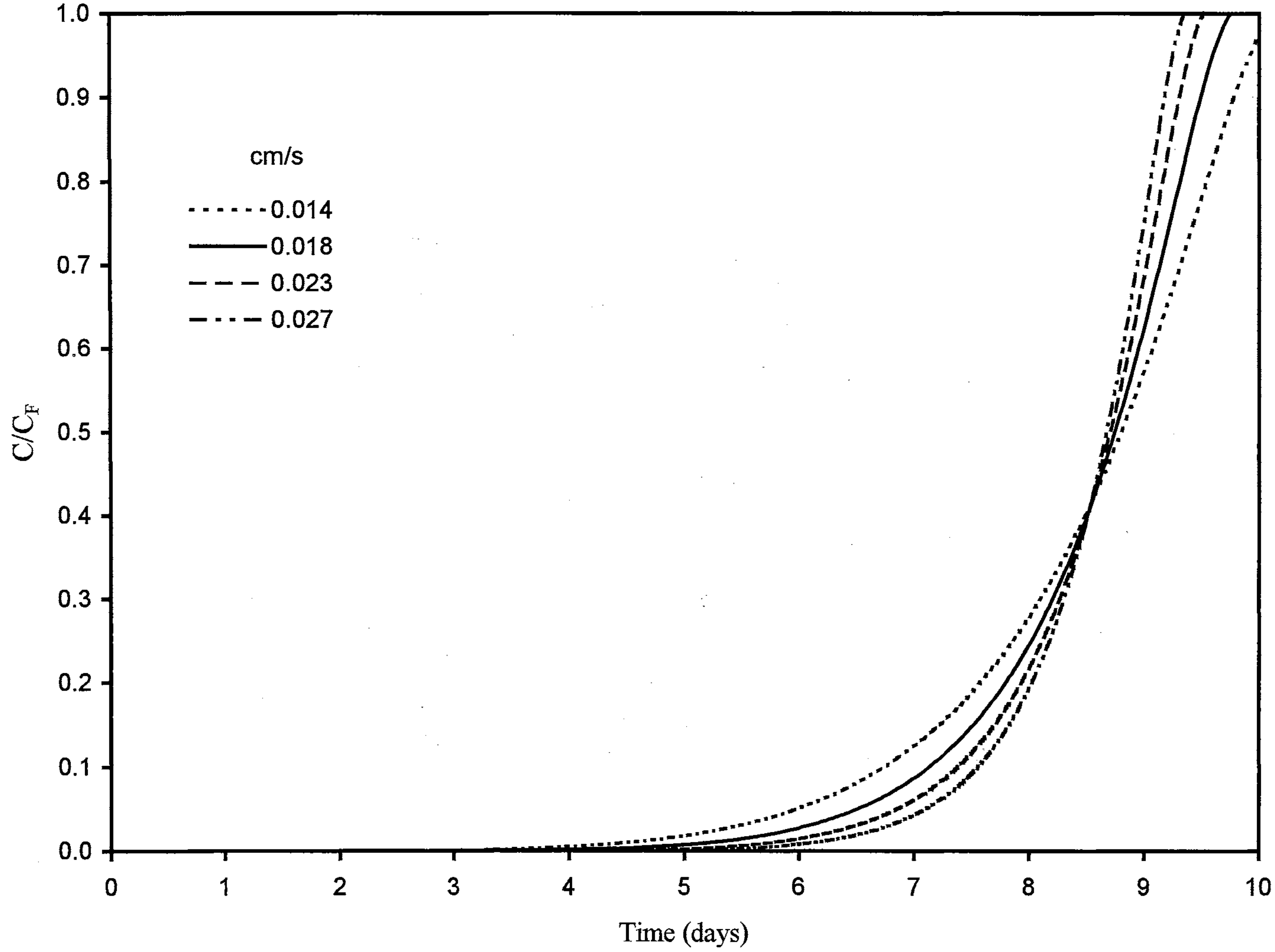

Figure 3. Comparison of sodium effluent profile with different mass-transfer coefficients.

The retention of a particular ionic species by the ion-exchanger is determined by the selectivity coefficient or the equilibrium constant. The mass-transfer coefficient affects the slope of the breakthrough curve. The breakthrough curve shows a sharpening effect as mass-transfer coefficient increases. In the case of mixed bed ion-exchange, the combination of selectivity coefficient and mass-transfer kinetics determines the effluent concentration profile.

Figures 4 and 5 present the liquid-phase profile of sodium and chloride ions in the bed. Higher mass-transfer coefficient resulted in increased sodium and chloride liquid-phase concentration at the top of the bed, when compared to the effluent concentration at lower mass-transfer coefficient. But in the lower portion of the mixed bed, low mass-transfer coefficient gave higher effluent concentration. Similar observations can be made with the resin-phase loading profile of sodium and chloride.

Figures 6 and 7 show the effect of mass-transfer coefficient on the resin phase loading of sodium and chloride in the mixed bed. At 2000 mins, 10% of the cation-exchange resin was saturated with sodium, while 60% of the anion-exchange resin had exhausted in the mixed bed. Earlier exhaustion of anion-exchange resin is expected since the cation-to-anion resin ratio was 2:1.

Chloride ion has a higher mass-transfer coefficient than the sodium ion. This corresponds to higher diffusivity of the chloride ion, almost 65% higher than the sodium ion at 25°C (Table I). Figures 8 and 9 show the predicted breakthrough profiles with mass-transfer coefficients corresponding to those used in Figures 4 to 7.

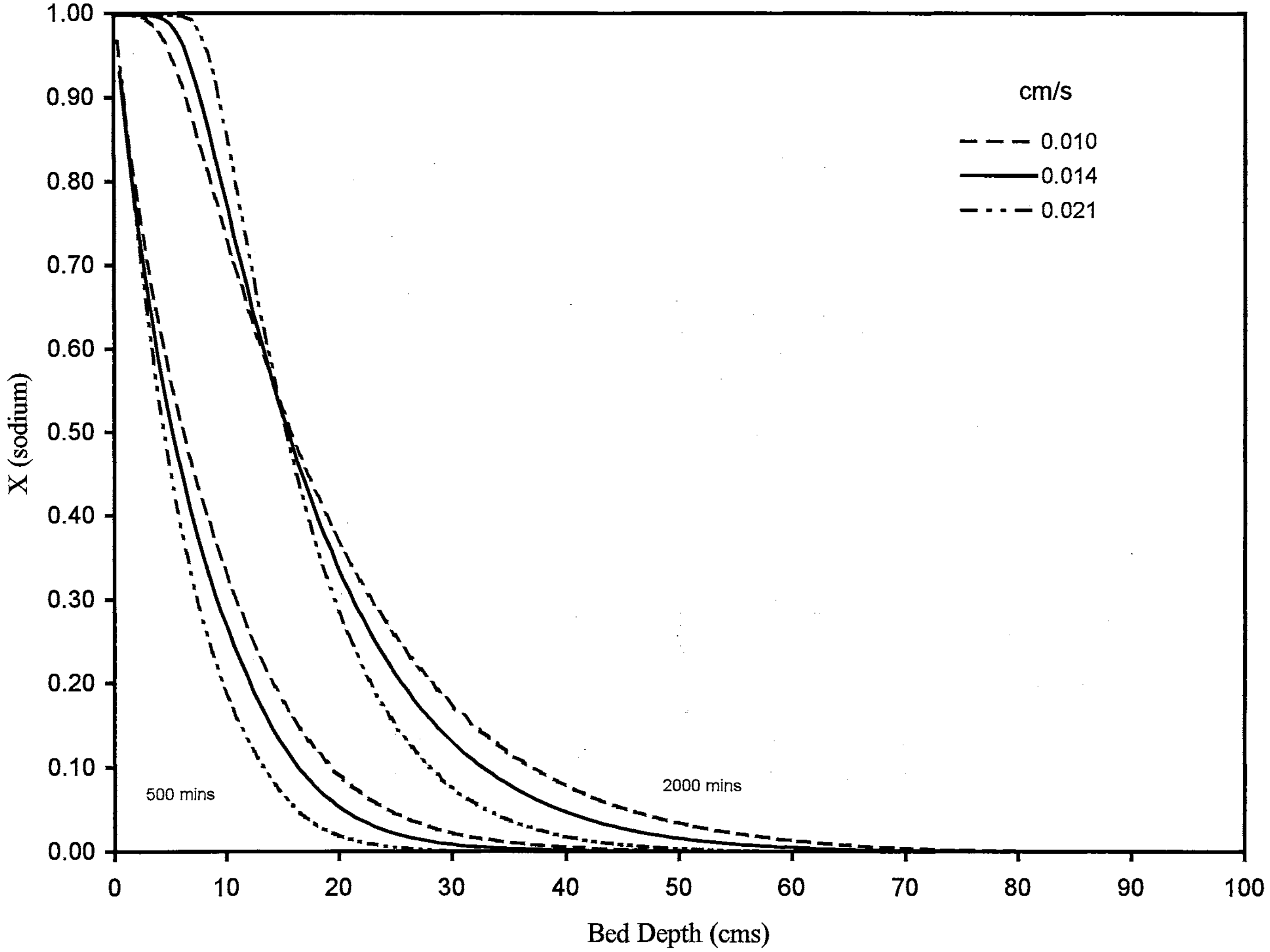

Figure 4. Liquid phase sodium concentration profiles with different mass-transfer coefficients.

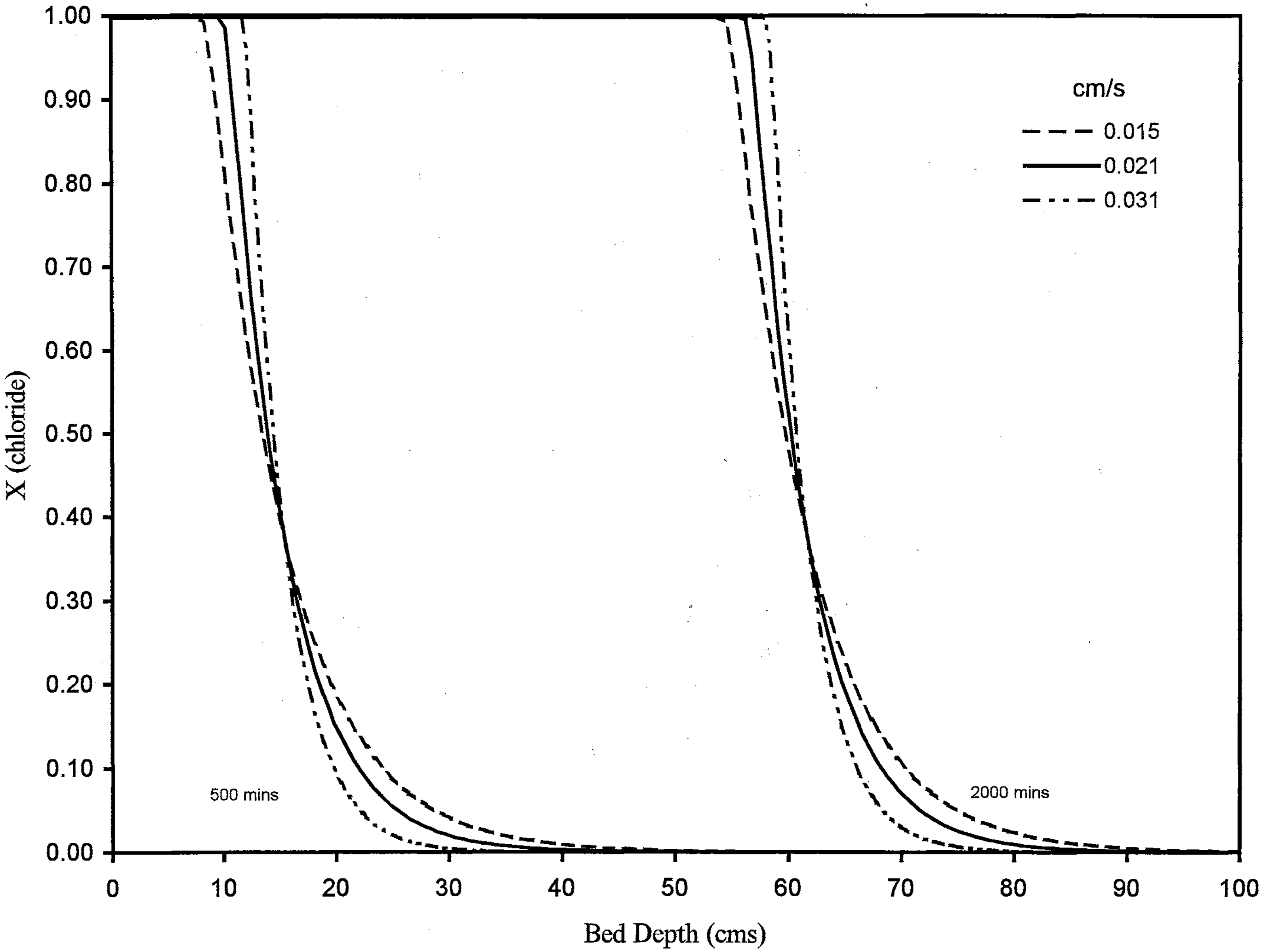

Figure 5. Liquid phase chloride profile with different mass-transfer coefficients.

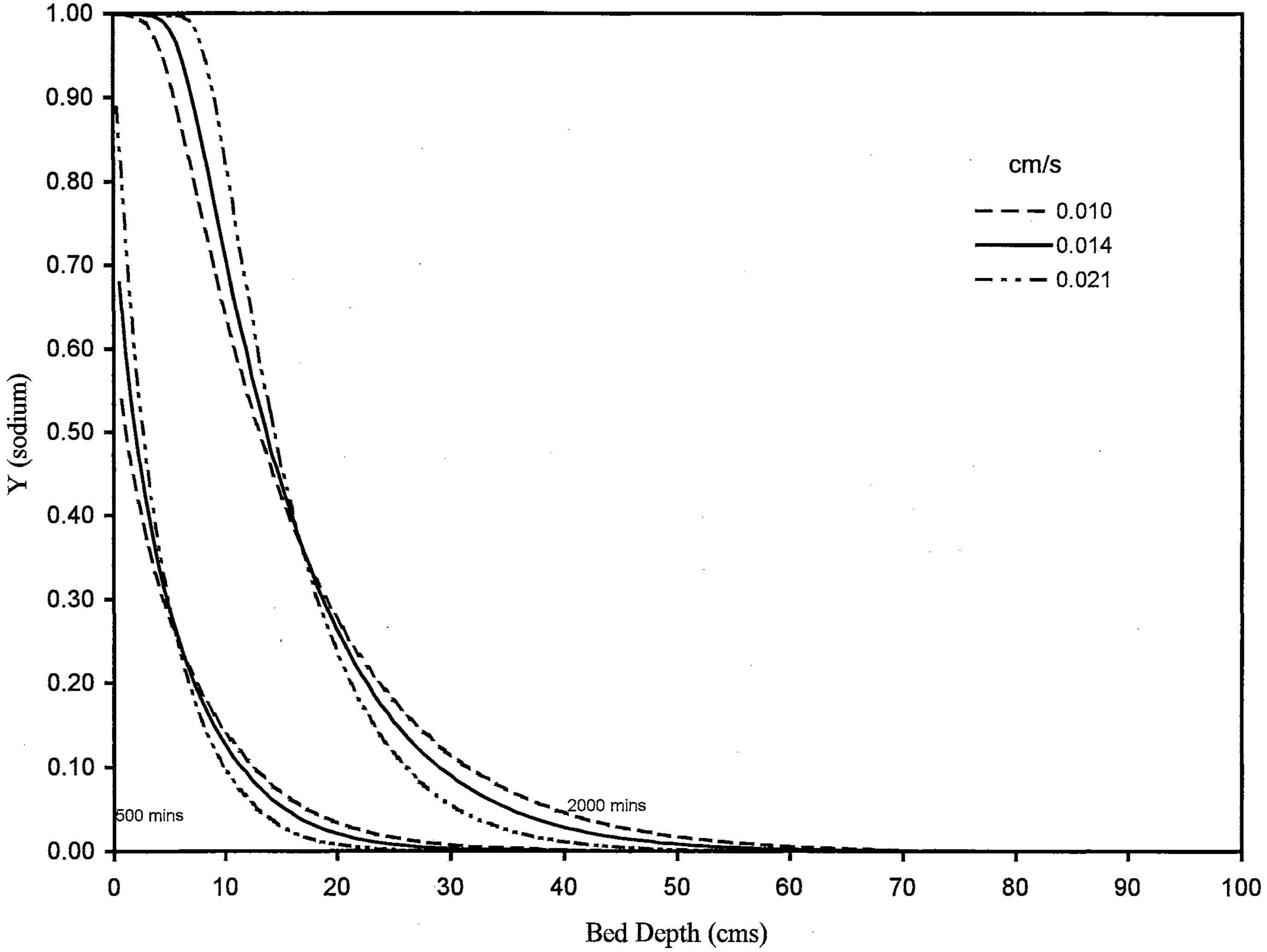

Figure 6. Resin-phase loading profile of sodium with different mass-transfer coefficients.

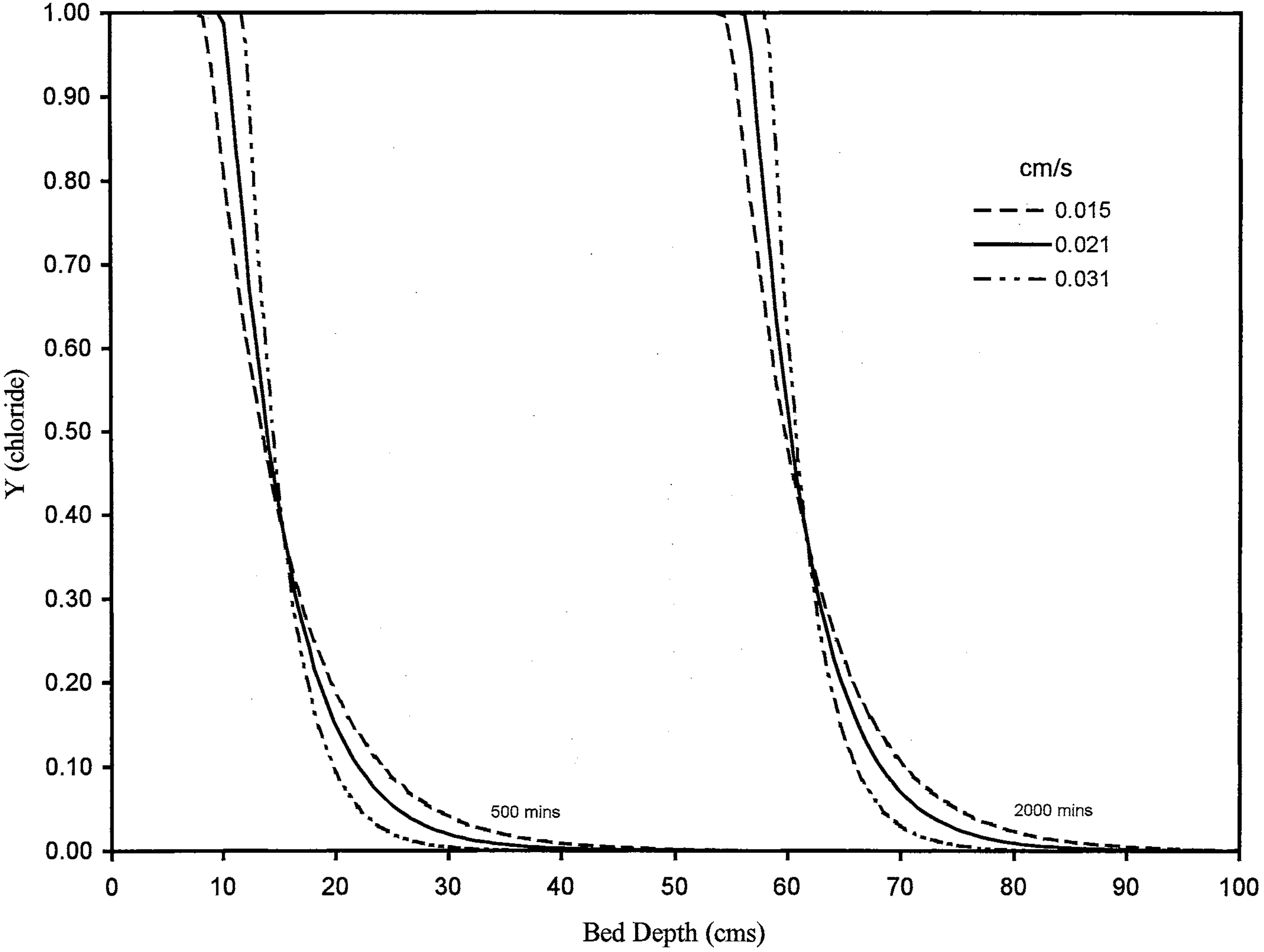

Figure 7. Resin-phase loading profile of chloride with different mass-transfer coefficients.

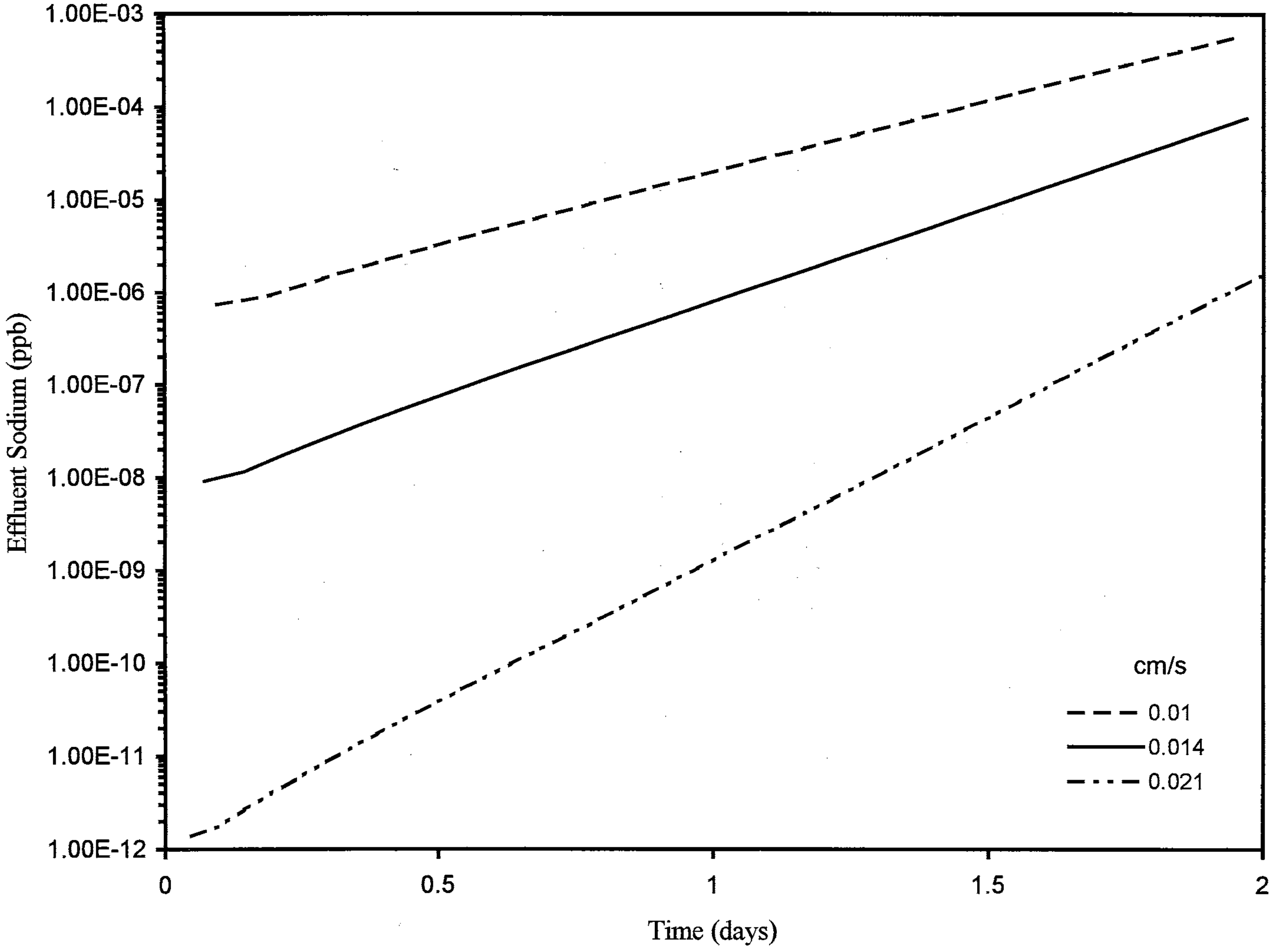

Figure 8. Effect of mass-transfer coefficient on sodium effluent profile.

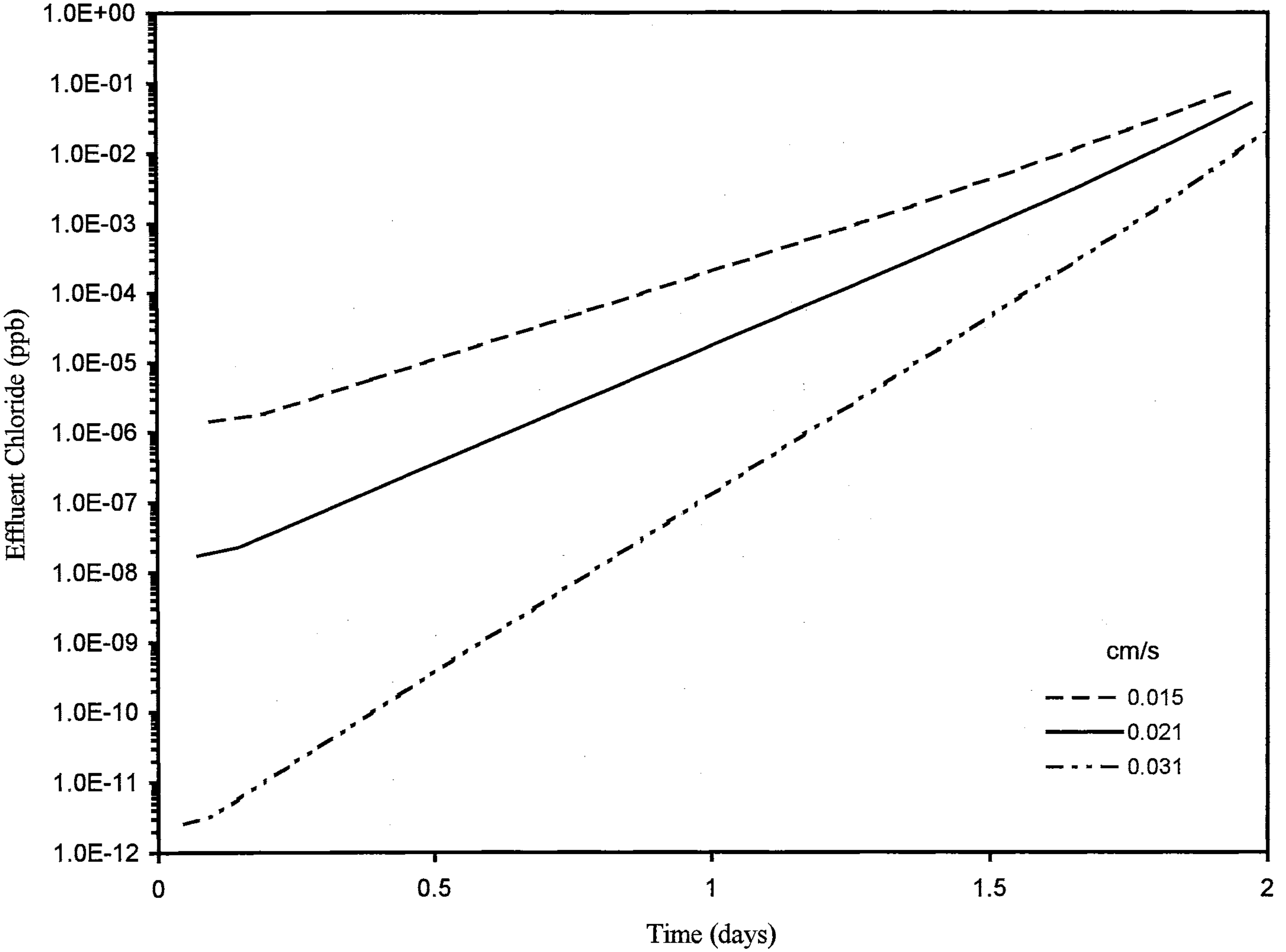

Figure 9. Effect of mass-transfer coefficient on chloride effluent profile.

Effect of R_i Correction on the Predicted Effluent Profiles

Diffusion, in the case of sodium chloride exchanging in a mixed bed, is multicomponent. The diffusivity of sodium and chloride is influenced by water ionization. The diffusivity also depends on the concentration of the different ions involved. The mass-transfer coefficient is assumed a constant in most deep-bed processes, but incorrect in the case of mixed bed ion-exchange. The concentration in the mixed bed changes and hence the diffusivity; this affects mass-transfer flux into the resin particle.

Haub and Foutch's (1986) model accounts for the effect of water ionization on diffusivity in this system. The column model also accounts for variation of diffusivity as concentration changes axially in the column. The R_i correction, as defined by Haub and Foutch (1986), is used in conjunction with a non-electrolyte mass-transfer correlation.

Figures 10 and 11 present the effect of applying R_i correction to predict effluent concentration history of sodium and chloride from an ion-exchange bed. Predicted effluent concentration was lower using the R_i correction. If R_i is greater than one, then the ion-exchange rate (Equation V-16) increases. The R_i factor is usually greater than one for sodium chloride exchange in the mixed bed. Therefore the ion-exchange rate is higher when compared to the rate calculated without the R_i correction; this results in a lower effluent concentration. The R_i correction influenced the chloride effluent profile more than the sodium profile.

Figures 12 and 13 show the numerically calculated effluent profiles using different mass-transfer correlations — Dwivedi and Upadhyay (1977), and Carberry

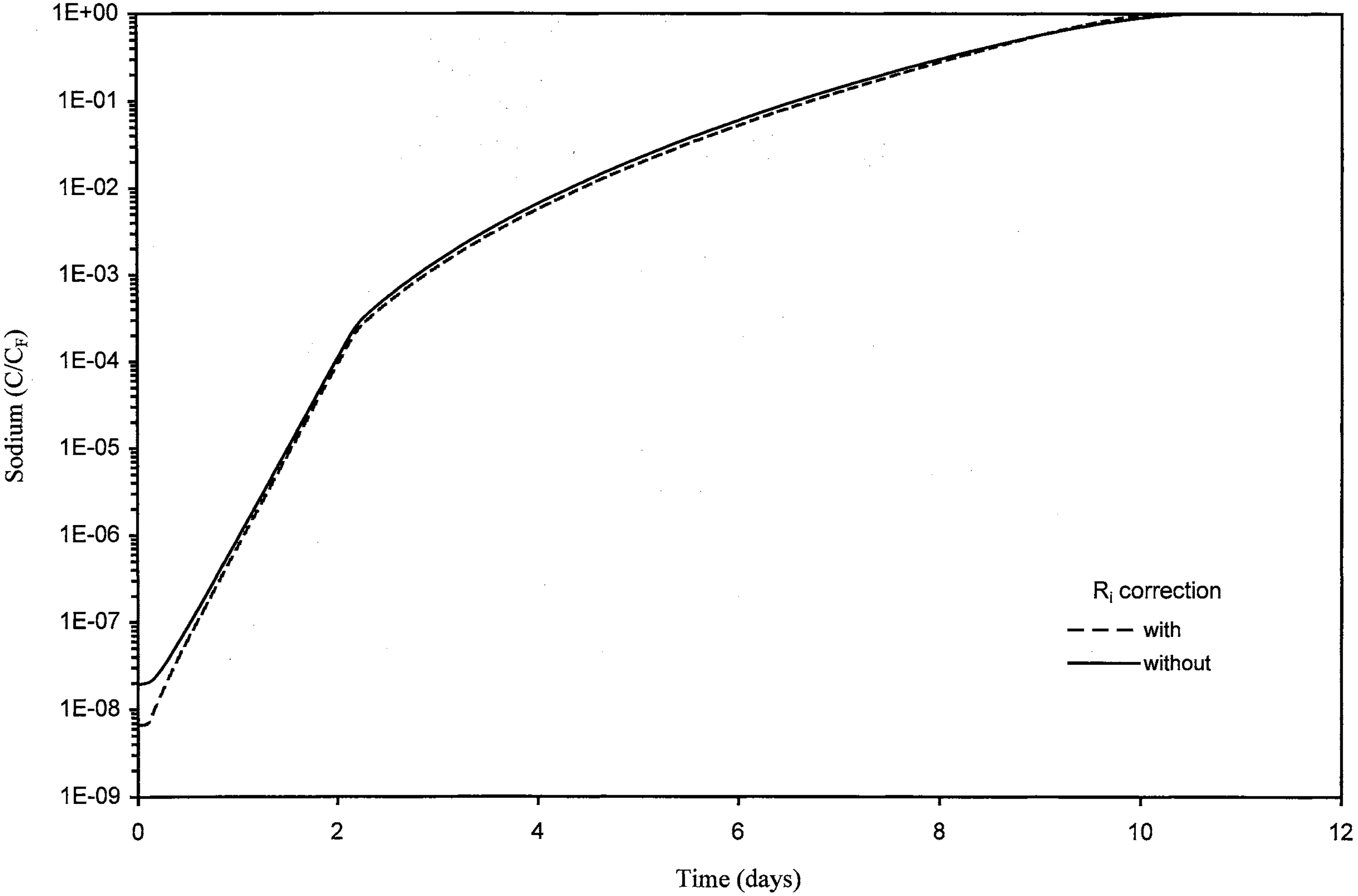

Figure 10. Effluent concentration profile using Carberry (1960) correlation

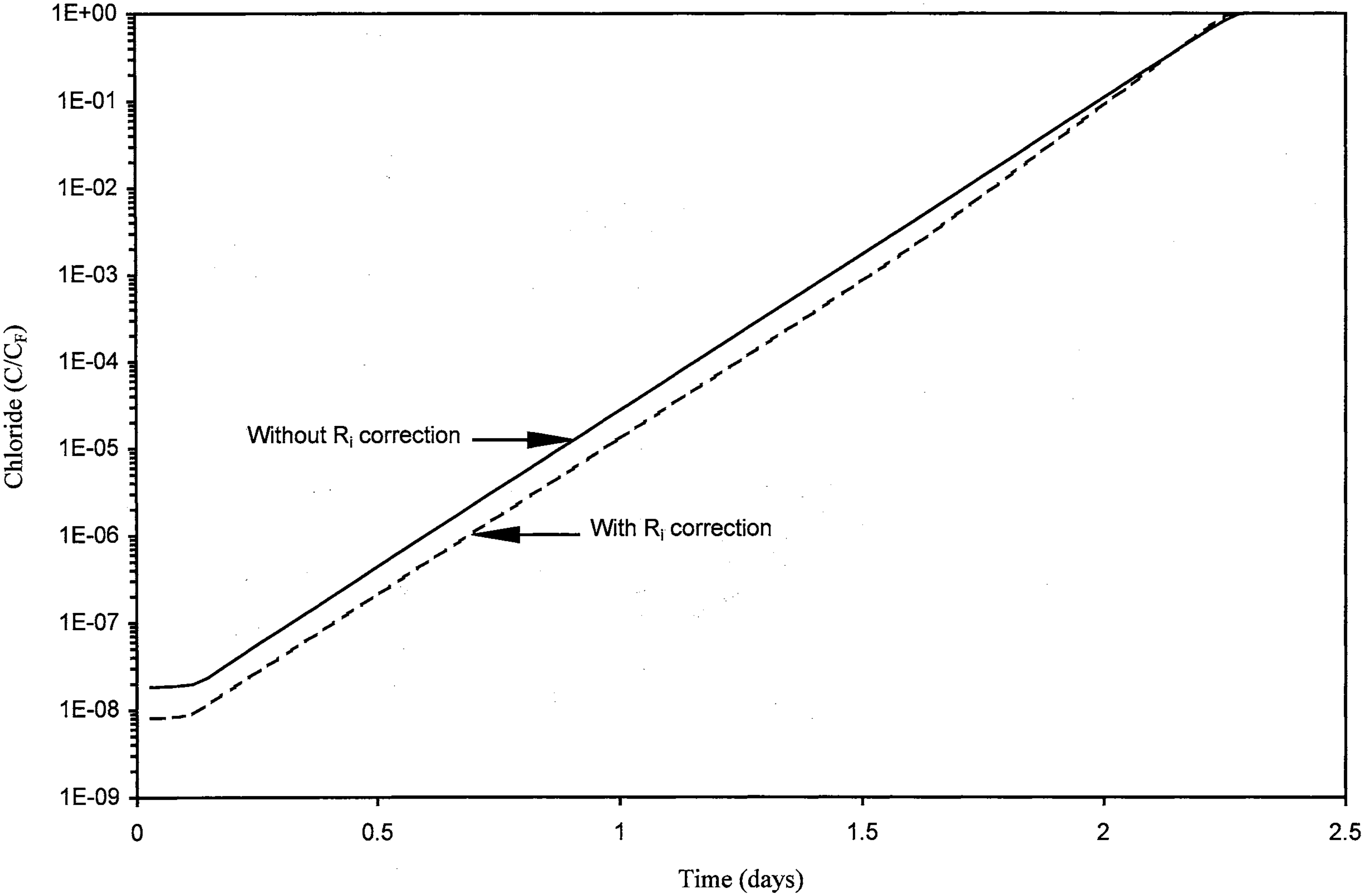

Figure 11. Chloride effluent profile using Carberry (1960) correlation for calculating the mass-transfer coefficient.

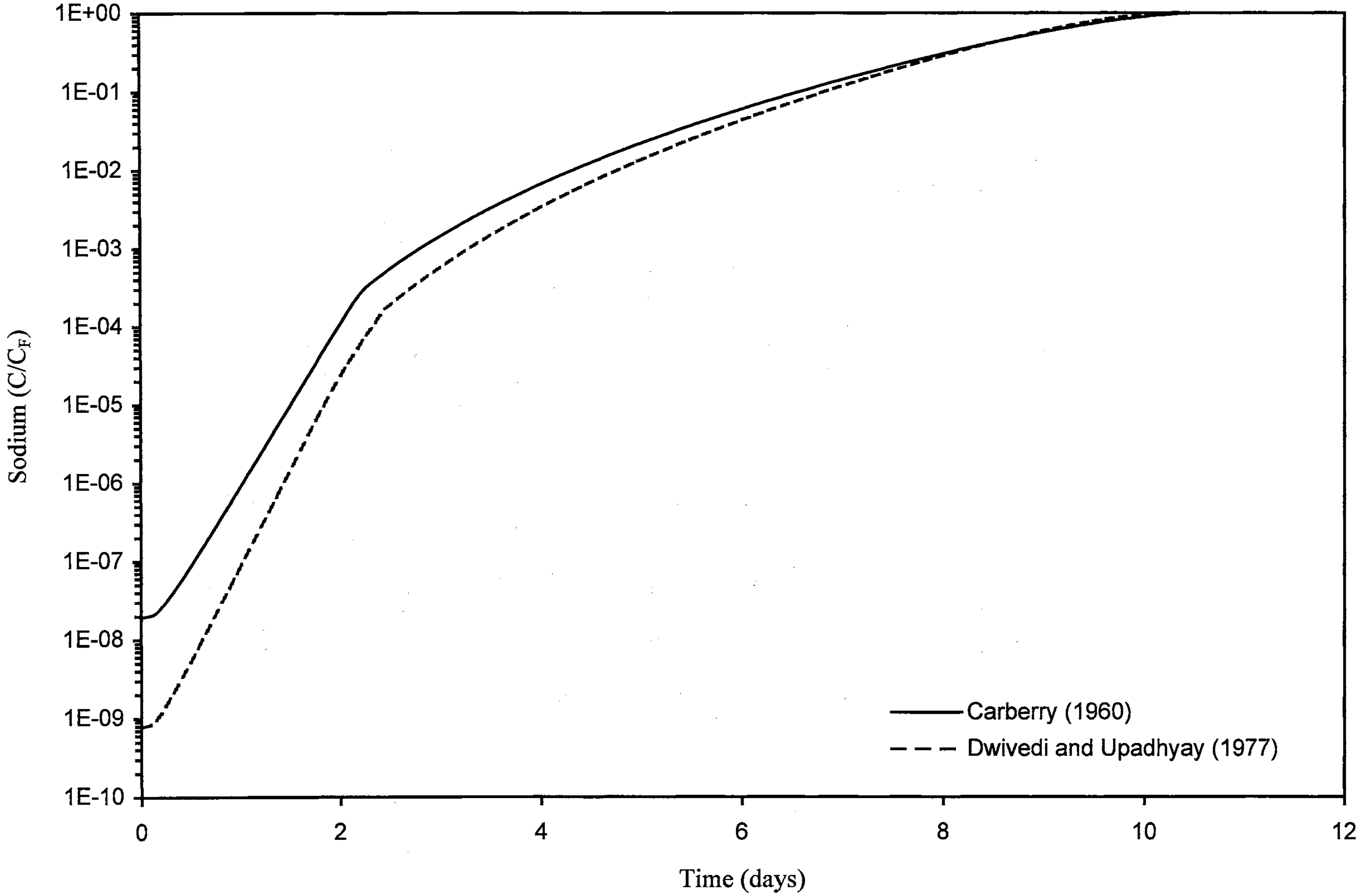

Figure 12. Predicted effluent profile using different mass-transfer correlations (without correction).

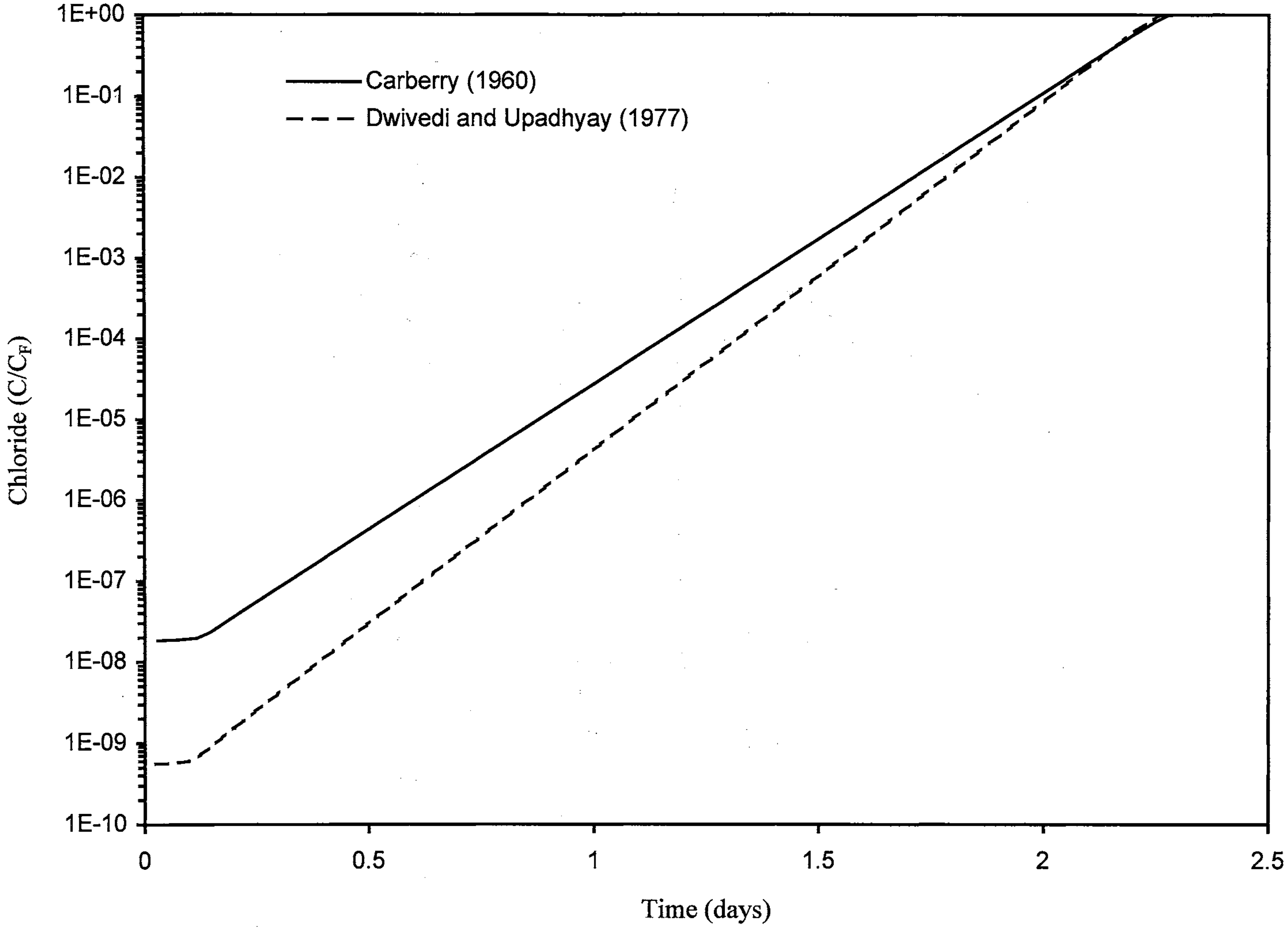

Figure 13. Chloride effluent profile using different mass-transfer coefficient correlations (without correction).

(1960) correlations. The calculated mass-transfer coefficients, for the operating conditions given in Table XIII, are shown in Table XIV.

TABLE XIV

Mass-Transfer Coefficients (cm/s) Predicted from Correlations

Ion	Dwivedi and Upadhyay (1977)	Carberry (1960)
Sodium	0.016	0.014
Chloride	0.025	0.021

Dwivedi and Upadhyay (1977) correlation predicts a higher mass-transfer coefficient compared to the Carberry (1960) correlation. In Figures 12 and 13, R_i correction has not been used in computing the effluent profiles. The higher mass-transfer coefficient results in lower initial leakage. Differences in mass-transfer coefficient are not critical as exchange progresses and the resin saturates. The predicted initial chloride leakage using Dwivedi and Upadhyay (1977) correlation (Figure 13) is lower than that predicted using Carberry (1960) correlation with the R_i correction (Figure 11).

Figures 14 and 15 compare the effect of using different exponents for the R_i factor on the predicted sodium and chloride effluent profiles. As the value of the exponent increases, the calculated R_i factor increases resulting in a higher ion-exchange rate. Hence a lower effluent concentration is predicted. The R_i correction with a calculated mass-transfer coefficient results in a mass-transfer parameter that varies in the column. This is a better representation of the transport of ionic species in mixed bed ion-exchange.

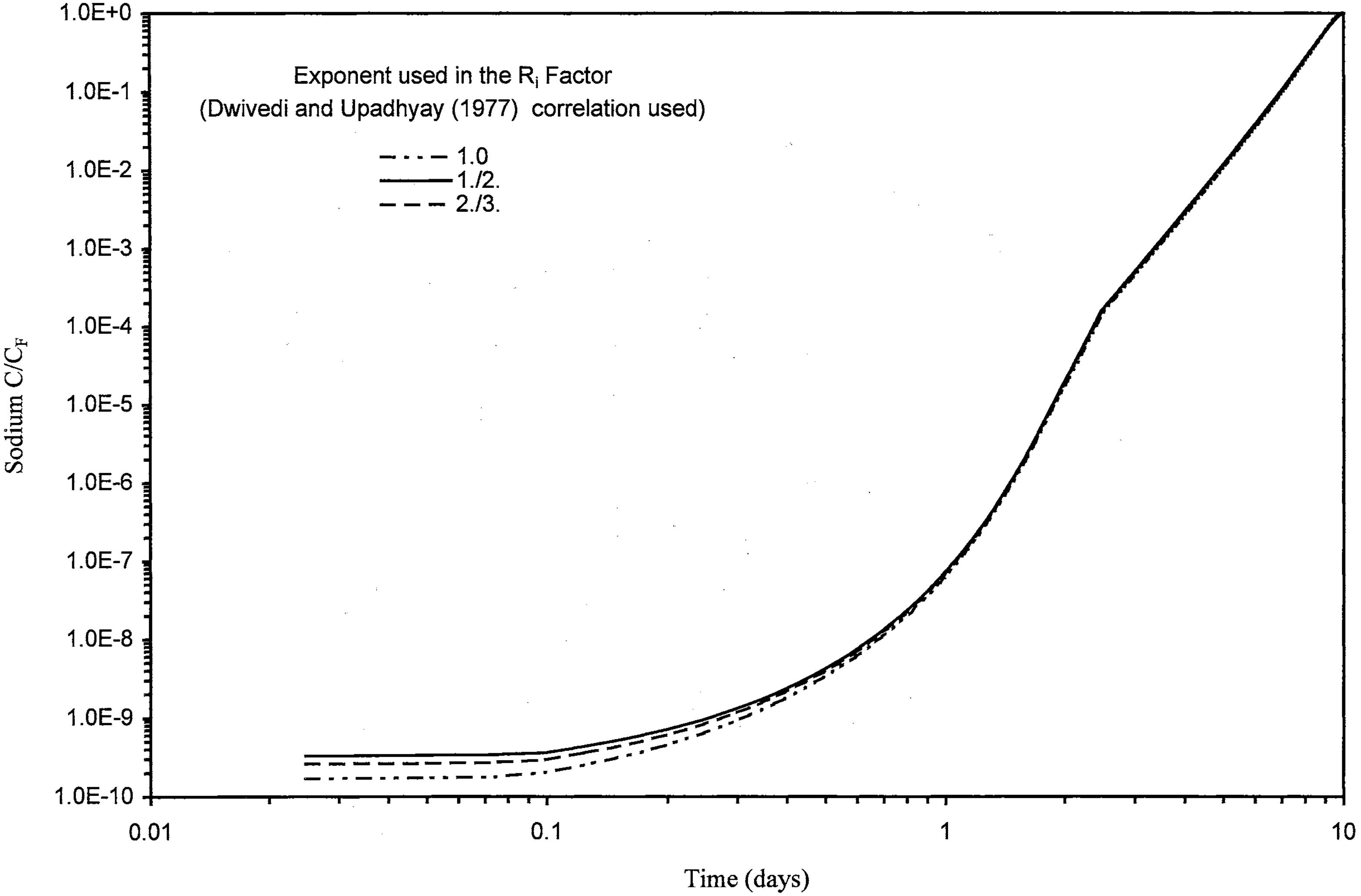

Figure 14. Effect of exponent used in the mass transfer correction on predicted effluent profile

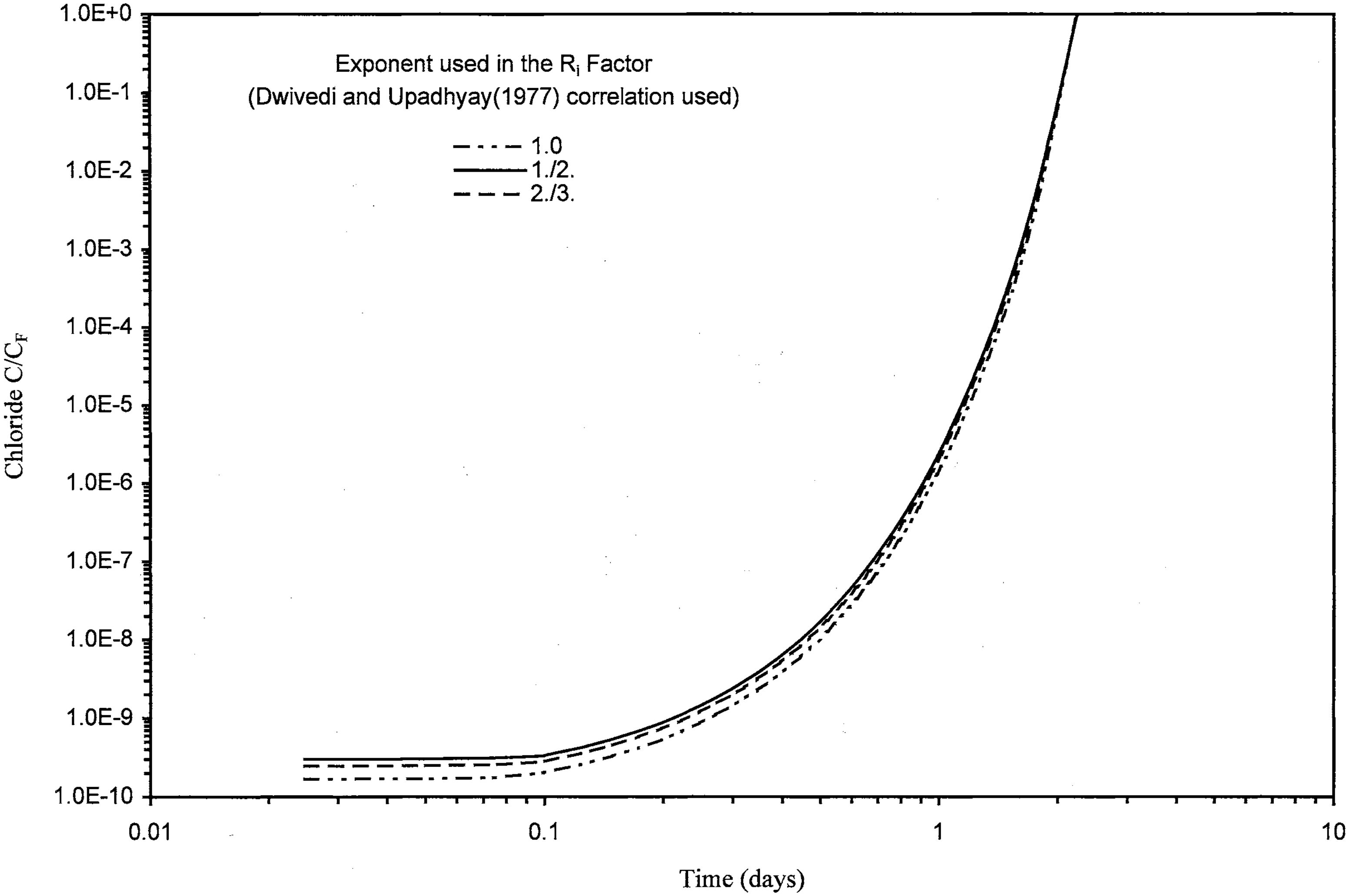

Figure 15. Comparison of predicted effluent profile with different exponents in the mass-transfer correction

The value of the exponent used in the R_i correction should be one. This value was obtained for a stagnant film model by Van Brocklin and David (1972), and Haub and Foutch's (1986) model for effective diffusivity was also derived using a stagnant-film model. The predicted ion-exchange rate is the highest when the exponent one is used for calculating R_i, compared to the rate predicted using the other exponents — one-half and two-thirds. The mass-transfer coefficient influenced the predicted effluent profile more than the changes in R_i correction.

Conclusions

Diffusivity of the sodium-chloride-water system has been analyzed using the Nernst-Planck equation. This is a multicomponent diffusion problem. Ionization of water influences the diffusion coefficient of the individual ionic species. The diffusion coefficient of individual species is influenced by the presence of other ions, and is also a function of concentration. Using this theoretical analysis, differences in existing ion-exchange mass-transfer coefficient data have been interpreted. The variation in experimental mass-transfer coefficient data due to differences in diffusivity has been explained.

The effect of mass-transfer coefficient on predicted effluent profiles of sodium and chloride from a mixed bed has been presented. The mass-transfer coefficient significantly affects the predicted initial ionic leakage. The effect of mass-transfer coefficient decreases as exchange progresses. The breakthrough curve is sharp at high mass-transfer coefficient when compared to breakthrough at lower mass-transfer coefficient.

Mass-transfer coefficients were calculated using Carberry (1960) and Dwivedi and Upadhyay correlation (1977). Carberry (1960) correlation predicts a lower mass-transfer coefficient when compared with Dwivedi and Upadhyay (1977) correlation. Dwivedi and Upadhyay (1977) correlation without the R_i correction predicts a lower initial leakage than that predicted using Carberry (1960) correlation with the R_i correction.

For numerical column-model calculations, Dwivedi and Upadhyay (1977) correlation for calculating mass-transfer coefficient is recommended. The R_i correction accounts for the variation in diffusivity as concentration changes, and needs to be used in conjunction with the mass-transfer correlation. The exponent used in the R_i correction should be one, to keep model consistency. The exponent in the R_i correction had a lower impact on the predicted initial leakage than the effect of mass-transfer coefficient.

CHAPTER VI

Conclusions and Recommendations

This work focused on two specific modeling issues in liquid-film diffusion-controlled mixed-bed ion exchange. Chapters II and III dealt with weak electrolyte mass transport modeling in mixed-bed ion exchange (MBIE). Chapters IV and V presented the effect of mass-transfer coefficient on film mass-transfer kinetics, and on predicted effluent profiles of sodium chloride exchange in a mixed bed.

A weak electrolyte mass transport model considering mass flux of dissociated and undissociated forms of the weak electrolyte is developed in Chapter II for MBIE. Previous models ignored the electrostatic influence of the dissociated (ionic) form on mass flux of other ions in the system. However, the model presented here accounts for such interactions. The model assumes that the ionic form, a counterion, exchanges with the resin, and the undissociated form undergoes an exchange-site interaction with the ion-exchange resin. This model is not specific to any weak electrolyte, but requires univalent ions in the system.

The weak-electrolyte mass-transport model, developed in Chapter II, is applied for amine transport in MBIE; the third chapter presents this work. Amines are weak electrolytes, and are encountered in MBIE operations in the power industry. The weak electrolyte model was used to model mass transport of the following amines: ammonia, morpholine, and ethanolamine. These amines were chosen since physiochemical properties were available, however, the model can be applied to exchange of any amine.

The model predictions for amine effluent concentrations were compared with data from Nuclear Electric (UK) power station and experimental data of Miller and Asay (1991). The predicted amine effluent concentration compared favorably with data. Model predictions for sodium were also compared with data. The predictions were in the range ± 10% when compared with data from Nuclear Electric (UK). However, the predictions of sodium effluent were unable to represent the data of Miller and Asay (1991). Industrial use of the model as a design and decision making tool has also been demonstrated — the model can be used to evaluate operating criteria, or system responses to change in variables.

In the fourth chapter, mass-transfer correlations used to predict the mass-transfer coefficient (MTC) in packed beds were studied. The MTC influences mass-transfer kinetics (ion-exchange rate), and hence the predicted effluent concentrations; therefore the need to study MTCs. Comparison of literature mass-transfer correlations with mixed-bed ion-exchange data (obtained at low influent solute concentrations) had not been done previously. In this work, MTC predictions from literature mass-transfer correlations have been compared with available sodium chloride mass transfer data.

MTCs calculated using Carberry's (1960) correlation and Dwivedi and Upadhyay's (1977) correlation were compared. The ion-exchange MTC data were correlated well (± 10%) by the Dwivedi and Upadhyay (1977) correlation. A lower MTC was predicted using Carberry (1960) correlation than the Dwivedi and Upadhyay (1977) correlation.

The effect of these MTC correlations on predicted effluent profiles were studied and presented in Chapter V. The MTC significantly affects the predicted initial ionic leakage; higher MTC results in lower initial ion concentrations in the effluent. The effect of MTC diminishes as ion-exchange progresses.

The differences in existing ion-exchange MTC data for sodium chloride has been theoretically analyzed using the Nernst-Planck equation in Chapter V. The influence of hydrogen and hydroxide concentration on sodium chloride diffusivity is presented. This demonstrates the multicomponent nature of this system.

Recommendations

The weak electrolyte mass transport model was limited to a single dissociative species. Inclusion of multiple dissociative species in the model must be considered. General models describing weak acidic or basic species, or a mixture of species, should be developed. The main problem that can be anticipated with this system is the roots generated by the equilibrium equation — multiple roots of the polynomial equation. Robust solution methods for solving the equilibrium equations should be sought. Error checks should be built into the computer code to check for valid roots. A tedious process would be to obtain all the roots of the polynomial and check validity. Multicomponent exchange should also be incorporated.

There is a lack of experimental data on physiochemical characterization of certain amines being studied as pH-control agents. This would force the model to assume transport properties and equilibrium interaction constants with the resin. Hence there is a need to develop a properties database for the amines.

The model was validated with experimental breakthrough data. Additionally, model predictions can be further validated by comparing liquid-phase concentration profiles in the bed. Experimentally determined bed profiles will provide information on local exchange kinetics, using this approach the mixed-bed ion-exchange model can be improved. There is lack of data on liquid-phase concentration profiles in the bed; hence additional experimental work can be performed.

To solve the column code numerically, a more advanced method needs to be implemented; for example, a finite element method — orthogonal collocation on finite elements — can be used to solve the column material balance. The advantage of using finite elements is the ability to control the size of the elements. Smaller elements can be used when there are steep gradients, and larger elements at other locations. A different numerical approach may require initial liquid-phase profiles of the exchanging species. Hence the effect of initial profiles on breakthrough curves needs to be carefully studied.

The experimental MTCs used in this study were for univalent ions. Experimental data for divalent species is insufficient. Theoretical analysis of diffusion at low concentration (in water) was done for a binary system, but analysis of a multicomponent system is relevant for multi-species exchange. Extension of the binary component analysis can be undertaken if sufficient experimental data for MTCs are available in a multi-species exchange system. The presence of weak electrolytes increases complexity of the analysis; nonetheless, such diffusion analysis will help in understanding local ion-exchange kinetics in the mixed bed.

BIBLIOGRAPHY

A Handbook of Ice (1927), Middle West Utilities Company

Abrams, I. M. (1969) Removal of Organics from Water By Synthetic Resinous Adsorbents, Chem. Eng. Progr. Symp. Ser., 65(97), 106-112

Afrashtehfar, S. and Cantwell, F. F. (1982) Chromatographic Retention Mechanism of Organic Ions on a Low-Capacity Ion Exchange Adsorbent, Anal. Chem., 54, 2422-2427

Amman, A. A. and Ruttiman, T. B. (1995) Simultaneous Determination of Small Organic and Inorganic Anions in Environemntal Water Samples by Ion-Exchange Chromatography, J. Chromatogr. A., 706, 259-269

Aminzadeh, K., Taha, T. R., Cornish, A. R. H., Kolansky, M. S. and Pfeffer, R. (1974) Mass Transport Around Two Spheres at Low Reynolds Numbers, Int. J. of Heat and Mass Transfer., 17, 1425-1436

Appel, P. W. and Newman, J. (1976) Application of the Limiting Current Method to Mass Transfer in Packed Beds at very Low Reynolds Numbers, AIChE J., 22 (6), 979-994

Baker, M. N. (1948) The Quest for Pure Water, The American Water Works Association, Inc, New York

Balto, B. A. and Pawlowski, L. (1987) Wastewater Treatment by Ion Exchange, E. & F. N. Spon, Ltd., London

Bar-Ilan, M. and Resnick, W. (1957) Gas Phase Mass transfer in Fixed Beds at Low Reynolds Numbers Ind. Eng. Chem., 49(2), 313-319

Barber, D. (1994) Personal Communication, Ontario Hydro, Canada

Bates, J. C. (1989) The Ion Exchange Behavior of Selected Amines, Proceedings of the workshop on Condensate Polishing for Deep Bed Purification Systems, Little Rock, Arkansas, May 31-June 2

Bates, J. C. (1993) Personal Communication, Nuclear Electric, UK

Bhandari, V. M., Juvekar, V. A. and Patwardhan, S. R. (1992) Sorption Studies on Ion Exchange Resins. 2. Sorption of Weak Acids on Weak Base Resins, Ind. Eng. Chem. Res., 31, 1073-1080

Bibler, J. P. (1990) Ion Exchange in the Nuclear Industry, in Recent Developments in Ion Exchange 2, P. A. Williams and M. J. Hudson, editors, Elsevier Applied Science, New York

Bird, R. B. Stewart, W. E. and Lightfoot, E. N. (1960) Transport Phenomena, John Wiley and Sons, New York

Bolde, W. B., White, T. and Groves, Jr. F. R. (1989) Continuous Fixed Bed Ligand Exchange: The Shrinking-Core Model, AIChE. J., 35(5), 849-852

Brattebo, H., Odegaard, H. and Halle, O. (1987) Ion Exchange for the Removal of Humic Acids in Water Treatment, Wat. Res., 21(9), 1045-1052

Bulusu, R. (1994) Development of a Column Model to Predict Multicomponent Mixed Bed Ion Exchange Breakthrough, MS Thesis, Oklahoma State University

Carberry, J.J. (1960) A Boundary-Layer Model of Fluid-Particle Mass Transfer in Mixed Beds, AIChE. J., 4, 460-462

Cooney, D. O. (1991) The Importance of Axial Dispersion in Liquid-Phase Fixed-Bed Adsorption Operations, Chem. Eng. Commun., 110, 217-231

Cornel, P. and Sontheimer, H. (1986) Sorption of Dissolved Organics From Aqueous Solution by Polystyrene Resins — I. Resin Characterization and Sorption Equilibrium, Chem. Eng. Sci., 41(7), 1801-1810

Croll, B. T. (1993) The Removal of Nitrate from Water Using Ion Exchange, Ion Exchange Processes: Advances and Applications, A. Dyer, M. J. Hudson, and P. A. Williams, Editors, The Royal Society of Chemistry, Cambridge, UK, 141-158

Cussler, E. L. (1976) Multicomponent Diffusion, Elsevier Scientific Publishing Company, Amsterdam

Cussler, E. L. (1984) Diffusion Mass Transfer in Fluid Systems, Cambridge University Press, New York

Dawson, D. A. and Trass, O. (1972) Mass Transfer at Rough Surfaces, Int. J. of Heat and Mass Transfer., 15, 1317-1336

Dobbs, R. A., Uchida, S., Smith, L. M. and Cohen, J. M. (1975) Ammonia Removal from Wastewater by Ligand Exchange, AIChE. Symp. Ser., 152(71), 157-163

Dunn, L. A. and Stokes, R. H. (1965) The Diffusion of Monocarboxylic Acids in Aqueous Solution at 25°C, Aust. J. Chem., 18, 285-196

Dwivedi, P. N. and Upadhyay, S. N. (1977) Particle-Fluid Mass Transfer in Fixed and Fluidized Beds, Ind. Eng. Chem., Process Des. Dev., 16(2), 157-165

EPRI TR-102952 (September 1993) Advanced Amine Application Guidelines, Palo Alto, California

EPRI TR-104299 (September 1994) Sodium Leakage from Condensate Polishers Under Alternate Amine Chemistry, Palo Alto, California

Evans, G. C. and Gerald, C. F. (1953) Mass Transfer from Benzoic Acid Granules to Water in Fixed and Fluidized Beds at Low Reynolds Numbers. Chem. Eng. Prog., 49(3), 135-140

Fogler, S. H. (1992) Elements of Chemical Reaction Engineering, Prentice Hall, Englewood Cliffs, New Jersey

Fountain, M. J. Greene, J. C. and Jones, M. G. (1990) The Effect of Amines on Ion-Exchange Resins, EPRI Workshop:The Use of Amines in Conditioning Steam/Water Cycles, Tampa, Florida, Paper 38

Foutch, G. L. (July 1991) Ion Exchange: How Particle Size Affects MBIE Breakthrough, Ultrapure Water, 26-29

Frey, D. D. (1986) Prediction of Liquid-Phase Mass-Transfer Coefficients in Multicomponent Ion Exchange: Comparison of Matrix, Film-Model, and Effective-Diffusivity Methods, Chem. Eng. Commun., 47, 273-293

Frisch, N. W. and Kunin, R. (1960) Kinetics of Mixed-Bed Deionization: I, AIChE. J., 6(4), 640-647

Fu, P. L. K. and Symons, J. M. (October 1990) Removing Aquatic Organic Substances by Anion Exchange Resins, Jour. AWWA., 70-77

Gaffney, B. J. and Drew, T. B. (1950) Mass Transfer from packing to Organic Solvents in Single Phase Flow Through a Column, Ind. Eng. Chem., 42(6), 1120-1127

Gilliland, E. R. and Baddour, R. F. (February 1953) The Rate of Ion Exchange, Ind. Eng. Chem. Res., 45(2), 330-337

Graham, E. E. and Dranoff, J. S. (1982) Application of the Stefan-Maxwell Equations to Diffusion in Ion Exchangers. 1. Theory, Ind. Eng. Chem. Fundam, 21(4), 360-365

Harries, R. R. and Ray, N. J. (1984) Anion Exchange in High Flow Rate Mixed Beds, Effluent and Water Treatment Journal, 24(4), 131-139

Harries, R. R. (1987) Ion Exchange Kinetics in Condensate Purification, Chemistry and Industry, 4, 104-109

Harries, R. R. (1988) The Role of pH in Ion Exchange Kinetics, Ion Exchange for Industry, M. Streat, Editor, Ellis Horwood Limited, Chichester, England, 314-325

Harries, R. R. (1991) Ion Exchange Kinetics in Ultra Pure Water Systems, J. Chem. Tech. Biotechnol., 51, 437-447

Haub, C. E. (1984) Model Development for Liquid Resistance-Controlled Reactive Ion Exchange at Low Solution Concentrations with Applications to Mixed Bed Ion Exchange, MS Thesis, Oklahoma State University

Haub, C. E. and Foutch, G. L. (1986a) Mixed-bed ion exchange at concentrations approaching the dissociation of water 2. Column model applications. Ind. Eng. Chem. Fundam., 25(3), 373-381

Haub, C. E. and Foutch, G. L. (1986b) Mixed-Bed Ion Exchange at Concentrations Approaching the Dissociation of Water. 2. Column Model Application, Ind. Eng. Chem. Fundam., 25(3), 381-385

Hayduk, W. and Laudie, H. (1974) Prediction of Diffusion Coefficients for Nonelectrolytes in Dilute Aqueous Solutions, AIChE. J., 20(3), 611-615

Helfferich, F. G. (1962) Ion Exchange. McGraw Hill Book Company, New York.

Helfferich, F. G. and Bennett, B. J. (1984) Weak Electrolytes, Polybasic Acids, and Buffers in Anion Exchange Columns I. Sodium Acetate and Sodium Carbonate Systems, Reactive Polymers, 3, 51-66

Helfferich, F. G. and Hwang, Y. (1988) Ion Exchangers as Catalysts, Ion Exchange for Industry, M. Streat, Editor, Ellis Horwood Limited, Chichester, England, 585-596

Helfferich, F. G. (1990) Ion-Exchange Equilibria of Amino Acids on Strong-Acid Resins: Theory, Reactive Polymers, 12, 95-100

Helfferich, F. G. (1990) Models and Physical Reality in Ion-Exchange Kinetics, Reactive Polymers, 13, 191-194

Hepp. D., Wein, G. and Bornak, W. (September 1987) Evaluate Amine Capability for Condenser Protection, Power, 67-70

Hines, A. L. and Maddox, R. N. (1985) Mass Transfer Fundamentals and Applications, Prentice-Hall Inc, New Jersey

Horvath, A. L. (1985) Handbook of Aqueous Electrolyte Solutions, Ellis Horwood Limited, Chichester, England

Hubner, P. and Kadlec, V. (1978) Kinetic Behavior of Weak Base Anion Exchangers, AIChE. J., 24(1), 149-154

Jolls, K. R. and Hanratty, T. J. (1969) Use of Electrochemical Techniques to Study Mass transfer Rates and Local Skin Friction to a Sphere in a Dumped Bed, AIChE. J., 15(2), 199-205

Karabelas, A., Wegner, T. H. and Hanratty, T. J. (1971) Use of Asymptotic Relations to Correlate Mass Transfer Data in Packed Beds, Chem. Eng Sci., 26, 1581-1589

Kataoka, T., Yoshida, H. and Ueyama, K. (1972) Mass Transfer in Laminar Region Between Liquid and packing material Surface in the Packed Bed, J. Chem. Eng. Jpn., 5(2), 132-136

Kataoka, T., Yoshida, H. and Yamada, T. (1973) Liquid Phase Mass Transfer in Ion Exchange Based on the Hydraulic Radius Model, J. Chem. Eng. Jpn., 6(2), 172-177

Kataoka, T. and Yoshida, H. (1976) Liquid Phase Diffusion Controlling in Irreversible Ion Exchange, J. Chem. Eng. Jpn., 6, 326-329

Kikuchi, K., Konno, H., Sugawara, T. and Ohashi, H. (1984) Mass Transfer Between Particles and Liquid in Dilute Fluidized Beds in the Low Reynolds Number Region, J. Chem. Eng. Jpn., 17(4), 438-440

Koloini, T., Sopcic, M. and Zumer, M. (1977) Mass Transfer in Liquid-Fluidized Beds at Low Reynolds Numbers, Chem. Eng. Sci., 32, 637-641

Kraaijeveld, G. and Wesselingh, J. A. (1993) The Kinetics of Film-Diffusion-Limited Ion Exchange, Chem. Eng. Sci., 48(3), 467-473

Kunii, D. and Suzuki, M. (1967) Particle-to-Fluid Heat and Mass Transfer in Packed Beds of Fine Particles, Int. J. Heat and Mass Transfer., 10, 845-850

Kunin, R. and McGarvey, F. X. (1951) Monobed Deionization with Ion Exchange Resins, Ind. Eng. Chem., 43(3), 734-740

Lange, N. A. (1985) Lange's Handbook of Chemistry, J. A. Dean, Editor, 13 edition, McGraw-Hill, New York

Leaist D. G. and Lyons, P. A. (1981) Multicomponent Diffusion of Electrolytes with Incomplete Dissociation. Diffusion in a Buffer Solution, J. Phys. Chem., 85, 1756-1762

Lee, G. C. (1994) The Ionic Mass Transfer Coefficients of Cation and Anion Exchange Resins at Various Flow Rates and Influent Concentrations in Single and Mixed Beds, PhD Thesis, Oklahoma State University

Levins, D. M. and Glastonbury, J. R. (1972) Particle-Liquid Hydrodynamics and Mass transfer in a Stirred Vessel, Part-II Mass Transfer, Trans. Instn. Chem. Engrs, 50, 132-145

Lin, K. H. (1975) Performance of Ion Exchange Systems in Nuclear Power Plants, AIChE. Symp. Ser., 71(152), 224-235

Livingstone, A. G. and Noble, J. B. (1993) Mass Transfer in Liquid-Solid Fluidized Beds of Ion Exchange Resins at Low Reynolds Numbers, Chem. Eng. Sci., 48(6), 1174-1178

Lou, J. (1993) Simulations of Borate Ion Exchange and Radial Flow for Reactor Water Clean Up Systems, MS Thesis, Oklahoma State University

Martinola, F. (1980) Ion Exchangers and Adsorbents—Versatile Aids for the Chemical Industry, Ger. Chem. Eng. 3, 79-88

McCune, L. K. and Wilhelm, R. H. (1949) Mass and Momentum Transfer in Solid Liquid Systems: Fixed abd Fluidized Beds, Ind. Eng. Chem. 41, 1124-1134

McNulty, J. T., Eumann, M., Bevan, C. A., and Tan, V. C. T. (1986) Anion Exchange Resin Kinetic Testing an Indispensable Diagnostic Tool for Condensate Polisher Troubleshooting, in 47th Annual Meeting International Water Conference, Pittsburgh, Pennsylvania

McNulty, J. T., Bevan, C. A., and Carlin, W. H. (July 14, 1992) Condensate Polishing and Blowdown Demineralization in Morpholine and in Morpholine/Boric Acid Matrices, Presented at IEX'92, Churchill College, Cambridge

Miers, J. A. (1995) Regulation of Ion Exchange Resins for the Food, Water and Beverage Industries, Reactive Polymers, 24, 99-107

Miller, A. D. and Asay, R. H. (June 18-20, 1991) Sodium Throw with Alternate Amine Chemistry, EPRI Condensate Polishing Workshop, Scottsdale, Arizona

Miyauchi, T., Matsumoto, K. and Yoshida, T. (1975) Liquid Film Coefficient of Mass Transfer in Low Peclet Number Region for Sphere Packed Beds, J. Chem. Eng. Jpn., 8(3), 228-232

Moison, R. L. and O'Hern, H. A., Ion Exchange Kinetics (1959), Chem. Engr. Progr. Symp. Ser., 24(55), 71-85

Muller, G. T. A. and Stokes, R. H. (1956) The Mobility of the Undissociated Citric Acid Molecule in Aqueous Solution, Trans. Faraday. Soc., 53(5), 642-645

Nelson, P. A. and Galloway, T. R. (1975) Particle-To-Fluid Heat and Mass Transfer in Dense Systems of Fine Particles, Chem. Eng. Sci., 30, 1-6

Newman, J. (1973) Electrochemical Systems, Prentice-Hall, Inc., Englewood Cliffs, New Jersey

Novak, L.T. (1976) Transport and Reactions of Ions in Soils, AIChE. Symp. Ser., 166(73), 344-360

Ohashi, H., Sugawara, T., Kikuchi, K. and Konno, H. (1981) Correlation of Liquid-Side Mass Transfer Coefficient for Single Particles and Fixed Beds, J. Chem. Eng. Jpn., 14(6), 433-438

Petruzzelli, D. and Helfferich, F. G. (1993) Migration and Fate of Pollutants in Soils and Subsoils, NATO ASI Series, Springer-Verlag, Heidelberg, Germany

Pfeffer, R. (1964) Heat and Mass Transport in Multiparticle Systems, Ind.Eng. Chem. Fundam., 3(4), 380-383

Rao, G. M. and David, M. M. (1964) Single-Particle Studies of Ion Exchange in Packed Beds: Cupric Ion-Sodium Ion System, AIChE. J., 10(2), 213-219

Radcliffe, D. F., Leng, J. L. and Thomas, G. (1982) Direct Measurement of External Mass Transfer in Packed Sorbent Beds, AIChE. J., 28(2), 344-345

Rahman, K. and Streat, M. (1981) Mass Transfer in Liquid Fluidized Beds of Ion Exchange Particles, Chem. Eng. Sci, 36(2), 293-300

Reid, R. C., Parusnitz, J. M. and Sherwood, T. K. (1977) The Properties of Gases and Liquids, Third edition, McGraw-Hill, New York

Robinson, R. A. and Stokes, R. H. (1955) Electrolyte Solutions, Academic Press Inc., Publishers, New York

Samuelson, O. (1963) Ion Exchange Separations in Analytical Chemistry, John Wiley and Sons, New York

Schwarzenbach, R. P., Gschwend, P. M. And Imboden, D. M. (1993) Environmental Organic Chemistry, John Wiley and Sons, Inc., New York

Selke, W. A., Bard, Y., Pasternak, D., and Aditya, S. K. (1956) Mass Tranfer Rates in Ion Exchange, AIChE. J., 2(4) 468-470

Semmens, M. J. (1975) A Review of Factors Influencing the Selectivity of Ion Exchange Resins for Organic Ions, AIChE. Symp. Ser., 71(152), 214-223

Smith, E. H. and Weber, W. J. (1989) Evaluation of Mass Transfer Parameters for Adsorption of Organic Compounds from Complex Organic Matrices, Environ. Sci. Technol., 23(6), 713-722

Snoeyink, V. L. and Jenkins, D. (1980) Water Chemistry, John Wiley and Sons, New York

Soldatov, V. S. (1988) Ion Exchanger Mixtures used as Artificial Nutrient Media for Plants, Ion Exchange for Industry, M. Streat, Editor, Ellis Horwood Limited, Chichester, England, 652-658

Stanek, V. (1994) Fixed Bed Operations: Flow Distribution and Efficiency, Ellis Horwood, New York

Stokes, R. H. (1965) Tracer Diffusion in Binary Solutions Subject to a Dimerization Equilibrium, J. Phys. Chem., 69(11), 4012-4016

Streat, M. (1988) Ion Exchange for Industry, Ellis Horwood Limited, Chichester, England, 337-442

Stumm, W. (1992) Chemistry of the Solid-Water Interface, John Wiley and Sons, Inc., New York

Tantirige, S. and Trass, O. (August 1984) Mass Transfer at Geometrically Dissimilar Rough Surfaces, Can. J. of Chem. Eng., 62, 490-496

Tateda, A. and Fritz, J. S. (1978) Mini-Column Procedure for Concentrating Organic Contaminants from Water, J. Chromatogr., 152, 329-340

Taylor, R. (1982) Solution of the Linearized Equations of Multicomponent Mass Transfer, Ind. Eng. Chem. Fundam., 21, 407-413

Thompson, R. H. (February 1991) Morpholine Advances as a Method for Reducing Iron Transport in Feedwater, Power, 26-32

Toor, H. L. (1964) Solution of the Linearized Equations of Multicomponent Mass Transfer: I, AIChE. J., 10(4) 448-455

Tournie, P., Laguerie, C. and Couderc, J. P. (1979) Correlations for Mass Transfer Between Fluidized Spheres and A Liquid, Chem. Engng Sci., 34, 1247-1255

Turner, J. C. R., Church, M. R., Johnson, A. S. W. and Snowdown, C. B. (1966) An Experimental Verification of the Nernst-Planck model for Diffusion in an Ion Exchange Resin, Chem. Eng. Sci., 21, 317-325

Van Vliet, B. M. and Weber, W. J. (1988) Particle Surface Roughness Effects on the Interfacial Mass Transfer Dynamics of Microporous Adsorbents, Chem. Eng. Commun., 68, 165-176

Van Brocklin, L. P. (1968) Ionic Migration Effects on Liquid-Resistance-Controlled Ion Exchange, PhD Thesis, University of Washington

Van Brocklin, L. P. and David, M. M. (1972) Coupled Ionic Migration and Diffusion During Liquid-Phase Controlled Ion Exchange, Ind. Eng. Chem. Fundam., 11(1), 91-99

Van Brocklin, L. P. and David, M. M. Ionic Migration Effects During Liquid Phase Controlled ion Exchange, AIChE. Symp. Ser., 152(71), 191-201

Vassiliou, B. and Dranoff, J. S. (1962) The Kinetics of Ion Exclusion, AIChE. J., 8(2), 248-250

Vitagliano, V. and Lyons, P. A. (1956) Diffusion in Aqueous Acetic Acid Solutions, J. Amer. Chem. Soc., 78, 4538-4542

Von Karman, T. (1939) The Analogy Between Fluid Friction and Heat Transfer, Trans. Am. Soc. Mech. Engrs., 61, 705-710

Wagner, J. D. and Dranoff, J. S. (1967) The Kinetics of Ion Exchange Accompanied by Irreversible Reaction. III. Film Diffusion Controlled Neutralization of a Strong Acid Exchanger by a Weak Base, J. Phys. Chem., 71(13), 4551-4553

Wakao, N. and Funazkri, T. (1978) Effect of Fluid Dispersion Coefficients on Particle-to-Fluid Mass Transfer Coefficients in Packed Beds, Chem. Eng. Sci., 33, 1375-1384

Wakao, N. and Kagei, S. (1982) Heat and Mass Transfer in Packed Beds, Gordon and Breach Science Publishers, New York

Water Quality and Treatment: A Handbook of Public Water Supplies (1971), The American Water Works Association, Third Edition, McGraw-Hill Book Company, New York

Wendt, R. P. (1965) The Estimation of Diffusion Coefficients for Ternary Systems of Strong and Weak Electrolytes, J. Phys. Chem., 69(4), 1227-1237

Wesselingh, J. A. and Krishna, R. (1990) Mass Transfer, Ellis Horwood, London

Wildhagen, G. R. S., Qassim, R. Y., Rajagopal, K. and Rahman, K. (1985) Effective Liquid-Phase Diffusivity in Ion Exchange, Ind. Eng. Chem. Fundam., 24, 423-432

Wilke, C. R. and Hougen, O. A. (1945) Mass Transfer in Flow of Gases THrough Granular Solids Extended to Low Modified Reynolds Numbers, Trans. AIChE., 41, 445-451

Williamson, J. E., Bazaire, K. E. and Geankoplis, C. J. (1963) Liquid Phase Mass transfer at Low Reynolds Numbers, Ind.Eng. Chem. Fundam., 2(2), 126-129

Wilson, E. J. and Geankoplis, C. J. (1966) Liquid Mass Transfer at Very Low Reynolds Numbers in Packed Beds, Ind. Eng. Chem. Fundam., 5(1), 9-14

Yakowitz, S. and Szidarovszky, F. (1989) An Introduction to Numerical Computations, Second Edition, Macmillan Publishing Company, New York

Yoon, T. K. (1990) The Effect of Cation to Anion Resin Ratio on Mixed-Bed Ion Exchange Performance at Ultra-Low Concentrations, PhD Thesis, Oklahoma State University

Yoshida, H. and Kataoka, T. (1987) Adsorption of Amines on H^+-Form Ion Exchanger, Chem. Eng. Sci., 42(7), 1805-1814

Yoshida, H., Shimizu, K. and Kataoka, T. (1990) Adsorption of Amines and Paints on H-Form Resin from Electrodeposition Wastewater, AIChE. J., 36(12), 1815-1821

Yutani, N., Ototake, N. and Fan, L. T. (1987) Statistical Analysis of Mass Transfer in Liquid-Solids Fluidized Beds, Ind. Eng. Chem. Res., 26, 343-347

Zarraa, M. A. (1992) Mass Transfer During the Removal of Dissolved Heavy Metals from Wastewater Flows in Fluidized Beds of Ion Exchange Resins, Chem. Eng. Technol. 15, 21-25

Zeechini, E. J. (1990) Solutions to Selected Problems in Multi-Component Mixed-bed Ion Exchange Modeling, PhD Thesis, Oklahoma State University

APPENDIXES

APPENDIX A

Numerical Solution of the MBIE Column Model

The column material balance Equation II-16 with the resin mass-transfer rate equation (II-21 or II-22) can be solved by using finite difference schemes. However, for computing the solution, here, a different approach is taken. The column material balance, Equation II-16 — a partial differential equation, is solved as an ordinary differential equation by change of variables. The resin mass-transfer equation is also re-written with the new variables. The ordinary differential equation is then solved using the method of characteristics.

In a finite difference scheme, an initial bulk-phase concentration profile needs to be generated for computing the solution. This process is very difficult in the case of MBIE due to the nonlinear nature of the exchange isotherm. However, a bulk-phase profile can be generated by making simplifying assumptions. The advantage of the computing strategy used here is that no initial bulk-phase concentration profiles are needed.

Two new variables are defined for changing the partial differential to an ordinary differential equation. The new variables are (Kataoka et al., 1976):

$$\tau = \frac{K_{f,i} C_{Total}^{Feed}}{d_p Q}\left(t - \frac{\varepsilon z}{u}\right) \tag{A-1}$$

$$\xi = \frac{K_{f,i}(1-\varepsilon)z}{ud_p} \tag{A-2}$$

Equation A-23 defines a dimensionless time and Equation A-2 defines dimensionless distance. Using the chain rule, the derivatives in Equation II-16 can be expressed by the new variables as:

$$\frac{\partial C_i}{\partial t} = \frac{\partial C_i}{\partial \tau}\left(\frac{\partial \tau}{\partial t}\right) + \frac{\partial C_i}{\partial \xi}\left(\frac{\partial \xi}{\partial t}\right) \tag{A-3}$$

$$\frac{\partial C_i}{\partial z} = \frac{\partial C_i}{\partial \tau}\left(\frac{\partial \tau}{\partial z}\right) + \frac{\partial C_i}{\partial \xi}\left(\frac{\partial \xi}{\partial z}\right) \tag{A-4}$$

$$\frac{\partial q_i}{\partial t} = \frac{\partial q_i}{\partial \tau}\left(\frac{\partial \tau}{\partial t}\right) + \frac{\partial q_i}{\partial \xi}\left(\frac{\partial \xi}{\partial t}\right) \tag{A-5}$$

Equations A-1 and A-2 can be differentiated to give:

$$\frac{\partial \tau}{\partial t} = \frac{K_{f,i}C_{\text{Total}}^{\text{Feed}}}{d_pQ} \qquad \frac{\partial \tau}{\partial z} = -\left(\frac{K_{f,i}C_{\text{Total}}^{\text{Feed}}\varepsilon}{d_pQu}\right) \tag{A-6}$$

$$\frac{\partial \xi}{\partial t} = 0 \qquad \frac{\partial \xi}{\partial z} = \frac{K_{f,i}(1-\varepsilon)}{d_pu} \tag{A-7}$$

Equations A-3 to A-7 are used in II-16 to obtain the material balance equation as:

$$\frac{\partial C_i}{\partial \xi} + \Phi\frac{C_{\text{Total}}^{\text{Feed}}}{Q}\frac{\partial q_i}{\partial \tau} = 0 \tag{A-8}$$

Introducing the variables:

$$X_i = \frac{C_i}{C_{\text{Total}}^{\text{Feed}}} \qquad Y_i = \frac{q_i}{Q}$$

Equation A-8 can be written as:

$$\frac{\partial X_i}{\partial \xi} + \Phi\frac{\partial Y_i}{\partial \tau} = 0 \tag{A-9}$$

with the constraints:

$$\sum X_i = 1.0 \qquad \sum Y_i = 1.0$$

The mass-transfer rate equation (II-21) is transformed using the new variables to give:

$$\frac{\partial Y_i}{\partial t} = K_{f,i} R_i a_s \left(C_i^o - C_i^*\right)\left(\frac{1}{Q}\right) \qquad \text{(replacing } q_i \text{ only)} \qquad \text{(A-10)}$$

Changing t to τ, using τ (from A-1) and differentiating, in Equation A-10 yields:

$$\frac{\partial Y_i}{\partial \tau} = R_i a_s d_p \left(C_i^o - C_i^*\right)\left(\frac{1}{C_{\text{Total}}^{\text{Feed}}}\right) \qquad \text{(A-11)}$$

R_i has been defined previously (Equation II-20). Recognizing that the product of the particle diameter and surface area of a sphere is six, the final expression for mass-transfer rate to the resin bead is given by:

$$\frac{\partial Y_i}{\partial \tau} = 6R_i\left(X_i - X_i^*\right) \qquad \text{(A-12)}$$

For a weak electrolyte, Equation A-12 is written as:

$$\frac{\partial Y_i}{\partial \tau} = 6R_i\left(X_i - X_i^*\right) + 6\left(X_{\text{Mol}} - X_{\text{Mol}}^*\right)$$

Equation A-10 and A-12 are solved for studying the dynamics of the MBIE column.

The equations and the variables defined until now have not been differentiated according to resin and ion properties. In a mixed-bed column, both cation-exchange and anion-exchange resins are present; their properties differ. The ionic species involved also have different characteristics — for example, different diffusivities lead to variations in calculated mass-transfer coefficients. Variation in property will yield different τ and ξ values (Equations A-1 and A-2). However, for purposes of a meaningful solution, there can be only one set of τ and ξ values.

A unique set of τ and ξ values can be obtained by defining a reference ion, either a cation or an anion and associated cation-exchange or anion-exchange resin. The reference ion needs to be chosen such that the diffusivity is well represented. For example: selecting the hydrogen ion (and the cation-exchange resin) will not represent the true diffusivity in a mixed-bed system containing Na^+, Cl^-, and OH^-. The hydrogen ion has a much higher diffusivity compared to the sodium or the chloride ion. Since diffusion is multicomponent, the ions do not diffuse by themselves but there is an effective diffusivity for the system. Since slower ions influence transport, sodium or chloride ion would be a good choice for the reference ion. After a reference ion has been selected, the τ and ξ values can be computed. For the other ions these values need to be multiplied by the ratio of the specific property.

In the amine system modeled here, the following ions are considered: $Amine^+$, Na^+, H^+, Cl^-, and OH^-. The reference ion selected here is the ionic form of the amine, exchanged by the cation-exchange resin. The following equations for the material balance can be written ($amine^+$ is denoted by subscript x; subscript 'a' denotes the anion-exchanger, and 'c' the cation-exchanger.):

$$\tau_x = \frac{K_{f,x} C_{Total}^{Feed}}{d_{pc} Q_c}\left(t - \frac{\varepsilon z}{u}\right) \text{ , and } \xi_x = \frac{K_{f,x}(1-\varepsilon)z}{u d_{pc}} \qquad \text{(defined with the reference ion)}$$

a) for exchanging cations (i = any cation):

$$\frac{\partial Y_i}{\partial \tau} = \frac{\partial Y_i}{\partial \tau_x}\left(\frac{\partial \tau_x}{\partial t}\right) = \frac{K_{f,x}}{K_{f,i}}\left(\frac{\partial Y_i}{\partial \tau_x}\right) \tag{A-13}$$

$$\frac{\partial X_i}{\partial \xi} = \frac{\partial X_i}{\partial \xi_x}\left(\frac{\partial \xi_x}{\partial \xi}\right) = \frac{K_{f,x}}{K_{f,i}}\left(\frac{\partial X_i}{\partial \xi_x}\right) \tag{A-14}$$

b) for exchanging anions (j = any anion):

$$\frac{\partial Y_j}{\partial \tau} = \frac{\partial Y_j}{\partial \tau_x}\left(\frac{\partial \tau_x}{\partial t}\right) = \frac{K_{f,x} d_{pa} Q_a}{K_{f,j} d_{pc} Q_c}\left(\frac{\partial Y_j}{\partial \tau_x}\right) \qquad \text{(A-15)}$$

$$\frac{\partial X_j}{\partial \xi} = \frac{\partial X_j}{\partial \xi_x}\left(\frac{\partial \xi_x}{\partial \xi}\right) = \frac{K_{f,x} d_{pa}}{K_{f,j} d_{pc}}\left(\frac{\partial X_j}{\partial \xi_x}\right) \qquad \text{(A-16)}$$

Now, Equations A-9 and A-12 can be specifically written for cations and anions by replacing the partial derivatives found in Equations A-13 to A-16. The equations are:

a) for cations (i = any cation; Φ_{cation} is the volume fraction of cation-exchange resin in the mixed-bed column)

$$\frac{\partial X_i}{\partial \xi_x} + \Phi_{cation} \frac{\partial Y_i}{\partial \tau_x} = 0 \qquad \text{(A-17)}$$

$$\frac{\partial Y_i}{\partial \tau_x} = 6R_i \frac{K_{f,i}}{K_{f,x}}\left(X_i - X_i^*\right) \qquad \text{(A-18)}$$

b) for anions (j = any anion; Φ_{anion} is the volume fraction of anion-exchange resin in the mixed-bed column)

$$\frac{\partial X_j}{\partial \xi_x} + \Phi_{anion} \frac{\partial Y_j}{\partial \tau_x} = 0 \qquad \text{(A-19)}$$

$$\frac{\partial Y_j}{\partial \tau_x} = 6R_j\left(X_j - X_j^*\right)\left(\frac{K_{f,j} d_{pc} Q_c}{K_{f,x} d_{pa} Q_a}\right) \qquad \text{(A-20)}$$

Equations A-17 and A-19 can be written in the form:

$$\frac{\partial X}{\partial \xi} = -\Phi \frac{\partial Y}{\partial \tau} \qquad \text{(A-21)}$$

Equation A-21 is the liquid-phase material balance equation for the different species involved. Equations A-18 and A-20 yield the ion-exchange rate. After calculating the ion-exchange rate, the liquid-phase material balance equation is solved.

The column material balance in the new form, Equation A-21, is solved by the method of characteristics. The solution method involves defining a grid structure for the calculation procedure (Figure 1). The X-axis on the grid is ξ and τ is along the Y-axis. An uniform grid is not a necessary condition.

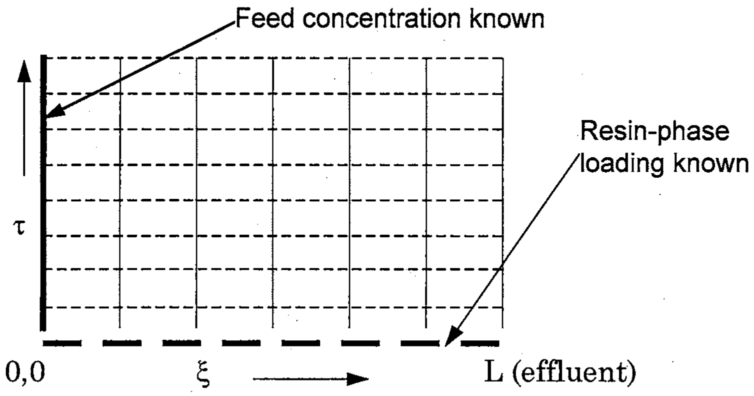

Figure 1. Grid structure for the numerical calculation

The solution is obtained by solving the system of equations along constant lines of ξ and τ; one variable is held constant while the other is evaluated. The solution is updated by incrementing the variable that was held constant and repeating the evaluation over the other variable.

The material balance equation has been transformed from solving a set of partial differential equations to a solution of ordinary differential equations. Hence techniques of solving ordinary differential equations are used. The choice of implicit or explicit method to be used depends on stability. Implicit methods are more stable than the explicit methods; however, implicit methods are more work intensive. In the solution here, a fourth order Adams-Bashforth method is used (Yakowitz and

Szidarovszky, 1989). The implementation of this solution requires function evaluations at previous four points. Hence to start the solution a Runge-Kutta algorithm is used.

The grid is defined by selecting incremental values of ξ and τ. The column is divided into finite number of slices depending on the selected incremental value of ξ ($\Delta\xi$). In each slice: 1) the liquid-phase material balance is computed and then the resin-phase loading, and 2) after ion-exchange calculations, solution equilibrium is calculated. These calculations are done over all the slices. Ion concentrations leaving the last slice is the effluent concentration. τ is updated and the solution is repeated over ξ.

APPENDIX B

Calculated Mass-Transfer Coefficient Comparisons

TABLE I

Experimental Properties

Property	Harries (1984)	Lee (1994)
Cation-exchange resin		
Name	Amberlite 200C	HGR-W2-H
Particle diameter (cm)		0.08
Name		650C-H
Particle diameter (cm)		0.065
Anion-exchange resin		
Name	Amberlite IRA 900	SBR-PC-OH
Particle diameter (cm)	0.079	0.06
Name	Amberlite IRA 458	550A-OH
Particle diameter (cm)	0.074	0.059
Cation-to-anion resin ratio	2:1	2:1
Temperature	20°C	25°C

TABLE II

Mass-Transfer Coefficient Comparisons

Bed void volume fraction	0.35			Carberry (1960)		Dwivedi and Upadhyay (1977)	
Description	Velocity cm/s (u)	Reynolds number	MTC cm/s (expt)	MTC cm/s (calc)	% dev from expt value	MTC cm/s (calc)	% dev from expt value
Mixed-bed data for chloride (Harries, 1984)							
Schmidt number=	564						
Amberlite IRA 900	2.5	55	2.07E-02	1.62E-02	-21.62	1.93E-02	-6.88
Amberlite IRA 900	3.33	74	2.47E-02	1.86E-02	-24.56	2.19E-02	-11.41
Amberlite IRA 458	2.5	52	2.00E-02	1.67E-02	-16.56	1.99E-02	-0.62
Amberlite IRA 458	3.33	69	2.55E-02	1.93E-02	-24.33	2.27E-02	-10.92
Mixed-bed data for chloride (Lee, 1994)							
Schmidt Number=	443						
SBR-PC-OH	1.64	31	1.92E-02	1.67E-02	-13.26	2.05E-02	6.55
SBR-PC-OH	2.3	44	2.17E-02	1.96E-02	-9.66	2.36E-02	8.54
SBR-PC-OH	2.95	56	2.50E-02	2.23E-02	-10.84	2.65E-02	5.83
550A-OH	1.64	31	2.10E-02	1.67E-02	-20.69	2.05E-02	-2.58
550A-OH	2.3	43	2.60E-02	1.98E-02	-23.73	2.39E-02	-8.24
550A-OH	2.95	55	2.74E-02	2.25E-02	-17.92	2.67E-02	-2.48
Mixed-bed data for sodium (Lee, 1994)							
Schmidt number=	656						
HGR-W2-H	1.64	42	1.40E-02	1.10E-02	-21.33	1.33E-02	-5.24
HGR-W2-H	2.3	58	1.66E-02	1.31E-02	-20.82	1.56E-02	-6.16
HGR-W2-H	2.95	75	1.97E-02	1.48E-02	-24.75	1.74E-02	-11.67
650C-H	1.64	34	1.29E-02	1.22E-02	-5.11	1.49E-02	15.81
650C-H	2.3	47	1.67E-02	1.46E-02	-12.57	1.75E-02	4.67
650C-H	2.95	61	1.76E-02	1.64E-02	-6.60	1.94E-02	10.46
Mono-bed data for chloride (Lee, 1994)							
Schmidt number=	443						
SBR-PC-OH	1.64	31	1.33E-02	1.67E-02	25.22	2.05E-02	53.81
SBR-PC-OH	2.3	43	1.66E-02	1.98E-02	19.47	2.39E-02	43.72
SBR-PC-OH	2.95	56	1.98E-02	2.23E-02	12.57	2.65E-02	33.63
Mono-bed data for sodium (Lee, 1994)							
Schmidt number=	656						
HGR-W2-H	1.64	42	1.24E-02	1.10E-02	-11.18	1.33E-02	6.99
HGR-W2-H	2.3	58	1.56E-02	1.31E-02	-15.75	1.56E-02	-0.14
HGR-W2-H	2.95	75	1.74E-02	1.48E-02	-14.80	1.74E-02	0.01

APPENDIX C

Concentration Effects on Multi-component Diffusion of NaCl in Water

Sodium chloride is completely ionized, at low solute concentrations, in water. The solution contains Na^+, Cl^-, H^+, and OH^- ions. Movement of a particular ion is dependent on the presence of other ions. Electrostatic influence of all ions in the aqueous environment will determine the movement of a species.

In the absence of an ionized solute or high concentration of the electrolyte, Fick's law can be used to model the sytem with a representative diffusivity. The ionic flux in this case cannot be modeled using Fick's law since electrostatic influences are not accounted. Hence the Nernst-Planck equation is used to model the NaCl-H_2O system. The Nernst-Planck equation is:

$$j_i = -D_i\left[\frac{\partial C_i}{\partial r} + \frac{Z_i C_i F}{RT}\frac{\partial \phi}{\partial r}\right] \tag{C-1}$$

Electroneutrality and charge conservation principles apply to this sytem. These principles are represented by:

$$\sum_{i=1}^{i=n} Z_i C_i = 0 \tag{C-2}$$

$$\sum_{i=1}^{i=n} Z_i j_i = 0 \tag{C-3}$$

i=Na^+, H^+, Cl^-, and OH^-.

Since the solute concentration is low, ionization of the solvent (water) needs to be considered. This can be represented by:

$$C_H C_O = k_w \tag{C-4}$$

Equation C-4 can be written as:

$$\frac{\partial}{\partial r}\left(C_H C_O\right) = 0 \tag{C-5}$$

or as:

$$\frac{\partial C_O}{\partial r} = -\frac{C_O}{C_H}\frac{\partial C_H}{\partial r} \qquad \text{or} \qquad \frac{\partial C_H}{\partial r} = -\frac{C_H}{C_O}\frac{\partial C_H}{\partial r} \tag{C-6}$$

To obtain ionic flux, Equation C-1 needs to be solved. The electric-potential gradient, second term in Equation C-1, is not a measured value. Hence direct solution of Equation C-1 is not possible. But the electric-potential gradient term can be re-written in terms of concentration gradient of the ions in the system. Differentiating the electroneutrality equation (C-2) with respect to r yields:

$$\frac{\partial C_{Na}}{\partial r} + \frac{\partial C_H}{\partial r} - \frac{\partial C_O}{\partial r} - \frac{\partial C_{Cl}}{\partial r} = 0 \tag{C-7}$$

Using Equation C-6, C-7 can be written as:

$$\frac{\partial C_{Na}}{\partial r} - \left(1 + \frac{C_H}{C_O}\right)\frac{\partial C_O}{\partial r} - \frac{\partial C_{Cl}}{\partial r} = 0 \tag{C-8}$$

Expanding Equation C-3:

$$j_{Na} + j_H - j_O - j_{Cl} = 0 \tag{C-9}$$

The ionic flux expression, Equation C-1, is substituted into Equation C-9, and the terms are re-grouped to yield:

$$-\frac{F}{RT}\frac{\partial \phi}{\partial r}=\frac{1}{\sum_{i=1}^{n} D_i C_i}\left[\sum_{i=1}^{n} D_i Z_i \frac{\partial C_i}{\partial r}\right] \tag{C-10}$$

Equation C-10 can be used for obtaining the sodium-ion flux as (Z_{Na} = 1):

$$j_{Na}=-D_{Na}\frac{\partial C_{Na}}{\partial r}+\frac{D_{Na}C_{Na}}{\sum_{i=1}^{n} D_i C_i}\left[\sum_{i=1}^{n} D_i Z_i \frac{\partial C_i}{\partial r}\right] \tag{C-11}$$

Expanding the terms in Equation C-11 and using Equation C-6 gives:

$$j_{Na}=\left[\frac{-D_{Na}\sum_{i=1}^{n} D_i C_i + D_{Na}^2 C_{Na}}{\sum_{i=1}^{n} D_i C_i}\right]\frac{\partial C_{Na}}{\partial r}+\frac{D_{Na}C_{Na}}{\sum_{i=1}^{n} D_i C_i}\left(D_H+\frac{D_O C_O}{C_H}\right)\frac{\partial C_H}{\partial r}-\frac{D_{Na}C_{Na}D_{Cl}}{\sum_{i=1}^{n} D_i C_i}\frac{\partial C_{Cl}}{\partial r} \tag{C-12}$$

Using Equations C-7 and C-6 the differential of hydrogen with respect to r in Equation C-12 can be replaced. With algebraic manipulation, the following relation can be obtained:

$$j_{Na}=\left[\frac{-D_{Na}\theta + D_{Na}^2 C_{Na}}{\theta}+\frac{\beta}{\theta(1+\chi)}\right]\frac{\partial C_{Na}}{\partial r}-\left[\frac{D_{Na}D_{Cl}C_{Na}}{\theta}+\frac{\beta}{\theta(1+\chi)}\right]\frac{\partial C_{Cl}}{\partial r} \tag{C-13}$$

where:

$$\theta=\sum_{i=1}^{n} D_i C_i \tag{C-14}$$

$$\chi=\frac{k_w}{C_H^2} \tag{C-15}$$

$$\beta=D_{Na}C_{Na}\left(D_H+D_O\chi\right) \tag{C-16}$$

Similarly for chloride-ion flux :

$$j_{Cl} = \left[\frac{-D_{Cl}\theta + D_{Cl}^2 C_{Cl}}{\theta} + \frac{\psi}{\theta(1+\chi)}\right]\frac{\partial C_{Cl}}{\partial r} - \left[\frac{D_{Na} D_{Cl} C_{Cl}}{\theta} + \frac{\psi}{\theta(1+\chi)}\right]\frac{\partial C_{Na}}{\partial r} \qquad \text{(C-17)}$$

where: θ is defined by Equation C-14, χ by Equation C-15, and

$$\psi = D_{Cl} C_{Cl}(D_H + D_O \chi) \qquad \text{(C-18)}$$

Equations C-13 through C-18 can be expressed in the form:

$$j_{Na} = D_{11}\frac{\partial C_{Na}}{\partial r} + D_{12}\frac{\partial C_{Cl}}{\partial r} \qquad \text{(C-19)}$$

$$j_{Cl} = D_{21}\frac{\partial C_{Na}}{\partial r} + D_{22}\frac{\partial C_{Cl}}{\partial r} \qquad \text{(C-20)}$$

where

$$\zeta = \frac{D_H C_H^2 + D_O K_w}{C_H^2 + K_w} \qquad \text{(C-21)}$$

$$D_{11} = \frac{1}{\sum_{i=1}^{n} D_i C_i}\left[-D_{Na}\sum_{i=1}^{n} D_i C_i + D_{Na}^2 C_{Na} + D_{Na} C_{Na}\zeta\right] \qquad \text{(C-22)}$$

$$D_{12} = \frac{(-1)}{\sum_{i=1}^{n} D_i C_i}\left[D_{Na} D_{Cl} C_{Na} + D_{Na} C_{Na}\zeta\right] \qquad \text{(C-23)}$$

$$D_{21} = \frac{(-1)}{\sum_{i=1}^{n} D_i C_i}\left[D_{Na} D_{Cl} C_{Cl} + D_{Cl} C_{Cl}\zeta\right] \qquad \text{(C-24)}$$

$$D_{22} = \frac{1}{\sum_{i=1}^{n} D_i C_i}\left[-D_{Cl}\sum_{i=1}^{n} D_i C_i + D_{Cl}^2 C_{Cl} + D_{Cl} C_{Cl}\zeta\right] \qquad \text{(C-25)}$$

Equation C-19 and C-20 need to be solved for obtaining the flux of sodium and chloride ions.

APPENDIX D

Computer Source Code Listing

```
*-----------------------------------------------------------------------------------------
*                School of Chemical Engineering
*                  Oklahoma State University
*
*         Weak electrolyte exchange model for MBIE
*         Vikram N. Chowdiah and Gary L. Foutch
*
*-----------------------------------------------------------------------------------------
          IMPLICIT INTEGER (I-N), REAL*8 (A-H,O-Z)
          REAL*8 KLN, KLX,LOAD,KLMR,KLOH,FLOW2, KLA,IONBAL,
     1  YNC(4,4000),YXC(4,4000),YCA(4,4000),
     2  RATN(4,4000),RATX(4,4000),RATC(4,4000),RATA(4,4000),
     3  XCA(4,4000),XAC(4,4000),XNC(4,4000),XXC(4,4000)
          DIMENSION N(4000)

          CHARACTER*15 OUTFILE,INFILE
          CHARACTER*25 AMINE_NAME
          CHARACTER*80 DESCRIPTION,DUMMY1,DUMMY2

          COMMON / PROP1 /TEMP,VOID_FRAC,BED_DIA, RES_HT
          COMMON / PROP2 /PDC,PDA,QC,QA
          COMMON / PROP3 /DEN,CP
          COMMON / PROP4 /RTF,AREA,VS
          COMMON / AMINE1 /DISS,DX,DMOR,WTA,TKNX
          COMMON / AMINE2 /AMINE_NAME
          COMMON / BAL /CFCAT,CFAN,IONBAL
          COMMON / DIFFUSION /DH,DO,DN,DC
          COMMON / MASS /KLX,KLN,KLA,KLOH,KLMR

c-------------------------------------------------------------------------------
          OPEN(3, FILE='readfile.in',status='old')
                 read(3,'(a)')infile
          close(3)
      OPEN(2,FILE=infile,STATUS='UNKNOWN')
                 READ(2,*)  KPBK, KPPR, TIME
                 READ(2,*)  YNO, YXO, YCO
                 READ(2,*)  PDC, PDA, QC, QA
                 READ(2,*)  CFN, CFC
                 READ(2,*)  VOL_FLOW, FFR, CHTIME
                 READ(2,*)  BED_DIA, RES_HT, VOID_FRAC
                 READ(2,*)  TAU, XI
                 READ(2,*)  TKCO,TKNH
                 READ(2,*)  FAR , FCR
                 READ(2,*)  TEMP, DEN
C--------------------------------------------------------------
c     dummy1 is just a description line in the data file
c     i_amine is an integer variable corresponding to a
c     particular amine.  the properties have been hard coded
c     in this program.  amines described here can only be used.
```

```
c
C-----------------------------------------------------------------
                    READ(2,'(A)') DUMMY1
                    READ(2,*)I_AMINE
C-----------------------------------------------------------------
c     if choice is 1 then enter ph as value1
c     if choice is 0 then enter total amine as value1
c          cannot enter ph and total amine-over specified problem
c
c     dummy2 is just a description line in the data file
C-----------------------------------------------------------------
                    READ(2,'(A)') DUMMY2
                    READ(2,'(A)') DUMMY2
                    READ(2,*)  CHOICE,VALUE1
                    READ(2,'(A)')  OUTFILE
                    READ(2,'(A)') DESCRIPTION
                    READ(2,*)  KNC,VNC
                    READ(2,'(A)') DUMMY2
                    READ(2,*)LEAK
                    IF(LEAK.EQ.1)THEN
                                write(6,*)' leak conditions  '
                                READ(2,*)STARTLEAK,STOPLEAK
                                READ(2,*)CFN_LEAK,CFC_LEAK
                    ENDIF
      CLOSE(2)

      ctime1=chtime/1440.    ! flow change time (conversion to days)
      KCONC = 0
      KSTEP = 0
      KFLOW = 0
      T = 0.

      CFN_START = CFN
      CFC_START = CFC

      CALL PROPERTY
      CALL AMINE_SELECT(I_AMINE)

      IF(CHOICE.EQ.1) THEN
                    PH = VALUE1
                    pOH = 14. - pH
                    CHII = 10.**(-PH)
                    COII = 10.**(-pOH)
                    coo=coii
                    cho=CHII
                    CAO = COO**2./DISS
                    CXO=COO
                    CAT = CAO + CXO

             ELSE IF(CHOICE.EQ.0) THEN

                    CAT = (VALUE1/WTA)*1.0E-3    ! PPM CONV TO MEQ/ML
                    COO = SQRT(DISS*CAT) ! INITIAL GUESS FOR NEWTON RAPHSON

                    CALL EQB3(DISS,CAT,COO,CAO,CHO,CXO,CFN,CFC)
                    COII = COO
                    CHII = CHO

             ENDIF

                    CFAN =  CFC + COII          !TOTAL ANIONS
                    CFCAT = CFN + CHII + CXO       !TOTAL CATIONS
                    CF = CFCAT
                    CTIME = CF
C-----------------------------------------------------------------
C
C      check ionic imbalance, else call IONBAL to balance
```

```
C
C--------------------------------------------------------------------
     ionbal = (abs(cfcat-cfan)/cfcat)*100.     ! ion balance in %
                  write(*,*)'   '
                  WRITE(*,*)' TOTAL CATIONS AND ANIONS ::: '
                  WRITE(*,534)CFCAT,CFAN,ionbal
 534        FORMAT(1X,'CATIONS =',E12.6,4X,'ANIONS =',E12.6,
   $       4X,' ION IMBALANCE % ',F9.3)

      IF( IONBAL.GT.5.0) THEN
                  CALL BALANCEION(PH,CFN,CFC)
                  STOP
      ELSE
                  WRITE(*,423)
 423        FORMAT(4X,'ION BALANCE WITHIN 5 % ERROR')
                  write(*,*)'  '
           ENDIF


 4321 IF(KFLOW.EQ.0)THEN
           VS = VOL_FLOW/AREA
     ELSE
           VS = FFR/AREA
     ENDIF

           CALL MTCOEFF     ! computes mass transfer coeffs

*--------------------------------------------------------------------
*    constants defined for the numerical procedure
*    (done here to reduce computational time)
*--------------------------------------------------------------------
     AM1 = KLMR/KLX
     AN1 = KLN/KLX
     AX1 = KLX/KLX
     AC1 = (KLA*PDC)/(KLX*PDA)
     AN2 = AN1*FCR
     AX2 = AX1*FCR
     AC2 = AC1*FAR
     QRATIO = QC/QA
     AH = DH/DN          ! diffusivity ratios for subroutines
     AX = DX/DN
     AO = DO/DC

*--------------------------------------------------------------------
*  Calculate total number of steps in distance (NT) down column
*--------------------------------------------------------------------
             CHTD = KLX*(1.-VOID_FRAC)*RES_HT/(VS*PDC)
             NT = CHTD/XI
                  write(6,*) nt
*--------------------------------------------------------------------
c      stop if NT greater than array size
*--------------------------------------------------------------------
                  if(nt.gt.4000) then
                        write(*,*)'  '
                        write(*,*)' not enough memory '
                        write(*,*)'  '
                        stop
                  endif

     if (kflow.eq.1) goto 4325
     flow2=KLX

     CALL OUTPUT(YXO,YNO,CF,VOL_FLOW,FFR,CTIME1,TAU,XI,NT,
    $   DESCRIPTION,OUTFILE)

             TAUPR = KLX*CF*(TIME*60.)/(PDC*QC)
           IF (KPPR.NE.1) GO TO 60
```

```
                    CALL HEADING1(TIME)
  60   CONTINUE

*------------------------------------------------------------------
*  Set initial resin loading throughout the entire column
*------------------------------------------------------------------
      MT = NT + 1
      DO 100 M=1,MT
      YNC(1,M)=YNO
      YXC(1,M)=YXO
      YCA(1,M)=YCO
      N(M) = 0
  100 CONTINUE
*------------------------------------------------------------------
*  Readjust NT for the second flow rate
*------------------------------------------------------------------
      if (kflow.eq.0) goto 4326
 4325   continue
           mmt = nt + 1
      do 1100 m=1,mmt
      mm = mt/mmt*m
      ync(1,m)=ync(1,mm)
      yxc(1,m)=yxc(1,mm)
      yca(1,m)=yca(1,mm)
 1100 continue
      if(kflow.eq.1) goto 4322

 4326 continue
*------------------------------------------------------------------
*  Calculate dimensionless program time limit
*  based on inlet conditions (Z=0)
*------------------------------------------------------------------
      TMAXC=QC*3.142*(BED_DIA/2.)**2.*RES_HT*FCR/(VOL_FLOW*CFN*60.)
      TMAXA=QA*3.142*(BED_DIA/2.)**2.*RES_HT*FAR/(VOL_FLOW*CFC*60.)
      IF(TMAXC.GE.TMAXA) THEN
            TMAX=TMAXC
           ELSE
            TMAX=TMAXA
      ENDIF
      TMAX1 = TMAX/1440.0    !CONVERSION TO DAYS
      TAUMAX = KLX*CF*(TMAX*60.)/(PDC*QC)
      WRITE(6,222)
      WRITE(6,223)TMAX1
      WRITE(6,224)
  222 FORMAT(' Program run time is based on total resin capacity')
  223 FORMAT(' and flow conditions.  The program will run for',F12.1)
  224 FORMAT(' days of column operation for the current conditions.')

      IF (KPBK.NE.1) GO TO 50
                    CALL HEADING2
   50  CONTINUE

*------------------------------------------------------------------
*  Initialize values prior to iterative loops
*
*------------------------------------------------------------------
      J = 1
      JK = 1
      TAUTOT = 0.
      JFLAG = 0
      MFLAG=0          !set to 1 after bed is completely aminated
      XNC(JK,NT) = 0.
      KK = 1
      tauflow=chtime*flow2*CTIME*60./PDC/QC

      IF(LEAK.EQ.1) THEN
                       TAULEAK = STARTLEAK*FLOW2*CF*60.0/PDC/QC
                    TSTOP = STOPLEAK*FLOW2*CF*60.0/PDC/QC
         write(6,*)'tauleak  =  ',tauleak
         write(6,*)'tstop    =  ',tstop
    ENDIF
*-------------------------------------------------------------------
*
* Time step loop within which all column calculations are
* implemented, time is incremented and outlet concentration checked
*-------------------------------------------------------------------

  1 CONTINUE
         KNC = KNC+1
         IF(LEAK.EQ.1)THEN
            IF(TAUTOT.GT.TSTOP)KSTEP=KSTEP+1
            IF(KSTEP.EQ.1)THEN
                   CFN = CFN_START
                   CFC = CFC_START
                   CF = CTIME
                   WRITE(6,*)' CONDENSER LEAK STOPS '
                   GOTO 98
            ENDIF

                  IF(TAUTOT.GT.TAULEAK)KCONC=KCONC+1
                  IF(KCONC.EQ.1)THEN
                           CFN = CFN_LEAK + CFN_START
                           CFC = CFC_LEAK + CFC_START
                           CF = CFN+CHII+CXO
                           WRITE(6,*)'  CONDENSER LEAK  '
                           WRITE(6,*)' '
                  ENDIF
         ENDIF
98    CONTINUE

                  if(chtime.ne.0.0)then
                           if(tautot.gt.tauflow) kflow=kflow+1
                  endif
         if (kflow.eq.1) goto 4321
4322  IF (TAUTOT.GT.TAUMAX) GOTO 138

*-------------------------------------------------------------------
* Correction of time step value for Adams-Bashforth Method
*-------------------------------------------------------------------
         IF (J.EQ.4) THEN
            JD = 1
           ELSE
            JD = J + 1
         ENDIF
*-------------------------------------------------------------------
* Set inlet liquid phase fractional concentrations for each
* Species in the matrix
*-------------------------------------------------------------------
   coo=coii
   cho=CHII
   CAO = COO**2./DISS
   CXO=COO
   CAT = CAO + CXO
   XCA(J,1) = CFC/CF
   XAC(J,1) = CAO/CF
   XNC(J,1) = CFN/CF
   xxc(j,1) = CXO/CF
*-------------------------------------------------------------------
* Loop to increment distance (bed length) at a fixed time
*-------------------------------------------------------------------
   DO 400 K=1,NT
         CXO = XXC(J,K)*CF
         CNO = XNC(J,K)*CF
         CCO = XCA(J,K)*CF
```

```
            CAO = XAC(J,K)*CF
            cat1 = cat
            CCT2 = CCO
            CNT2 = CNO
            CH1 = CHO
            CO1 = COO
            ca1 = cao
            CX1 = CXO
            YN = YNC(J,K)
            YC = YCA(J,K)
            IF(N(K).EQ.0)THEN
            YX = YXC(J,K)
               IF (YX .LT.0.99) THEN
                      CALL CR (CHO,CNO,CXO,AH,AX,YN,YX,CNI,CXI,RN,RX,CTI,
     $            TKNH,TKNX,cao,cai)
                      XXI = CXI/CF
                      XNI = CNI/CF
                      xai = cai/cf
               ELSE
                      N(K)=1
               ENDIF
            ELSE
                      IF(YN.LT.1.0) THEN
                                CALL BULK (TKNX,CXO,CNO,YN,AX,RN,CNI)
                                XNI = CNI/CF
                       ELSE
                                XNI=0.0
                                RN=0.0
                       ENDIF
            ENDIF
*
      IF (YC .LT. 1.0) THEN
             CALL BULK (TKCO,COO,CCO,YC,AO,RIA,CCI)
               XCI = CCI/CF
      ELSE
               XCI = 1.0
               RIA = 0.0
      ENDIF
*
            IF(N(K).EQ.0)THEN
                      RATEA = 6.0*(xac(j,k)-xai)*AM1
                      RATEX = 6.*RX*(XXC(J,K) - XXI)*AX1
            ENDIF
      RATEN = 6.*RN*(XNC(J,K) - XNI)*AN1
      RATEC = 6.*RIA*(XCA(J,K)-XCI)*AC1
      IF (K .EQ. 1) THEN
             IF(N(K).EQ.0)THEN
                      RATX(J,1) = RATEX
                      RATA(J,1) = RATEA
                      YXC(JD,1) = YXC(J,1)+(TAU*RATX(J,1)+TAU*RATA(J,1))
                      if(yxc(jd,1).gt.1.0)yxc(jd,1)=1.0
             ENDIF
            RATN(J,1) = RATEN
            RATC(J,1) = RATEC
            YNC(JD,1) = YNC(J,1)+TAU*RATN(J,1)
            YCA(JD,1) = YCA(J,1)+TAU*RATC(J,1)*QRATIO
                      IF (YNC(JD,1).GT.1.0) YNC(JD,1) = 1.0
                      IF (YCA(JD,1).GT.1.0) YCA(JD,1) = 1.0
      ENDIF
            IF (N(K).EQ.0) THEN
                 LOAD = YXC(JD,K)-YXC(J,K)
                XAC(J,K+1)=XAC(J,K)-LOAD*fcr*XI/TAU
                IF(XAC(J,K+1).LT.0.0)XAC(J,K+1)=0.0
            ENDIF
*
      IF (K.LE.2) THEN
                      CALL RUNGE(XI,RN,XNC(J,K),XNI,AN2,XNC(J,K+1))
               IF(N(K).EQ.0) THEN
                    CALL RUNGE(XI,RX,XXC(J,K),XXI,AX2,XXC(J,K+1))
               ENDIF
                    CALL RUNGE(XI,RIA,XCA(J,K),XCI,AC2,XCA(J,K+1))
      ELSE
              COEN=55.*RATEN-59.*RATN(J,K)+37.*RATN(J,K-1)-9.*RATN(J,K-2)
           XNC(J,K+1) = XNC(J,K) - (XI/24.)*COEN*FCR
                    IF(N(K).EQ.0)THEN
             COEX=55.*RATEX-59.*RATX(J,K)+37.*RATX(J,K-1)-9.*RATX(J,K-2)
           XXC(J,K+1) = XXC(J,K) - (XI/24.)*COEX*FCR
                    ENDIF
             COEC=55.*RATEC-59.*RATC(J,K)+37.*RATC(J,K-1)-9.*RATC(J,K-2)
           XCA(J,K+1) = XCA(J,K) - (XI/24.)*COEC*FAR
      ENDIF
*------------------------------------------------------------------
*  Determine concentrations for next distance step and recalculate
*  bulk phase equilibria
*------------------------------------------------------------------
           IF(N(K).EQ.0)THEN
                    CXO = XXC(J,K+1) * CF
                    CAO = XAC(J,K+1) * CF
            ENDIF
      CNO = XNC(J,K+1) * CF
      CCO = XCA(J,K+1) * CF
      COO = CO1 + (CCT2 - CCO)
           IF(N(K).EQ.0)THEN
                    CAT = CAt1 - (CX1 - CXO) - (ca1 - cao)
                    CHO = CH1 + (CNT2 - CNO) + (CX1-CXO)
           ELSE
                    CAT = CAT1 + (CNT2-CNO)
           ENDIF
      CALL EQB3(DISS,CAT,COO,CAO,CHO,CXO,CNO,CCO)
      XXC(J,K+1) = CXO/CF
      XAC(J,K+1) = CAO/CF
*------------------------------------------------------------------
*  Determine rates at constant xi for solutions of the tau
*  material balance
*------------------------------------------------------------------
      YN = YNC(J,K+1)
      YC = YCA(J,K+1)
*
           IF(N(K+1).EQ.0)THEN
           YX = YXC(J,K+1)
              IF (YX .LT.0.99) THEN
                    CALL CR (CHO,CNO,CXO,AH,AX,YN,YX,CNI,CXI,RN,RX,CTI,
     $              TKNH,TKNX,cao,cai)
                    XXI = CXI/CF
                    XNI = CNI/CF
                    xai = cai/cf
              ELSE
                    N(K+1)=1
              ENDIF
           ELSE
                    IF(YN.LT.1.0) THEN
                         CALL BULK (TKNX,CXO,CNO,YN,AX,RN,CNI)
                         XNI = CNI/CF
                     ELSE
                         XNI=0.0
                         RN=0.0
                     ENDIF
           ENDIF
*
      IF (YC .LT. 1.0) THEN
              CALL BULK (TKCO,COO,CCO,YC,AO,RIA,CCI)
              XCI = CCI/CF
      ELSE
              XCI = 1.0
            RIA = 0.0
      ENDIF
*
          IF(N(K+1).EQ.0)THEN
                    RATA(J,K+1) = 6.0*(XAC(J,K+1)-xai)*AM1
                    RATX(J,K+1) = 6.*RX*(XXC(J,K+1) - XXI)*AX1
          ENDIF
      RATN(J,K+1) = 6.*RN*((XNC(J,K+1)) - XNI)*AN1
      RATC(J,K+1) = 6.*RIA*((XCA(J,K+1))-XCI)*AC1
*------------------------------------------------------------------
*  Integrate Y using adams-bashforth (calculate next particle loading)
*------------------------------------------------------------------
      IF (KK.LE.1) THEN
             YNC(JD,K+1) = YNC(J,K+1) + TAU*RATN(J,K+1)
      YXC(JD,K+1) = YXC(J,K+1)+(TAU*RATX(J,K+1)+TAU*RATA(J,K+1))
             YCA(JD,K+1) = YCA(J,K+1) + TAU*RATC(J,K+1)*QRATIO
      ELSE
          IF(J.NE.1) GOTO 208
                    J1=4
                    GOTO 209
 208        J1 = J-1
 209        COEN=3.*RATN(J,K+1)-RATN(J1,K+1)
                    YNC(JD,K+1)=YNC(J,K+1)+(TAU/2.)*COEN
            IF(N(K+1).EQ.0)THEN
                    COEX =3.*RATX(J,K+1)-RATX(J1,K+1)
                    coeA=3.*ratA(j,k+1)-ratA(j1,k+1)
                    YXC(JD,K+1)=YXC(J,K+1)+((TAU/2.)*COEX +(tau/2.)*coeA)
             ENDIF
                    COEC=3.*RATC(J,K+1)-RATC(J1,K+1)
                    YCA(JD,K+1)=YCA(J,K+1)+(TAU/2.)*COEC*QRATIO
          ENDIF
                    if((yxc(jd,k+1)+ync(jd,k+1)).gt.1.0) then
                              yxc(jd,k+1)=1.0 - ync(jd,k+1)
                    endif
                    IF (YCA(JD,K+1).GT.1.0) YCA(JD,K+1) = 1.0
*------------------------------------------------------------------
*  Print concentration profiles
*------------------------------------------------------------------
      IF (KPPR.NE.1) GO TO 350
                    IF (TAUTOT.LT.TAUPR) GO TO 350
                    JFLAG = 1
                    ZA = FLOAT(NT)
                    ZB = FLOAT(K-1)
                    Z = ZB*RES_HT/ZA
                    KOUNT = KOUNT+1
      IF (KOUNT.NE.(KOUNT/10*10)) GOTO 350
*------------------------------------------------------------------
*  Open data file
*------------------------------------------------------------------
      OPEN(8, FILE=OUTFILE,STATUS='UNKNOWN')
             CXO = (XXC(J,K)*CF)/1E-3*WTA
             CAO = (XAC(J,K)*CF)/1.0E-3*WTA
             CNO = (XNC(J,K)*CF)/1E-6*23
             write(8,35)z,ync(j,k),yxc(j,k),CAO,cxo,cno,n(k)
 350 CONTINUE
 400 CONTINUE
  29 FORMAT (' ',4(4X,E8.3),5X,F4.2)
  35 FORMAT (' ',F10.5,5(2X,f10.5),2x,I3)
*------------------------------------------------------------------
*   Print breakthrough curves
*------------------------------------------------------------------
      IF (KPBK.NE.1) GO TO 450
          kk =2
          ppbna=cno/1.e-6*23
          ppbcl=cco/1.e-6*35.5
          ppmmor =cat/1e-3*wta
          TAUTIM = TAUTOT*PDC*QC/(flow2*CTIME*60.)/1440.
```

```
              T = TAUTIM
              pH=14.+LOG10(COO)
                 IF(KNC.EQ.20)THEN
                 KNC = 0
              OPEN(8,FILE=OUTFILE,STATUS='UNKNOWN')
              WRITE(8,139)TAUTIM,PPBNA,PPMMOR,PPBCL,PH
              WRITE(6,139) TAUTIM,ppbna,ppmmor,ppbcl,pH
  139   FORMAT(F9.3,6X,f9.3,4X,F9.3,6X,F9.3,4X,F4.2)
                 ENDIF
  450  CONTINUE

       JK = J
       IF (J.EQ.4) THEN
                 J = 1
               ELSE
                 J = J+1
       ENDIF
*-----------------------------------------------------------------
*  End of loop, return to beginning and step in time
*-----------------------------------------------------------------
       IF (JFLAG.EQ.1) STOP
       TAUTOT = TAUTOT + TAU
       IF(TAUTIM.GE.VNC)GOTO 138
       GOTO 1
 138  STOP
       END
*
       SUBROUTINE CR (CHO,CNO,CXO,AH,AX,YN,YX,CNI,CXI,RN,RX,CTI,
      $ TKNH,TKNX,cao,cai)
       IMPLICIT REAL*8 (A-H,O-Z)
*
       S = (CHO+CNO+CXO)*(AH*CHO+CNO+AX*CXO)
       DENOM1 = TKNH+(1-TKNH)*YN+(TKNX-TKNH)*YX
       DENOM2 = AH*TKNH+(1-AH*TKNH)*YN+(AX*TKNX-AH*TKNH)*YX
*
*     Calculate Interfacial Concentrations
*
              CNI = YN*(SQRT(S/DENOM1/DENOM2))
              IF (CNI.LT.0.0) CNI=0.0
              CXI = CNI*TKNX*YX/YN
              IF (CXI.LT.0.0) CXI=0.0
              CHI = CNI*TKNH*(1-YN-YX)/YN
              IF (CHI.LT.0.0) CHI=0.0
              CTI = CNI+CHI+CXI
              CTO = CXO+CHO+CNO
              CTR = CTI/CTO
              CNR = CNI/CNO
              CXR = CXI/CXO
              BBB = 1.+ CTR
              AAX = CXO-CXI
              AAN = CNO-CNI
*
*     Calculate Ternary Effective Diffusivities
*
       IF (ABS(AAN).GE.(CNO/100000.)) GOTO 57
              CNI = CNO
              DENN = 1.0
              GOTO 58
 57    DENN = 2.*(CTR*CNR-1.)
        CCC = CNR-1.
        DENN = DENN/(BBB*CCC)
 58    IF (ABS(AAX).GE.(CXO/100000.)) GOTO 59
              CXI = CXO
              DEX = 1.0
              GOTO 61
 59    DEX = 2.*(CTR*CXR-1.)
        BBX = CXR-1.
       DEX = DEX/(BBX*BBB)
 61    CONTINUE
*
*      Calculate Ri's for components
*
      EPN = 2./3.
      RN = (ABS(DENN))**(EPN)
      RX = (ABS(DEX))**(EPN)
      if(cno.ne.0.0)then
      cai = tknx*yx*cni/yn
      if(cai.gt.cao)cai=cao
      endif
*
      RETURN
      END
*
      SUBROUTINE BULK (TKNA,CAO,CNO,YN,AO,RIC,CNI)
*        subroutine to calculate Ri and the interface concentration
*         using the bulk phase neutralization model
*
      IMPLICIT REAL*8 (A-H,O-Z)
      Y = CAO/CNO
      IF (YN.GT.1.0) YN = 1.0
      IF (YN.LT.0.000001) THEN
              YP = SQRT((CAO/CNO + 1./AO) * (CAO/CNO + 1.))
              DE = 2.*AO*(YP - CAO/CNO - 1.) / (1.-AO)
              XNI = 0.0
            ELSE
              S = TKNA*(1. - YN)/YN
              XNI = SQRT(((AO*Y+1.)*(Y+1.))/((AO*S+1.)*(S+1.)))
              DE = 2.*AO*(S*XNI+XNI-Y-1.)/((1.-AO)*(1.-XNI))
      ENDIF
      CNI = XNI*CNO
      RIC = (ABS(DE))**(2./3.)
      RETURN
      END
*
       SUBROUTINE EQB3(DISS,CAT,COO,CAO,CHO,CXO,CNO,CCO)
       IMPLICIT REAL*8 (A-H,O-Z)
*
*      New equilibrium subroutine
*      cations and anions are included in the charge balance
*
       F(X,CAT,DISS,CNO,CCO)=X**3.+((DISS+CCO-CNO)*X**2)-
     $  ((1.E-14+(CAT+CNO-CCO)*DISS)*X)-DISS*1.E-14
      DF(X,CAT,DISS,CNO,CCO)=3.*X**2+ (2.*(DISS+CCO-CNO)*X) -
     $  (1.E-14+(CAT+CNO-CCO)*DISS)
*
       EPS = 1.0E-9
       X0 =  COO
       X = X0 -F(X0,CAT,DISS,CNO,CCO)/DF(X0,CAT,DISS,CNO,CCO)
       DO WHILE ((ABS(X-X0)/x).GT.EPS)
             X0 = X
             X = X0 - F(X0,CAT,DISS,CNO,CCO)/DF(X0,CAT,DISS,CNO,CCO)
       END DO
       COO = X
       CHO = 1.E-14/COO
       CXO = (COO + CCO) - (CHO + CNO)
       CAO = CAT - CXO
       RETURN
       END
*
      SUBROUTINE PROPERTY()
      IMPLICIT REAL*8 (A-H,O-Z)

c-----------------------------------------------------------------------------
c           set ion propertites
```

```
c
c-----------------------------------------------------------------------------
      COMMON / PROP1 /TEMP,VOID_FRAC,BED_DIA, RES_HT
            COMMON / PROP2 /PDC,PDA,QC,QA
            COMMON / PROP3 /DEN,CP
            COMMON / PROP4 /RTF,AREA,VS
      COMMON / DIFFUSION /DH,DO,DN,DC

      CP = 1.43123+TEMP*(0.000127065*TEMP-0.0241537)
      RTF = (8.931D-10)*(TEMP+273.16)
      AREA = 3.1415927*(BED_DIA**2)/4.

      XLAMH = 221.7134+5.52964*TEMP-0.014445*TEMP*TEMP
      XLAMN = 23.00498+1.06416*TEMP+0.0033196*TEMP*TEMP
      XLAMO = 104.74113+3.807544*TEMP
      XLAMC = 39.6493+1.39176*TEMP+0.0033196*TEMP*TEMP
      DN = RTF*XLAMN          ! diffusion coefficient (sodium)
      DO = RTF*XLAMO          ! diffusion coefficient (hydroxide)
      DC = RTF*XLAMC          ! diffusion coefficient (chloride)
      DH = RTF*XLAMH          ! diffusion coefficient (hydrogen)

      RETURN
      END

            SUBROUTINE MTCOEFF
            IMPLICIT REAL*8 (A-H,O-Z)
            REAL*8 KLX,KLN,KLA,KLOH,KLMR
c-------------------------------------------------------------------------------------
c           calculate mass transfer coeffs
c
c-------------------------------------------------------------------------------------

            COMMON / PROP1 /TEMP,VOID_FRAC,BED_DIA, RES_HT
            COMMON / PROP2 /PDC,PDA,QC,QA
            COMMON / PROP3 /DEN,CP
            COMMON / PROP4 /RTF,AREA,VS
            COMMON / AMINE1 /DISS,DX,DMOR,WTA,TKNX
            COMMON / DIFFUSION /DH,DO,DN,DC
            COMMON / MASS /KLX,KLN,KLA,KLOH,KLMR

               F1(R,S) = 1.15*VS/(VOID_FRAC*(S**(2./3.))*(R**0.5))
               F2(R,S) =1.85*VS*((VOID_FRAC/(1.-VOID_FRAC))**(-1./3.))/
     1           (VOID_FRAC*(S**(2./3.))*(R**(2./3.)))

      REC = PDC*100.*VS*DEN/(VOID_FRAC*CP)
      REA = PDA*100.*VS*DEN/(VOID_FRAC*CP)
      SCX = (CP/100.)/DEN/DX
      SCN = (CP/100.)/DEN/DN
      SCA = (CP/100.)/DEN/DC
      smr = (cp/100.)/den/dmor
      SCO = (CP/100.)/DEN/DO

             IF (REC.LT.20.) THEN
                     KLN = F2(REC,SCN)
                     KLX = F2(REC,SCX)
                     KLMR = F2(REC,SMR)
               ELSE
                     KLN = F1(REC,SCN)
                     KLX = F1(REC,SCX)
                     KLMR = F1(REC,SMR)
             ENDIF
             IF (REA.LT.20.) THEN
                     KLA = F2(REA,SCA)
                     KLOH = F2(REA,SCO)
               ELSE
                     KLA = F1(REA,SCA)
                     KLOH = F1(REA,SCO)
```

```
        ENDIF
      RETURN
      END
*
      SUBROUTINE AMINE_SELECT(IA)
      IMPLICIT REAL*8 (A-H,O-Z)
      CHARACTER*25 AMINE_NAME

      COMMON / PROP1 /TEMP,VOID_FRAC,BED_DIA, RES_HT
      COMMON / PROP2 /PDC,PDA,QC,QA
      COMMON / PROP3 /DEN,CP
      COMMON / PROP4 /RTF,AREA,VS
      COMMON / AMINE1 /DISS,DX,DMOR,WTA,TKNX
      COMMON / AMINE2 /AMINE_NAME
      COMMON / DIFFUSION /DH,DO,DN,DC
C
C-----------------------------------------------------------
C     DEPENDING ON IA, THE AMINE PROPERTIES ARE OBTAINED
C     ALL VALUES ARE HARD CODED
C-----------------------------------------------------------
C     IA = 1        MORPHOLINE
C     IA = 2        AMMONIA
C     IA = 3        ETA
C     IA = 4
C-----------------------------------------------------------
      IF(IA.EQ.1)THEN
            XLAMX = 60.0
            DISS = 3.14E-6
            DX = RTF*XLAMX     ! diffusion coefficient (morpholine)
            WTA = 87.0
            DMOR = 1.058E-5
            AMINE_NAME=' MORPHOLINE '
            TKNX = 2.1

      ELSE IF(IA.EQ.2)THEN
            XLAMX =1.40549*TEMP+39.1537 ! FOR AMMONIA ONLY
            DISS = 1.78E-5
            DX = RTF*XLAMX
            WTA = 17.0
            DMOR = 2.288E-5
            AMINE_NAME=' AMMONIA '
            TKNX = 1.1
      ELSE IF(IA.EQ.3)THEN
            XLAMX = 47.2
            DISS = 3.16E-5
            DX = RTF*XLAMX
            WTA = 61.0
            DMOR = 1.24E-5
            AMINE_NAME=' ETHANOL AMINE'
            TKNX = 2.7

      ELSE IF(IA.EQ.4)THEN
            XLAMX = 45.0
            DISS = 5.01E-5
            DX = RTF*XLAMX
            WTA = 89.14
            DMOR = 0.926E-5
            AMINE_NAME = ' AMP  '
            TKNX = 2.5
      ENDIF
            RETURN
            END

      SUBROUTINE BALANCEION(PH,CFN,CFC)
      IMPLICIT REAL*8 (A-H,O-Z)
      REAL*8 IONBAL
      COMMON / BAL /CFCAT,CFAN,IONBAL
```

```
       WRITE(*,*)'  '
       WRITE(*,*)'----------- BALANCE IONIC COMPOSITION -----------'
       WRITE(*,800)
800  FORMAT(4X,' CURRENT VALUES========> ')
       WRITE(*,801)IONBAL,PH
801  FORMAT(4X,'IONIC IMBALANCE % ',F10.4,2X,'pH  ',F6.4)
       WRITE(*,802)CFN,CFC
802  FORMAT(4X,'SODIUM CONC ',E12.6,2X,' CHLORIDE CONC ',E12.6)

       write(*,*)'  '
       write(*,*)'  '
       write(*,*)'     Enter the number corresponding to your choice'
       write(*,*)'  '
       write(*,*)'      1 ---> To change pH              '
       write(*,*)'      2 ---> To change SODIUM CONC (in meq/ml)  '
       write(*,*)'      3 ---> To change CHLORIDE CONC (in meq/ml)'
       write(*,*)'  '
       write(*,'(a \)')'      Enter number of choice  ====>  '
       read(*,*)nu
       WRITE(*,*)'  '
       WRITE(*,*)'  '
       if(nu.eq.1)then
               write(*,'(a \)')' Enter new value for pH ==> '
               read(*,*)PH
       else if(nu.eq.2) then
       write(*,'(a \)')'Enter new value for SODIUM conc (meq/ml)==> '
               read(*,*)CFN
       else if(nu.eq.3) then
       write(*,'(a \)')'Enter new value for CLORIDE conc (meq/ml)==> '
               read(*,*)CFC
       endif

       return
       end
       SUBROUTINE OUTPUT(YXO,YNO,CF,VOL_FLOW,FFR,CTIME1,TAU,XI,NT,
  $ DESCRIPTION,OUTFILE)
       IMPLICIT REAL*8 (A-H,O-Z)
       REAL*8 KLX,KLN,KLA,KLOH,KLMR,IONBAL
       CHARACTER*15 OUTFILE
       CHARACTER*25 AMINE_NAME
   CHARACTER*80 DESCRIPTION

       COMMON / PROP1 /TEMP,VOID_FRAC,BED_DIA, RES_HT
       COMMON / PROP2 /PDC,PDA,QC,QA
       COMMON / PROP3 /DEN,CP
       COMMON / PROP4 /RTF,AREA,VS
       COMMON / AMINE1 /DISS,DX,DMOR,WTA,TKNX
       COMMON / AMINE2 /AMINE_NAME
       COMMON / BAL /CFCAT,CFAN,IONBAL
       COMMON / DIFFUSION /DH,DO,DN,DC
       COMMON / MASS /KLX,KLN,KLA,KLOH,KLMR

       OPEN(UNIT=8,FILE=OUTFILE,STATUS='UNKNOWN')
               DO 9 I = 1,2     !write results to terminal and data file
                       IF (I.EQ.1) THEN
                               IN = 6
                       ELSE
                               IN = 8
                       ENDIF

       WRITE(IN,534)CFCAT,CFAN,ionbal
534  FORMAT(1X,'CATIONS =',E12.6,4X,'ANIONS =',E12.6,
  $       4X,' ION IMBALANCE % ',F9.3)
       WRITE (IN,10)
       WRITE (IN,11)
 10  FORMAT (' MIXED BED SYSTEM PARAMETERS:')
 11   FORMAT (' ')

        WRITE (IN,12) YXO,YNO
        WRITE (IN,13) PDC,VOID_FRAC
        WRITE (IN,14) QC,QA
        WRITE (IN,15) CF,VOL_FLOW,BED_DIA,RES_HT
 12   FORMAT (' RESIN REGENERATION',3X,': YXO =',F5.3,6X,
  $    'YNO =',F5.3)
 13   FORMAT (' RESIN PROPERTIES',5X,': PDC =',F6.4,5X,'VOID_FRAC =',
  $      F6.4)
 14   FORMAT (' RESIN CONSTANTS',6X,': QC  =',F6.4,5X,'QA  =',F6.4)
 15   FORMAT (' COLUMN PARAMETERS',4X,': CF  =',E10.4,' VOL_FLOW =',
  $       E9.4,5X,'BED_DIA =',F6.2,2X,'RES_HT =',F5.1)
        WRITE(IN,'(A)')' AMINE USED ::   ',AMINE_NAME
        write(IN,11)
        write(IN,123)VOL_FLOW,ffr
123    format(4x,'Initial flow = ',e10.5,4x,'Final flow = ',e10.5)
        write(IN,124)ctime1
124    format(4x,'Flowrate Change time (days) =   ',f10.4)
        write(IN,11)
        write(IN,11)
        WRITE (IN,16) DX,DN,DH
        WRITE (IN,17) CP,DEN,TEMP
 16   FORMAT (' IONIC CONSTANTS',6X,': DX  =',E10.4,'  DN =',E10.4,
  1      2X,'DH  =',E10.4)
 17   FORMAT (' FLUID PROP.',9X,' : CP  =',F7.5,4X,' DEN =',F6.3,
  1      4X,' TEMP =',F4.1)
        WRITE (IN,11)
        WRITE (IN,19)
 19   FORMAT (' CALCULATED PARAMETERS')
        WRITE (IN,11)
        WRITE (IN,21) TAU,XI,NT
        WRITE (IN,22) KLN
        WRITE (IN,88) KLX,KLA
 21   FORMAT (' INTEGRATION INCREMENTS   : TAU =',F7.5,5X,'XI  ='
  $   ,F7.5, 5X,'NT  =',I6)
 22   FORMAT (' TRANSFER COEFFICIENTS    : KLN =',E10.4)
 88   FORMAT (' ',25X,'  KLX =',E10.4,'  KLA = ',E10.4)
        write(IN,125)klmr,KLOH
125    format(8X,'KLMR(mol amine)=   ',e10.5,4X,'KLOH =  ',E10.5)
        WRITE (IN,23) VS
 23   FORMAT (' SUPERFICIAL VELOCITY     : VS =',F7.3)
        write(IN,11)
        write(IN,'(A)')description
9    CONTINUE
        RETURN
        END
C-----------------------------------------------------------------
        SUBROUTINE HEADING1(TIME)
        IMPLICIT REAL*8 (A-H,O-Z)
        DO 10 I = 1,2
                IF(I.EQ.1)THEN
                        IN = 6
                ELSE
                        IN = 8
                ENDIF
                WRITE (IN,30)
                WRITE (IN,31) TIME
                WRITE (IN,30)
                WRITE (IN,33)
                WRITE (IN,30)
10    CONTINUE
 30   FORMAT (' ')
 31   FORMAT (' CONCENTRATION PROFILES AFTER ',F5.0,' MINUTES')
 33   FORMAT (' ',6X,'Z',4X,'YNC(j,k)',4X,'YXC(j,k)',4X,'CAO',
  1      6X,'CXO',5X,'CNO',5x,' N(k) ')
        RETURN
```

```
          END

C---------------------------------------------------------------------
          SUBROUTINE HEADING2
          IMPLICIT REAL*8 (A-H,O-Z)
          DO 10 I = 1,2
                    IF(I.EQ.1)THEN
                              IN = 6
                    ELSE
                              IN = 8
                    ENDIF
                    WRITE (IN,26)
                    WRITE (IN,25)
                    WRITE (IN,26)
                    WRITE (IN,27)
                    WRITE (IN,26)
10    CONTINUE
 25   FORMAT (' BREAKTHROUGH CURVE RESULTS:')
 26   FORMAT (' ')
 27   FORMAT (' ',5X,'T(DAYS)',6X,'SODIUM',6X,'AMINE',7X,'CHLORIDE',
  1        7X,'pH')
            RETURN
            END

          SUBROUTINE RUNGE(XI,R,XIN,XS,F,XOUT)
          IMPLICIT REAL*8 (A-H,O-Z)

                    F1 = XI*6.0*R*(XIN-XS)*F
                    F2 = XI*6.0*R*((XIN+F1/2.0)-XS)*F
                    F3 = XI*6.0*R*((XIN+F2/2.0)-XS)*F
                    F4 = XI*6.0*R*(XIN+F3-XS)*F
          XOUT = XIN - (F1+ 2.0*F2 +2.0*F3 +F4)/6.0
          RETURN
          END
```

Sample Input Data File

```
1,0,100.0D0                     !KPBK, KPPR, TIME
0.00185,0.00185,0.00185         !YNO, YXO, YCO
0.1D0,0.066D0,1.85,1.0           !PDC, PDA, QC, QA
1.74D-8,1.74d-8                  ! sodium and chloride conc(meq/ml)
3.03d4,6.06D4,0.0               ! flow rate cahnge time in mins
152.0,100.0,0.35                !DIA, CHT, VD
0.001D0,0.005D0                 !TAU, XI
17.0,1.5                        !TKCO, TKNH
0.5,0.5                         !FAR, FCR
25.0,0.995                      !TMP,DEN
1-MORPHOLINE   2-AMMONIA   3-ETA  4-AMP
3
ENTER 1 AND THEN THE PH OR ELSE ENTER 0 AND TOTAL AMINE(ppm)
(ONLY ONE CHOICE ALLOWED)
1,9.65
teste.dat                       !OUTPUT DATA FILE     [amine]
 morpholine used NE simultions
0,30.0                          !KNC, VNC (simulate till....in days)
leak simulation parameters
0                               ! 1 TO SIM LEAK, 0 FOR NONE
14400,14700                     !TIME TO START AND STOP LEAK
1.74D-4,1.74D-4                 !LEAK CONC OF SOD AND CL-
```

VITA

Vikram N. Chowdiah

Candidate for the Degree of

Doctor of Philosophy

Thesis: LIQUID-FILM DIFFUSION CONTROLLED ION-EXCHANGE MODELING — STUDY OF WEAK ELECTROLYTE MASS TRANSPORT AND FILM MASS-TRANSFER KINETICS

Major Field: Chemical Engineering

Biographical:

Education: Graduated from National High School, Bangalore, India in May 1981; completed pre-university education from National College, Bangalore, India in May 1983; received Bachelor of Engineering in Chemical Engineering from Bangalore University, India in May 1988; received Master of Science in Chemical Engineering from Oklahoma State University in December 1990. Completed the requirements for the Doctor of Philosophy Degree at Oklahoma State University in May 1996.

Professional Experience: Research Scholar in Atmospheric Science, Indian Institute of Science, Bangalore, India from August 1988 to July 1989. Graduate teaching assistant and research associate at the School of Chemical Engineering, Oklahoma State University, September 1989 to May 1995.

Professional Memberships: American Institute of Chemical Enginers, Omega Chi Epsilon